Sustainable Design of Wastewater Treatment Systems: Evaluations of Operational Flexibility and Phototrophs for Resource Recovery

by

Jeremy S. Guest

A dissertation submitted in partial fulfillment
of the requirements for the degree of
Doctor of Philosophy
(Environmental Engineering)
in the University of Michigan
2012

Doctoral Committee:

Professor Nancy G. Love, Co-Chair
Associate Professor Steven J. Skerlos, Co-Chair
Professor Lutgarde Raskin
Professor Donald Scavia
Glen T. Daigger, CH2M HILL

Acknowledgements

I would like to acknowledge the following sources of financial support for this research:

- Department of Civil and Environmental Engineering, University of Michigan;
- Graham Environmental Sustainability Institute, University of Michigan;
- Rackham Graduate School, University of Michigan;
- National Science Foundation;
- Hampton Roads Sanitation District (HRSD).

I would like to thank the staff in the Department of Civil and Environmental Engineering, with special attention to Rick Burch and Tom Yavaraski for making all laboratory work possible, and Nancy Osugi and Kimberly Gauss for their help with too many items to list. Experimental components of this work were made possible through the efforts of Siddharth Dev and Harsha Hebbale (undergraduate students at the University of Michigan), who are two of the most devoted and hardworking researchers with whom I have had the pleasure to work. Lipid analyses were made possible by Phil Savage and Robert Levine (Department of Chemical Engineering).

I would like to thank my committee members, Dr. Lutgarde Raskin, Dr. Donald Scavia, Dr. Glen Daigger, and Dr. Charles Bott, for their mentoring and thoughtful contributions over the last several years. Beyond guidance on the specific research topics contained in this dissertation, I would like to thank Lut for being a role model for an aspiring faculty member and Dr. Daigger for being a role model for an aspiring engineer. I would also like to take this opportunity to thank Dr. Mark van Loosdrecht (TU Delft) for his mentoring both in research and in my development as a member of the wastewater community, and for the opportunity to spend a month in the Department of Biotechnology at TU Delft. I would like to thank the students in the Environmental Biotechnology Group at TU Delft for their inspiration and thoughtful discussions on all things biotechnology, and Mari and Thomas for the bike rides.

I would like to thank my co-advisors, Dr. Nancy Love and Dr. Steven Skerlos, for their patience, mentoring, and guidance. They both have a deep and genuine interest in the

intellectual and professional development of their students; a simple fact that creates a safe haven for intellectual freedom and exploration. I cannot say enough about how grateful I am to have them both as mentors, except to say that I will make it my mission to provide my future students with similar experiences.

I would like to thank my Ph.D. Support Group, namely Monica Higgins, Sherri Cook, and Andrew Henderson, for their help in maintaining forward motion throughout my degree. I would like to thank members of the Love Research Group (past and present), with special thanks to Kevin Gilmore and Wendell Khunjar. I would like to thank members of the Environmental Biotechnology Group and EASTlab, with special thanks to Ameet Pinto for his trust and friendship, and for the influential role he has played in my intellectual and professional development over the last 6 years. I would also like to thank Dr. Thomas DiStefano (Bucknell University), for being a constant source of support, for his mentoring, and for helping keep it all in perspective.

I would like to thank my parents for their constant support and understanding, and for instilling in me a sense of responsibility and a genuine desire to improve this world through everyday behavior and whatever career path I choose. I would like to thank my siblings for their encouragement over the years, and for being role models in every aspect of their lives.

Most importantly, I would like to thank my wife, Eileen, and our son, Liam. Eileen's support and dedication made this dissertation possible, and Liam has provided us with the most profound motivation to complete this degree and move on to the next chapter in our lives.

Preface

The lack of improved sanitation is a global crisis, with 2.5 billion people still without access [1]. The work presented in this dissertation seeks to advance the sustainability of wastewater treatment systems, taking for granted the provision of such services for the protection of public health. It is not my intent for this work to be regarded as distinct from improving access to sanitation in developing communities, but rather to contribute to this effort by advancing our understanding of how to develop engineering solutions that match locality-specific needs, that add value to sanitation systems, and that improve their capacity to endure.

In addressing these and other global concerns [2], it becomes necessary to re-envision the way we design engineered infrastructure to meet human needs. In the wastewater field, our use of water as a carrier for human excreta dates back to Roman times, with modern sewerage networks born out of the mid-19th century London cholera outbreak and the work of Sir Joseph Bazalgette. Following the installation of collection systems came recognition of the need for treatment and the observation that oxidation of sewage reduced its potency [3]. One of the first treatment processes of modern times was the use of porous earth to filter and aerobically treat sewage [4]. Finally, in the early 1900's, Ardern and Lockett discovered that if you aerate sewage in a container, let it settle, and only replace the supernatant with fresh sewage (thereby leaving the settleable biological solids in the container), treatment would become much more rapid [5]: thus, the *Activated Sludge* process was born, and has since been a cornerstone of wastewater treatment systems [6, 7].

As we consider the future of our industry, we will undoubtedly continue to take advantage of the discoveries and inventions that have inspired more advanced treatment systems over the last half-century (e.g., [8-10]). Beyond improvements to treatment technology, however, we will also re-consider the design of infrastructure for the provision of water and sanitation services to a rapidly growing and urbanizing society [11, 12]. Given that many of the benefits of such redesign may not be immediately or

locally observed, social and economic barriers will continue to deter such innovation. It is my hope that the work presented here may, in some small measure, contribute to the development of planning and design processes that will more accurately characterize sustainability trade-offs of design decisions, and that will empower decision-makers to achieve harmony among local, regional, and global goals for sustainability.

Table of Contents

List of Figures

List of Tables

List of Appendices

Chapter 1
Introduction

We are pushing the Earth's limits in terms of sustaining a stable global environment, in particular through anthropogenic activities resulting in climate change, biodiversity loss, and alteration of the global nitrogen and phosphorus cycles [2]. Sustainability science and engineering is an emerging field that seeks to address these complex problems through interdisciplinary and collaborative efforts [13]. The field itself is about the dynamic interactions between nature and society [14-16], about accepting the complexity of social-ecological systems [17], and is defined by the challenges it seeks to overcome (rather than the disciplines it employs) [18]. In the context of wastewater engineering, the challenges we face include a lack of access to improved sanitation [1], lack of funding in the face of aging and deteriorating infrastructure [19], decreased availability of freshwater resources [20], increasingly stringent effluent permit requirements (e.g., [21]), increasing susceptibility of receiving environments [22], and emerging performance indicators not traditionally considered in design and operation decisions (e.g., life cycle greenhouse gas emissions) [23]. As we begin to pursue sustainability in the wastewater industry, it is important that we reconsider the way we design wastewater infrastructure, and transition from traditional cost-benefit analyses to design processes that address environmental, ecological, social, economic, and functional factors that influence system sustainability [24].

Sustainable design, as a discipline, is in its infancy. Many of the developments in the field have emerged from Mechanical, Industrial, and Chemical Engineering, gaining momentum around the concept of green engineering – the design of processes or products to avoid waste generation [25, 26]. Just as it has been observed that the majority of product or process costs are determined by the early stages of design [27], it is believed that the same is true for life cycle environmental impacts [28]. Within Civil and Environmental Engineering, the need for more sustainable urban infrastructure has been identified [29-31], with recent efforts including low impact development (LID) for stormwater management [32], the construction of low energy buildings [33], the

development of construction materials with lesser environmental impacts [34], and the recovery of resources from waste [11, 35, 36]. In comparison to engineering disciplines focused on products or production processes, Civil and Environmental Engineering has arguably made less progress in the development and application of sustainable design tools and concepts. A contributing factor is society's reliance on existing infrastructure and the impetus to maintain its current level of performance at all times. To transition to more sustainable infrastructure, however, we must create opportunities to re-envision the provision of civil services to growing populations [31] and develop the tools to understand the implications of our design decisions.

In the wastewater field, recent advancements in the application of sustainability-thinking have taken three main forms: (i) resource recovery from wastewater [11, 35, 37], (ii) considering broader impacts in process or infrastructure selection (e.g., public acceptance, global warming potential) [24, 38-42], and (iii) expanding appropriate sanitation coverage globally [43, 44]. Although they often appear independent of one another in the literature, these three research areas are directly related: to facilitate the global implementation of appropriate sanitation systems (item iii), it is vital that we consider what benefit these systems can provide to communities (item i) and understand their broader impacts (item ii) for installations to be successful (for a more thorough discussion of sanitation system implementation in developing world scenarios, see [45, 46]). Therefore, the inclusion of broader impacts in wastewater treatment plant (WWTP) planning and design may promote the adoption of innovative resource recovery technologies – a synergistic relationship that may facilitate the pursuit of more sustainable wastewater systems.

Standard components of WWTP projects include performance and cost assessments. For performance assessments, researchers and practitioners rely on simulators (e.g., GPS-X^{TM}) to better understand the likely behavior of the WWTP [47]. Recent advancements in the literature often focus on explicitly characterizing sources of uncertainty [48] to enable decision-makers to make more informed design choices. Economic assessments, in addition to being a cornerstone of practice, have also been applied in the research literature using well-established approaches such as net present value and life cycle costing [49]. In order to quantify the broader environmental impacts of a wastewater treatment system, life cycle assessment (LCA) has been widely used – a tool to quantify the environmental impacts of a given product or process by evaluating

the emissions resulting from all related processes within the system's boundary [50]. Due to the standardization of this methodology [51], it has been widely applied with reasonable consistency in the wastewater literature [38]. In contrast, social factors in WWTP planning and design are the least standardized, with approaches to ranging from the use of social metrics in developed world studies (e.g., acceptability to stakeholders [52]) to a focus on the process of community participation in developing world projects [45, 46]. Although this array of assessment tools exists, the comprehensive integration of these tools for WWTP design has not been demonstrated in the literature. In addition to offering insight into design decisions among traditional treatment technologies, the integration of these tools would also enable more comprehensive evaluations of emerging resource recovery technologies to better understand the performance, economic, environmental, and social implications of their implementation.

Resource recovery from wastewater is not a new concept (e.g., [53]). Typically, three resources are identified as potentially recoverable from wastewater: water, nutrients, and energy [24, 35]. Although traditional wastewater treatment strategies do not preclude utilities from achieving water reuse, their reliance on aerobic chemotrophic bacteria significantly diminish the potential for energy and nutrient recovery from wastewater. Considering on-going concerns surrounding climate change and anthropogenic impacts on nitrogen and phosphorus cycles [2], there is a real need for technological and strategic developments in the areas of nutrient and energy recovery from wastewater. Relevant technologies in these areas include anaerobic processes for methane production [54, 55], anaerobic processes for direct electricity production [56], nutrient recovery via precipitation as struvite ($MgNH_4PO_4$-$6H_2O$) [57], and the use of phototrophic microorganisms for nutrient assimilation and energy production [58]. [Note: The term *phototrophic microorganism* is used here to include both microalgae and photosynthetic bacteria. Although the term *microalgae* was once commonly used to encompass both eukaryotes and bacteria, the term is reserved here for phototrophic, eukaryotic microorganisms.] Given the need for locality-specific sustainability solutions, each of these technologies may have circumstances under which they are the most sustainable alternative. Anaerobic technologies, in particular, have been widely implemented across the globe, while struvite precipitation systems have been installed at WWTPs in recent years to recover nutrients (often) from centrate. There is a long history of using phototrophic microorganisms for wastewater treatment (e.g., [59]), with

the most common types of phototrophic systems being ponds/lagoons or, more recently, high rate algal ponds. The goals for such systems tend not to include energy or nutrient recovery, however, as these systems are often constructed in areas where low maintenance and construction costs are preferable or a necessity [60]. As a result, the wastewater industry has very limited experience with the use of phototrophic bioprocesses for simultaneous wastewater treatment and biofuel feedstock production (e.g., lipids for biodiesel or biogas, carbohydrates for bioethanol or biogas), and any future advancements in this technology will require investments from both industry and academia.

To date, the full-scale implementation of phototrophic resource recovery technologies has been inhibited by technological barriers that prevent them from being cost-effective [58], not the least of which is a lack of understanding of phototroph physiology in engineered processes. Promising elements of phototrophic technologies include the potential benefits of larger scale installations [61] (e.g., large, centralized WWTPs), and that their use for energy recovery in wastewater treatment does not preclude the use of technologies that recover energy via the biochemical oxidation of organic carbon (i.e., anaerobic processes). To take advantage of these characteristics, a great deal of research is required. In addition to required improvements to photobioreactor design [58] and downstream processing [62], a critical barrier in realizing the potential of phototrophs for resource recovery from wastewater is a lack of understanding of cell physiology in engineered bioprocesses – the central focus of the phototrophic work presented in this dissertation.

To be able to design systems capable of enriching carbon-accumulating phototrophs, it is necessary to understand the dynamic behavior of these microorganisms and to be able to model their performance in an engineered process. What we need, therefore, is to gain a fundamental understanding of the kinetic and stoichiometric behavior of phototrophic microorganisms in both lit and dark conditions before we can evaluate this technology with a broader set of sustainability factors. Only with this kind of understanding will we be able to answer the question whether or not resource recovery via phototrophic microorganisms is a technology that is consistent with the sustainability goals of the wastewater industry.

The overarching goal of this dissertation is to advance the sustainability of wastewater systems. Although concepts surrounding sustainable wastewater infrastructure have advanced in recent years (e.g., [11, 30, 31, 63, 64]), a defined methodology to develop designs and elucidate trade-offs across dimensions of sustainability (social, economic, environmental, functional), space (local, regional, global), and time (present, future) does not exist. In particular, social barriers have been poorly addressed and there is a severe lack of integration in quantitative assessments of economic, environmental, and functional sustainability. This limitation not only impacts the industry's ability to develop more sustainable designs and evaluate configuration alternatives, but it also prevents the comparative evaluation of traditional with emerging technologies in wastewater management (e.g., the use of phototrophic microorganisms for energy recovery). In order to address social factors, we have developed a planning and design process for wastewater treatment systems that is centered on a process of continuous stakeholder participation (Chapter 3) and that is enhanced through communication tools and lessons learned from the social sciences literature (Chapter 4). To provide stakeholders with the best available information in the context of WWTP design, we have also integrated state of the art tools to assess the performance, cost, and life cycle environmental impacts of WWTP designs (Chapter 5). Although these tools have been developed independent of one another in the literature, their integration creates opportunities to elucidate tensions and synergistic relationships among goals for sustainability. Ultimately, this methodology and the case study used for its demonstration (Chapter 5) offer insight into broader themes of WWTP sustainability, improve designs in novel ways, and provide a framework to evaluate emerging technologies in wastewater management. Finally, having identified the likely benefits of resource recovery from wastewater via phototrophic microorganisms but the lack of an understanding of cell physiology in engineered systems, we have developed a process model (Chapter 6) to enable the evaluation of phototrophic microorganisms as a resource recovery technology. Through these efforts, this dissertation advances the sustainability of wastewater treatment systems by facilitating sustainable design and decision-making in the context of WWTP design and operation.

Chapter 2
Background

2.1. Sustainable Design

2.1.1. Pillars of Sustainability

Since the publication of *Our Common Future* [65] by the Brundtland Commission in 1987, the term *sustainable* has become the centerpiece of a broad movement across academic disciplines [66] and industry [67]. Although the literal meaning of the term has been retained (i.e., "the capacity to endure" [68]), it has grown to imply a broader perspective that acknowledges the interdependence of social, environmental, and economic systems. Although other perspectives on sustainability science exist (e.g., [69]), the tripartite model (social, environmental, and economic pillars) of sustainability science has continued to be been a core theme in recent years [70]. Despite this fact, sustainability research in the natural sciences and technology fields has been plagued by a lack of knowledge integration across these three disciplines [71] (technology data not shown). In the work presented in this dissertation we structure our discussion using the tripartite model of sustainability, with the explicit inclusion of performance characteristics as a core element in the design of engineered systems.

2.1.2. Approaches to Sustainability Evaluations

The IWA Operations and Maintenance specialist group has generated a list of performance indicators (addressing environmental, personnel, quality of service, etc.) for the evaluation of WWTPs [23] which has been applied by others to better characterize both the impact on receiving streams and the cost of wastewater treatment [72]. However, the methodology proposed by the specialist group was meant for the selection, measurement, and reporting of performance indicators at a fully-operational WWTP; the process of identifying or pursuing improvements at such a plant was an afterthought. Apart from this IWA document, there is a body of literature that has sought to elucidate the sustainability of a given WWTP or treatment process through the use of various criteria. In particular, life cycle impact assessment (LCA) has been widely used

to estimate environmental impacts [39, 41, 73, 74] and social criteria have been used for projects in the developing world [46, 75]. The vast majority of this work, however, has relied on the comparison of alternatives post-design, which limits researchers' ability to elucidate tensions between WWTP design and specific environmental and social impacts. In contrast, this dissertation will integrate assessment tools in such a way as to enable rapid environmental, cost, and performance evaluations of a given conceptual or detailed design, which creates opportunities to improve our understanding of how design and operational decisions (e.g., solids residence time) influence the various aspects of system sustainability.

Distinct from the LCA and social science literature, it is not surprising that significant effort has been expended in the optimization of WWTP designs with the objective of either a minimization of effluent pollutant concentrations (e.g., NH_4^+) or a minimization of cost. Very recently, however, some studies have pursued the minimization of environmental impacts [76, 77], where environmental impacts are placed in the objective function of a single- or multi-objective optimization problem. Biswas and colleagues used a multi-objective optimization methodology for WWTP process selection that included an "environmental cost" constraint, but this parameter was essentially a treatment reliability constraint (they did not evaluate environmental impacts) [78]. To date, no sustainable design methodology has been published that integrates emerging concerns for environmental and social sustainability with traditional considerations of cost and performance in such a way as to create opportunities for innovation. To do this, a comprehensive framework must be assembled that creates flexibility in design conceptualization (i.e., not impose new constraints or objective functions) while providing a structured framework for comparative assessments. This is a central objective of the sustainable design methodology developed in this dissertation, which is presented in Chapters 3-5.

2.1.3. Resource Recovery from Wastewater

As we pursue more sustainable wastewater systems, however, it is important to note that there is no single technology or process that will always be optimal: sustainability is subject to locality-specific considerations [79] that may include land availability, permit requirements, and stakeholder acceptance of WWTP unit processes and recovered resources. By first focusing on what can be recovered from wastewater (rather than what must be removed), wastewater infrastructure may begin to be described as

resource recovery systems [24]. This shift in thinking may allow wastewater management systems to not only mitigate environmental impacts and protect human health, but to also have a net benefit for the environment [80]. As we consider the need for locality-specific solutions to wastewater management, it should not be surprising that the sustainability of resource recovery from wastewater will vary from plant to plant. Wastewater is a renewable resource from which water [11, 81], energy [56, 82], and materials [37, 83-85] can be recovered [11, 35]. The most common drivers to achieve resource recovery include a local need for such resources (e.g., water reuse in Singapore [86]) or to generate revenue or offset costs (e.g., on-site energy recovery [87]). Recent LCAs typically demonstrate that resource recovery also results in net reductions in broader environmental impacts in localities where and end use for such resources exists [38].

Although it has been speculated that the use of wastewater would reduce the broader environmental impacts of phototroph-to-biodiesel production processes [88], it is unknown how phototrophic bioprocesses would influence the life cycle environmental impacts of wastewater treatment systems. Although phototrophic microorganisms may appear to have enormous potential for energy and nutrient recovery from wastewater [89], we must develop a much more thorough understanding of the performance of bioprocesses designed for this purpose before we can actually estimate the net environmental impacts of the use of phototrophs for resource recovery from wastewater. The work presented in Chapter 6 of this dissertation will help fill this knowledge gap and contribute to future assessments of the relative sustainability of this emerging technology.

2.2. Bioprocess Modeling

2.2.1. Current Approaches to Wastewater Bioprocess Modeling

The first presentation of the widely adopted International Water Association (IWA) Activated Sludge Model No. 1 (ASM1) was in 1987 [90]. Since that time the ASM series has grown to include ASM2 [91] and ASM2d [92] for the modeling of enhanced biological phosphorus removal (EBPR), and ASM3 [93] to include organic carbon storage by all heterotrophs. The ASMs are pseudo-mechanistic, deterministic models that simulate biological wastewater treatment through the characterization of specific processes (e.g., aerobic heterotrophic growth) using a set of state variables (e.g., readily biodegradable

substrate, S_S). In general, the wastewater industry relies heavily on the ASMs and they are widely applied by researchers, consultants, and utility personnel to improve treatment efficiency, design new WWTPs, and simulate process changes and upsets. A pseudo-mechanistic model for anaerobic digestion (Anaerobic Digestion Model 1, ADM1) has also been developed [94, 95] and is increasingly used. The ASMs cannot directly link with ADM1, however, because they use different state variables. A fact that presents a challenge for plant-wide modeling and that must be overcome for any new bioprocess models.

To develop plant-wide models that include both activated sludge and anaerobic digestion processes, integration techniques for ASMs and ADM1 have been developed. At present, there are three main approaches to plant-wide dynamic WWTP modeling: (1) the *interfaces* approach [96-99], (2) the *standard supermodel* approach [100, 101], and (3) the *tailored supermodel* approach [102]. A summary of these approaches can be found in Grau et al. [103]. A number of software packages are commercially available for whole-plant simulations (e.g., GPS-X™, BioWin, WEST®), taking advantage of both the *interfaces* (e.g., GPS-X™) and *supermodel* (e.g., BioWin) approaches for whole-plant modeling. Although the supermodel approach is sometimes used in practice, there are two key benefits in the use of interfaces: (i) modelers can use well-established models like the ASMs and ADM1, and (ii) new models for innovative unit processes can simply be added to an existing WWTP model with transformers (rather than having to develop an entirely new supermodel). Although developing state variable transformers (to interface between one model and another) may present challenges [103], supermodel approaches require the development of new state variables and processes which can be a significant barrier to the adoption of new models. The interfaces approach, therefore, is particularly useful in the development of new models (e.g., for phototrophic microorganisms) and their coupling with existing activated sludge and digestion models for whole-plant modeling. As such, this approach was used for the development of the phototrophic process model for stored lipids (X_{TAG}, which may be converted to X_{LI} in ADM1) and carbohydrates (X_{PG}, which may be converted to X_{SU} in ADM1) in Chapter 6 of this dissertation.

2.2.2. Lumped Sum Metabolic Models

As we consider where to begin in the development of new bioprocess models, one of the areas identified as having not received sufficient attention in wastewater modeling is the

use of lumped sum metabolic models [104]. *Lumped sum* metabolic models are distinct from *metabolic flux* models in that the latter are developed for *in silico* modeling of gene expression across an organism's genome while the former focus on inputs and outputs of metabolisms to enhance bioprocess understanding [104, 105]. In the field of wastewater treatment, lumped sum metabolic models have been particularly helpful in understanding experimental observations of competition between polyphosphate accumulating organisms (PAOs) [106-109] and glycogen accumulating organisms (GAOs) [110, 111], and in the modeling of other organisms subjected to feast/famine conditions [112, 113]. To date, however, metabolic models of phototrophic metabolisms have been limited to *flux* models [114, 115], with the intent of evaluating metabolic engineering strategies for biofuel development. In contrast, Chapter 6 of this dissertation introduces a lumped sum metabolic model for phototrophic unit processes that is consistent with current wastewater bioprocess modeling approaches. In addition to enabling its incorporation into existing WWTP simulators, this approach also enables users to add well-established chemotrophic models (e.g., ASM2d) to better understand competition and synergies among microorganisms that would likely be present in a WWTP setting.

2.2.3. Modeling Uncertainty

There are a number of sources of uncertainty in WWTP modeling that include the context (or boundary identification), inputs, parameters, and both the structure and implementation of the model itself [116]. Commonly discussed sources include influent characteristics and fractionation [117], biomass kinetic parameters [118, 119], and even biomass stoichiometry [120-122]. In an effort to account for these uncertainties, researchers commonly use methods such as Monte Carlo to determine model outputs based on a range and distribution of model inputs [48, 117, 123-126]. Among other advantages of including uncertainty analysis in design refinement is the ability to perform risk-based probabilistic design which may offer economic advantages to WWTPs by reducing capital investments while considering trade-offs such as risk of non-compliance with permit requirements [123, 125, 127]. At the very least, however, performing uncertainty analyses enables designers to more robustly characterize the likely performance of a process or treatment plant and more explicitly address specific sources of uncertainty in design [48].

Beyond process modeling and predictions of effluent quality and costs, uncertainty assessments have been limited in wastewater literature. In particular, published wastewater LCAs have seemed to rely exclusively on either (i) real data from a WWTP (e.g., [73, 128]) or (ii) a single set steady-state simulation (e.g., [129, 130]). Although sensitivity analysis is a key component of LCA, it is typically only applied to the inventory and impact assessment stages in wastewater LCAs. The application of uncertainty assessment to account for WWTP modeling uncertainties, therefore, has been severely lacking in the wastewater literature. In contrast to past wastewater LCAs, this dissertation will introduce a framework that combines state-of-the-art approaches for wastewater uncertainty assessment with LCA (Chapter 5) to better understand the broader environmental impacts of design and operations decisions.

2.3. Phototrophs as an Emerging Technology

2.3.1. A Role for Phototrophic Microorganisms in Resource Recovery

The role of phototrophic microorganisms as a resource recovery technology in wastewater management dates back to the 1950's in published literature by Oswald and colleagues [131] at the University of California, Berkeley. These researchers recommended the harvesting of phototrophic microorganisms from stabilization lagoons for anaerobic digestion [131, 132], and even experimentally investigated the coupling of phototroph production with anaerobic digestion in a completely closed system (except for light transmission into the reactor) [133]. Although these studies achieved their intended result, there was little follow-up in the academic literature in the 1960's and 1970's, and researchers were skeptical about the benefit of using phototrophic microorganisms for the generation of renewable energy (in the form of methane) because of nutrient, water, and land requirements [134]. It was clear at the time, however, that phototrophs did have the potential to provide agriculture with an appreciable supply of fertilizer, and it was hypothesized that lipid accumulation might improve the feasibility of energy recovery [135].

Advances since the work of Oswald and colleagues include (i) further investigation of algal biomass in anaerobic digesters [136-140], (ii) the use of algae in MFCs [141-143], (iii) the "revival" of the closed system concept tested by Oswald and Golueke [133] but with the inclusion of a MFC [144], and (iv) the accumulation of lipids in phototrophic microorganisms for the production of biodiesel [58, 62]. In particular, research into lipid

accumulation [145-148] and processing to biodiesel [58, 61, 62, 149] has exploded in recent years because of its potential implications for transportation-based fuels [150]. Although the production of biodiesel from phototrophic microorganisms results in life cycle environmental impacts throughout the production chain [61], the potential use of wastewater as a source of nutrients and water has been identified as an opportunity to reduce the life cycle environmental impacts of the production process [88]. Experimentation and modeling of phototrophs in this context, however, has been severely limited.

2.3.2. Organic Carbon Storage in Phototrophic Microorganisms

The key to energy recovery via phototrophic microorganisms is their ability to convert light energy and carbon dioxide (CO_2) into organic carbon. Organic carbon in a cell is largely associated with macromolecules including proteins, polysaccharides, lipids, and nucleic acids. Of particular relevance to energy recovery is the ability of phototrophic microorganisms to accumulate both lipids [146, 151] and polysaccharides [152, 153] for intracellular energy storage. Despite the advantages of polysaccharide accumulation coupled with anaerobic digestion [136], the vast majority of energy-recovery research has focused on lipid accumulation [62, 154, 155]. Among lipid-accumulation studies, most have used pure cultures of phototrophic microorganisms and synthetic algal media [145, 148, 156, 157] which have little relevance to wastewater. More recent studies have used actual wastewaters for cultivation [158], with researchers using both pure cultures (e.g., [159]) and mixed consortia (e.g., [160]) in experimentation. One of the key challenges in trying to predict the life cycle environmental impacts, performance, and cost of this technology, however, is that the vast majority of published work in this field is limited to data collection on the timescale of days (e.g., once per day [159-161] or even less frequent [162-164]). Despite the fact that researchers regularly draw conclusions about the kinetics of growth and carbon storage from such experiments – ultimately leading to speculation about the full-scale design of such processes (see examples summarized in [158]) – the lack of regard for diurnal cycles and the dynamics of growth, organic carbon storage, and organic carbon mobilization result in a severely limited understanding of the performance (and potential) of such systems. [Note: The term *dynamic* is used here to characterize a process or behavior that changes in response to changing environmental conditions (e.g., a change in growth rate as nutrients are depleted).] It is important to note that WWTPs have their own range of wastewater

compositions and (justifiably) operate using enriched rather than pure cultures. As a result, phototrophic microorganisms grown in wastewater will have to compete with heterotrophic bacteria, ammonia and nitrite oxidizing bacteria, and predators in a non-ideal nutrient stream. These complicating factors will undoubtedly impact the performance of phototrophic microorganisms and their potential for energy recovery in wastewater management – a key driver for the phototrophic process model developed as part of this dissertation (Chapter 6).

Much of the earliest research on macromolecule content in phototrophic microorganisms stems from its use as a dietary supplement in mariculture [165], the cultivation of marine organisms for food and other products. In comparisons of phytoplankton species for their nutritional value, researchers in the 1980's recognized that the dynamics of organic polymer storage in phototrophic microorganisms were both a function of species and growth phase (stationary versus exponential growth) [152]. Although the vast majority of research since that time has focused on lipid accumulation, some observations have also been related to polysaccharide accumulation. In particular, intracellular polysaccharide accumulation has been linked to nutrient-rich growth under light conditions [166] with a positive correlation with light intensity [167], and in nitrogen-deplete, lit conditions [152, 153]. Under dark conditions stored polysaccharides fuel protein synthesis and cell division [168], and their degradation has also been observed in light under nitrogen and sulfate limited conditions in cyanobacteria [166]. Beyond these observations, however, there is little known about mechanisms for enhanced polysaccharide accumulation in phototrophic microorganisms.

Courchesne and colleagues [155] classify ongoing research strategies for enhanced lipid production by phototrophic microorganisms into three categories: (i) *biochemical engineering* – manipulating environmental conditions to create physiological stress such as nutrient starvation or high salinity to channel metabolic fluxes to lipid accumulation, (ii) *genetic engineering of metabolic genes* – modifying a cell's genome to overexpress one or more key enzymes (especially rate-limiting enzymes) to channel metabolites to lipid biosynthesis in recombinant microalgal strains, or (iii) *genetic engineering of regulatory elements* – modifying a cell's genome to overexpress transcription factors regulating the metabolic pathways involved in the accumulation of target metabolites. The challenges associated with genetic engineering include the need for axenic cultures [169], the expense of gene modification, and the lack of public acceptance [170]

associated with genetically modified organisms. Biochemical engineering, on the other hand, merely takes advantage of natural characteristics of a given set of microorganisms – an approach relied upon in chemotrophic wastewater bioprocesses.

The design of wastewater treatment processes is based on the fundamental principle that we can create the physiological conditions that select for the microorganism function we desire. An example of this concept can be seen in the selection for polyphosphate accumulating organisms (PAOs) at enhanced biological phosphorus removal (EBPR) WWTPs. By first exposing mixed liquor (a solution of suspended WWTP biomass) to anaerobic, simple carbon-rich conditions and then to aerobic, carbon-limited conditions, a treatment system will enrich for PAOs because their metabolism will give them a competitive advantage over most other microorganisms (assuming appropriate solids retention time, pH, etc.). This process of enrichment allows for the cultivation of diverse communities of microorganisms that will perform a desired function and offer a level of functional redundancy that may enhance performance stability [171]. Therefore, as we consider how best to pursue enhanced intracellular carbon storage as a tool to achieve resource recovery from wastewater, it seems logical to begin with the *biochemical engineering* approach.

In the application of this approach to phototrophic microorganisms, there are three environmental conditions that are particularly relevant: (i) lit, nutrient-replete conditions under which cells grow and multiply, (ii) lit, nutrient-deplete conditions under which cells reduce their rate of division and accumulate intracellular organic carbon, and (iii) dark conditions under which cells switch to aerobic, chemoheterotrophic growth and degrade intracellular storage products. Although nitrogen limitation is the most commonly reported trigger for lipid-accumulation in phototrophic microorganisms, phosphorus and other nutrient deficiencies have also been reported to induce lipid accumulation (as have temperature, light, and salinity) [146, 154, 172]. The trade-off in subjecting cells to nutrient-limited conditions, however, is that cells decrease their rate of division (and possibly polysaccharide accumulation) which will have implications for total energy recovery and nutrient uptake [155]. As we continue to investigate the potential for phototrophic microorganisms as a resource recovery technology in wastewater treatment, it is vital that we consider the role cell physiology will play in intracellular lipid and polysaccharide storage and nitrogen and phosphorus assimilation.

2.3.3. Modeling Phototrophic Microorganisms

The study of phototrophic microorganisms has a long history that has stemmed from concerns of harmful blooms in marine [173] and freshwater [174] aquatic environments. In particular, there has been extensive research surrounding the environmental conditions that promote harmful blooms (e.g., [175, 176]). Seemingly separate from these studies has been the pursuit of engineered systems that use phototrophs. In the wastewater industry, the use of phototrophic microorganisms has principally been in waste stabilization lagoons – facultative systems (containing both aerobic and anaerobic zones) that have been traditionally designed based on empirical considerations [59]. In addition to the treatment of raw sewage and primary effluent, phototrophs have also been used in tertiary treatment to either inactivate pathogenic organisms (e.g., in maturation ponds) [177] or to achieve nutrient polishing (often, but not exclusively, using biofilm-based systems) [178-180]. One barrier to innovation in these systems, however, has been their apparent simplicity. Lagoons and ponds are often presented as low-cost, low-tech, low-maintenance options (as compared to activated sludge systems) – so why add complexity to a system whose advantage is simplicity? Additional challenges to the development of wastewater treatment models for lagoon- and pond-based systems are that (i) they are often unmixed and (ii) light presents a unique challenge because it cannot be mixed. As a result, spatial differences in nutrient concentrations, temperature, light intensity, etc., add enough complexity and variability from locality-to-locality to deter modeling efforts. Therefore, one challenge we face in developing innovative phototroph-based wastewater treatment systems is a lack of well-proven, widely-adopted phototrophic wastewater process models to predict system performance.

Recent advances in the modeling of phototroph-bacterial wastewater treatment systems include the development of mechanistic models for high rate algal ponds (which have a shallow raceway design) [181], for chemostats treating inhibitory pollutants [182], and for biofilms achieving secondary effluent polishing [183]. Of particular interest are the models of Wolf et al. [183] and Jupsin et al. [181] which have been developed for wastewater-related systems and calibrated using experimental data with mixed-microbial communities. In particular, the Wolf kinetic and metabolic model (termed PHOBIA) is of interest because it includes processes for the production of extracellular polymeric substance (EPS) and internally stored polyglucose by phototrophs [184]. Much like ASM3 [93] for heterotrophs, the PHOBIA model assumes that phototrophs grow on

stored polyglucose. Divergent from the ASM3, however, is the assumption that this only occurs in the dark. Due to the absence of information on the kinetics of polyglucose storage, Wolf and colleagues assumed the rate of storage was directly coupled to growth rate. This was handled by multiplying growth rate by a fixed factor to get the rate of polyglucose storage or EPS production. The justification for this assumption was attributed to work by Neu and Lawrence [185], who microscopically identified EPS formation in a biofilm with river water inocula, and the work of Horn et al. [186], who examined only EPS dynamics in a heterotrophic bacterial community. Neither of these studies, however, investigated the dynamics of intracellular carbon storage or the formation of EPS by phototrophic microorganisms. Wolf and colleagues acknowledged that the lack of data related to internal carbon storage and EPS formation was a challenge for phototrophic models, and took the approach of using ranges of factors to better understand the sensitivity of the PHOBIA model to rates of EPS and polyglucose formation [183]. The selected range for EPS was not justified, and the range for internal carbon storage was based on a phototrophic bacterial reference [187] and a study on poly-beta-hydroxybutyrate storage by WWTP mixed liquors [188].

As we consider the use of phototrophic microorganisms as an energy recovery technology (in addition to a unit process for wastewater treatment), intracellular organic carbon storage (as lipids or polysaccharides) will be an important factor that must be considered. This preliminary inclusion of the organic polymers EPS and polyglucose in the PHOBIA mechanistic model, therefore, provides an excellent starting point, as does experience with PAO storage polymers in ASM2d [92]. What we still lack, however, is a wastewater process model that includes independent processes for intracellular carbon storage as lipids and polysaccharides such that the potential use of phototrophic microorganisms as an energy feedstock for biodiesel or methane can be evaluated; a need we seek to address in this dissertation (Chapter 6).

Chapter 3
A New Planning and Design Paradigm to Achieve Sustainable Resource Recovery from Wastewater

3.1 Introduction

Water and wastewater system decisions have been traditionally driven by considerations of function, safety, and cost-benefit analysis. The emphasis on costs and benefits would be acceptable if all relevant factors could be included in the analysis, but unfortunately many relevant factors are routinely excluded. Coupled with failures to fully engage the public in decision-making processes, this can impede progress toward achieving sustainable solutions. Ignoring broader social issues that impact the adoption of sustainable solutions prolongs not only global environmental and ecological problems, but also unjust public health and social conditions in the developing world.

Within the water and wastewater management industry, discussions of sustainable development have often focused on water stress [20, 189]: a hazard that is exacerbated by other global stressors such as climate change, demographic and land use changes, increasing population, and urbanization [20]. In addition to water stress, water and wastewater management practices contribute to nutrient imbalances and a host of environmental detriments such as eutrophication [190], discharge of pharmaceuticals and other emerging contaminants [191], and a loss of biodiversity in receiving streams [192]. Efforts to address these issues across regional and global scales are hindered by the historical disconnect between the water quality and water quantity factions of the

water profession. Although our understanding of sustainability is constantly evolving, the water and wastewater design process retains its foundation in engineering traditions established in the early 20th century [11]. As we chart a path in the 21st century, we contend that wastewater contains resources worthy of recovering and that the development of technologies, practices, and policies that enable cost effective recovery will have broad geopolitical implications.

The primary problem we face is not the availability of technology for resource recovery, but the lack of a socio-technological design methodology to identify and deploy the most sustainable solution in a given geographic and cultural context. We acknowledge that the most sustainable solution may not result in maximum, or any, recovery of resources from wastewater. Instead a sustainable water and wastewater decision-making process considers environmental, economic, and social ramifications of decisions across spatial and temporal scales to achieve the best balance identified by the project stakeholders. A central element of sustainability is that *stakeholders* are defined broadly to include utility managers, operators, regulators, local government officials, end-users, public interest groups, and other parties impacted by the project. The objective of this paper is to identify elements of such a decision-making methodology that can provide all stakeholders with the tools needed to advance sustainability, as well as to suggest a set of guiding principles for resource recovery systems in the water industry.

3.2 Wastewater as a Renewable Resource

Sustainability demands that we acknowledge wastewater as a renewable resource from which water [193], materials (e.g., fertilizers [37], bioplastics [84]), and energy [193]) can be recovered. By shifting away from today's paradigm, which focuses on what must be *removed* from wastewater, to a new paradigm focusing on what can be *recovered*, sanitation systems may begin to be described as resource recovery systems (RRS) – a conceptual transformation that could allow the perceived impact of wastewater on communities to become a net positive [192].

Water recovery. Water reclamation and reuse (or water recycling) can provide additional water resources in water stressed areas. Successful examples include the Orange County Water District (California, U.S.) and the Upper Occoquan Sewage Authority (Virginia, U.S.), which have each been achieving indirect potable reuse for over

30 years. A large "systems-level" example of reuse can be seen in Singapore's "four national taps" strategy. That island nation has a diverse water portfolio which includes 1) imported water from Malaysia, 2) local water supplies, 3) desalination, and 4) indirect potable reuse of reclaimed water (NEWater). In fact, with the opening of the Changi plant in 2010, NEWater will meet 30% of Singapore's drinking water demand [194]. A successful example of *direct* potable reuse is found in Windhoek, Namibia, where water resources are particularly sparse [195].

Energy recovery. The most common form of energy recovery from wastewater is methane (CH_4)-containing biogas produced during the anaerobic treatment of wastewater and the digestion of solids collected and generated. Anaerobic reactors are in use throughout the world, producing CH_4 that can 1) be combusted on-site for heat or electricity generation, 2) be cleaned and sold to a local natural gas provider, or 3) be cleaned and used as fuel for vehicles. Other examples of wastewater energy recovery include microbial fuel cells [196] and the extraction of latent heat for buildings' heating and cooling [82].

Material recovery. The use of biosolids as a fertilizer is a well-documented application that is becoming increasingly common in the U.S. [197] and U.K. [198]. There have also been recent developments in the harvesting of struvite ($MgNH_4PO_4$) from solids treatment processes [199] as well as the recovery of nutrients from source-separated urine [37]. For instance a significant portion of the vegetables consumed in Kampala, Uganda, are produced in backyard gardens using storage-sterilized, source-separated urine [200].

Resource recovery systems (RRS). Water, energy, and materials recovery from wastewater can all be achieved with existing technologies, and new technological approaches are on the horizon [11]. Despite such advances, our observation is that wastewater systems contribute to a greater proportion of negative impact on regional hydrological cycles than on energy and materials consumption. Indeed, is the recent, heavy focus by the water industry on energy sustainability *causing us to miss the major point of water sustainability?* We propose a reorientation of (stakeholders') thinking towards addressing the impact of wastewater technologies on regional and global hydrological cycles first, then assess whether these approaches are negatively impacting global energy, climate, and/or material(s) sustainability. By utilizing this

approach, our planning and design processes will evolve toward applying available technologies that have the maximal benefit for regional and global goals for water resource quality and availability, while simultaneously reducing negative impacts on other aspects of sustainability when possible. Note that although an RRS may not include energy or material recovery in a specific instance, what matters most is that decisions in the water industry do not significantly impede regional or global action plans for energy and/or material sustainability (which are unlikely to include the water industry to a significant degree in the foreseeable future). Once we understand which technologies best contribute to sustainability from this regional and global perspective, we must strive to learn how best to implement these technologies in a manner that is socially acceptable from the local perspective.

Barriers to the successful implementation of RRS. Given the availability of technologies to recover resources from wastewater, *why don't we use them more often*? Reasons include a lack of agreed upon sustainability goals and targets (see [201]) and the absence of a holistic design methodology capable of including sociological factors. The importance of sociological factors is illustrated by San Diego (U.S.) [202], a coastal city with a semi-arid climate and population >1.3 million. The city relies on the importation of water a distance of 390 and 715 km from the Colorado River and Sacramento-San Joaquin Delta, respectively. In recent years, imported water (containing discharge from over 200 wastewater treatment plants) has constituted up to 90% of San Diego's water supply. To provide more water from local sources, two reclamation plants were constructed with the capacity to recycle just over 25% of the local water demand. In an attempt to encourage reuse, the U.S. EPA mandated that one of the plants would operate at 75% capacity and produce water for non-potable reuse. However, public rejection of the plan has resulted in returning 73% of the water produced by this plant to the sewer for treatment at the local wastewater treatment plant before discharge to the ocean. Despite having technology *in place* to recover a major fraction of wastewater, the failure to simply use it demonstrates the need to include social sustainability factors in the planning and design process.

The San Diego example teaches us that there is more to sustainability than economics and process performance. Public and political pressures coupled with opposition from the media have significantly restricted the use of reclaimed water [203] and not just in San Diego: also Toowoomba, Australia [40], and the California locales of San Ramon-

Dublin [204] and Los Angeles [204]. The reclamation of water is a volatile issue that challenges cultural and historical notions of water, resulting in perceived risks that engineers and scientists often believe to be unjustified [40, 205]. In order to engage successfully with the public it is important that engineers and decision makers understand the socio-political context of stakeholders' existence [206] including: forms of relevant experience, past relations with expert and decision-making bodies, and the distinctive forms and styles through which diverse publics make sense of expert knowledge – concerns nicely captured by Jasanoff's notion of *civic epistemology* [207]. Beyond the challenge of understanding civic epistemology, additional barriers to the advancement of water and wastewater systems may include the lack of political will [44, 208] and the absence of an enabling environment (policies, legislative frameworks, financing, and modes of public discourse) [44, 206, 209].

To date, the water industry has been poorly equipped to address factors outside of the traditional engineering scope. We believe that this can be traced to the long standing and narrowly defined approaches that are used to train water industry professionals. This shortcoming – as well as the institutional compartmentalization that impedes integrated water resource management [11, 210] – must be remedied to make progress in developing and deploying sustainable water management strategies.

3.3 The Pursuit of Sustainability in Water Management

Since sustainability does not exist at a single project level, our overall goal must be to harmonize RRS design at the local level with the goal of *global* sustainability. Guiding principles at the local level that impact the global sustainability goals of the water industry are provided in Table A1 in Appendix A. Following all these principles simultaneously is usually impossible in a given project and therefore we require context-specific assessment techniques to evaluate alternatives and a means to resolve tradeoffs among them. Representative methods to evaluate project alternatives from the sustainability perspective are described in the following paragraphs.

Environmental and ecological assessment. Life cycle assessment (LCA) is a tool traditionally used to elucidate the environmental and ecological impacts of products or processes throughout their life cycle. For instance, Sydney Water (Australia) in collaboration with the University of New South Wales produced a comprehensive LCA of

their integrated water and wastewater infrastructure to forecast environmental and ecological impacts through the year 2021 [73]. While this approach provides guidance on the impact of specific emissions expected from design choices, it can only serve as an input to a broader stakeholder decision-making process which must resolve the tradeoffs that inevitably emerge: 1) between different environmental and ecological impacts, 2) across spatial and temporal scales, and 3) across the categories of guiding principles listed in Table A1 that also include considerations of economics, societal acceptance and equity, and functional performance.

Economic assessment. Life cycle costing (LCC) can start to address the economic dimension of sustainability by estimating capital, operational, and maintenance costs, as well as costs from upstream and downstream processes [49]. The absence of LCC approaches has led to implementation failures in both industrialized [211] and developing countries [212]. Although LCC could improve the economic sustainability of a given project, neither it nor other economic assessment techniques are appropriate for the evaluation of other sustainability dimensions. Recent progress has been made in the use of environmental valuation – a tool that monetizes environmental and ecological impacts – but the monetization of externalities (including social impacts such as morbidity and mortality effects) has met with a number of criticisms (see [213]). Ultimately, if the objective of the assessment is to evaluate a project's sustainability characteristics, the monetization of nonmarket impacts is inappropriate since it forces a value mapping by the decision makers which, even if it could be done 'correctly', eliminates the independence of environmental and social dimension bases; an outcome that is contrary to the sustainable development principle of balancing considerations across all three categories [214]. Instead LCC should be used along with other assessment tools such as LCA for the environmental and ecological dimensions, and new tools should be developed to help assess the social dimension(s) [215].

Social assessment. Ideally social dimensions could be included in an LCA framework but this has proven difficult [214]. One of the great challenges associated with social life cycle evaluations is the existence of several hundred indicators [216]. Although risk assessments have been used to quantify potential impacts on public health, few methods have been developed for the water industry to incorporate a broader set of social indicators into the planning and design process (e.g., those listed in Table A1).

Recent work includes that of Hunkeler [216] using employment as a mid-point variable and Ashley et al. evaluating stakeholder perception and understanding [52].

Resolving tradeoffs in decision-making. After the assessment of project alternatives in each dimension of sustainability, decision makers must resolve the tradeoffs that will inevitably exist. One tool that can provide a framework for comparative sustainability assessments is multi-criteria decision analysis (MCDA): a class of formal approaches to decision-making that allow stakeholders to take explicit account of multiple criteria [217]. Of particular value to sustainability decision-making is MCDA's ability to resolve tradeoffs among qualitative and quantitative metrics, and for the process to evolve as stakeholder preferences are articulated [217].

Stakeholder participation is a vital component of sustainability that has not been universally applied in the planning and design of water systems [218]. The importance of appropriately-timed stakeholder participation in decision-making is not unique to the water industry and has been acknowledged as a key component of socio-technological planning and design methodologies in natural resource management [217] and sustainability projects [70].

Box 1: Decision-making in a developing world context

In a development setting, beneficiaries are often poor and reside in under-developed communities. The word *project* encompasses more than the physical structure that is designed and constructed. Projects must account for the local social and cultural setting and include input from the people who will ultimately operate, manage, and benefit from the whole endeavor [219]. Therefore project designers must establish the appropriate ownership, skills, and management capacity to support the effort while at the same time designing the physical structure. In addition to environmental and economic sustainability elements, designers should consider the following social factors: socio-cultural respect, community participation, gender roles, and political cohesion [46].

3.4 Challenges and the Path Forward

As we pursue a more sustainable water industry, management strategies must evolve to address the broad set of challenges listed in Table A2 in Appendix A. Our water systems must become integrated RRS that 1) match water supply with demand (both in

location and level of treatment), 2) enable the efficient recovery of resources, and 3) acknowledge the significance of environmental, economic, and social aspects of sustainability throughout the planning and design process.

Stakeholder participation in planning and design. The successful implementation of more sustainable solutions requires that the social dimension of technology be acknowledged via both assessment techniques [52, 70] and participatory planning [40, 52, 70, 218]. Through the respectful inclusion of stakeholders in the decision-making process, project managers can facilitate positive social learning, minimize and resolve conflicts, elicit and use local knowledge, and achieve greater public and stakeholder acceptance of water management decisions [218]. The sustained participation of stakeholders can be achieved through regular workshops that are designed to facilitate meaningful contributions and build trust among participants (Figure 3.1).

A more thorough discussion of stakeholder participation in water industry projects may be found elsewhere [52, 206, 217, 218]. These articles discuss the importance of community values and mechanisms for their inclusion in planning and design. The next step is for these approaches to be extended to RRS in pursuit of sustainable water systems as a critical element of global sustainability.

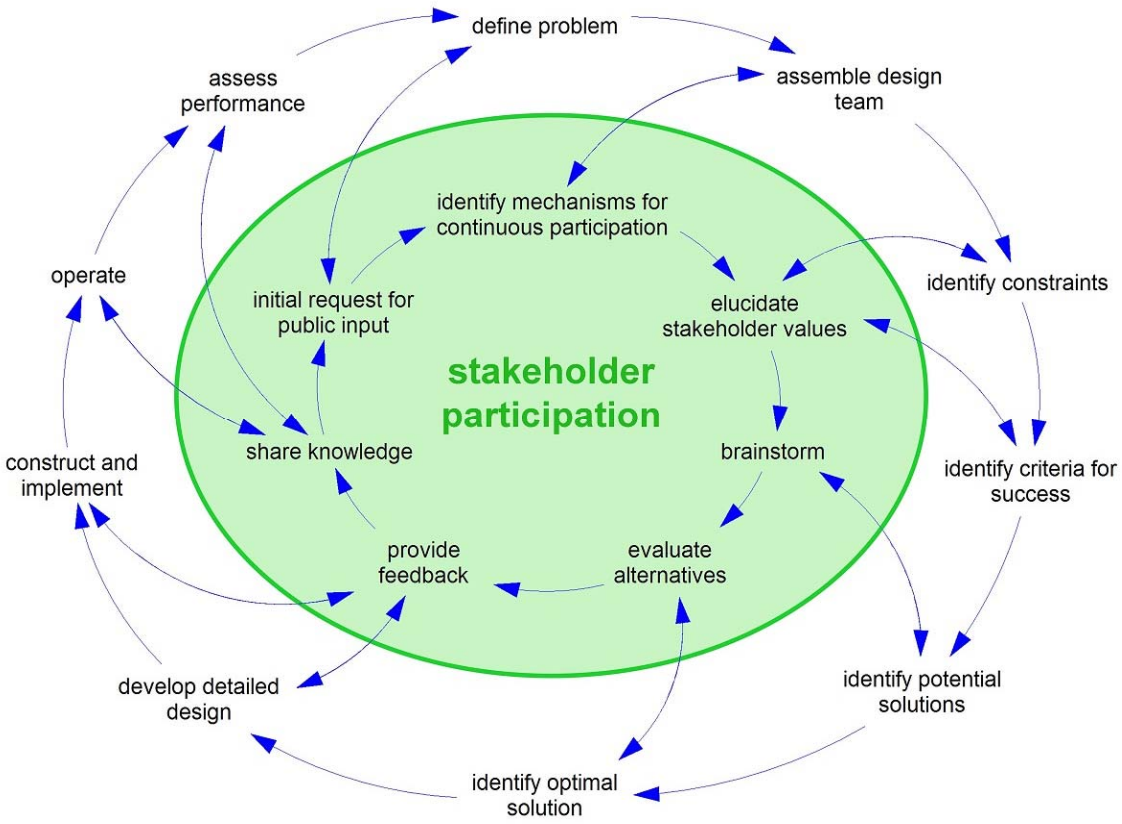

Figure 3.1. A recommended planning and design process that connects engineering (outer loop) with sustained stakeholder participation (inner loop). Double-headed arrows connecting the technical design process with stakeholder participation represent workshops held throughout the planning and design of a water system. This depiction bears resemblance to the *Framework for Environmental Health Risk Management* [220] in that the technical decision-making process relies on stakeholder participation throughout.

The transition toward sustainability. For over 100 years, drinking water and wastewater treatment have existed for the protection of human health. Although successful, we now rely on infrastructure and management strategies that are not sustainable in the 21st century. Envisioning wastewater as a renewable resource offers exciting opportunities for the water industry to contribute to global sustainability through the recovery of water, energy, and materials. Achieving this objective will require coordination and cooperation among the different sectors of water and wastewater management to set achievable sustainability targets for the water industry.

After the identification of industry-wide targets, a research and implementation strategy will be necessary to identify and support their pursuit, recognizing that water recovery

may be the most important strategic focus due to the disproportionate impact of water and wastewater systems on the sustainability of water resources (as compared to energy and materials resources). Next, place-based definitions of sustainability will need to be developed using a socio-technological planning and design methodology. Finally, through both industry-wide leadership and locality-based initiatives, it will then become possible to identify the best practices that promote sustainable resource recovery systems in water and wastewater management.

This will not be a "one size fits all" endeavor. Methods for evaluating the sustainability of alternatives in a local (or place-based) context are needed, along with an inherently subjective process for resolving tradeoffs across spatial scales, temporal scales, and sustainability dimensions (social, environmental, and economic). Furthermore, the pursuit of sustainable systems must not take place in a vacuum between only experts. The planning and design process will require collaboration across stakeholder sectors building on the expertise of a broad set of disciplines. The importance of undertaking this challenge cannot be understated. As the water industry discovers new technological solutions contributing to environmental protection, public health, and global sustainability, it must recognize that these solutions will not be adopted unless greater attention is given to stakeholder interests as a central element of a sustainable planning and design paradigm.

3.5 Acknowledgements

The authors acknowledge financial support from the Graham Environmental Sustainability Institute at the University of Michigan which facilitated a workshop on this topic and provided partial funding for the lead author. We thank the anonymous reviewers of this manuscript for their constructive comments.

3.6 Author Biographical Statement

Jeremy S. Guest is a Ph.D. student in the Civil and Environmental Engineering Department at the University of Michigan, and a graduate fellow of the Graham Environmental Sustainability Institute. Steven J. Skerlos is an associate professor of Mechanical Engineering at the University of Michigan. James L. Barnard is the global practice & technology leader for advanced biological treatment at Black and Veatch

Corporation. M. Bruce Beck is a professor and eminent scholar in the Warnell School of Forestry and Natural Resources at the University of Georgia. Glen T. Daigger is the senior vice president and chief wastewater process engineer at CH2M HILL. Helene Hilger is an associate professor of Civil and Environmental Engineering at the University of North Carolina at Charlotte. Steven J. Jackson is an assistant professor at the School of Information at the University of Michigan. Karen Karvazy is a senior project manager at Chastain-Skillman, Inc. Linda Kelly is the managing director of public communication for the Water Environment Federation. Linda Macpherson is a reuse principal technologist at CH2M HILL. James R. Mihelcic is a professor of Civil and Environmental Engineering at the University of South Florida. Amit Pramanik is a senior program director at the Water Environment Research Foundation. Lutgarde Raskin is a professor of Civil and Environmental Engineering at the University of Michigan. Mark C. M. van Loosdrecht is a professor of environmental biotechnology at Delft University of Technology and the scientific director Asellus at KWR Water Cycle Research Institute. Daniel Yeh is an assistant professor of Civil and Environmental Engineering at the University of South Florida. Nancy G. Love is a professor and chair of Civil and Environmental Engineering at the University of Michigan. Please address correspondence regarding this article to nglove@umich.edu.

Chapter 4
The Use of Qualitative System Dynamics to Identify Sustainability Characteristics of Decentralized Wastewater Management Alternatives

Reprinted from Guest, J. S.; Skerlos, S. J.; Daigger, G. T.; Corbett, J. R. E.; Love, N. G., The use of qualitative system dynamics to identify sustainability characteristics of decentralized wastewater management alternatives. *Water Sci. Technol.* **2010,** *61*, (6), 1637-1644., with permission from the copyright holders, IWA Publishing.

4.1. Introduction

With an aging infrastructure and increasingly stringent nutrient removal requirements, decentralized wastewater treatment systems have the potential to be cost-effective solutions in the 21st century [221]. Beyond simple economics, however, it has been widely recognized that decentralized systems have the potential to be a more efficient and sustainable approach to wastewater treatment [222]. A key advantage of decentralized treatment is the potential for the source-separation of waste streams – a management strategy that offers exciting opportunities for the recovery of resources from wastewater including nutrients, energy, and water [37, 222].

Although technologies and processes for decentralized treatment and the recovery of resources from wastewater are available, the lack of a comprehensive planning and design methodology incorporating sociological factors has left innovative wastewater projects susceptible to failure (e.g., water reuse in San Diego as discussed elsewhere [24]). In order to facilitate the implementation of decentralized wastewater treatment systems, we must develop planning and design tools that can address a broader set of factors (e.g., social and institutional barriers [223]) and account for the dynamic interactions among the many variables influencing system sustainability. To this end, we will discuss the use of qualitative system dynamics and complementary quantitative tools for practitioners to identify and better understand interactions among different aspects of

sustainability during the planning and design of decentralized wastewater treatment systems. This paper will discuss the hypothetical application of these qualitative tools in the context of an ongoing sanitation infrastructure upgrade in the Capital Regional District, Canada.

4.2. Sustainability Metrics in Wastewater Management

To facilitate the adoption of more sustainable wastewater management strategies, a set of *guiding principles* for water and wastewater systems has been proposed (see Guest et al. [24] for a discussion in the context of a broad body of literature). These guiding principles are general and do not apply contextually at the functional level of wastewater management decisions: the project-level. This is important since a locality's set of physical and social considerations may be unique and therefore there is always a need to contextualize and balance global sustainability objectives so that they are tangible to the stakeholders. Furthermore, a need to balance competing sustainability objectives (e.g., economic, environmental, social) always exists at a project-level.

4.2.1. The Triple Bottom Line

Often, the incorporation of sustainability in engineering decision-making has taken the form of the *Triple Bottom Line* (TBL). The TBL identifies three categories of criteria that must be considered in decision-making: economic, environmental, and social. The TBL may also be known as profit/planet/people or economy/ecology/equity. No matter how it is referred to, it simply suggests that criteria from each of the three categories have been identified and considered in the final decision. These criteria may be in the form of qualitative or quantitative metrics and are discussed in the following paragraphs.

Economic Metrics. Economic metrics are typically the easiest to quantify. Standard to every project are capital, operational, and maintenance costs. Life cycle costing (LCC) is a methodology that seeks to further develop decision makers' understanding of cost comparisons among alternatives by elucidating cost drivers and identifying cost tradeoffs in the life cycle of a project [49]. When considering infrastructure upgrades, it has also been recommended that comparisons be made not in terms of average costs, but in terms of incremental costs [11]. Incremental costs, in this context, have been defined as the cost difference between the alternative under consideration and the cost that will be avoided if the alternative is selected.

Economists may also contend that methods such as contingent valuation (a survey-based method for the monetization of externalities) are appropriate for evaluating environmental or ecological impacts and may provide insight for policy makers [224]. However, the elimination of independent evaluation tools for the environmental or social dimensions of sustainability is contrary to the sustainable development principle of balancing considerations across all three categories and the monetization of ecological and certain social externalities has received significant criticism (e.g., [225]).

Environmental/Ecological Metrics. A number of environmental and ecological metrics have been developed to compare one product or process to another. The terms *environmental* and *ecological* are often used interchangeably to include consideration of air, soil, water, and non-human life. Although a distinction between the two will be made in the causal loop diagram below (ecology will specifically include criteria related to the interaction of non-human organisms and their environment), combined they form one category of the traditional TBL. Environmental/ecological metrics have benefited greatly from the development of life cycle assessment (LCA), a methodology to determine the environmental impacts of a product or process across its life cycle.

LCA metrics utilized in the wastewater literature (e.g., [73]) may fall into one of two categories: inventory-based or impact-based. Inventory is one of the steps of LCA, and is essentially an accounting process to quantify the inputs to (e.g., energy and natural resources) and outputs from (e.g., emissions to air and water) a process across its life cycle. Impact-based metrics, on the other hand, predict an environmental or ecological impact that would result (based on characterization factors) from the inputs or outputs identified during the inventory stage (e.g., global warming potential). Although inventory-based metrics offer the advantage of source-number transparency and the removal of characterization-based biases, their repercussions may be more difficult to understand (e.g., what does 1 kg of aquatic cadmium emissions really mean?). Impact-based metrics, however, may present data in more relatable terms (e.g., potential human health impacts), but they lack the transparency of inventory-based metrics and their uncertainties are much larger. Both types are acceptable, but users should be aware of the advantages and disadvantages of the metrics they use.

Social Metrics. Although metrics related to human safety and health (e.g., risk assessments) are relatively well-developed, other human aspects of engineering

projects are often overlooked. Social considerations related to institutional governance (e.g., permitting structure, utility structure) may be included in the decision-making process [223], but less common is the incorporation of cognitive or normative aspects of the human dimension [226]. Examples of social metrics include political cohesion, employment, and public awareness and understanding. These types of metrics are more commonly applied in the developing world [75], and may lack explicit definition in developed world projects.

Directly related to social metrics is the process by which they are incorporated into the planning and design of a wastewater system. In order to earnestly pursue social sustainability, it is vital that appropriately timed stakeholder participation be achieved [223]. Although this participatory planning process is a means rather than an end, it is a component of planning and design that must be considered in evaluating the sustainability of a wastewater management strategy [24, 52].

4.2.2. Beyond the Triple Bottom Line

Functional Metrics. The need for a broader set of functional metrics is becoming increasingly apparent as we try to design systems that are able to manage changing human (e.g., population, settlement patterns), environmental (e.g., water availability, climate stability), and engineered (e.g., mixed versus source-separated waste streams) parameters without having to completely replace infrastructure [227]. Examples of functional metrics include adaptability, flexibility, robustness, resilience, reliability, and manageability: concepts which have been discussed thoroughly in the context of socio-ecological systems [228]. Some of these metrics may also be included in other categories of the TBL. For instance, metrics such as adaptability or flexibility of a wastewater management alternative may also be classified as economic concerns (by projecting the likelihood of potential expenses to adapt the system), but including a fourth category may help direct attention to functional metrics that can identify differences among alternatives that may be obscured if only metrics that fit into the TBL are utilized.

4.3. Qualitative Tools for Planning and Design

In order to comparatively evaluate wastewater management alternatives using the sustainability metrics identified above, decision makers must understand the

interconnectedness of various criteria and have a means to predict how a given decision will influence each aspect of sustainability (economic, environmental/ecological, social, functional). Decision makers must also gain an understanding of stakeholder preferences through a participatory planning process designed to elucidate stakeholder values. Challenges associated with these tasks include the need to cope with subjective information and uncertainty in the decision-making process. We begin here with a description of tools that can help elucidate stakeholder values and find ways to plan, design, and implement projects that simultaneously meet broader sustainability objectives.

4.3.1. Force Field Diagrams

A force field diagram is a simple, graphical way to characterize the factors influencing a decision. It does not offer specific solutions, but it identifies a list of items that must be considered [11]. This representation has been used to help stakeholders identify potential barriers to project success (i.e., restraining forces), and provides a foundation for more complex and dynamic diagrams. It also provides some direction for addressing implementation barriers, as it is usually expected that removing restraining forces is a more effective approach than bolstering advancing forces (i.e., factors that are pushing the project forward).

To demonstrate the concept of a force field diagram, here we interpret an on-going project in the Capital Regional District (CRD), Canada. The CRD is transitioning from the discharge of screened wastewater to the marine environment to a comprehensive wastewater management process – including secondary treatment, biosolids management, and resource recovery– and is considering a range of alternatives in the continuum between “centralized” and “decentralized” infrastructure. The layout in Figure 4.1 is a preliminary example of a force field diagram for the identification of forces influencing the decision of whether or not to implement decentralized wastewater management.

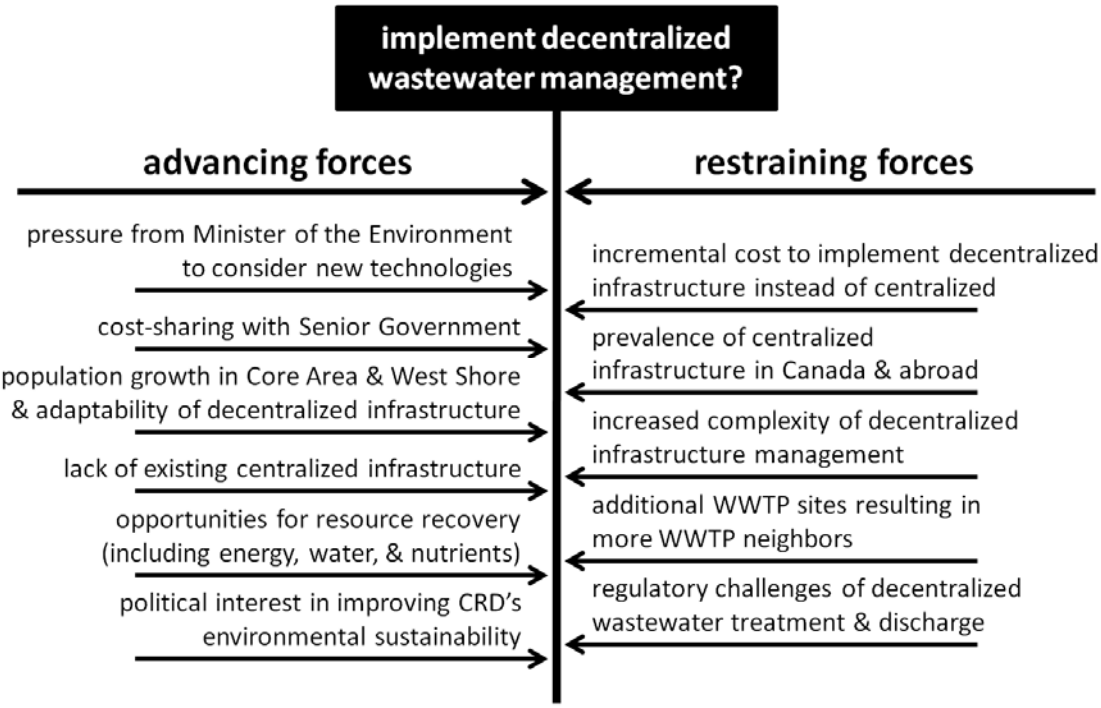

Figure 4.1. A hypothetical force field diagram with advancing and restraining forces related to the selection of decentralized wastewater management as part of the CRD planning and design process for liquid stream management. This diagram was generated by the authors based on personal observations and reports collected from the project website [229].

One shortcoming of force field diagrams is that they do not illustrate the interactions among restraining and advancing forces, and instead give the impression that if each restraining force is removed the proposed system will be successful. Another shortcoming is that force field diagrams do not on their own advance sustainability factors but rather consider advancing and restraining factors with respect to proposed project decisions – regardless of their sustainability. In other words, if the question being asked is tangential to sustainability, or biased towards a specific aspect of the TBL or beyond, then the approach itself does not necessarily promote sustainable solutions.

4.3.2. Causal Loop Diagrams

The forces or factors influencing a project can be viewed in the context of the broader, non-linear system through the use of qualitative system dynamics. Qualitative system dynamics uses causal loop diagrams (CLDs) for the visualization of feedback thinking, providing users with the ability to identify potential unintended consequences of their decisions [230]. CLDs are a core tool in systems thinking [231] and may facilitate

participatory diagramming – a valuable component in the growing application of systems thinking to water management [232]. To demonstrate this tool, a hypothetical CLD has been created (Figure 4.2) based on our interpretation of the CRD project. Although the relationships identified in Figure 4.2 may be intuitive, there are many complex interactions that are easily overlooked without the development of a diagram that specifically illustrates the dynamic relationships among factors.

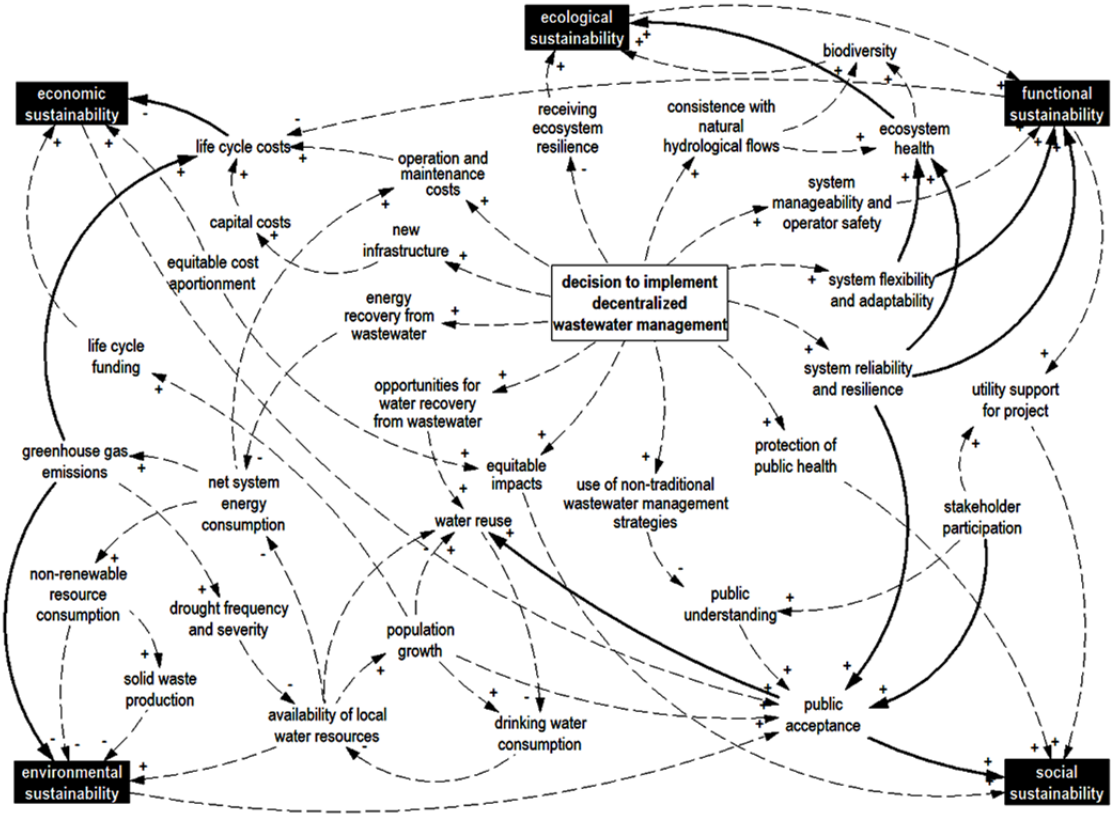

Figure 4.2. A hypothetical CLD illustrating the impact on each sustainability *stock* for a utility switching from the marine discharge of screened wastewater to a decentralized wastewater management system. A "+" at the head of an arrow indicates that the variable at the tail end causes a change in the variable at the arrow head in the same direction. A "-" indicates a change in the opposite direction. The arrows in this figure are not comprehensive, but represent a preliminary set of relationships worthy of discussion. Arrows discussed in the text are bold. This diagram was generated by the authors based on personal observations and reports collected from the project website [229].

In Figure 4.2, the four sustainability categories (economic, environmental/ecological, social, and functional) are represented as five qualitative *stock variables* – entities that may improve or diminish depending upon the factors influencing them (environmental and ecological stocks have been separated to distinguish between the two). By

evaluating infrastructure alternatives in this way, decision makers can track the impact of a given wastewater management strategy through the loops and improve their understanding of how it will influence each category of sustainability. For example, how will the decision to implement decentralized wastewater management impact economic sustainability? The capital costs and projected operation and maintenance costs will always be quantified, but greenhouse gas (GHG) emissions may only be thought of as a criterion for environmental sustainability. As Figure 4.2 illustrates, however, GHG emissions may influence the life cycle costs of the project, particularly if these emissions become taxed or capped. Beyond this however, Figure 4.2 reminds us that the emission of GHGs may contribute to changes in the local water cycle that include the reduced availability of quality water or increased sensitivity of receiving waters. The selection of a management strategy that reduces GHG emissions, therefore, would reduce the likelihood that a utility would incur these additional costs. Further, recognizing that climate change might alter the assumptions driving the design, an emphasis on infrastructure resilience and adaptability may support solutions that simultaneously improve ecological sustainability as well as functional sustainability.

The CLD also highlights other considerations that are of contemporary interest beyond economic and environmental sustainability. For instance, the importance of stakeholder participation and public understanding are aspects of social sustainability that are clearly related to functional sustainability (Figure 4.2). Specifically, the influence of system reliability and resilience on public acceptance is unique in that the impact of the former on the latter transcends the specific project and may be tied to public awareness of past successes or failures. To draw a parallel, we can consider the implementation of decentralized “package” wastewater treatment plants in the 1970’s designed to enable high-density lot development. These systems often failed due to a lack of an operational and maintenance support system, contributing to the negative impression many designers had of decentralized wastewater management. Although it is clear from Figure 4.2 that many aspects of decentralized wastewater management will move sustainability stocks in the right direction, it is important to note that system performance will influence stocks beyond functional sustainability. Projects implemented in a less than perfect manner can negatively influence social sustainability because of their impact on cognitive [233] and affective [234] aspects of decision-making – factors that

have been identified by others to play a significant role in social learning and both individual and collective decision-making [226].

4.4. The Pursuit of Sustainability By Way of Transparency

With over one hundred definitions of sustainability having been proposed, it is clear that the concept can be challenging to articulate. In order to orchestrate an inclusive and successful planning and design process, it is vital that both qualitative and quantitative tools be used to enhance the transparency of comparisons being made. In particular, stakeholders must understand the metrics used and how they fit into the context of sustainability as it pertains to their wastewater infrastructure project.

4.4.1. The Use of Qualitative Tools to Understand the Broader Context

As discussed above, examples of quantitative tools include LCA, LCC, and risk assessment. By using qualitative tools to put quantitative outputs into a broader context, practitioners can greatly enhance the transparency of the decision-making process. By developing a project-specific CLD, stakeholders can identify causal loops that are of particular importance to them and can identify barriers to project success. This method of interactive modeling has had success in increasing public understanding of the value of water conservation in Las Vegas (United States), where a CLD and quantitative model were used to illustrate the system dynamics of residential water consumption to a public audience [235]. This model only quantified factors influencing water consumption (e.g., per capita water use and population), but was found to stimulate discussion among stakeholders and "help build the consensus and support resource managers need[ed] to implement their decisions" [235]. The benefits of interactive modeling is not unique to water projects, and similar results have been observed with the use of interactive "dialogue mapping" as discussed by Conklin [236].

Although there are many relationships among sustainability system variables that we, at present, have no means of quantifying (e.g., the impact of stakeholder participation on the demand for reuse water), merely understanding and diagrammatically representing their connections may have a significant impact on the transparency of decision-making. Even without quantifiable parameters, qualitative models may: (*1*) bring added transparency to the planning and design process, (*2*) inspire new thinking, (*3*) expose potential unintended consequences and project barriers, and (*4*) identify metrics that are

measurable that will provide insight into the CLD loops of interest. Such uses of qualitative system dynamics have been found to be effective in natural resource management [217] and in automotive policy design [237], and may be equally influential in the management of wastewater resources.

4.4.2. Combining Qualitative and Quantitative Tools in Decision-Making

After the identification of alternatives, the development of project-specific CLDs, and the selection of a comprehensive set of metrics, decision makers must undertake the task of resolving the inevitable tradeoffs between and among sustainability aspects. One analytical tool that can provide a framework for comparative sustainability assessments is multi-criteria decision analysis (MCDA). MCDA is a class of formal approaches to decision-making that allow individuals or groups to explore decisions while taking explicit account of multiple criteria [238]. Some of the advantages of MCDA identified by Belton and Stewart [238] include its ability to: (*1*) provide structure for the problem, (*2*) account for multiple, conflicting criteria, (*3*) add transparency to the decision-making process, and (*4*) help decision makers learn about their own and others' values and judgments. MCDA has been widely utilized as a decision aid in a number of resource management fields (e.g., energy [239]), as well as water resource [240] and wastewater management projects [64, 241].

In order for MCDA to be effective for the wastewater planning and design process, it must provide a means to resolve tradeoffs among qualitative (e.g., public understanding) and quantitative (e.g., energy consumption) metrics and evolve as stakeholder preferences are articulated. Using global and local targets for sustainability (e.g., "our wastewater management system should be GHG-neutral"), stakeholders can develop a CLD, identify loops of interest, and apply weightings based on their value judgments. Weighting the criteria is one of the most important and challenging aspects of applying MCDA [242]. Eliciting people's preferences may lead to inconsistent data [243] resulting in criteria weightings that may have large uncertainties [242, 244]. Even if stakeholder preferences are elicited through a participatory planning process, cognitive biases may arise from the participation process itself – leading to skewed weightings of criteria [245]. In addition to the complexities of eliciting stakeholder values, there are also uncertainties associated with the decision-making process itself that must be included in the comparative analysis (e.g., selection of the appropriate goals and objectives) [246].

Although there are a number of processes to elucidate stakeholder preferences and minimize epistemic uncertainty [244, 247], there exists a level of uncertainty from human input that may be irreducible because of the inherent variability of socio-political systems [246]. Despite these challenges with MCDA and other participatory decision-making tools, it is important to note that stakeholder participation can improve the public acceptance of a decision and provide valuable insight to the planning and design process through local knowledge and creative thought; especially in the case of complex, poorly structured problems [244, 247]. For this reason we must continue to use and develop tools that will facilitate stakeholder participation in the pursuit of more sustainable wastewater systems.

4.5. Conclusion

In the simplest of terms, our pursuit of sustainability should involve solving problems without creating new ones. Unfortunately, it is highly unlikely that an improvement in one aspect of sustainability will not have tradeoffs with other aspects. Through the use of force field diagrams and CLDs in a participatory planning and design process, individual metrics can be placed in the broader context of sustainability so that stakeholders may better understand the impacts of their decision. Ultimately, these tools will help qualitatively assess whether the alternative being considered would be a shift toward or away from a more sustainable wastewater management system. In other words, stakeholders can simply ask themselves: "if our goal is sustainability, are we moving in the right direction?"

4.6. Acknowledgements

We acknowledge the Graham Environmental Sustainability Institute at the University of Michigan which provided partial funding for the lead author. The authors would also like to thank the anonymous reviewers of this manuscript for their constructive comments.

Chapter 5
Quantitative Sustainable Design for Wastewater Treatment Plant Process Refinement: An Evaluation of Operational Flexibility

J.S. Guest[1], N.G. Love[1], S. Snowling[2], C.B. Bott[3], G.T. Daigger[4], S.J. Skerlos[5,*]

[1] Department of Civil & Environmental Engineering, University of Michigan
[2] Hydromantis Environmental Software Solutions, Inc.
[3] Hampton Roads Sanitation District
[4] CH2M HILL
[5] Department of Mechanical Engineering, University of Michigan

5.1. Introduction

With aging infrastructure [19] and increasingly stringent effluent quality requirements, utilities across the United States are making large investments toward the replacement and upgrade of existing wastewater treatment plants (WWTPs). Such upgrades often result in the construction and operation of more advanced treatment processes, processes which have been observed to achieve net reductions in effluent nutrients but at the expense of other life cycle impacts and higher operational costs [248]. Although environmental or economic burdens may be partially reduced by use of design optimization [47, 249, 250], a holistic sustainable design methodology for the wastewater industry is still lacking.

In the literature, a number of sustainability assessment frameworks have been proposed (e.g., the Human Hierarchy [251], Social-Ecological Systems [228]), but these frameworks can be difficult to employ in practice. As a result, industry has commonly used the concept of the *triple bottom line* (TBL), which simply means that environmental/ ecological, social, and economic factors have been considered. The lack of standardization in TBL analysis, however, can lead to its misuse and the erosion of the

TBL as a guiding principle in design. Along these same lines, the application of sustainable design in the wastewater industry has suffered from a lack of transparency in decision-making and the absence of a standardized methodology.

In the pursuit of more sustainable WWTPs, decision-making processes should address performance, economic, environmental, and social factors [24], and do so in a way that incorporates locality-specific elements. A reasonable goal for such a process is to balance local sustainability (which may have local water quality, cost, and stakeholder preferences as primary concerns) with the pursuit of regional and global sustainability (which may have more of an emphasis on non-traditional emissions and life cycle environmental impacts). Although social factors can be addressed (to a degree) through a participatory planning process [24, 252], a process is still needed by which designs can be quantitatively compared to elucidate the performance, environmental, and economic trade-offs. It may not always be possible to achieve designs that simultaneously improve local and global sustainability efforts, but such a process could elucidate trade-offs that may inform decision-making processes at the local level.

Although much recent effort has focused on performing comparative evaluations of the life cycle environmental impacts (using life cycle assessment, LCA) of configuration alternatives (e.g., [41, 128, 253, 254]), fewer published studies have included cost assessments in their comparative evaluations (e.g., [248, 255]). More recent advancements toward the integration of economic and environmental assessments includes the work of Wang and colleagues [256], who evaluated the reduction of N_2O emissions as a financing mechanism (via their sale as carbon credits) to upgrade WWTPs for nitrogen removal. Independent of these advancements toward integrating environmental and economic considerations has been the development of more rigorous simulation approaches to better predict the likely performance of a specific WWTP design [48, 124, 126]. Simulation-based uncertainty assessments have been limited in their application to cost analysis in the literature [125], and have not been applied in connection with LCA. In particular, it has recently been shown that influent composition may play an important role in WWTP greenhouse gas emissions [257], but such factors are generally not addressed in WWTP LCAs. Also missing is the use of diurnal simulation to predict life cycle and economic performance in a holistic way, as the bulk of LCA and economic studies rely on steady-state data despite observations that steady-

state simulations may result in artificial performance differences between compared designs [47].

To develop more sustainable WWTP designs, what is needed is a methodology by which performance (specifically in terms of diurnal effluent quality), life cycle environmental impacts, and costs can be quantified together under uncertainty to elucidate trade-offs between design decisions. Here we present a quantitative sustainable design methodology that addresses social, performance, environmental, and economic factors, and apply it to refine the design of a WWTP upgrade. Designs were developed through coordination with utility and consultant stakeholders, and were assessed by way of Monte Carlo, diurnal simulations, LCA, and cost analysis. This quantitative process is the backbone of a larger planning and design process [24] that has an overarching goal to advance both local and global sustainability efforts.

5.2. Quantitative Sustainable Design Methodology

5.2.1. Case Study

The Chesapeake-Elizabeth Wastewater Treatment Plant (WWTP) is located in Virginia Beach, Virginia (USA) and has a design capacity of 24 million gallons per day (MGD). Although the Chesapeake-Elizabeth WWTP currently uses a high rate activated sludge (HRAS) process for secondary treatment, pending nutrient limits will require an upgrade to an enhanced biological phosphorus removal (EBPR) process. In addition to HRAS, existing unit processes at the plant include secondary clarification with ferric chloride addition for phosphorus removal, disinfection via sodium hypochlorite, gravity thickening of waste activated sludge (WAS), centrifugation of thickened sludge, and on-site incineration of centrifuge cake.

As part of the Chesapeake Bay initiative, Chesapeake-Elizabeth will have a waste load allocation of 3-8 mg-(N)·L^{-1} total nitrogen (TN) and 0.7 mg-(P)·L^{-1} total phosphorus (TP) at design flow on an annual average basis. In preparation for this permit change, the Hampton Roads Sanitation District (HRSD) is planning an upgrade of the Chesapeake-Elizabeth WWTP to achieve biological nitrogen and phosphorus removal. The centerpiece of this upgrade is the construction of a 5-stage Bardenpho process followed by denitrification filters, where a 5-stage Bardenpho process consists of five sequential zones (anaerobic-anoxic-aerobic-anoxic-aerobic) with an internal recycle between the

first aerobic and anoxic zones. In general, processes are sized such that the minimum anaerobic, anoxic, and aerobic SRTs are achieved under both winter and summer conditions (with winter controlling). In the case of Chesapeake-Elizabeth, the selected total SRT of the system is proportional to the reactor volume required – this is due to existing secondary clarifiers that cannot be easily (or cheaply) replaced. Likewise, anaerobic, anoxic, and aerobic volumes are proportional to their respective design SRTs. Although nitrifiers are highly sensitive to low temperatures (making winter aerobic SRT a key design parameter), anaerobic and anoxic growth rates are less sensitive to temperature changes. Therefore, if a process is designed for minimum anaerobic, anoxic, and aerobic SRTs under winter conditions, the ability of operators to decrease the total system SRT under summer conditions will be limited by minimum anaerobic and/or anoxic SRTs (with aerobic summer SRT typically in excess of what is required to maintain nitrification). The prospect of superfluous aerobic SRT under summer conditions raises the question of whether or not an alternative design can be developed to meet performance goals while reducing life cycle costs and environmental impacts.

Although the 5-stage Bardenpho process is capable of achieving high levels of biological nutrient removal year round, the prospect of an annual average permit offers the plant the opportunity to offset higher effluent nitrogen levels in the winter with lower levels in the summer. Rather than relying on high levels of BNR at all times, there is the opportunity to shift to a BNR process with higher effluent TN in the winter months if it offers other benefits (e.g., in terms of lower costs or environmental impacts). The relative sustainability of operational flexibility in the form of a full-scale seasonal process change at the Chesapeake-Elizabeth WWTP, however, is unknown.

5.2.2. Alternative Design – Seasonal Process Change

As an alternative to the Standard Design defined by a year-round 5-stage Bardenpho process, we have developed a Seasonal Design that enables operation as a 5-stage Bardenpho under summer months and operation as an Anaerobic-Anoxic-Oxic (A2O) process in the winter months. This process transformation may be achieved by making the second anoxic zone (ANX2) a swing zone, capable of being aerated during winter months. A key difference between the 5-stage Bardenpho and A2O processes is that the A2O process consolidates anoxic conditions into a single stretch of the reactor basins. This change reduces the capacity (all else equal) of the secondary treatment

process to denitrify as it relies exclusively on internal recycle pumping to deliver nitrate to the anoxic zone.

For this case study, conceptual designs of two alternative upgrades are studied here: (1) the Standard Design, which consists of a year-round 5-stage Bardenpho process, and (2) the Seasonal Design, which consists of a secondary treatment process that can be operated as a 5-stage Bardenpho in the summer and as an A2O process in the winter. Both design alternatives include the construction of new primary clarifiers, denitrification filters, an acetic acid (HAc) delivery system (to provide HAc as an electron donor for denitrification), an incinerator scrubber blowdown treatment system (to treat wastewater generated by on-site incinerators), and gravity belt thickeners, as well as capacity increases to secondary sludge pumping systems. Based on the site layout, both designs would use existing HRAS tankage by converting it to aerobic and anoxic tankage toward the end of the biological process, and secondary clarifiers would be unchanged. All unit processes were designed based on annual average flow (24 MGD) with the largest, most critical unit operation out of service. The key factors in reactor sizing were (i) maximum mixed liquor suspended solids (MLSS) concentration (dictated by existing clarifiers) and (ii) winter design SRTs. A maximum MLSS of 3,100 mg-(TSS)·L^{-1} based on acceptable solids loading rates to existing secondary clarifiers under annual average (largest unit out of service) and maximum month (all units in service) conditions. As a result of the fixed design MLSS, any increase in design SRT resulted in increased reactor volume.

Anaerobic (ANA), anoxic (ANX), and aerobic (AER) SRTs for design were selected based on utility and consultant input. Under winter conditions, the design values for the Standard Design were 1.0 (ANA), 2.0 (ANX), and 10 (AER) days. The Standard Design volume ratio of ANX1:ANX2 was designed at 1.0:1.5 to take advantage of endogenous respiration in the second anoxic zone. Design values for the Seasonal Design were 1.0 (ANA), 1.5 (ANX), and 10 (AER) days. This reduction in ANX SRT of 0.5 days was deemed reasonable because it provided a sufficient safety factor for reliable performance (equivalent to the reliability of an ANX SRT of 2.0 days in the Standard Design) given that the whole of the ANX zone would be consolidated and less dissolved oxygen would enter the zone. Additionally, the ANX1:ANX2 volume ratio was reduced to 1.0:1.0 to maintain sufficient anoxic volume during A2O operation. Target total SRTs under summer conditions were selected to be 70% of winter design values, resulting in

anaerobic/anoxic/aerobic SRTs of 0.7/1.4/7.0 days and 0.7/2.1/6.0 days for the Standard and Seasonal Designs, respectively. By switching the second anoxic zone from anoxic conditions (in summer) to aerobic conditions (in winter), the Seasonal Design allows the utility to partially uncouple winter AER SRT from summer AER and ANX SRTs, achieving the necessary minimum aerobic SRT in winter conditions while disproportionally increasing the anoxic volume fraction in summer.

Another key difference between the Standard and Seasonal designs is the sizing of denitrification filters. Based on existing design standards, denitrification filters were sized to meet hydraulic loadings of 4.0 gal·min^{-1}·ft^{-2} for the Standard Design and 3.5 gal·min^{-1}·ft^{-2} for the Seasonal Design assuming 2 of 12 units are out of service at any time and annual average flow. Other than different design parameters for the secondary treatment process (different anoxic SRTs and ANX1:ANX2 ratios) and denitrification filter loadings (4.0 vs. 3.5 gal·min^{-1}·ft^{-2}), all other unit processes and pieces of equipment were designed using consistent design standards [6, 7] (see Appendix B).

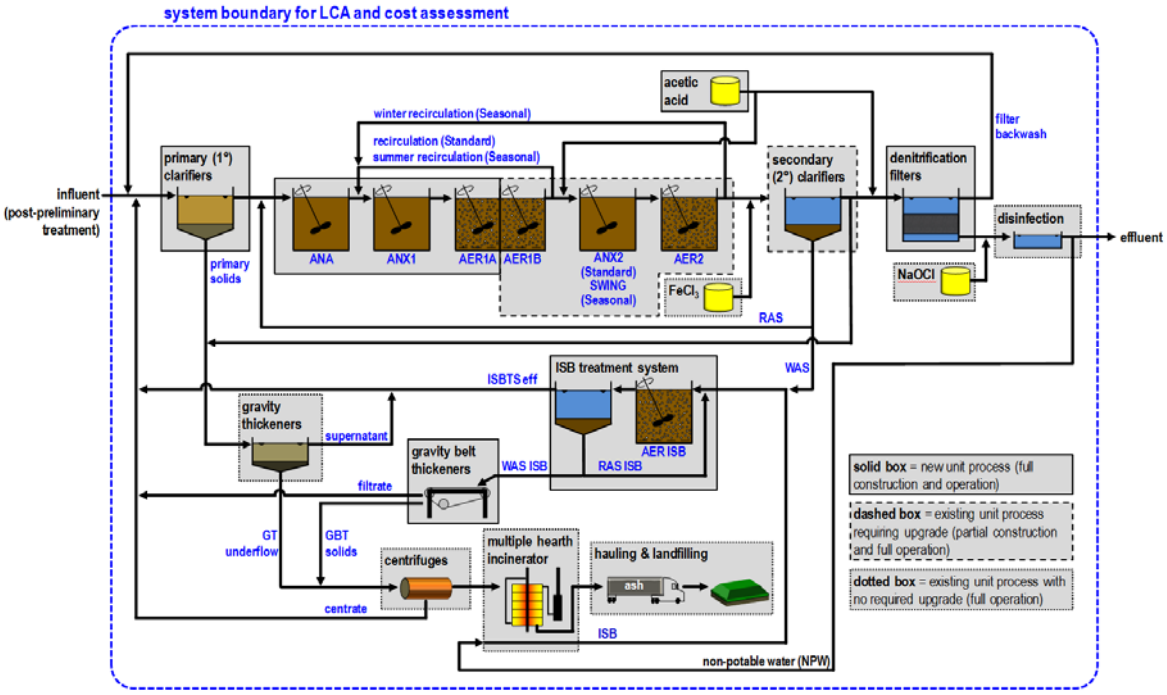

Figure 5.1. System boundary for LCA and cost assessment.

5.2.3. Performance Assessment

Performance of the WWTP designs was simulated using GPS-X™ (Hydromantis Environmental Software Solutions, Inc.; Hamilton, Canada). All processes within the system boundary (Figure 5.1) except disinfection, incineration, and ash hauling and landfilling were explicitly modeled in GPS-X^{TM}, using the Mantis2 model for biological process modeling. A weekday and a weekend dry weather diurnal flow pattern were modeled from hour-by-hour data, and a characteristic hydrograph was established for infiltration and inflow resulting from rain events. Each simulation was run to steady state, followed by a dynamic simulation period of 10 days. The first 3 days of each dynamic simulation was a dry weather, weekday diurnal. It was observed that every model parameter used for the performance, life cycle impact, and cost assessments (except effluent nitrite) was within 0.3% of the previous day's value after 3 days of dynamic simulation; nitrite was within 1.3% (data not shown). Data was collected from simulation results from days 4 through 10, which were simulated as a Wednesday morning through Tuesday night and included random rain events consistent with the frequency and intensity of rain events recorded by HRSD from 2005-2010.

5.2.4. Cost Assessment

Cost estimates of unit processes within the system boundary (Figure 5.1) were achieved using equations derived from CAPDET [258] and CapdetWorks^{TM} (v2.5e; Hydromantis Environmental Software Solutions, Inc.; Hamilton, Canada). For each unit process, the following costs were quantified: construction and equipment cost ($), operational labor cost ($\cdot yr^{-1}$), maintenance labor cost ($\cdot yr^{-1}$), material and supply cost ($\cdot yr^{-1}$), chemical cost ($\cdot yr^{-1}$), and energy cost ($\cdot yr^{-1}$). These values were then used to determine the present worth of a given design and simulation scenario assuming a discount rate of 8%.

5.2.5. Life Cycle Impact Assessment

Goal Scope and Definition. The functional unit for this study was the treatment of HRSD influent wastewater (as characterized by the probability density functions in Table 5.1) over 40 years, with effluent TP less than or equal to 0.7 mg-(P)$\cdot L^{-1}$, effluent TN less than or equal to 5.5 mg-(N)$\cdot L^{-1}$, and residual solids disposed of at a municipal solid waste landfill. The system boundary excluded sources of impact from utility infrastructure upstream of the wastewater treatment plant (collection system, gaseous emissions in

collection system, electricity for pumping, etc.; Figure 5.1). First-order (direct emissions and discharge) and second-order (electricity generation, chemical manufacturing, etc.) processes during the construction and operation of the WWTP were included in the system boundary. The end-of-life phase of the WWTP was not assessed as it was expected to be negligible compared to the construction and operating phases (consistent with assumptions in [130, 259]).

Inventory Analysis. Data for the inventory analysis of the construction phase was generated in two steps. First, the volume of earthwork (excavation), sand (for denitrification filters), and reinforced concrete was estimated using equations derived from CAPDET [258] and CapdetWorks™. Next, the volume of reinforced concrete was used as a multiplier for the estimation of other construction phase processes and materials as described by Doka [260] (consistent with approach taken in [130]). This approach is based on inventory data from a series of publications ([261, 262], in Swiss German) leading back to the diploma work of Fahner and colleagues who quantified materials and processes required to convert a flat field into an operating WWTP using receipts from construction, planning documents, and information directly from material suppliers, vendors, contractors, and designers ([263], in Swiss German). These multiplicative factors include items such as: reinforcing steel; steel, aluminum, copper, and plastics for control panels (excluding precious metals); bitumen for asphalt; electricity; and a number of other materials and processes (see Appendix C). Although we are evaluating upgrades rather than new plant construction, it was assumed that these multiplicative factors would still be applicable as many of the same WWTP components would still have to be constructed (new pump and blower buildings, new paving, etc.). The sensitivity of the results to this assumption was evaluated by varying multiplicative factors (discussed in more detail in Uncertainty and Sensitivity Analysis section, below). Inventory data for these processes was based on U.S. data whenever possible, and the sensitivity of the results to these assumptions was evaluated (see Table 5.2).

Operation-phase inventory data were generated using the following steps. First, direct emissions from the WWTP were estimated using data from GPS-X™ simulations. Effluent nutrients (including ammonium, nitrate/nitrite, organic nitrogen, COD, and soluble total phosphorus) and chemical consumption (HAc for denitrification and ferric chloride for phosphorus precipitation) were directly quantified. Biogenic gaseous

emissions of nitrous oxide (N_2O) at the WWTP were estimated using the emission factor approach [264] with a value of 0.005 kg-(N_2O-N) per kg-(N) discharged (for "effluent" biogenic N_2O emissions) or denitrified (for "WWTP" biogenic N_2O emissions). The sensitivity of the results to assumed N_2O emissions factors were evaluated across ranges from the literature (see Table 5.2). Electricity consumption during operation was estimated using (i) required airflow and pumping rates from GPS-X™ simulations and (ii) continuous equations derived from CAPDET [258] and CapdetWorks™ for all unit processes (including pumping and various mechanical operations such as gates, arms, rakes, etc.). Polymer and hypochlorite use, natural gas and fuel oil (for incineration) consumption, and ash production were estimated based on correlations in monthly data (e.g., polymer used per kg of solids centrifuged) at the Chesapeake-Elizabeth WWTP.

The life cycle emissions and raw materials required for all materials (e.g., HAc), processes (e.g., electricity production and delivery), and wastes (e.g., construction waste) were quantified using the ecoinvent database accessed via SimaPro (v7.2.4; PRé Consultants; Amersfoot, The Netherlands). The specific ecoinvent processes used can be found in Appendix C.

Impact Assessment. The impact categories and characterization factors of the U.S. EPA's Tool for the Reduction and Assessment of Chemical and other Environmental Impacts (TRACI 2; v3.03) [265] were used. TRACI mid-point indicators include acidification, carcinogenics, ecotoxicity, eutrophication, global climate change, non-carcinogenics, respiratory effects, ozone depletion, and smog formation. No normalization was performed beyond the use of TRACI characterization factors and no grouping, weighting, or aggregation of impact categories was used. Sensitivity analyses were performed and are discussed in more detail below.

5.2.6. Uncertainty and Sensitivity Analyses

Monte Carlo analysis with Latin Hypercube Sampling (LHS) was used for uncertainty analysis. LHS is a sampling technique that evenly samples from the parameter space to reduce the number or runs required to produce representative and reproducible results [266]. Uncertainty analysis was performed on a total of 9 parameters: average daily influent flow, rainfall, dry weather influent BOD_5, influent BOD_5:TKN ratio, influent BOD_5:TP ratio, nitrifier maximum specific growth rate, oxygen half saturation coefficient

for heterotrophs, ammonium half saturation coefficient for ammonia oxidizing bacteria (AOB), and temperature. The probability density function (PDF) and pertinent values for each parameter are listed in Table 5.1. The values and PDFs of all influent parameters are based on daily and monthly plant-specific data from 2005-2010. All values and PDFs for kinetic parameters are from recently published WWTP modeling sensitivity analyses [124, 126].

Table 5.1. Input uncertainty for model parameters.

ID	Parameter	Distribution	Minimum & Maximum (uniform) or Average & Standard Deviation (normal)	Units
1	dry weather influent flow	uniform	18 (min); 23 (max)	MGD
2	rainfall	empirical [b,c]	NA	MGD
3	influent BOD_5	normal [b]	243 (avg); 19 (stdev)	$mg \cdot L^{-1}$
4	influent BOD:TKN ratio [d]	normal [b]	5.7 (avg); 0.79 (stdev)	mg-$(BOD_5) \cdot L^{-1}$ per mg-$(N) \cdot L^{-1}$
5	influent BOD:TP ratio [e]	normal [b]	41 (avg); 2.5 (stdev)	mg-$(BOD_5) \cdot L^{-1}$ per mg-$(P) \cdot L^{-1}$
6	nitrifier maximum specific growth rate [f]	uniform	0.77 (min); 0.92 (max)	d^{-1}
7	oxygen half saturation coefficient for heterotrophs	uniform [g]	0.1 (min); 0.3 (max)	mg-$(COD) \cdot L^{-1}$
8	ammonium half saturation coefficient for AOB	uniform [g]	0.5 (min); 1.5 (max)	mg-$(N) \cdot L^{-1}$
9	temperature	uniform [b]	12 (min); 28 (max)	°C

[a] The plant experiences roughly 1 MGD of influent from rain events on average. The values for dry weather influent flow exclude flow from rain events, which were simulated as a separate, independent parameter.

[b] Observed distribution based on HRSD data.

[c] Empirical distribution characterized by HRSD data. See Supporting Information for additional details.

[d] Influent ammonium was set to 74% of the influent TKN concentration based on the median value of HRSD data.

[e] Influent soluble phosphorus was set to 80% of the influent TP concentration; no data from HRSD was available for soluble phosphorus.

[f] AOB and nitrite oxidizing bacteria (NOB) decay were fixed at 0.17 d^{-1}, and NOB maximum specific growth rate was set to 0.1 d^{-1} greater than the AOB maximum specific growth rate based on this default assumption in GPS-X™.

[g] Distribution and values are consistent with assumption in [126].

LHS was used to generate a set of 500 values for each parameter listed in Table 5.1. These values were compiled into 500 discrete sets of input parameters, where an input parameter set was defined by a single value for each of the 9 parameters. Each input parameter set was used to simulate the performance of both the Standard and the Seasonal designs, resulting in a total of 1,000 dynamic simulations (500 for each

design). Comparisons between designs were made based on the differences in performance, environmental impacts, and costs for each individual input parameter set. It should be noted that because temperature was varied uniformly from 12-28 °C and 18 °C was arbitrarily selected as the separation between summer and winter performance, 37.5% of simulations (and operational time) would be under winter conditions and the remaining simulations would be under summer conditions. Temperature was monotonic and it was assumed the plant operation would only switch twice per year (once at the start of winter and once at the end).

Table 5.2. Sensitivity analysis overview.

Parameter	Default Value	Likely Minimum Value	Likely Maximum Value
Life Cycle Inventory			
Energy Source – Fraction Supplied by Coal [a]	0.342 [b]	0.141 [c]	0.632 [c]
N_2O Emission Factor – In WWTP [kg-(N_2O-N)·kg-(N denitrified)$^{-1}$]	0.005 [d]	0.0002 [e]	0.0059 [e]
N_2O Emission Factor – In Effluent [kg-(N_2O-N)·kg-(N in effluent)$^{-1}$]	0.005 [d]	0.005 [f]	0.046 [g]
Construction Multiplication Factor per m^3 Concrete – All Individual Materials & Processes	1x Fahner factor [h]	0.5x Fahner factor [h]	4x Fahner factor [h]
Cost Analysis			
Electricity Unit Cost [$·kWh^{-1}]	0.065 [i]	0.06	0.10

[a] Any changes to the coal fraction were compensated for with increase or decrease in the fraction electricity from nuclear power. The balance of electricity replaced by (or in place of) coal was assumed to be nuclear.
[b] Fraction based on 2010 data for the Commonwealth of Virginia [267].
[c] 25th percentile (likely minimum) and 75th percentile (likely maximum) of coal fractions by state for 2010 [267].
[d] [264]
[e] [256, 268]
[f] [256, 264]
[g] [256, 269]
[h] Factors developed in [263], and used by others (e.g., [130, 260])
[i] HRSD current pricing.

5.2.7. Implementation

MATLAB (MathWorks; Natick, Massachusetts) was used for LHS and, through operation of GPS-X™ in batch mode, the execution of the methodology as a whole. The MATLAB code used for simulation and preliminary data consolidation can be found in Appendix G. The code used for cost analysis and LCA can be found in Appendix H. The largest

computational burden in this approach stemmed from the GPS-X^{TM} simulations, averaging roughly 20 minutes per run (where a run includes a single steady state and 10 day dynamic simulation) on a 64-bit Windows 7 desktop with 3.16 GHz processor (6 MB cache) and 4.0 GB of RAM. This computation time, coupled with the use of Monte Carlo, was an influential factor in deciding to evaluate only two design alternatives.

5.3. Results and Discussion

5.3.1. WWTP Performance

Actual SRT values across simulations for winter and summer conditions matched design values with averages (+/- standard deviations) of 13.0 +/- 0.2 days and 9.0 +/- 0.1 days for the Standard Design, and 12.5 +/- 0.2 days and 8.7 +/- 0.1 days for the Seasonal Design. EBPR was consistently achieved, but to varying degrees between the two designs. The soluble phosphorus concentration entering the secondary clarifiers (before chemical precipitation) had average values of 0.5 and 1.1 mg-(P)·L^{-1} for the Standard and Seasonal Designs, respectively (Figure 5.2a), with summer and winter performance of the Seasonal Design differing greatly (0.6 vs. 1.8 mg-(P)·L^{-1}, respectively). Any residual phosphorus above 0.7 mg-(P)·L^{-1} for each individual simulation set was assumed to be precipitated with ferric chloride (this was the origin of ferric chloride use estimates).

Effluent TN constraints were also met with average values of 5.0 and 4.8 mg-(N)·L^{-1} for the Standard and Seasonal Designs, respectively. The Standard Design achieved similar TN removal under summer and winter conditions with median values of 4.4 and 4.0 mg-(N)·L^{-1}, respectively. As expected, the Seasonal Design had a greater difference between summer and winter performance, with effluent TN median values of 2.1 and 6.9 mg-(N)·L^{-1}, respectively (Figure 5.2b).

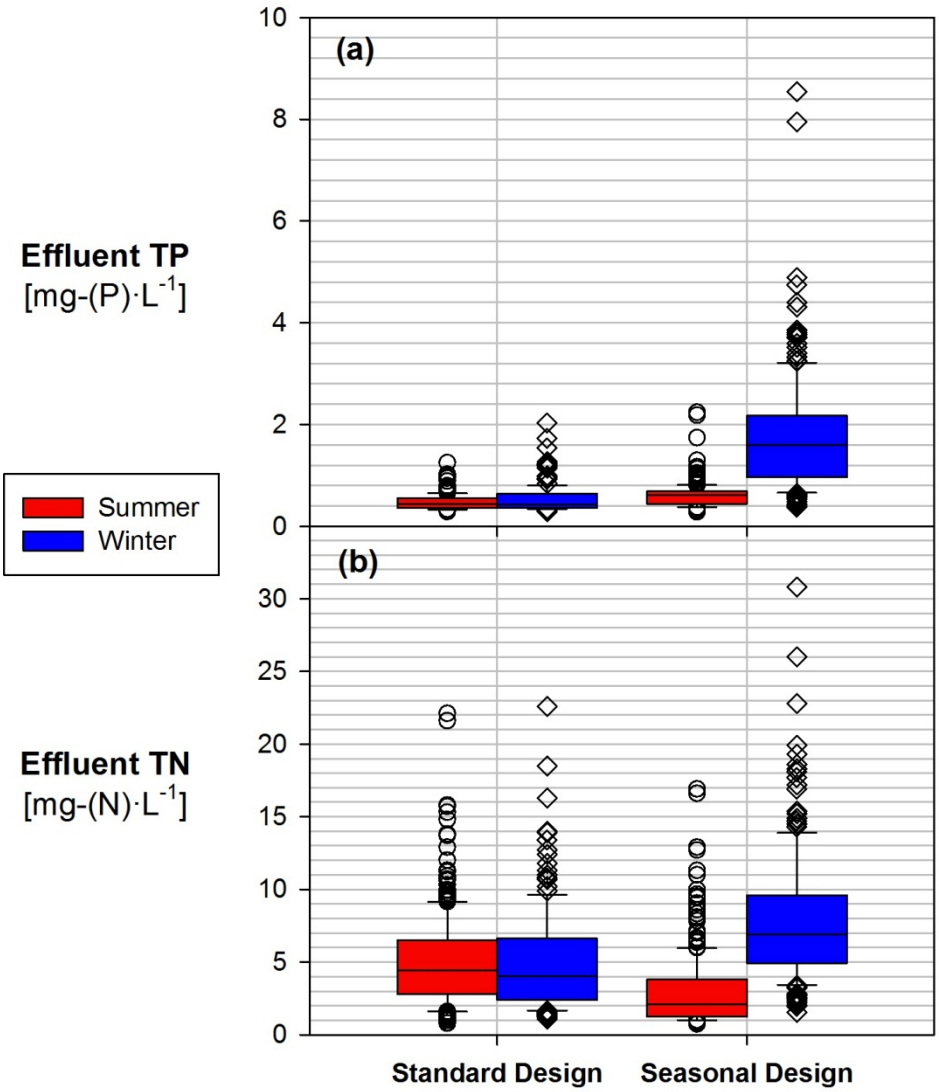

Figure 5.2. Box and whisker plot of effluent (a) TP and (b) TN of Standard and Seasonal Designs. The boxes represent the span of the lower (25th percentile) and upper (75th percentile) quartiles of 312 (summer) and 188 (winter) simulations. The horizontal line within each box represents the median, and the vertical lines ("whiskers") represent the 10th and 90th percentiles, and symbols denote data points outside of the 10th and 90th percentiles.

As expected, the Seasonal secondary treatment process had higher effluent nutrient concentrations during A2O operation in the winter compared to 5-stage Bardenpho operation in the summer. Overall, each design consistently achieved near complete nitrification, creating the opportunity to achieve greater TN removal with the addition of more electron donor to the anoxic zones. For the analyses presented here, HAc addition was flow paced at a fixed ratio for each set of simulations. Specifically, HAc was added to achieve the following target concentrations (in mg-(COD)·L^{-1}) in ANX2 and

denitrification filter (DF) influent: 42/22 (ANX2/DF) for Standard Design summer and winter operation; 30/22 for Seasonal Design summer; and 0/30 for Seasonal Design winter. The increased level of HAc addition to the Standard Design ANX2 zone was required to achieve effluent total nitrogen concentrations on par with Seasonal Design annual average performance. In particular, it was the extended summer anoxic SRT of 2.1 days for the Seasonal Design (as compared to 1.4 days for the Standard Design) and, specifically, the increased ANX1 SRT that lead to lower levels of effluent nitrate with less HAc addition. Ultimately, this reduction in the use of HAc addition (averaging a 22% reduction in summer and 69% reduction in winter, or 40% annual average) was a major component of cost and life cycle environmental impact differences between designs (discussed in more detail below).

5.3.2. Cost Assessment

A summary of the results of the cost analysis can be seen in the first row of data in Table 5.3. It was estimated the Seasonal Design would cost $4.5 million more to construct than the Standard Design. This additional expense is largely due to the additional denitrification filter area required for winter operation as well as the additional diffusers, air headers and piping, and redundant internal recycle withdrawal points (during A2O operation the internal recycle is withdrawn from AER2 rather than AER1B). Some construction cost savings are achieved with the reduced reactor volume required for the Seasonal Design, but these savings do not overcome the additional costs identified above.

Although the Standard Design was less expensive to construct, the Seasonal Design consistently costs less to operate. In fact, the Seasonal Design has a payback period of 2.7 years and would only be equivalent to the Standard Design in net present worth at an interest rate of 37% (a value of 8% was assumed for analyses presented here). This difference is due almost exclusively to the savings in electron donor over the life cycle of the plant. The Seasonal Design uses, on average, 2,800 fewer $L \cdot d^{-1}$ of acetic acid and achieves comparable annual average TN removal. Due to the magnitude of these savings, the cost analysis results are highly sensitive to the price of acetic acid. The default cost used in this analysis has been 1.57 $\$ \cdot L^{-1}$ [270], but a price of 0.366 $\$ \cdot L^{-1}$ would result in equivalent net present values for the Standard and Seasonal Designs.

Table 5.3. Summary of present worth and LCA comparisons between Standard and Seasonal Designs.

Indicator	Absolute Construction Impact		Impact of Upgrade From Standard to Seasonal Design [Seasonal minus Standard]		
	Standard	**Seasonal**	**Construction**	**Summer Operation** (40 years)	**Winter Operation** (40 years)
Present Worth [million $]	47.2	51.7	4.5	***(11.2)*** +/- 0.8	***(34.9)*** +/- 2.5
Acidification [thousand H+ moles eq]	918	909	***(9)***	***(12,300)*** +/- 3,100	***(32,600)*** +/- 4,800
Carcinogenics [tonnes benzene eq]	43.0	42.6	***(0.4)***	***(165)*** +/- 30	***(461)*** +/- 40
Ecotoxicity [tonnes 2,4-D eq]	24,200	23,900	***(200)*** [a]	***(123,000)*** +/- 23,000	***(340,000)*** +/- 38,000
Eutrophication [tonnes N eq]	26.1	25.8	***(0.3)***	***(518)*** +/- 767	2,810 +/- 3,690
Global warming [tonnes CO_2 eq]	4,890	4,840	***(50)***	***(47,100)*** +/- 7,600	***(124,000)*** +/- 9,000
Non carcinogenics [tonnes toluene eq]	456,000	451,000	***(5,000)***	***(1,200,000)*** +/- 230,000	***(3,310,000)*** +/- 300,000
Ozone depletion [kg CFC-11 eq]	0.206	0.204	***(0.002)***	***(7.16)*** +/- 0.69	***(20.6)*** +/- 1.5
Respiratory effects [tonnes $PM_{2.5}$ eq]	7.23	7.16	***(0.07)***	***(64.8)*** +/- 16.7	***(172)*** +/- 23
Smog [kg NO_x eq]	11.2	11.1	***(0.1)***	***(112)*** +/- 18	***(320)*** +/- 24

* Note: Parentheses are around negative values. Negative values mean the Seasonal Design had a lower value than the Standard Design (i.e., the Seasonal design cost less or has less of an environmental impact).

[a] Values in column of construction differences do not necessarily match values in Construction Impact column due to rounding for presentation in table.

[b] Values are averages +/- standard deviation.

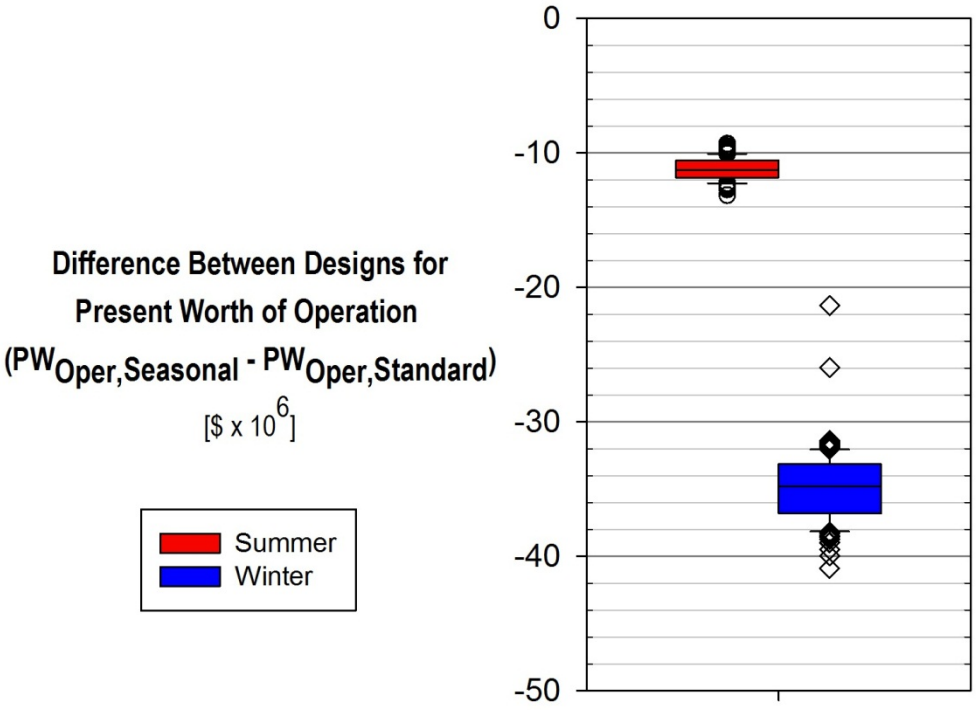

Figure 5.3. Box and whisker plot of difference between the Seasonal and Standard Design present worth of operation. The boxes represent the span of the lower (25th percentile) and upper (75th percentile) quartiles of 312 (summer) and 188 (winter) simulations. The horizontal line within each box represents the median, and the vertical lines ("whiskers") represent the 10th and 90th percentiles, and symbols denote data points outside of the 10th and 90th percentiles.

Although the promise of reduced electricity use often motivates design refinement, electricity savings of only 3.1 +/- 4.0% are expected with the switch to the Seasonal Design. Electricity savings accounted for only 1.1% of the operational cost savings, largely resulting from reductions in aeration demand of 5.8 +/- 6.3% in the summer and 4.3 +/- 2.8% in the winter condition. These savings are not a strong contributor to the values listed in Table 5.3, but would cause the Seasonal Design to have a lower operational present worth if both designs used equivalent volumes of electron donor (Figure 5.4; P << 0.00001 based on a paired, one-tailed t-test). The net present value of the Standard Design, in this instance, would be less expensive than the Seasonal Design by $3.7 million.

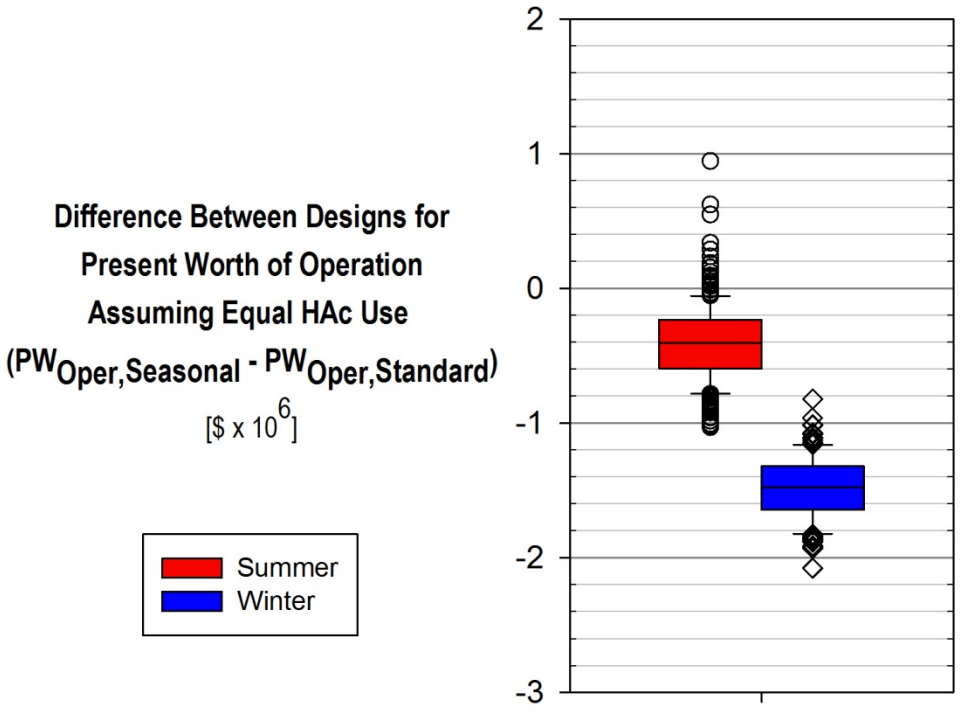

Figure 5.4. Box and whisker plot of difference between the Seasonal and Standard Design present worth of operation assuming equal use of acetic acid as an electron donor. The boxes represent the span of the lower (25th percentile) and upper (75th percentile) quartiles of 312 (summer) and 188 (winter) simulations. The horizontal line within each box represents the median, and the vertical lines ("whiskers") represent the 10th and 90th percentiles, and symbols denote data points outside of the 10th and 90th percentiles. Note that two outliers (positive 6.70 and 9.19 million $) from the winter condition were not plotted to preserve a legible axis scale.

5.3.3. Life Cycle Environmental Impacts

Overall, the Seasonal Design resulted in fewer environmental impacts in all impact categories except eutrophication (Figure 5.5). The reduced environmental impacts for the construction of the Seasonal Design were only 1.0% in each category, which is not likely to be significant relative to the uncertainty of the operation phase impacts. The majority of operational differences were again the result of differential HAc use (Table 5.4), but an advantage to switching to the Seasonal Design was still observed due to other factors (discussed below).

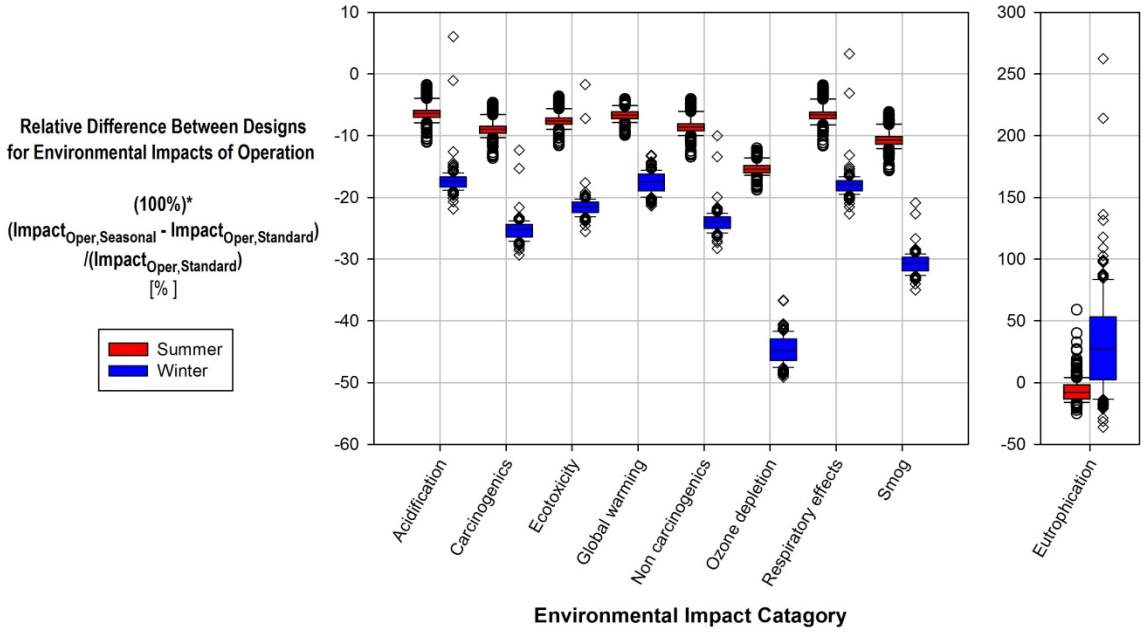

Figure 5.5. Box and whisker plot of relative difference between the Seasonal and Standard Design life cycle environmental impacts. The boxes represent the span of the lower (25th percentile) and upper (75th percentile) quartiles of 312 (summer) and 188 (winter) simulations. The horizontal line within each box represents the median, and the vertical lines ("whiskers") represent the 10th and 90th percentiles, and symbols denote data points outside of the 10th and 90th percentiles. Eutrophication has a separate y-axis scale due to its larger variability.

Table 5.4. Fraction of LCA life cycle impact differences (Seasonal minus Standard Design; presented in Figure 5.5) that result from different levels of HAc use between Standard and Seasonal Designs.

Life Cycle Impact	Summer (avg +/- stdev)	Winter (avg +/- stdev)
Acidification [%]	69 +/- 26	77 +/- 78
Carcinogenics [%]	84 +/- 18	91 +/- 9
Ecotoxicity [%]	77 +/- 17	88 +/- 71
Eutrophication [%]	-180 +/- 3,300	-21 +/- 329
Global warming [%]	81 +/- 14	93 +/- 4
Non carcinogenics [%]	82 +/- 20	89 +/- 11
Ozone depletion [%]	95 +/- 7	102 +/- 4
Respiratory effects [%]	72 +/- 29	75 +/- 44
Smog [%]	87 +/- 16	92 +/- 5

In addition to reducing exogenous electron donor requirements, the Seasonal Design resulted in an average reduction in electricity consumption of 3.1 +/- 4.7% and 3.1 +/- 2.4% for summer and winter operation, respectively. This reduction in electricity consumption reduced environmental impacts in all categories (although not to the same

degree as differential HAc use), and accounts for 13 +/- 25% and 6 +/- 4% of differences in operation phase greenhouse gas (GHG) emissions for summer and winter months. Ultimately, even if the Standard Design were able to achieve equivalent TN removal with the same amount of exogenous electron donor, the Seasonal Design would result in statistically significant reductions in almost all environmental impact categories (Figure 5.6). P values << 0.00001 were calculated for all categories except winter ozone and winter eutrophication based on a paired, one-tailed t-test. Both winter ozone and winter eutrophication were shown to increase with the shift to the Seasonal Design (P << 0.00001 based on a paired, one-tailed t-test). Although the increase in winter ozone impacts was statistically significant, the life cycle impacts of the two designs were within 0.9% of each other on average. Differences in eutrophication, however, stemmed largely from WWTP effluent which was responsible for 47 +/- 13% of life cycle eutrophication across all simulations, and was relatively insensitive to changes in assumptions of chemical or electricity use.

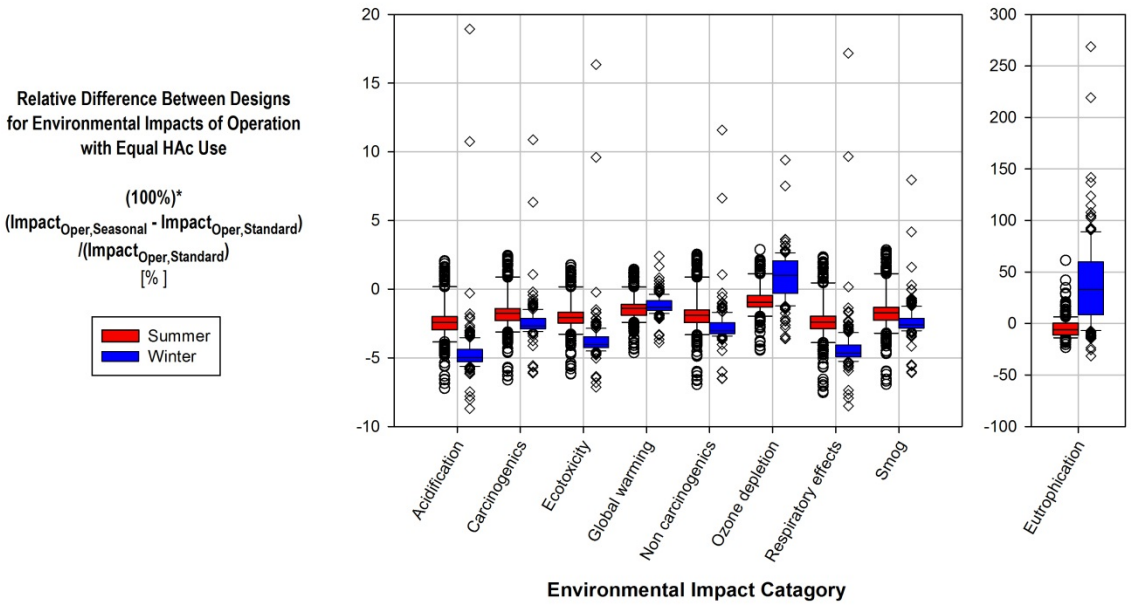

Figure 5.6. Box and whisker plot of relative difference between the Seasonal and Standard Design life cycle environmental impacts assuming equal use of acetic acid as an exogenous electron donor. The boxes represent the span of the lower (25th percentile) and upper (75th percentile) quartiles of 312 (summer) and 188 (winter) simulations. The horizontal line within each box represents the median, and the vertical lines ("whiskers") represent the 10th and 90th percentiles, and symbols denote data points outside of the 10th and 90th percentiles. Eutrophication has a separate y-axis scale due to its larger variability.

5.3.4. Exogenous Electron Donors as a Source of WWTP Environmental Impacts

The result that HAc is one of the key contributors to the differences in environmental impacts is somewhat surprising, especially considering that chemical consumption (although often included) has not been a focal point of WWTP LCAs [38]. As we consider the addition of HAc and its impacts on the WWTP, it is helpful to discuss it in the context of the addition of 1 mg-(COD)·L^{-1}. At the average influent flow of 20.5 MGD (plus incinerator scrubber blowdown flow of 1 MGD), the addition of 1 mg-(COD)·L^{-1} to the denitrification filters results in 1.06 million liters of HAc over the 40 year life cycle of the plant (or 73 liters per day). Adding 1 mg-(COD)·L^{-1} to the influent to the ANX2 zone, however, which includes forward flow (20.5 MGD) as well as RAS flow (roughly 70% of influent flow) and liquid streams from the incinerator scrubber blowdown and solids handling processes (e.g., the gravity belt thickeners; roughly 17% of influent flow), results in an acetic acid use of nearly 2.0 million liters of acetic acid over 40 years (or 136 liters per day). The life cycle implications of these levels of addition can be seen in Table 5.5.

Table 5.5. Costs and life cycle impacts of the addition of 1 mg-(COD)·L^{-1} of HAc to ANX2 and denitrification filter influent.

Parameter	Addition of 1 mg-(COD)·L^{-1} of Acetate to ANX2	Addition of 1 mg-(COD)·L^{-1} of Acetate to Denitrification Filters
Annual Chemical Cost [$/yr]	78,000	42,000
Present Worth of Chemical Cost [$]	930,000	500,000
Acidification [thousand H+ moles eq]	660	350
Carcinogenics [tonnes benzene eq]	12	6.2
Ecotoxicity [tonnes 2,4-D eq]	7,800	4,200
Eutrophication [tonnes N eq]	14	7.6
Global warming [tonnes CO_2 eq]	3,200[a]	1,700
Non carcinogenics [tonnes toluene eq]	81,000	43,000
Ozone depletion [kg CFC-11 eq]	0.58	0.31
Respiratory effects [tonnes $PM_{2.5}$ eq]	3.6	1.9
Smog [kg NO_x eq]	8.2	4.4

[a] As a basis for comparison, 3,200 tonnes CO_2 eq. would be emitted from the use of 5.1 million kWh assuming the Commonwealth of Virginia's current electricity source mix [267]. This electricity consumption would be observed over the lifetime of the plant if the average internal recycle were increased from 53.3 to 57.1 MGD (3.8 MGD increase).

Although this work has shown that significant reductions in life cycle environmental impacts may be achieved by modifying design parameters for a single configuration (i.e., anoxic SRT and ANX1:ANX2 volume ratios under summer conditions), another approach may be to simply replace HAc with an alternative substrate. As an example, a comparison between HAc and methanol (MeOH) based on ecoinvent characterization

factors is listed in Table 5.6. If the same ratio of COD added to N denitrified were observed for MeOH, environmental impacts of exogenous electron donor use may be reduced by 58-92% (right-most column in Table 5.6). These differences, however, are based solely on ecoinvent inventories for HAc and MeOH production. Other factors, including proximity of production facilities and details of a given supplier's production processes, will influence the actual magnitude of environmental impacts. In the event that HRSD could acquire a local waste product and use it as electron donor, the life cycle impacts (depending on how the waste product was treated in the life cycle inventory) could also be drastically reduced. This type of synergistic relationship has been observed at a 5-stage Bardenpho plant in North Carolina, which receives acetic acid waste from a pharmaceutical company at minimal cost. The decision to switch electron donors, however, is one that should be made after assessments of local availability and in collaboration with utility personnel.

Table 5.6. Comparison of ecoinvent impact factors for HAc and methanol on a mass and COD basis.

Impact category	**Acetic acid, 98% in H2O, at plant/RER U** [per kg] *	**Methanol, at plant/GLO U** [per kg] *	**Acetic Acid, HAc** [per kg of COD]	**Methanol, MeOH** [per kg of COD]	**Impact Reduction via Switch from HAc to MeOH**
Acidification [H+ moles eq]	0.318	0.0692	0.298	0.0461	84%
Carcinogenics [kg benzene eq]	0.00555	0.000585	0.00519	0.00039	92%
Ecotoxicity [kg 2,4-D eq]	3.75	0.399	3.50	0.266	92%
Eutrophication [kg N eq]	0.00681	0.000739	0.00637	0.000493	92%
Global warming [kg CO_2 eq]	1.54	0.736	1.44	0.491	66%
Non carcinogenics [kg toluene eq]	39.0	4.60	36.5	3.06	92%
Ozone depletion [kg CFC-11 eq]	2.81E-07	1.64E-07	2.62E-07	1.09E-07	58%
Respiratory effects [kg $PM_{2.5}$ eq]	0.00175	0.000265	0.00163	0.000177	89%
Smog [g NO_x eq]	0.00394	0.00106	0.00368	0.000709	81%

* Titles of columns 2 and 3 are the unique names of the ecoinvent inventories used in this analysis.

5.3.5. Nutrient Limits and Implications for Design

The primary responsibilities of a WWTP are to protect public health and the aquatic environment. As we seek to make our designs more environmentally sustainable, we are also seeking to prevent local, regional, and global emissions that would result in environmental deterioration and transitions to unstable ecosystems (e.g., see the Planetary Boundaries concept by Rockström et al. [2]). In this study, we have included eutrophication as a life cycle environmental impact. The sources of eutrophication include all processes and materials for which life cycle inventory data was acquired from ecoinvent, as well as the direct emissions from the WWTP. This analysis revealed that the largest single contributor (47 +/- 13%) to the WWTP's life cycle nutrient emissions is the effluent. Environmental impacts of effluent are distinct from other life cycle impacts because they are directly regulated by local permitting agencies. If we assume that meeting effluent permit requirements will provide sufficient protection for the local receiving environment such that it can assimilate discharged nutrients without detrimental impacts (which, we acknowledge, may be overly optimistic), then we may be free to pursue design alternatives that reduce other life cycle environmental impacts.

In this case study, the structure of the HRSD's permits (i.e., load limits on an annual average basis rather than a shorter timescale) has created opportunities for operational flexibility that could achieve statistically significant reductions in life cycle environmental impacts of acidification, carcinogenics, ecotoxicity, global warming, non-carcinogenics, respiratory effects, and smog. These regional and global impact reductions, however, come at the expense of seasonal variability in effluent nutrients entering the local aquatic environment. Ultimately, the fate and impact of effluent nutrients will depend on the receiving environment, and not all WWTPs have such flexibility in their effluent permits. The Chesapeake-Elizabeth WWTP discharges near the mouth of the Chesapeake Bay, immediately adjacent to the Atlantic Ocean. Although the Bay has undoubtedly suffered from high levels of nutrient inputs from anthropogenic activities [271], point sources represent only a fraction of the nitrogen discharged to the Bay [272]. Additionally, the growth of phytoplankton in response to discharged nutrients in the bay may not be as significant of a problem in winter months. Depending on the ultimate fate of effluent from the Chesapeake-Elizabeth WWTP (which is influenced by hydrodynamics at the mouth of the Bay), the discharged nutrients may or may not influence observable eutrophication

in the Bay. If this is the case, the winter increase in discharged nitrogen and phosphorus with the Seasonal Design may be at little local environmental cost.

5.4. Conclusions

Here we have developed a quantitative sustainable design methodology to evaluate upgrade alternatives for the Chesapeake-Elizabeth WWTP. With a flexible permit structure that allows for variable effluent quality over the course of the year, the opportunity exists to implement operational flexibility in the form of a seasonal secondary treatment process change: from a 5-stage Bardenpho process (in summer) to an A2O process (in winter). By using Monte Carlo, dynamic simulations, LCA, and present worth analysis, we have elucidated the advantages and disadvantages of such an upgrade. Although the Seasonal Design would require a larger capital investment, the differential use of electron donor could result in a payback period of a few years and the upgrade would reduce life cycle environmental impacts in all but one category (eutrophication). The magnitude of operational cost savings and operational environmental impact reductions are highly sensitive to estimated differential electron donor use (between the Standard and Seasonal Designs), but even at equivalent usage rates a net benefit in almost all impact categories would be observed. The opportunity to pursue this level of operational flexibility is made possible by Chesapeake-Elizabeth's annual average permit, which is a result of the sensitivity and flow characteristics of the receiving environment.

Although the stakeholders engaged in this case study were limited to HRSD personnel and consultants, this quantitative sustainable design methodology could also be used to engage a broader set of stakeholders including regulators, representatives from environmental interest groups (e.g., the Conservation Fund), and up-stream utilities in the Chesapeake Bay Watershed. By integrating these WWTP modeling efforts with tributary and Bay models, workshop participants could use this framework to better understand the implications of regulatory and design decisions on specific stakeholders and the larger Chesapeake Bay system. Ultimately, the sustainable design of WWTPs must balance local, regional, and global considerations. From an environmental perspective, designs should (at a minimum) prevent the transgression of thresholds that would result in non-linear impacts and the catastrophic failure of ecosystems. If we entrust regulatory agencies with the protection of our local environment through the

imposition of permits, and we impose those permits as constraints in the design process, we are then free to pursue more sustainable WWTPs through the application of a quantitative sustainable design methodology (presented here) coupled with a larger qualitative planning and design process [24, 252]. The ultimate objective of such a methodology is to advance the performance, social, economic, and environmental sustainability of WWTPs while balancing local objectives with regional and global goals for sustainability.

The framework presented here also offers the opportunity to evaluate the implications of alternative approaches to design. For example, as we expand the traditional design methodology to better address environmental factors, life cycle environmental impacts may be included as part of the objective function or as constraints to the design process. In particular, the inclusion of environmental criteria as constraints has three advantages: (i) it is consistent with today's practice of including performance constraints, (ii) it represents the environment as a limiting factor that requires us to operate within a set of impact boundaries for economic and social systems to be sustained [2], and (iii) it avoids the direct comparison of environmental versus economic trade-offs, as well as trade-offs across environmental criteria that may be incommensurable or incompatible [247]. Although the imposition of additional constraints in a design process tends to lead to lesser designs, such constraints may also push WWTP designers to view process design through a new lens that will inspire novel configurations and design concepts that will advance the various dimensions and scales (spatial and temporal) of sustainability simultaneously.

Chapter 6
A Metabolic Model of Organic Carbon Accumulation by Unicellular Phototrophic Microorganisms for Process Design

J.S. Guest[1], M.C.M. van Loosdrecht[2], S.J. Skerlos[1,3], N.G. Love[1]*

[1] Department of Civil & Environmental Engineering, University of Michigan
[2] Department of Biotechnology, Delft University of Technology
[3] Department of Mechanical Engineering, University of Michigan

6.1. Introduction

Phototrophic microorganisms have significant potential as alternative energy sources in the 21st century. Of particular relevance to energy recovery is the ability of phototrophic microorganisms to accumulate both lipids [146] and polysaccharides [152, 153] for intracellular energy storage. Research into lipid accumulation [145-148] and the conversion of phototrophic microorganisms to biodiesel [58, 61, 62] has rapidly increased in recent years because of its potential implications for transportation-based fuels [150]. There is also interest in polysaccharide storage for energy production [273] or at least the use of polysaccharide residual post-lipid extraction for energy production [274]. To develop enrichment processes for energy production systems with unicellular phototrophic microorganisms, it is helpful to be able to model their diurnal behavior to enhance our understanding of how phototrophs accumulate storage materials, and to apply that knowledge to the development of resource recovery technologies for sewage treatment.

Much like in engineered bioprocesses that use chemotrophic microorganisms [113], storage compounds can provide phototrophic cells with a means to balance their electron donor supply during short-term changes in environmental conditions (e.g., a switch from light to dark conditions [275]). Predicting the conditions that control the rate and extent to which these storage compounds are formed is key to the development of

effective phototroph-based bioprocess technologies. For this reason, computational models are needed that explicitly predict the behavior of storage compounds independent of the rest of the cellular material.

Here we develop a lumped sum metabolic model for carbon-accumulating unicellular phototrophic microorganisms, following the approach used by others for the modeling of polyphosphate [106-109] and glycogen accumulating organisms [110, 111] (PAOs, GAOs). This approach is distinct from recent genome-scale metabolic flux models of phototrophic microorganisms that are designed to evaluate metabolic engineering approaches *in silico* [114, 115], in that the interrelated complex processes occurring simultaneously in the cell are represented as a function of a single parameter upon which all are dependent [105]. The use of lumped sum metabolic models by other disciplines has been used successfully to predict the competitive growth behavior of mixed microbial communities when grown under conditions that impose various selective pressures [104].

We have developed our model using the known metabolic pathways of *Chlamydomonas reinhardtii*, a model green alga. *C. reinhardtii* has been extensively studied [276], its metabolic pathways are well characterized [114, 115, 276], and it is capable of both lipid and polysaccharide storage [277]. Furthermore, as a member of the green algae, it is in the largest taxonomic group in which oleaginous phototrophs have been identified and may be ubiquitous in diverse habitats [154]. Consequently, we believe that *C. reinhardtii* serves as a model organism that is sufficiently representative of phototrophs that are likely to proliferate in bioprocess systems used to recover energy from sewage. To demonstrate the applicability of the model to a mixed phototrophic culture, we performed experiments in flat panel cyclostats originally inoculated with biomass from a pilot-scale phototrophic system at a wastewater treatment plant.

6.2. Experimental Methods

6.2.1. Culturing

Inocula and growth medium. Inocula were collected from an Algae Wheel pilot-plant located after the secondary treatment process at the Hopewell Regional Wastewater Treatment Facility (City of Hopewell, Virginia, U.S.A.). Upon arrival, biomass was homogenized, operated in semi-batch mode for four days with daily light/dark cycles with

increasing light intensity each day, and filtered through a mesh (0.6 mm pore size) before being added to photobioreactors. Cultures were maintained using a modified Allen's BG-11 medium [278] with silicate [279] and adjusted nitrogen and phosphorus concentrations to reduce excess nitrogen but maintain phosphorus-limited growth. Medium was prepared using distilled water (ASTM Type II) with the following nutrient concentrations ($mg \cdot L^{-1}$): $NaNO_3$ (750), K_2HPO_4 (78), $MgSO_4 \cdot 7H_2O$ (75), $CaCl_2$ (27), $Na_2SiO_3 \cdot 9H_2O$ (58), citric acid (6.0), ferric ammonium citrate (6.0), $Na_2 \cdot EDTA \cdot 2H_2O$ (1.04), Na_2CO_3 (20), H_3BO_3 (2.86), $MnSO_4 \cdot H_2O$ (1.55), $ZnSO_4 \cdot 7H_2O$ (0.22), $Na_2MoO_4 \cdot 2H_2O$ (0.39), $CuCl_2 \cdot 2H_2O$ (0.054), $CoCl_2 \cdot 6H_2O$ (0.040). For nitrogen replete and phosphorus replete experiments, additional $NaNO_3$ or K_2HPO_4, respectively, were added to the levels indicated for each experiment.

Photobioreactors. Three flat plate photobioreactors with internal dimensions of 487 mm x 258 mm x 30 mm (height x width x depth) were constructed from 9.5 mm thick UV-stabilized acrylic (Trident Plastics, Inc.; Richmond, Virginia) and filled to 3.0 L. All photobioreactors were operated as cyclostats subjected to a daily light/dark cycle. [Note: Cyclostats are chemostats subjected to repeatedly a varying light or temperature regime where cells are in a dynamic equilibrium of balanced growth and are appropriately poised for the characterization of model parameters [280].] All three cyclostats were operated at a dilution rate of 0.41 d^{-1} +/- 0.01 d^{-1} and subjected to a light:dark regime of 14:10 hours. Light was provided from both sides of the reactors by a total of 16 fluorescent bulbs (Maxum™ 5000 48 inch F40-T12 MB, Full Spectrum Solutions; Jackson, Michigan). The surface irradiance on each side of the cyclostats was 400 +/- 18 $\mu E \cdot m^{-2} \cdot s^{-1}$ PAR (photosynthetically active radiation, 400-700 nm), as measured with a quantum meter (Apogee MQ-303; Logan, Utah). Average irradiance within each reactor was calculated using the following equation, which is based on the Beer-Lambert law (described in more detail in [281]):

$$I_{avg} = 2 \cdot I_0 \cdot \frac{1}{b_{reactor}} \left(1 - e^{-a_C \cdot X_{VSS} \cdot b_{reactor}}\right) \cdot \frac{1}{a_C \cdot X_{VSS}} \qquad \text{(E6.1)}$$

All nomenclature is defined in Section 6.7. The system was vented with a fan to reduce heat buildup, and mixing was achieved by sparging reactors continuously with air at a rate of approximately 0.2-0.3 $L_{air} \cdot L_{reactor}^{-1} \cdot min^{-1}$. pH was maintained below 7.55 (typical pH was 7.35-7.55) using a pH controller (EW-05802-25, Cole Parmer; Vernon Hills, Illinois) that operated solenoid valves to deliver CO_2 gas when needed to decrease the

reactor pH. Photobioreactors were cleaned weekly by temporarily removing biomass, bleaching reactors, and reintroducing biomass after filtration through mesh (0.6 mm pore size). Examples of microscope images from each of the three photobioreactors can be seen in Appendix J.

6.2.2. Analytical Methods

Total and volatile suspended solids. Total solids concentrations (dry mass) were determined in duplicate by filtration through a pre-rinsed, pre-combusted, pre-weighed glass fiber filter with a pore size of 0.7 μm (Whatman GF/F, Item #0987472, Fisher Scientific; Pittsburgh, Pennsylvania) [282]. Filters were dried at 105 °C for at least 1 hour and desiccated for a minimum of 30 minutes prior to weighing. Volatile solids were determined by combusting samples in a muffle furnace at 550 °C for 20 minutes followed by at least 30 minutes of desiccation prior to weighing.

Proteins. Total protein content was measured in duplicate using the micro-bicinchoninic acid (micro BCA) method (Item #23235, Thermo Scientific; Rockford, Illinois) modified with an alkaline digestion step [283] consistent with previous work in our lab [284]. Briefly, cells were resuspended in 1 N NaOH, incubated at 100 °C for 20 minutes, cooled to room temperature, and diluted 1:20 (sample volume:final volume) to dilute the NaOH to 0.05 N prior to the addition of micro BCA reagents and reading absorbance in triplicate microplate wells at 562 nm. Bovine serum albumin (BSA) standards (Item #23210, Thermo Scientific; Rockford, Illinois) were treated identically to samples.

Lipids. Total lipids were measured as fatty acid methyl esters (FAMEs) using the method of Levine and colleagues [285]. Briefly, reactor samples with a known solids concentration were pelleted (2,000xg at 4 °C for 15 minutes) in duplicate glass tubes (targeting 15-40 mg of dry solids per tube) and dried at 65 °C for 16-24 hours prior to storage at 4 °C. Immediately preceding transesterification, acidified methanol was prepared by slow (drop-wise) addition of 5 mL of acetyl chloride to methanol and diluting to 100 mL with methanol. A stir bar and 2 mL of acidified methanol were added to each glass tube with dried biomass pellet before sealing with Teflon-lined caps. Tubes were heated to 100 °C for 90 minutes with vigorous stirring, after which they were allowed to cool before 1 mL of distilled and deionized (ASTM Type I) water was added to stop the reaction. FAMEs were extracted into 4 mL of n-heptane containing 250 mg L^{-1} of

tricosanoic acid methyl ester (C23:0 FAME) as an internal standard (Item #91478, Sigma-Aldrich®; St. Louis, Missouri). Tubes were vortexed for 45 seconds and centrifuged (2,000xg for 10 minutes) before transferring approximately 2 mL of the upper layer of the n-heptane-FAME mixture to a GC vial. FAMEs were identified and quantified by GC-FID with single injections (1 µL; 10:1 split ratio; 260 °C inlet temperature) onto a HP-InnoWax column (30 m x 0.32 mm x 0.25 µm; J&W 1909BD-113, Agilent Technologies; Santa Clara, California) initially at 150 °C. After a 3 min hold, the temperature was ramped at 6 °C·min^{-1} to 260 °C and held for 9 min. Helium was the carrier gas at a constant flow rate of 1.0 mL·min^{-1}. FID detector temperature was 300 °C, and N_2 served as the makeup gas (25 mL·min^{-1}). The relative standard deviation of the internal standard across all runs was 0.9% and duplicate injections were shown to differ 1.5% on average for total lipids. Peaks were identified using an analytical standard (Supelco® 37 Component FAME Mix, Item #47885-U, Sigma-Aldrich®; St. Louis, Missouri) and quantified assuming the response ratio of each FAME (mg FAME·peak area^{-1}) was equal to that of the internal standard (consistent with EN14103 [286] with use of C23:0 in place of C17:0). The method used to compartmentalize measured lipid concentrations into (i) storage polymers and (ii) functional lipids (i.e., lipids fulfilling any role other than energy storage) is described in Section 6.4.1.

Carbohydrates. Total and soluble (i.e., non-pelletable) carbohydrates were measured in duplicate using the method of Dubois [287] with the following modifications. After the addition of 80% phenol and sulfuric acid, samples were digested at 90 °C for 5 minutes and allowed to cool to room temperature for 30 minutes in the dark before reading absorbance in triplicate wells at 490 nm using a µQuant microplate reader (Item #MQX200, BioTek; Winooski, Vermont). This process included the digestion step; however, it was not expected to measure all cell-associated carbohydrates. Although a short, heated digestion has been shown to consistently quantify intracellular carbohydrate-based storage polymers, a much longer digestion process may be required to make cellular structural components available for colorimetric measurement [288]. For the purposes of this study, we were particularly interested in the accumulation or depletion of storage polymers, which were expected to be readily measured with the short digestion. The method used to compartmentalize measured carbohydrate concentrations into (i) storage polymers and (ii) functional carbohydrates (i.e., carbohydrates fulfilling any role other than energy storage) is described in Section 6.4.1.

Nitrate and soluble phosphate. Samples were filtered through pre-rinsed 0.22 μm membranes (Item #GSWP 025 00, Fisher Scientific; Pittsburgh, Pennsylvania) prior to storage. Nitrate samples were stored in plastic centrifuge tubes at -20 °C until analysis. Nitrate concentrations were determined via triplicate injections using a DX-100 Ion Chromatograph (Dionex; Sunnyvale, California) with RFIC IonPac AG16 guard column, an IonPac AS14 analytical column, and eluent containing 3.5 mM Na_2CO_3 and 1.0 mM $NaHCO_3$. Soluble phosphorus samples were stored at 4 °C in acid-washed (HCl) glassware until analysis. Phosphate was quantified via the ascorbic acid method (Method 4500-P-E; [289]) modified for analysis in a microplate.

6.3. Model Formulation

6.3.1. Metabolism

The metabolic model consists of a total of 10 reactions (Figure 6.1), the details of which can be seen in Table 6.1 and are discussed in more detail below. Although many of the reactions specified are common among phototrophic microorganisms, the metabolic pathways used to construct the model are based on *C. reinhardtii* as a model organism.

With light as their energy source, phototrophs carry out light-dependent reactions to generate ATP, $NADPH_2$, and oxygen (from H_2O), and light-independent reactions (commonly referred to as “dark reactions”) to convert carbon dioxide (CO_2) into organic matter. Once CO_2 is fixed into organic matter, that material may be built into biomass, stored as intracellular polyglucose (X_{PG}) or triacylglycerol (X_{TAG}), or metabolized via oxidative phosphorylation. In addition to metabolizing recently-fixed organic carbon, most phototrophs are capable of utilizing stored or extracellular organic carbon as an energy (and carbon) source. Although cells differ in their ability to use various forms of extracellular organic carbon [290], it is reasonable to assume that all cells are capable of metabolizing intracellular organic carbon pools that they themselves stored. For the purposes of this model, it is assumed that cells do not use extracellular organic carbon (either because of a lack of availability or a lack of ability), and instead only grow heterotrophically (or mixotrophically) using stored organic carbon (as X_{PG} or X_{TAG}) as their energy and carbon source.

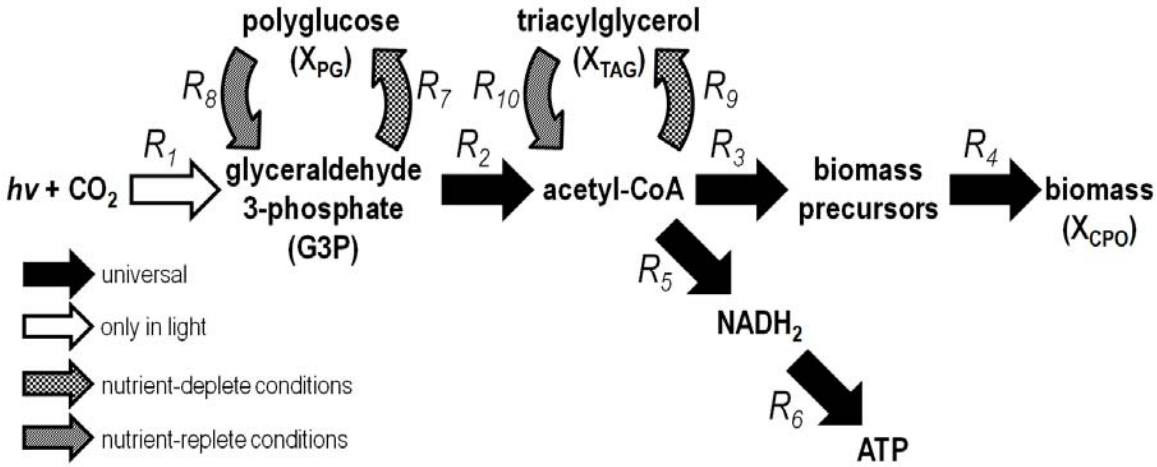

Figure 6.1. Schematic representation of the lumped sum metabolic model for carbon-accumulating phototrophic organisms (X_{CPO}) capable of accumulating intracellular lipids (as triacylglycerol, X_{TAG}) and polysaccharides (as polyglucose, X_{PG}).

Table 6.1. Summary of reactions included in the metabolic model on a C-mole basis.

Rate	Reaction	Stoichiometry	Citations
R_1	Synthesis of G3P from CO_2	α_p *hv* + CO_2 → $^1/_3$ G3P + O_2	[291, 292]
R_2	Synthesis of acetyl-CoA from G3P	$^1/_3$ G3P → $^1/_3$ acetyl-CoA + $^2/_3$ $NADH_2$ + $^2/_3$ ATP + $^1/_3$ CO_2	[114, 115]
R_3	Synthesis of biomass precursors from acetyl-CoA	½ (1 + δ_x + δ_N) acetyl-S-CoA + 0.2 NO_3^- + (α_m – ½ δ_N) ATP → $CH_{1.8}O_{0.5}N_{0.2}$ + (δ_x + δ_N) CO_2 + (2 δ_x – 0.1) $NADH_2$	[112, 293]
R_4	Polymerization of biomass precursors & maintenance	$CH_{1.8}O_{0.5}N_{0.2}$ + $\left(\alpha_X + \frac{m_{ATP}}{\mu}\right)$ ATP → $\frac{1}{n}$ $(CH_{1.8}O_{0.5}N_{0.2})_n$	[112, 294]
R_5	Carbon source catabolism	$^1/_2$ acetyl-CoA → 1 CO_2 + $^3/_2$ $NADH_2$ + $^1/_2$ $FADH_2$ + $^1/_2$ ATP	[115]
R_6	Oxidative phosphorylation	1 $NADH_2$ + $^1/_2$ O_2 → δ_{PO} ATP	[105, 295]
R_7	Synthesis of PG from G3P	$^1/_3$ G3P + $^1/_6$ $(glucose)_n$ + $^1/_6$ ATP → $^1/_6$ $(glucose)_{n+1}$	[296, 297] [114, 115]
R_8	Synthesis of G3P from PG	$^1/_6$ $(glucose)_{n+1}$ + $^1/_6$ ATP → $^1/_6$ $(glucose)_n$ + $^1/_3$ G3P	[298]
R_9	Synthesis of TAG from acetyl-CoA	$^{25}/_{51}$ acetyl-CoA + $^{23}/_{51}$ ATP + $^{42}/_{51}$ $NADPH_2$ + $^3/_{51}$ $NADH_2$ + $^1/_{51}$ CO_2 → $^1/_{51}$ TAG	[114, 154]
R_{10}	Synthesis of acetyl-CoA from TAG	$^1/_{51}$ TAG + $^2/_{51}$ ATP → $^{24}/_{51}$ $NADH_2$ + $^{21}/_{51}$ $FADH_2$ + $^1/_{51}$ CO_2 + $^{25}/_{51}$ acetyl-CoA	[115, 298]

Photosynthesis and production of acetyl-CoA. It is assumed that the end products of photosynthesis (**R_1**) are glyceraldehyde-3-phosphate (G3P) and diatomic oxygen (O_2).

Although cells may have auxiliary routes of electron transfer to match energy and reducing power conversion (from light energy) with metabolic needs [292] – including the use of cyclic photophosphorylation for additional ATP during photoautotrophic growth [299] – we assume these pathways are active at a rate designed to meet the ATP and $NADPH_2$ needs of carbon fixation and no more [291]. Once G3P is produced, it is converted to pyruvate via the Embden-Meyerhof-Parnas (EMP) pathway [115] and decarboxylated to form acetyl-CoA [114] (**R_2**).

Biomass synthesis. The synthesis of active biomass (anabolism) was assumed to take place in two steps [112]: (i) the synthesis of biomass precursors (monomers including amino acids, hexose, ribose, deoxyribose, fatty acid, etc.), **R_3**; and (ii) the polymerization of those precursors into active biomass (X_{CPO}), **R_4**. The elemental biomass composition of phototrophic microorganisms (and composition of biomass precursors) was initially assumed to be $CH_{1.8}O_{0.5}N_{0.2}$ based on the observations of Roels for a range of microorganisms [293]. Production of biomass precursors was assumed to occur with some fraction, δ_x, of acetyl-CoA being dissimilated to generate reducing equivalents [300], and an additional fraction (δ_N) required for the reduction of nitrate prior to assimilation (Table 6.2). The value for δ_N assumes the reducing power was generated via catabolism, R_5, and ATP generated during catabolism offsets ATP needs during polymerization of active biomass, R_3. The polymerization of biomass precursors and maintenance followed the approach of van Aalst-van Leeuwen and colleagues [112], with an assumed value, α_x, for the amount of ATP required for polymerization of precursors to active biomass [294]. The specific ATP consumption due to maintenance (m_{ATP}) must be calculated based on observation, and was assumed to be constant (consistent with Beeftink [301] and others).

Catabolism and oxidative phosphorylation. It was assumed that catabolism of acetyl-CoA (**R_5**) occurs via the tricarboxylic acid (TCA) cycle [115], resulting in the production of $NADH_2$. To meet energy demands in the cell, ATP may then be produced from $NADH_2$ via oxidative phosphorylation (**R_6**). The efficiency of this process can be expressed as the P/O ratio (δ_{PO}), which represents the moles of ATP produced per mole of $NADH_2$ oxidized [105]. Although the P/O ratio can vary with growth conditions [295], we follow the typical approach to lumped-sum metabolic modeling by maintaining a fixed ratio [302-304].

Polyglucose (PG) storage and mobilization. Phototrophic microorganisms have been shown to store polysaccharides in numerous forms including starch (e.g., green algae [296, 297]), chrysolaminarin (e.g., diatoms [305]), and glycogen (e.g., cyanobacteria [306]). Many of these storage polymers are formed simply by condensation of nucleoside diphosphate sugars [297, 298, 305]. Assuming that G3P is converted to glucose 6-phosphate via gluconeogenesis [114, 115], the only ATP expense of its storage is for polymerization at a cost of 1 ATP per molecule of glucose. It was assumed here, therefore, that the storage of polysaccharides is simply in the form of polyglucose ($\mathbf{R_7}$), which is equivalent to starch or glycogen. For the mobilization of stored PG reserves ($\mathbf{R_8}$), glucose monomers are removed from intracellular PG chains in the form of glucose 6-phosphate, which was then assumed to be converted to G3P via the EMP pathway.

Triacylglycerol (TAG) storage and mobilization. Phototrophic microorganisms have been shown to store lipids in numerous forms. Of particular relevance to downstream energy harvesting processes is the storage of neutral lipids, which are often produced in the form of triacylglycerol (TAG) comprised of long-chain fatty acids (C:16 to C:18) [154]. It was assumed here that fatty acids ultimately stored as neutral lipids are synthesized from acetyl-CoA to form palmitic acid (C:16) and attached to a glycerol molecule at the termination of synthesis, resulting in TAG with an elemental composition of $C_{51}H_{98}O_6$ ($\mathbf{R_9}$). It was assumed that G3P will be present in the cell during TAG synthesis and will be the precursor for glycerol. For the purposes of this model, therefore, acetyl-CoA is reverted back to G3P by simply reversing $\mathbf{R_2}$, and G3P is then converted to L-glycerol 3-phosphate. It was assumed that ATP is only required for the production of palmitic acid from acetyl-CoA, and no ATP is required for the activation of the palmitic acid molecules during TAG synthesis [114]. For the mobilization of TAG reserves ($\mathbf{R_{10}}$), TAG is first hydrolyzed to glycerol and fatty acids by lipases. Glycerol is then phosphorylated to glycerol 3-phosphate and oxidized to dihydroxyacetone phosphate, which is then isomerized to G3P [115]. Palmitate requires 1 ATP for activation to palmitoyl-CoA [298] before being degraded to 8 molecules of acetyl-CoA while producing both $FADH_2$ and $NADH_2$.

Table 6.2. Metabolic model parameter descriptions and value estimates.

Parameter	Description	Estimated Value	Units
δ_x	CO_2 production from the synthesis of 1 C-mole of biomass from acetyl-CoA	0.266[a]	C-moles of CO_2 produced per C-mole of biomass
δ_N	CO_2 production from the catabolism of acetyl-CoA to generate reducing power for NO_3^- reduction for assimilation.	0.436[b]	C-moles of CO_2 produced per C-mole of biomass
α_M	ATP requirement for synthesis of biomass precursors from acetyl-CoA	0.66[c]	moles ATP per C-mole of biomass
α_X	ATP required for polymerization of biomass precursors (monomers) to active biomass	1.5[d]	moles of ATP per C-mole of biomass
δ_{PO}	efficiency of oxidative phosphorylation (P/O ratio) in mitochondria	2.0[e]	moles of ATP produced per mole of $NADH_2$ oxidized

[a] Acetate via the glyoxylate cycle and isocitrate-lyase [300].

[b] Calculated based on the molar ratio of 0.2 moles of N required per C-mole of biomass formed and the requirement of 8 electrons per mole of N reduced from NO_3^- to NH_3. Reducing power was assumed to be generated via acetyl-CoA catabolism (R_5).

[c] [295], consistent with assumption by [112]

[d] [294] consistent with assumption by [112]

[e] [307]

6.3.2. Determination of Model Stoichiometry

Although not all of the internal reactions identified above can be measured, these reactions can be related to observable rates to enable modeling of the system [105]. First, linear equations representing the rate of change of each component in the metabolic model were written for each of two metabolic conditions: (i) nutrient-replete conditions (Appendix K; Table K2), when cells mobilize carbon reserves, and (ii) nutrient-deplete conditions (Appendix K; Table K3), when cells store organic carbon. Each set of linear equations included a degree of reduction balance [293] and – consistent with past lumped-sum metabolic models [109, 112] – assumes that there was no net accumulation of $NADH_2$, ATP, biomass precursors, acetyl-CoA, or G3P. Linear equations were solved using Wolfram Mathematica 8.0.1.0 (Wolfram Research, Inc.; Champaign, IL) to determine stoichiometric relationships among *specific* rates (where "specific" means the rate has been normalized to biomass concentration): phototrophic carbon fixation (q_{phot}); growth (μ); PG formation (q_{PG}); TAG formation (q_{TAG}); and

maintenance (m_{ATP}). Linear equation solutions and corresponding stoichiometric constants may be found in Table 6.3.

Table 6.3. Linear equation solutions and derived stoichiometric yields.

Description [Units]	**Nutrient-Replete Metabolism**	**Nutrient-Deplete Metabolism**
Linear Equation Solutions		
Specific Rate of Photosynthesis [(C-moles CO_2 fixed to G3P)·(C-mole biomass)$^{-1}$·(hr)$^{-1}$]	$q_{PHOT}^{NR} = \frac{\mu^{NR}}{Y_{XCPO}^{NR}} + \frac{q_{PG}^{NR}}{Y_{PG}^{NR}} + \frac{q_{TAG}^{NR}}{Y_{TAG}^{NR}} + \frac{m_{ATP}^{NR}}{Y_{ATP}^{NR}}$	$q_{PHOT}^{ND} = \frac{\mu^{ND}}{Y_{XCPO}^{ND}} + \frac{q_{PG}^{ND}}{Y_{PG}^{ND}} + \frac{q_{TAG}^{ND}}{Y_{TAG}^{ND}} + \frac{m_{ATP}^{ND}}{Y_{ATP}^{ND}}$
Specific Rate of CO_2 Production [(C-moles CO_2)·(C-mole biomass)$^{-1}$·(hr)$^{-1}$]	$q_{CO2}^{NR} = -\mu^{NR} - q_{PG}^{NR} - q_{TAG}^{NR}$	$q_{CO2}^{ND} = -\mu^{ND} - q_{PG}^{ND} - q_{TAG}^{ND}$
Specific Rate of O_2 Production [(C-moles O_2)·(C-mole biomass)$^{-1}$·(hr)$^{-1}$]	$q_{O2}^{NR} = \frac{1479}{1020}\,\mu^{NR} + q_{PG}^{NR} + \frac{145}{102}\,q_{TAG}^{NR}$	$q_{O2}^{ND} = \frac{1479}{1020}\,\mu^{ND} + q_{PG}^{ND} + \frac{145}{102}\,q_{TAG}^{ND}$
Stoichiometric Yields		
yield of PG on CO_2 fixed to G3P [(C-moles PG)·(C-mole CO_2 fixed to G3P)$^{-1}$]	$Y_{PG}^{NR} = \frac{18 + 34\,\delta_{PO}}{15 + 34\,\delta_{PO}}$	$Y_{PG}^{ND} = \frac{18 + 34\,\delta_{PO}}{21 + 34\,\delta_{PO}}$
yield of TAG on CO_2 fixed to G3P [(C-moles TAG)·(C-mole CO_2 fixed to G3P)$^{-1}$]	$Y_{TAG}^{NR} = \frac{153 + 289\,\delta_{PO}}{69 + 389\,\delta_{PO}}$	$Y_{TAG}^{ND} = \frac{153 + 289\,\delta_{PO}}{144 + 410\,\delta_{PO}}$
yield of biomass on CO_2 fixed to G3P [(C-moles biomass)·(C-mole CO_2 fixed to G3P)$^{-1}$]	$Y_{XCPO}^{NR} = Y_{XCPO}^{ND} = \frac{90 + 170\delta_{PO}}{45 + 90\,\alpha_m + 90\,\alpha_X + 174\,\delta_{PO} + 165\,\delta_{PO}\delta_N + 45\,\delta_X - 15\,\delta_{PO}\delta_X}$	
yield of ATP on CO_2 fixed to G3P [(moles of ATP)·(C-mole CO_2 fixed to G3P)$^{-1}$]	$Y_{ATP}^{NR} = Y_{ATP}^{ND} = \frac{9 + 17\,\delta_{PO}}{9}$	

* Note: The coefficient in front of the mu in the O_2 production calcs would be 1071/1020 rather than 1479/1020 if ammonia were the nitrogen source.

6.3.3. Kinetic Modeling

The structure of the kinetic model was established using (i) the linear equation solutions presented in Table 6.3, (ii) kinetic models and data from the literature, and (iii) experimental data from batch and cyclostat operation of all three photobioreactors.

Nutrient uptake. Consistent with the extensive literature on phytoplankton modeling, it was assumed that nutrient (N and P) uptake followed Michaelis-Menten kinetics [308]

and that growth would be limited by a single nutrient following Droop formulation (i.e., cell quota model) [309]. One modification to the cell quota model was to raise the expression of relative pool size (the minimum N or P ratio divided by the actual ratio, or Q_{min}/Q) to the power of 4. This modification was made after experimental observations showed that organic carbon storage occurred rapidly upon nutrient depletion. It is worth noting that empirical corrections to response functions (i.e., applying exponents to curves with values from 0 to 1) are not without precedent in phytoplankton modeling [310].

Nutrient uptake was assumed to be independent of internal stores of the respective nutrient [308]. Eventually we may consider including switching functions such that uptake of all nutrients will cease as any nutrient (N or P) becomes limiting [311, 312]; however, this has not been included in the current version of the model. To account for changing growth rates under dark conditions, a dark reduction term, η_{dark}, was added to nutrient uptake rates (a similar but simplified approach as compared to [313]).

Phototrophic kinetics. The light-dependency of photoautotrophic growth was approached as in the PHOBIA model [183] but with one modification (the introduction of K_γ, discussed below). Briefly, light dependency was modeled using the Eilers-Peeters relationship [314], which includes the effects of photoinhibition at high levels of irradiance. Photoadaptation was addressed using the approach of Duarte and Ferreira [315] by including chlorophyll:carbon ratio as a state variable, R, which influences the initial slope of the photosynthesis-irradiance curve. The final expression, f_I, expressing the cell's maximum relative photosynthetic productivity at time t (as a unitless term with a value from 0 to 1) becomes:

$$f_I = \frac{I}{I + I_n \cdot (0.25 - 5R) \cdot \left(\frac{I^2}{I_{opt}^2} - \frac{2 \cdot I}{I_{opt}} + 1 \right)} \quad \text{(E6.2)}$$

Distinct from previous works, the adaptation of the chlorophyll:carbon ratio (originally characterized by [316]) was modified to be a continuous equation for convenience. This was achieved with the addition of K_γ in the first parenthetical expression in the photoadaptation rate equation (Table 6.5).

Organic carbon storage. It has been widely observed that many phototrophic microorganisms accumulate lipids under lit conditions in the absence of nitrogen,

although phosphorus has mixed impacts on lipid storage in eukaryotic algae [146]. Additionally, some species have been observed to accumulate polysaccharides in the absence of nitrogen [152, 153]. Based on our experimental results, it was assumed that TAG and PG storage occur when growth is arrested due to lacking nitrogen, and that PG storage (but not TAG storage) occurs when growth is arrested due to phosphorus. It was also assumed that cells have some maximum possible storage capacity per cell for both PG (f_{PG}^{max}) and TAG (f_{TAG}^{max}). Consistent with modeling of polyhydroxybutyrate storage kinetics [317], it was assumed that cells accumulate polysaccharides and lipids at the greatest rate when none are within the cell and that they gradually decrease their rate of accumulation as they approach their maximum storage capacity. In the absence of compelling evidence to suggest the rate expressions for accumulation are more complex, we chose the relatively simple representation of:

$$\frac{q_{PG}}{\hat{q}_{PG}} = 1 - \left(\frac{f_{PG}}{f_{PG}^{max}}\right)^{\beta_1} \quad \text{(E6.3)}$$

$$\frac{q_{TAG}}{\hat{q}_{TAG}} = 1 - \left(\frac{f_{TAG}}{f_{TAG}^{max}}\right)^{\beta_2} \quad \text{(E6.4)}$$

where f_{PG} and f_{TAG} are the relative fractions of stored substrate with units of C-moles of PG or TAG per C-mole of biomass, respectively.

Mobilization of stored organic carbon. It was assumed that stored substrate degradation was limited by nitrogen, phosphorus, or the relative fraction of stored substrate (as f_{PG} and f_{TAG}). Based on the assumption that all cells (X_{CPO}) in the cyclostats have the ability to store both PG and TAG, and that stored PG (X_{PG}) and TAG (X_{TAG}) in the reactor are divided evenly among the cells, the rates of degradation of X_{PG} and X_{TAG} must be linked to prevent unrealistic growth rates. To this end, the relative fractions of each storage polymer were transformed to equivalent units and combined to create a new term, f_s, representing the relative fraction of stored substrate (C-moles of PG equivalents per C-mole of biomass):

$$f_S(t) = f_{PG}(t) + f_{TAG}(t) \cdot \frac{Y_{PG}^{NR}}{Y_{TAG}^{NR}} \quad \text{(E6.5)}$$

An important note is that the X_{PG} and X_{TAG} utilization equations (for growth and for maintenance) are structured such that X_{PG} will be used simultaneously with X_{TAG}.

Although recent findings of Siaut and colleagues showed that stored polysaccharides were mobilized before stored lipids when cultures of *C. reinhardtii* were switched from lit, nutrient-deplete conditions to dark, nutrient-replete conditions [277], stored X_{PG} and X_{TAG} were frequently mobilized simultaneously in many of the mixed cultures tested here. X_{PG} and X_{TAG} utilization did, however, differ in the rate and extent of their degradation, where X_{PG} was regularly degraded more rapidly and to a greater extent than X_{TAG}. To address this, a term "ρ" was added to the Monod expression to account for the disproportional rate and extent of mobilization of X_{PG}, such that the relative rates of growth on X_{PG} and X_{TAG} could be described as:

$$\frac{\mu_{XCPO}}{\widehat{\mu}_{XCPO}} = \frac{\rho f_{PG}}{K_{STO} + \rho f_{PG} + f_{TAG} \cdot \frac{Y_{PG}^{NR}}{Y_{TAG}^{NR}}} \quad \text{(E6.6)}$$

and

$$\frac{\mu_{XCPO}}{\widehat{\mu}_{XCPO}} = \frac{f_{TAG} \cdot \frac{Y_{PG}^{NR}}{Y_{TAG}^{NR}}}{K_{STO} + \rho f_{PG} + f_{TAG} \cdot \frac{Y_{PG}^{NR}}{Y_{TAG}^{NR}}} \quad \text{(E6.7)}$$

Maintenance and endogenous respiration. Consistent with assumptions by Beeftink [301] and others (e.g., [302]), it was assumed that the specific maintenance rate (in units of moles ATP per C-mole biomass per time) was constant. The maintenance ATP demand was distributed between the degradation of X_{PG} and X_{TAG} when available, supplemented with endogenous respiration as needed. The approach followed that of Beeftink and colleagues [301] who reconciled the models of Herbert [318] and Pirt [319]. This approach results in maintenance energy demand being met exclusively by stored substrate as f_{PG} and f_{TAG} approach f_{PG}^{max} and f_{TAG}^{max}, respectively, and by endogenous respiration as f_{PG} and f_{TAG} approach zero.

6.3.4. Model Structure

In accordance with the format of presentation of other process models [320], a Petersen Matrix [321] was used. A Petersen Matrix consists of a stoichiometric matrix (Table 6.4) and a vector of transformation rate equations (Table 6.5). The state variables and transformation processes are characterized with indices *i* and *j*, respectively. The stoichiometric coefficients are presented in the stoichiometric matrix (v_{ji}), and

transformation rate equations are presented as vector ρ_j. The rate of production of component *i* (in units of $Mass_i \cdot Length^{-3} \cdot Time^{-1}$), therefore, is the sum of each stoichiometric coefficient in column *i* multiplied by each transformation rate *j* ($r_i = \sum v_{ji} \cdot \rho_j$; over all processes *j*).

Table 6.4. Stoichiometric matrix of model processes.

Process	State Variable									
	R g-(Chl)·g-(C)$^{-1}$	**X_{CPO}** moles-(C)·L^{-1}	**X_{PG}** moles-(C)·L^{-1}	**X_{TAG}** moles-(C)·L^{-1}	**S_{CO2}** moles-(C)·L^{-1}	**S_{O2}** moles-(O_2)·L^{-1}	**S_{NO}** moles-(N)·L^{-1}	**S_P** moles-(P)·L^{-1}	**X_{NO}** moles-(N)·L^{-1}	**X_P** moles-(P)·L^{-1}
Photoadaptation (P_1)	1									
Nitrate Uptake (P_2)							-1		1	
Phosphorus Uptake (P_3)								-1		1
Photoautotrophic Growth (P_4)		1			-1	$\frac{1479}{1020}$			$-Q_{N,min}$	$-Q_{P,min}$
Growth on Stored PG (P_5)		1	$-\frac{Y_{PG}^{NR}}{Y_{XCPO}}$		$\frac{Y_{PG}^{NR}}{Y_{XCPO}} - 1$	$-\frac{Y_{PG}^{NR}}{Y_{XCPO}} + \frac{1479}{1020}$			$-Q_{N,min}$	$-Q_{P,min}$
Growth on Stored TAG (P_6)		1		$-\frac{Y_{TAG}^{NR}}{Y_{XCPO}}$	$\frac{Y_{TAG}^{NR}}{Y_{XCPO}} - 1$	$-\frac{Y_{TAG}^{NR}}{Y_{XCPO}}\frac{145}{102} + \frac{1479}{1020}$			$-Q_{N,min}$	$-Q_{P,min}$
PG Degradation for Maintenance (P_7)			-1		1	-1				
TAG Degradation for Maintenance (P_8)				-1	1	$-\frac{145}{102}$				
Endogenous Respiration (P_9)		-1			1	$-\frac{1479}{1020}$			*	*
PG Storage (P_{10})			1		-1	1				
TAG Storage (P_{11})				1	-1	$\frac{145}{102}$				

** X_{CPO}-associated nitrogen and phosphorus was assumed to not be bioavailable after endogenous respiration. Inert material (including inert N and P) was not included in this model formulation.*

Table 6.5. Kinetic equations for model processes.

Process [units]	Rate
Photoadaptation (P_1) [g-(Chl)·g-(C)$^{-1}$·hr^{-1}]	$\left(\frac{0.2 * \frac{I}{I_n}}{K_\gamma + \frac{I}{I_n}}\right) \cdot \left(0.01 + 0.03\frac{\ln\left(\frac{I}{I_n} + 0.005\right)}{\ln(0.01)} - R\right)$
Nitrate Uptake (P_2) [moles-(N)·L^{-1}·hr^{-1}]	$\hat{V}_{NO} \cdot \frac{S_{NO}}{K_{NO} + S_{NO}} \cdot \max[f_I, \eta_{dark}] \cdot X_{CPO}$
Phosphorus Uptake (P_3) [moles-(P)·L^{-1}·hr^{-1}]	$\hat{V}_P \cdot \frac{S_P}{K_P + S_P} \cdot \max[f_I, \eta_{dark}] \cdot X_{CPO}$
Photoautotrophic Growth (P_4) [moles-(biomass as C)·L^{-1}·hr^{-1}]	$\hat{\mu}_{XCPO} \cdot \min\left[1 - \left(\frac{Q_{N,min}}{Q_N}\right)^4, 1 - \left(\frac{Q_{P,min}}{Q_P}\right)^4\right] \cdot \min\left[f_I, \left(1 - \frac{\rho f_{PG} + f_{TAG} \cdot \frac{Y_{PG}^{NR}}{Y_{TAG}^{NR}}}{K_{STO} + \rho f_{PG} + f_{TAG} \cdot \frac{Y_{PG}^{NR}}{Y_{TAG}^{NR}}}\right)\right] \cdot X_{CPO}$
Growth on Stored PG (P_5) [moles-(biomass as C)·L^{-1}·hr^{-1}]	$\hat{\mu}_{XCPO} \cdot \min\left[1 - \left(\frac{Q_{N,min}}{Q_N}\right)^4, 1 - \left(\frac{Q_{P,min}}{Q_P}\right)^4\right] \cdot \left(\frac{\rho f_{PG}}{K_{STO} + \rho f_{PG} + f_{TAG} \cdot \frac{Y_{PG}^{NR}}{Y_{TAG}^{NR}}}\right) \cdot X_{CPO}$
Growth on Stored TAG (P_6) [moles-(biomass as C)·L^{-1}·hr^{-1}]	$\hat{\mu}_{XCPO} \cdot \min\left[1 - \left(\frac{Q_{N,min}}{Q_N}\right)^4, 1 - \left(\frac{Q_{P,min}}{Q_P}\right)^4\right] \cdot \left(\frac{f_{TAG} \cdot \frac{Y_{PG}^{NR}}{Y_{TAG}^{NR}}}{K_{STO} + \rho f_{PG} + f_{TAG} \cdot \frac{Y_{PG}^{NR}}{Y_{TAG}^{NR}}}\right) \cdot X_{CPO}$
PG Degradation for Maintenance (P_7) [moles-(PG as C)·L^{-1}·hr^{-1}]	$m_{ATP} \cdot \left(\frac{Y_{PG}^{NR}}{Y_{ATP}}\right) \cdot \left(\frac{\rho f_{PG}}{K_{STO} + \rho f_{PG} + f_{TAG} \cdot \frac{Y_{PG}^{NR}}{Y_{TAG}^{NR}}}\right) \cdot X_{CPO}$
TAG Degradation for Maintenance (P_8) [moles-(TAG as C)·L^{-1}·hr^{-1}]	$m_{ATP} \cdot \left(\frac{Y_{TAG}^{NR}}{Y_{ATP}}\right) \cdot \left(\frac{f_{TAG} \cdot \frac{Y_{PG}^{NR}}{Y_{TAG}^{NR}}}{K_{STO} + \rho f_{PG} + f_{TAG} \cdot \frac{Y_{PG}^{NR}}{Y_{TAG}^{NR}}}\right) \cdot X_{CPO}$
Endogenous Respiration (P_9) [moles-(biomass as C)·L^{-1}·hr^{-1}]	$m_{ATP} \cdot \left(\frac{Y_{XCPO}}{Y_{ATP}}\right) \cdot \left(1 - \frac{\rho f_{PG} + f_{TAG} \cdot \frac{Y_{PG}^{NR}}{Y_{TAG}^{NR}}}{K_{STO} + \rho f_{PG} + f_{TAG} \cdot \frac{Y_{PG}^{NR}}{Y_{TAG}^{NR}}}\right) \cdot X_{CPO}$
PG Storage (P_{10}) [moles-(PG as C)·L^{-1}·hr^{-1}]	$\hat{q}_{PG} \cdot \left(1 - \left(\frac{f_{PG}}{f_{PG}^{MAX}}\right)^{\beta_1}\right) \cdot \max\left[\left(\frac{Q_{N,min}}{Q_N}\right)^4, \left(\frac{Q_{P,min}}{Q_P}\right)^4\right] \cdot f_I \cdot X_{CPO}$
TAG Storage (P_{11}) [moles-(TAG as C)·L^{-1}·hr^{-1}]	$\hat{q}_{TAG} \cdot \left(1 - \left(\frac{f_{TAG}}{f_{TAG}^{MAX}}\right)^{\beta_2}\right) \cdot \left(\frac{Q_{N,min}}{Q_N}\right)^4 \cdot f_I \cdot X_{CPO}$

6.3.5. Model Calibration and Validation

Model calibration. For calibration of kinetic parameters, batch studies were conducted by stopping influent and effluent flow from the reactor and altering the light:dark regime. Reactors were spiked with nitrogen, phosphorus, and micronutrients as needed to observe nutrient replete, N-limited, and P-limited conditions under both lit and dark scenarios for extended periods of time (3-6 days). All calibration studies were run at the same light intensity as the cyclostat daytime operation. All trends (e.g., mobilization of stored X_{PG} and X_{TAG} in the dark) were observed in at least two reactors, but calibration and validation was done using only data from photobioreactor 3.

The model was calibrated by minimizing the total relative error between measured and modeled data, where relative error (RE) for a given compound (*k*) across the number of time points (N) was defined as follows [302]:

$$\mathrm{RE}_k = \sum_{i=1}^{\mathrm{N}} \left[\frac{n_k^{\mathrm{measured}}(\mathrm{t}_i) - n_k^{\mathrm{model}}(\mathrm{t}_i)}{n_k^{\mathrm{measured}}(\mathrm{t}_i)} \right]^2 \quad \text{(E6.8)}$$

The total error between experimental data and the model was the sum of the relative error across all time points for X_{CPO}, f_{PG}, and f_{TAG}. Measurements were taken for all compounds at all time points, and relative errors for each indicator and each time point were weighted equally. Thus:

$$\text{Total Relative Error} = \sum \mathrm{RE}_k \quad \text{(E6.9)}$$

where k = X_{CPO}, f_{PG}, and f_{TAG}.

Model calibration was achieved iteratively using data from three batch experiments on a single photobioreactor. For the light and dark growth studies, initial relative cell quotas (the ratio Q/Q_{min}) were independently calibrated to any value between 1 and 3 based on the maximum observed biomass concentration during the batch study. Initial relative quotas of 1.0 were used for the organic carbon accumulation study. First, the maximum specific X_{PG} storage rate ($\hat{q}_{PG}$), maximum specific X_{TAG} storage rate ($\hat{q}_{TAG}$), maximum fraction of stored X_{PG} (f_{PG}^{MAX}), maximum fraction of stored X_{TAG} (f_{TAG}^{MAX}), and storage inhibition constants (β_1 and β_2) were estimated using data from a batch study under lit, nitrogen-deplete conditions. Next, the maximum specific growth rate ($\hat{\mu}_{XCPO}$), the stored substrate saturation constant (K_{STO}), optimal irradiance (I_{OPT}), PG relative preference

factor (ρ), maximum nutrient uptake rates ($\widehat{V}_{NO}$ and $\widehat{V}_{P}$) and dark reduction factor (η_{dark}), and the specific maintenance rate (m_{ATP}) were estimated was estimated using data from a batch studies under lit and dark, nutrient-replete conditions. All parameter estimations were achieved using the GRG Nonlinear solver tool using forward derivatives in Microsoft Excel.

Model validation. For the validation study, a single photobioreactor was operated in batch mode with a 14 hour light period under reduced irradiance followed by a 10 hour dark period. The surface irradiance during the light cycle was 150 +/- 6 $\mu E \cdot m^{-2} \cdot s^{-1}$ PAR. Soluble phosphorus was maintained in excess of 8 mg-(P)$\cdot L^{-1}$ with a spike of nitrate at the start of the light (30 mg-(N)$\cdot L^{-1}$) and dark (200 mg-(N)$\cdot L^{-1}$) cycles.

6.4. Results and Discussion

6.4.1. Normalization of X_{CPO}

To calibrate and validate the model, it was necessary to convert experimental measurements of VSS, protein, lipids, and carbohydrates into concentrations of X_{CPO}, X_{TAG}, and X_{PG}. It was assumed that functional biomass, X_{CPO}, consisted of protein, lipids, carbohydrates, and some additional material contributed to its mass (this would include nucleic acids as well as cell-associated carbohydrates that were not measured with the rapid acid digestion method). It was also assumed that X_{CPO} would have a constant relative composition, meaning a constant ratio among its cell components. Protein was used as the normalizing factor using minimum and maximum ratios across all experiments (except the validation study). The minimum observed ratios of lipid:protein and carbohydrate:protein were 0.15 mg-(total lipids)$\cdot$mg-(protein)$^{-1}$ and 0.19 mg-(measured carbohydrates)$\cdot$mg-(protein)$^{-1}$. [Note: This ratio of carbohydrate:protein for total cell content is very low. However, analytical methods used here were not meant to capture all cell carbohydrates, and the actual ratio of carbohydrate:protein in the cell was likely much higher.] Based on measured protein concentrations, these ratios were used to define the mass of measured lipids and carbohydrates associated with X_{CPO}. The difference between measured lipids and X_{CPO}-associated lipids was assumed to be X_{TAG}, and the difference between measured carbohydrates and X_{CPO}-associated carbohydrates was assumed to be X_{PG}. Finally, VSS of X_{CPO} was estimated based on the maximum ratio of protein:VSS of 0.48 mg-(protein)$\cdot$mg-(VSS)$^{-1}$.

6.4.2. Photobioreactor Performance

The cyclostats operated with very low effluent phosphorus concentrations, often below the minimum reporting level of 0.05 mg-(P)·L^{-1}. Furthermore, effluent nitrate concentrations were typically greater than 10 mg-(N)·L^{-1}. Volatile suspended solids (VSS) concentrations in the cyclostats increased over the course of the lit cycle and decreased during night operation, with typical values for ranging from roughly 1,400 to 2,200 mg-(VSS)·L^{-1}. Regardless of the batch conditions they were transferred to, the cultures that originated from the cyclostats rapidly adapted to their new environments as we would expect them to. This was observed through linear behavior (i) in lit, nutrient replete conditions where growth and stored polymer mobilization were both rapid and linear for the first several hours of each study, and (ii) in lit, nutrient deplete conditions where storage of polymers was rapid and linear.

The absorption coefficient, a_c, was determined to be 0.049 m^2·g-$(VSS)^{-1}$ (VSS was 93 +/- 3% of TSS, resulting in an equivalent a_c of 0.46 m^2·g-$(TSS)^{-1}$). This resulted in an average irradiance across the reactors of 250-360 μE·m^{-2}·s^{-1} during normal cyclostat operation (depending on the VSS concentration). Although we recognize that the absorption coefficient will change with different light intensities or physiological conditions (e.g., a_c will decrease as light intensity increases [322]), this value was used to estimate the average light intensities across all experiments and is consistent with how light intensity was modeled in other studies [323].

6.4.3. Model Calibration

A total of three batch experiments (nutrient-replete light, nutrient-replete dark, and N-deplete light) from a single cyclostat were used for model calibration. The calibrated parameters are listed in Table 6.6. Minimum nutrient quotas were fixed based on the assumed biomass composition ($CH_{1.8}O_{0.5}N_{0.2}$) and a N:P molar ratio of 10:1 ($Q_{min,N}$ = 0.2 moles-(N)·mole-(biomass as C)·L^{-1}; $Q_{min,P}$ = 0.02 moles-(P)·mole-(biomass as C)·L^{-1}). It is worth noting, however, that the ratio of N:P in phototrophic microorganisms may not be fixed and cells may adapt to their environment to achieve co-limitation if within the acceptable range of N:P and given enough time [324].

Table 6.6. Calibrated model parameters for Cyclostat 3.

Description	Parameter	Fitted Value	Units
maximum specific growth rate	$\hat{\mu}_{XCPO}$	0.081	moles-(biomass as C)·mole-(biomass as C)$^{-1}$·hr^{-1}
optimal irradiance	I_{OPT}	130	μE·m^{-2}·s^{-1}
stored substrate saturation constant	K_{STO}	2.4	moles-(PG as C)·moles-(biomass as C)$^{-1}$
PG relative preference factor	ρ	5.0	unitless
maximum specific nitrate uptake rate	$\hat{V}_{NO}$	0.048	moles-(N)· mole-(biomass as C)$^{-1}$·hr^{-1}
maximum specific phosphate uptake rate	$\hat{V}_{P}$	0.0052	moles-(P)· mole-(biomass as C)$^{-1}$·hr^{-1}
specific maintenance rate	m_{ATP}	0.026	moles-(ATP)· mole-(biomass as C)$^{-1}$·hr^{-1}
dark nutrient uptake reduction factor	η_{dark}	0.55	unitless
maximum specific PG storage rate	$\hat{q}_{PG}$	0.028	moles-(PG as C)·mole-(biomass as C)$^{-1}$·hr^{-1}
maximum specific TAG storage rate	$\hat{q}_{TAG}$	0.016	moles-(TAG as C)·mole-(biomass as C)$^{-1}$·hr^{-1}
power coefficient for PG storage inhibition	β_1	3.1	unitless
power coefficient for TAG storage inhibition	β_2	1.2	unitless
maximum relative ratio of stored PG to biomass	f_{PG}^{MAX}	0.78	moles-(PG as C)·mole-(biomass as C)$^{-1}$
maximum relative ratio of stored TAG to biomass	f_{TAG}^{MAX}	1.4	moles-(TAG as C)·mole-(biomass as C)$^{-1}$

The model fit the batch experimental data well using the parameters presented in Table 6.6. In comparing experimental data to model data across all calibration experiments, R^2 values of 0.95 and 0.96 were achieved for f_{PG} (Figure 6.2) and f_{TAG} (Figure 6.3), respectively. A R^2 value of 0.94 was also achieved for X_{CPO}, but it should be noted that the range of values observed during the experiment was limited.

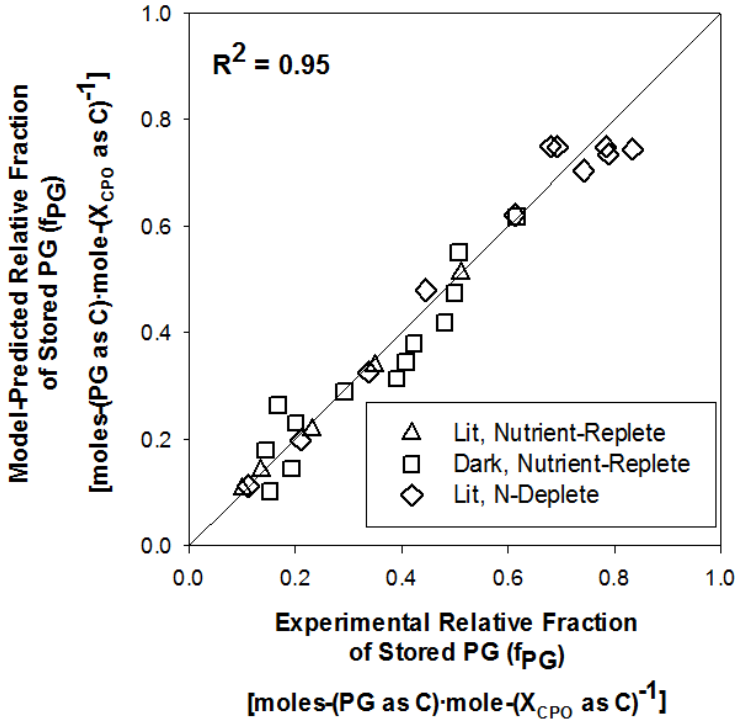

Figure 6.2. Comparison between experimental and model-predicted fractions of stored PG (f_{PG}).

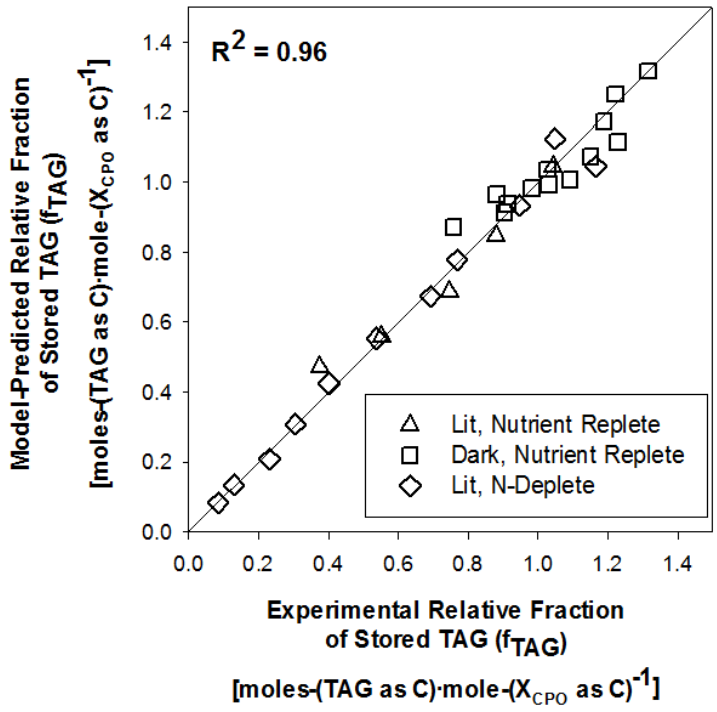

Figure 6.3. Comparison between experimental and model-predicted fractions of stored TAG (f_{TAG}).

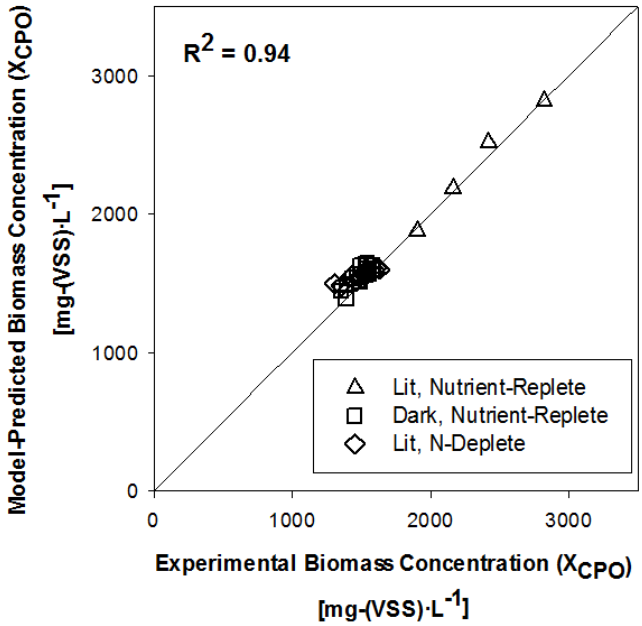

Figure 6.4. Comparison between experimental and model-predicted biomass concentrations (X_{CPO}).

6.4.4. Growth and Maintenance

Comparisons between measured and modeled X_{CPO} concentrations over time can be seen in Figure 6.5. The maximum specific growth rate was estimated to be 0.081 (C-moles biomass)·(C-mole biomass)$^{-1}$·hr^{-1} with an optimal irradiance of 130 μE·m^{-2}·s^{-1}. Although irradiance was not deliberately varied during the calibration study experimentation (in fact, surface irradiance was fixed), the varying composition of the cultures during experiments resulted in average photobioreactor irradiances from 120-270 μE·m^{-2}·s^{-1}. It was for this reason that an optimal irradiance value was estimated.

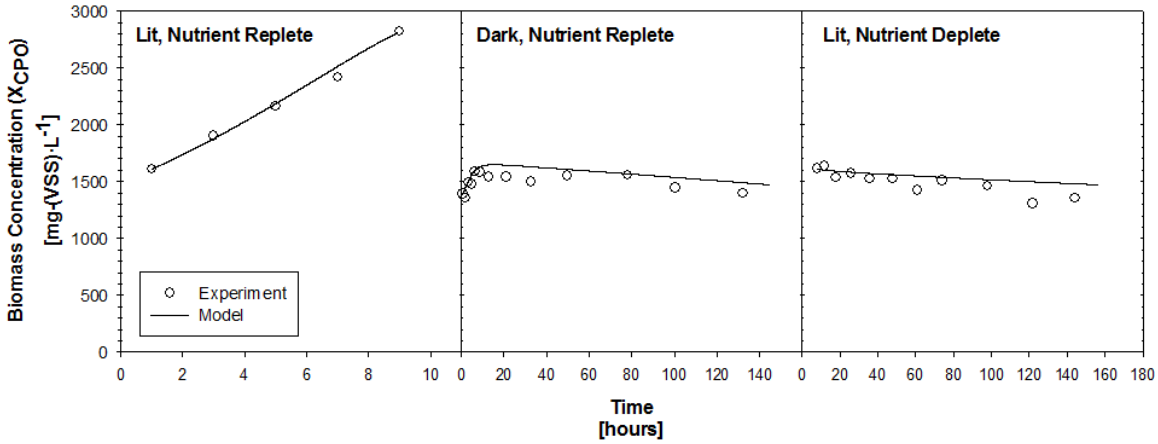

Figure 6.5. Comparison between experimental data and model predictions for biomass concentration (X_{CPO}).

Calibrated values of specific ATP maintenance rates for lumped sum metabolic models can vary greatly [302]. Rates of basal metabolism, however, have been estimated to be roughly 4-7% of maximum specific growth rates across several groups of phototrophic microorganisms (see summary in [325] for diatoms, green algae, and cyanobacteria).

Using the stoichiometric yields Y_{XCPO}^{ND} and Y_{ATP}^{ND} presented in Table 6.2, the estimated specific maintenance rate of 0.026 moles-(ATP)·mole-(biomass as C)$^{-1}$·hr^{-1} (Table 6.5) can be shown to be equivalent to an endogenous respiration rate of 0.0032 hr^{-1}. This value is 4.0% of the calibrated maximum specific growth rate, which is similar to the values summarized by Zhao et al. [325].

6.4.5. Carbohydrate and Lipid Storage and Mobilization

Comparisons between measured and modeled f_{PG} and f_{TAG} over time can be seen in Figures 6.6 and 6.7, respectively. Although carbohydrate storage was regularly observed under both nitrogen- and phosphorus-deplete conditions, lipid storage under phosphorus limitation was drastically slower than when under nitrogen-deplete conditions. Additionally, the maximum lipid content observed in one lit P-deplete study was less than 0.05 moles-(TAG as C)·mole-(biomass as C)$^{-1}$ after more than 3 days when phosphorus concentrations were low enough to result in a net biomass loss and a PG accumulation of 0.29 moles-(PG as C)·mole-(biomass as C)$^{-1}$.

The maximum PG storage capacity of the culture was estimated to be 0.78 moles-(PG as C)·mole-(biomass as C)$^{-1}$, with a maximum specific PG storage rate of 0.028 moles-(PG as C)·mole-(biomass as C)$^{-1}$·hr^{-1}. Although the maximum specific rate of lipid storage was slower than PG storage (43% slower on a C-mole basis), the maximum storage capacity of lipids was nearly 80% higher than that of PG on a C-mole basis (f_{TAG}^{MAX} was calibrated to 1.4 moles-(TAG as C)·mole-(biomass as C)$^{-1}$).

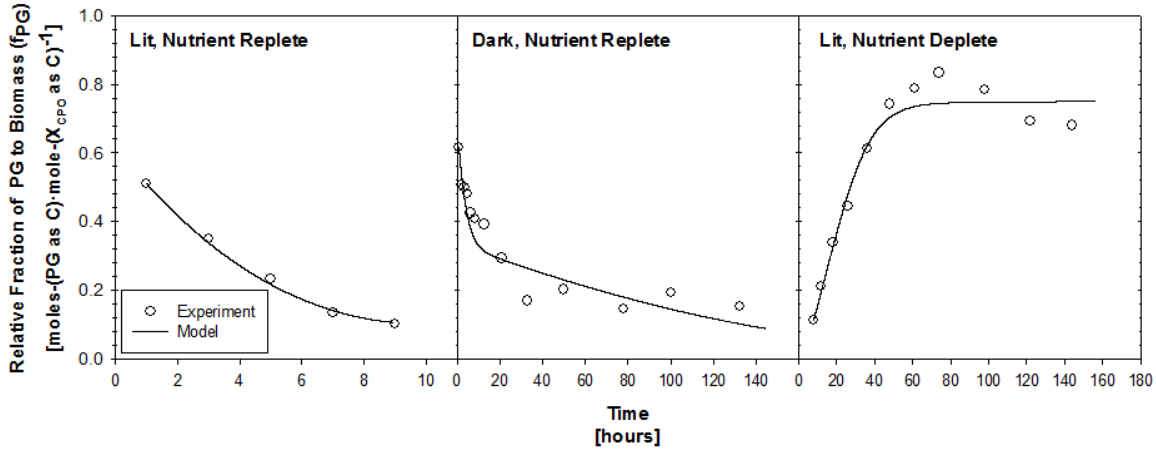

Figure 6.6. Comparison between experimental data and model predictions for the relative fraction of X_{PG} per biomass (f_{PG}).

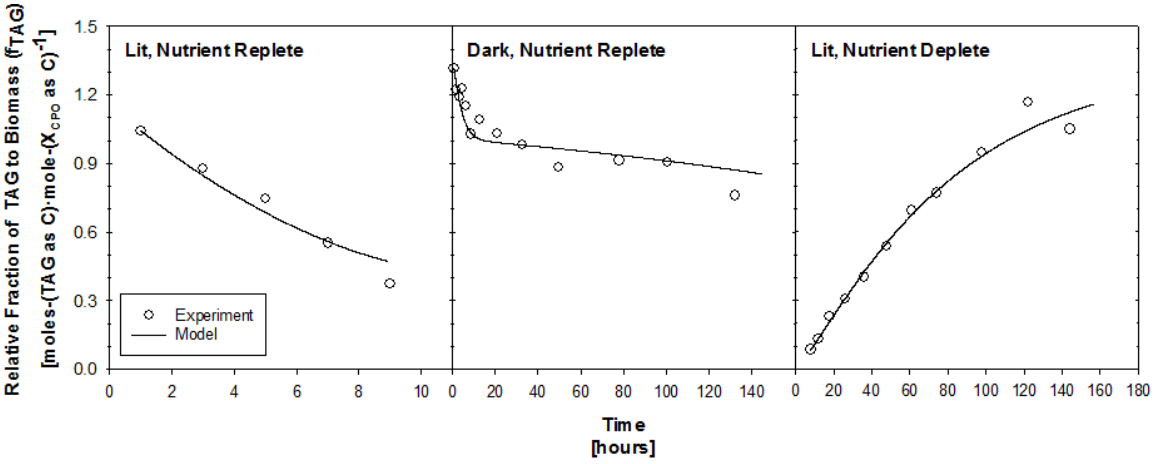

Figure 6.7. Comparison between experimental data and model predictions for the relative fraction of X_{TAG} per biomass (f_{TAG}).

Once cultures with stored carbohydrates were provided with nutrients, rapid mobilization of stored carbohydrate reserves was consistently observed under both lit and dark conditions (Figure 6.6). Lipid mobilization was also observed (Figure 6.7), but at a reduced rate as compared to carbohydrates. Given that the theoretical yield of biomass on TAG was 1.2x that of PG (Y_{PG}^{NR} divided by Y_{TAG}^{NR}), it is not surprising that cells stored and mobilized PG (lower energy compound) more quickly.

FAME analysis revealed that stored lipids were predominantly long chain fatty acids (C16 and C18; Figure 6.8). During N-deplete batch studies in all three cyclostats, C16:0 (palmitic acid) was the primary C16 fatty acid (FA) stored, while observed C18 FAs

storage was spread among C18:0 (stearic acid), C18:1 (oleic and elaidic acids), C18:2 (linoleic and linolelaidic acids), and C18:3 (α-linolenic acid). Although individual forms of C18 FAs were observed at greater concentrations than C16:0 in some experiments, C16:0 was consistently observed to follow storage and mobilization dynamics. For this reason, it is reasonable to maintain the assumption that stored lipids are in the form of C16:0 for the lumped sum metabolic model.

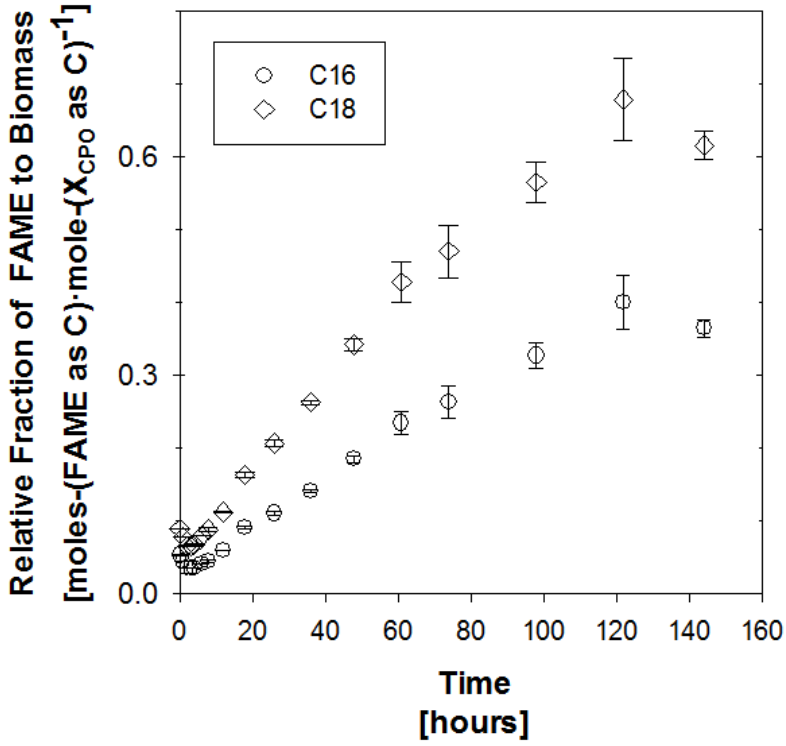

Figure 6.8. Relative fractions of C16 (predominantly C16:0) and C18 (spread among C18:0, C18:1, C18:2, and C18:3) fatty acids (measured at FAMEs) to biomass.

6.4.6. Model Validation

Although the model was able to calibrate well across the three calibration experiments with a single set of parameter values, these values were not able to describe the validation study as well. The key elements of the validation study that made it distinct from calibration studies were (i) less light was used during the lit-phase, and (ii) the culture was shifted to the dark before it had appreciable time (e.g., greater than 48-96 hours) to accumulate high levels of carbohydrates and lipids. The average light intensity within the reactor during the validation study was 98 +/- 8 $\mu E \cdot m^{-2} \cdot s^{-1}$ PAR. Based on the calibrated model parameters, this irradiance resulted in a light dependency term (f_I)

ranging from 0.94-0.99 during the lit phase of the validation study – a value at the top of the range observed in the calibration studies (which ranged from 0.82-1.00). Despite this fact, the model underestimated the initial growth rate and the initial rates of X_{PG} and X_{TAG} degradation (Figure 6.9).

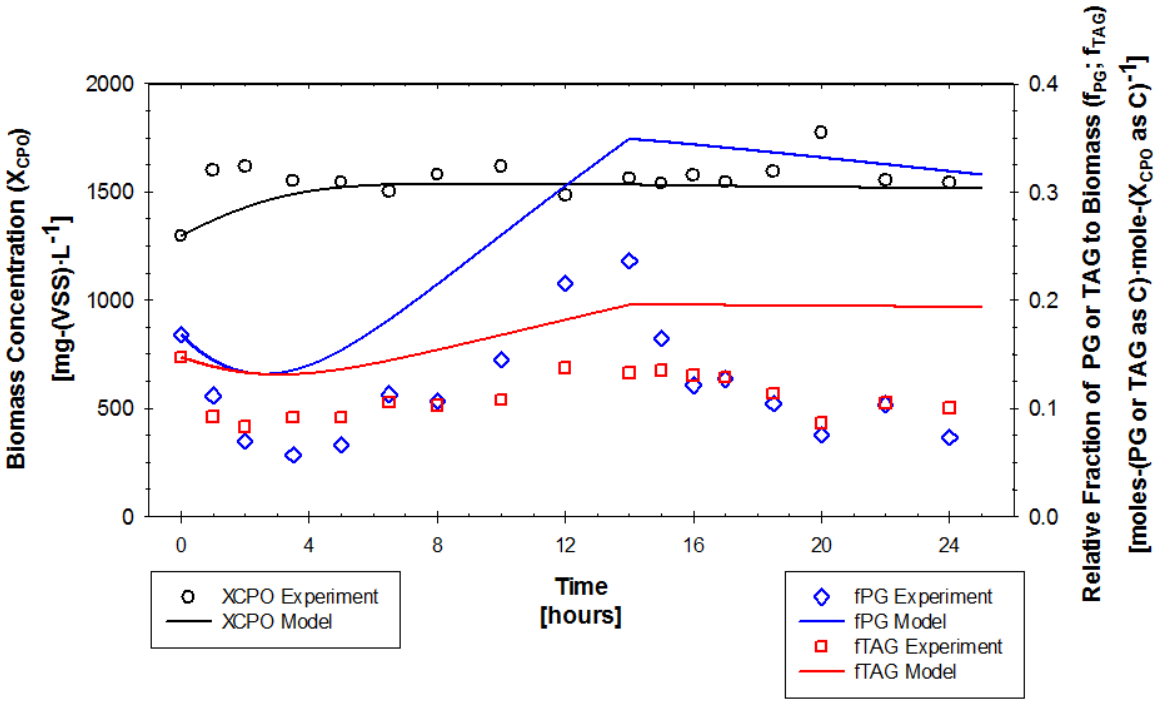

Figure 6.9. Comparison between experimental data and model predictions for the validation study for the concentration of biomass (X_{CPO}, left axis), relative fraction of X_{PG} per biomass (f_{PG}, right axis), and relative fraction of X_{TAG} per biomass (f_{TAG}, right axis). The culture was lit from hours 0 to 14 and in the dark from 14 to 24. Nutrient spikes were given at hours 0 and 14.

The calibrated model does predict the overall trends, but fails to capture the dynamics (i.e., the rapidly changing rates or growth, organic carbon mobilization and storage) of the system. One possible explanation for this is simply that calibrated parameters, although meeting the criteria of the GRG Nonlinear Method for the Excel Solver, are not optimal to describe the system. To evaluate whether the model structure can describe the validation study data, the parameters were re-calibrated to the validation study data. This calibration resulted in Figure 6.10 and the parameter values listed in Table 6.7, which are presented alongside their relative difference from the calibration values in Table 6.6. The calibrated parameter values were roughly 58% different, on average, from the values presented in Table 6.6, but the model was able to better capture the observed trends in biomass and the relative fractions of X_{PG} and X_{TAG} to biomass. Although it is possible that calibration may be improved with additional experimental

data, other explanations for the disconnect between the calibration and validation studies may be explained by the model structure.

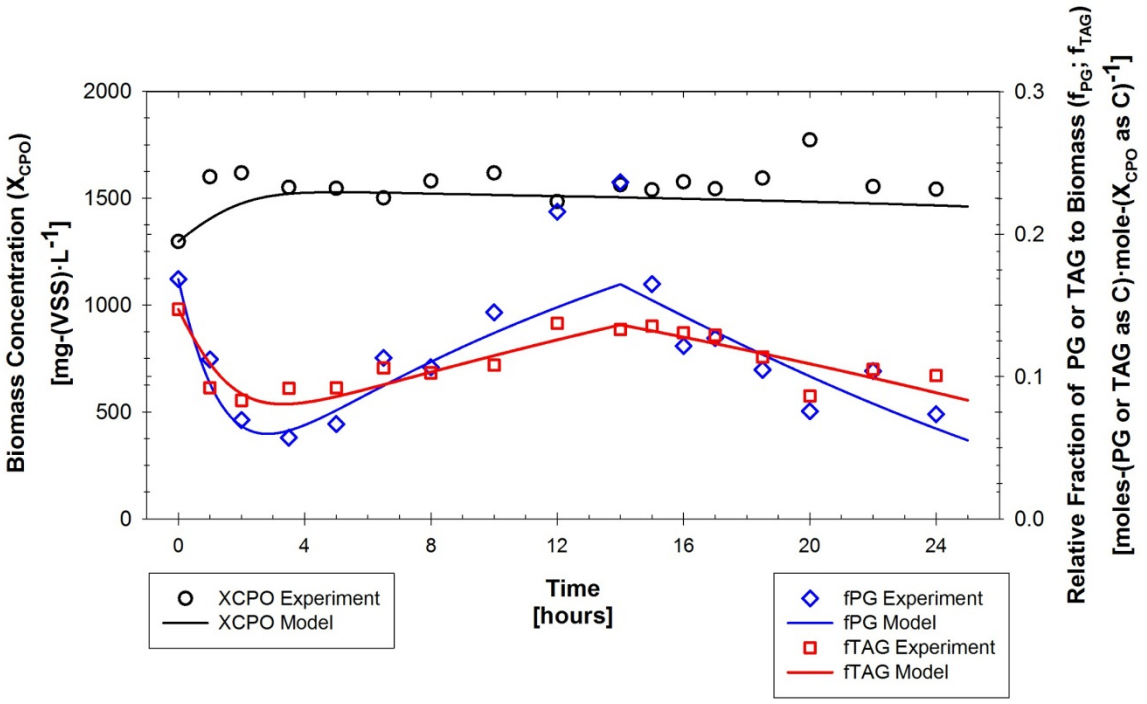

Figure 6.10. Comparison between experimental data and re-calibrated model predictions for the validation study for the concentration of biomass (X_{CPO}, left axis), relative fraction of X_{PG} per biomass (f_{PG}, right axis), and relative fraction of X_{TAG} per biomass (f_{TAG}, right axis). The culture was lit from hours 0 to 14 and in the dark from 14 to 24. Nutrient spikes were given at hours 0 and 14.

Table 6.7. Re-calibration of model parameters using validation study data.

Parameter	New Fitted Value	Relative Difference from Value in Table 6.6	Units
$\hat{\mu}_{XCPO}$	0.128	58%	moles-(biomass as C)·mole-(biomass as C)$^{-1}$·hr^{-1}
I_{OPT}	215	67%	μE·m^{-2}·s^{-1}
K_{STO}	0.22	-91%	moles-(PG as C)·moles-(biomass as C)$^{-1}$
ρ	2.1	-57%	unitless
$\hat{V}_{NO}$	0.059	24%	moles-(N)· mole-(biomass as C)$^{-1}$·hr^{-1}
$\hat{V}_{P}$	0.0052	0%	moles-(P)· mole-(biomass as C)$^{-1}$·hr^{-1}
m_{ATP}	0.097	270%	moles-(ATP)· mole-(biomass as C)$^{-1}$·hr^{-1}
η_{dark}	0.55	0%	unitless
$\hat{q}_{PG}$	0.027	-3%	moles-(PG as C)·mole-(biomass as C)$^{-1}$·hr^{-1}
$\hat{q}_{TAG}$	0.032	97%	moles-(TAG as C)·mole-(biomass as C)$^{-1}$·hr^{-1}
β_1	1.1	-65%	unitless
β_2	0.5	-57%	unitless
f_{PG}^{MAX}	0.70	-10%	moles-(PG as C)·mole-(biomass as C)$^{-1}$
f_{TAG}^{MAX}	1.10	-21%	moles-(TAG as C)·mole-(biomass as C)$^{-1}$

On key characteristic of the model structure is that all processes in the model are continuously active. Rather than having discrete processes that turn on or off in the presence or absence of a trigger (e.g., a response function for TAG storage that has a value of 1 in N-deplete conditions and a value of 0 in N-replete conditions), the model relies on continuous equations that are always active. This model characteristic leads to tension between processes that, to a degree, dampens model behavior. Attempts were made to reduce the impacts of these tensions by, for example, raising the relative N and P quota size to the 4th power (an example of the response function with and without this change can be seen in Figure 6.11). With initial relative N and P quotas (Q/Q_{min}) for the validation study (taken from the calibrated value of a separate experiment) of 1.4, this results in a response term for growth processes of 0.78 and a response term for storage processes of 0.22.

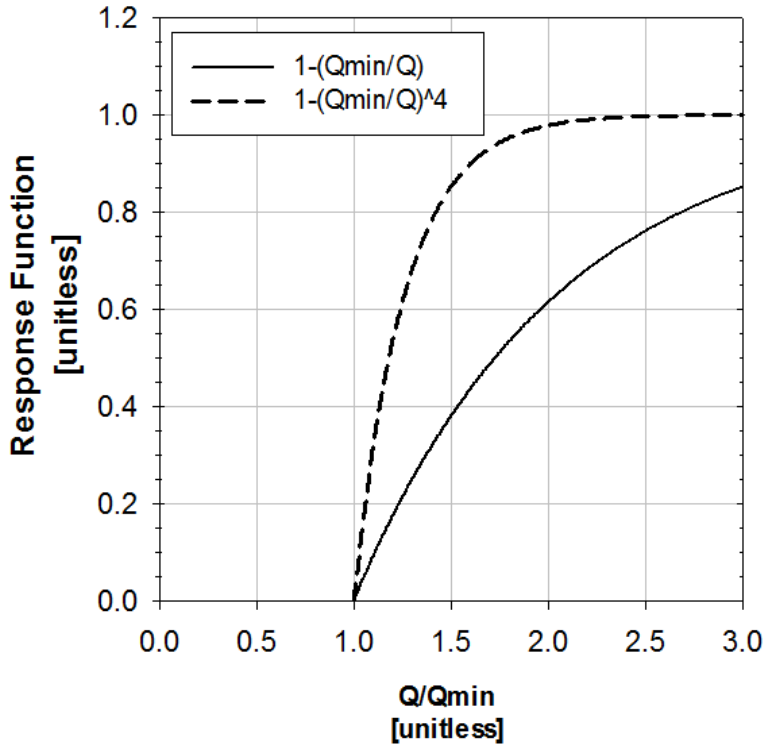

Figure 6.11. Two response functions for nutrient-limited growth: (i) original Droop formulation (solid line) and (ii) modified function for more rapid response.

Given the structure of the growth processes (P4, P5, and P6), net X_{CPO} growth at the start of the validation study was greater than 70% of the maximum specific growth rate. The initial points on the X_{CPO} curve, however, would require a $\hat{\mu}_{XCPO}$ an order of magnitude higher than the calibrated value to match the model to the experimental data. Given that the calibrated $\hat{\mu}_{XCPO}$ and m_{ATP} values match the magnitude of values in the literature and fit the calibration studies in higher irradiance, it would be more appropriate for future studies to focus on evaluating alternative model structures (e.g., discrete switching functions) to characterize short-term, low light studies of this nature.

6.5. Conclusions

There are distinct advantages to developing a lumped sum metabolic model for process modeling, not the least of which is the mechanical friction provided by developing stoichiometric relationships in terms of fundamental biochemical parameters (e.g., P/O ratio). The development of the model presented here does rely on basic assumptions about which metabolic pathways are used, but the selection of the model green alga *C. reinhardtii* has resulted in a metabolic model built on pathways that have been identified

in a wide range of phototrophic microorganisms (e.g., the EMP pathway). The model presented here was able to calibrate very well to longer-term studies of culture growth, as well as PG and TAG storage and mobilization. All calibration studies were run with a surface irradiance of 400 $\mu E \cdot m^{-2} \cdot s^{-1}$ PAR on each of two sides of the photobioreactors, which is a reasonable value for naturally-lit photobioreactors [151]. For the prediction of lower light performance, the model relied on photosynthesis-irradiance response relationships developed in the limnology literature over many decades [314, 315, 326]. Although recent phototroph modeling advancements have included more explicit nutrient process descriptions (e.g., [327]) and the storage and depletion of organic carbon reserves (e.g., [313]), the focus of such modeling efforts is still often focused on natural environmental systems. As such, much of the data used to calibrate such models are on timescales of days or longer. Access to hourly (or even more frequent) experimental data has been severely limited in the literature, and existing model structures are often ill-equipped to handle such timescales. Future work on the advancement of process modeling of phototrophic microorganisms, therefore, must include a balanced effort between utilization of well-established phototrophic models and a re-structuring of such models to more accurately describe process dynamics at shorter timescales that are relevant to engineered bioprocesses.

6.6. Acknowledgements

The authors would like to acknowledge financial support from the Graham Environmental Sustainability Institute and the Rackham Graduate School, both at the University of Michigan, for partial funding for the first author. The authors would also like to acknowledge Siddharth Dev and Harsha Hebbale, undergraduate students at the University of Michigan, for their assistance in maintaining the photobioreactors and performing experiments, as well as Phillip Savage and Robert Levine (Dept. of Chemical Engineering, University of Michigan) for assistance with the analysis of FAMEs.

6.7. Nomenclature

Table 6.8. Definitions of nomenclature used throughout manuscript.

Parameter	Description	Units
α_M	ATP requirement for synthesis of biomass precursors from acetyl-CoA	moles-(ATP)·mole-(biomass as C)$^{-1}$
α_p	light energy efficiency factor	unitless
α_X	ATP required for polymerization of biomass precursors (monomers) to active biomass	moles-(ATP)·mole-(biomass as C)$^{-1}$
β_1	power coefficient for PG storage inhibition	unitless
β_2	power coefficient for TAG storage inhibition	unitless
δ_N	CO_2 production from the catabolism of acetyl-CoA to generate reducing power for NO_3^- reduction for assimilation.	moles-(CO_2 as C)·mole-(biomass as C)$^{-1}$
δ_{PO}	efficiency of oxidative phosphorylation (P/O ratio) in mitochondria	moles-(ATP)·mole-($NADH_2$)$^{-1}$
δ_x	CO_2 production from the synthesis of 1 C-mole of biomass from acetyl-CoA	moles-(CO_2 as C)·mole-(biomass as C)$^{-1}$
η_{dark}	dark nutrient uptake reduction factor	unitless
$\boldsymbol{\mu}$	specific growth rate	moles-(biomass as C)·mole-(biomass as C)$^{-1}$·hr^{-1}
$\hat{\boldsymbol{\mu}}_{\mathbf{XCPO}}$	maximum specific growth rate	moles-(biomass as C)·mole-(biomass as C)$^{-1}$·hr^{-1}
ρ	PG relative preference factor	unitless
a_c	PAR absorption coefficient on a volatile suspended solids (VSS) or total suspended solids (TSS) basis	m^2·g-(VSS or TSS)$^{-1}$
$b_{reactor}$	thickness of reactor along light path	m
f_I	irradiance response function	unitless
f_{PG}	ratio of stored polyglucose to cells	moles-(PG as C)·mole-(biomass as C)$^{-1}$
$\mathbf{f}_{\mathbf{PG}}^{\mathbf{MAX}}$	maximum relative ratio of stored PG to biomass	moles-(PG as C)·mole-(biomass as C)$^{-1}$
f_S	ratio of stored organic carbon (PG and TAG in PG equivalents) to biomass	moles-(PG as C)·mole-(biomass as C)$^{-1}$
$\mathbf{f}_{\mathbf{TAG}}^{\mathbf{MAX}}$	maximum relative ratio of stored TAG to biomass	moles-(TAG as C)·mole-(biomass as C)$^{-1}$
f_{TAG}	ratio of stored lipids to cells	moles-(TAG as C)·mole-(biomass as C)$^{-1}$
I_{avg}	average PAR irradiance within the photobioreactor	μE·m^{-2}·s^{-1}

Table 6.8 - Continued

Parameter	Description	Units
I_n	maximum incident irradiance ("irradiance at noon")	$\mu E \cdot m^{-2} \cdot s^{-1}$
I_{OPT}	optimal irradiance	$\mu E \cdot m^{-2} \cdot s^{-1}$
I_{opt}	optimum irradiance	$\mu E \cdot m^{-2} \cdot s^{-1}$
K_{NO}	nitrate (as nitrogen source) half saturation coefficient	moles-(N)$\cdot L^{-1}$
K_P	phosphorus half saturation coefficient	moles-(P)$\cdot L^{-1}$
K_{STO}	stored substrate saturation constant	moles-(PG as C)·moles-(biomass as C)$^{-1}$
K_γ	parameter to transform adaptation expressions of [316] into continuous equation	unitless
m_{ATP}	specific maintenance rate	moles-(ATP)·mole-(biomass as C)$^{-1}\cdot hr^{-1}$
q_{CO2}	specific rate of net CO2 production	moles-(CO_2 as C)·mole-(biomass as C)$^{-1}\cdot hr^{-1}$
q_{O2}	specific rate of net O2 production	moles-(O_2)·mole-(biomass as C)$^{-1}\cdot hr^{-1}$
q_{PG}	specific PG storage rate	moles-(PG as C)·mole-(biomass as C)$^{-1}\cdot hr^{-1}$
$\hat{\mathbf{q}}_{\mathbf{PG}}$	maximum specific PG storage rate	moles-(PG as C)·mole-(biomass as C)$^{-1}\cdot hr^{-1}$
q_{phot}	specific rate of CO_2 fixation to G3P	moles-(G3P as C)·mole-(biomass as C)$^{-1}\cdot hr^{-1}$
q_{TAG}	specific TAG storage rate	moles-(TAG as C)·mole-(biomass as C)$^{-1}\cdot hr^{-1}$
$\hat{\mathbf{q}}_{\mathbf{TAG}}$	maximum specific TAG storage rate	moles-(TAG as C)·mole-(biomass as C)$^{-1}\cdot hr^{-1}$
R	chlorophyll:carbon ratio	g-(*Chl a*)·g-(C)$^{-1}$
S_{CO2}	carbon dioxide	moles-(C)$\cdot L^{-1}$
S_{NO}	soluble nitrate	moles-(N)$\cdot L^{-1}$
S_{O2}	oxygen	moles-(O_2)$\cdot L^{-1}$
S_P	soluble phosphorus	moles-(P)$\cdot L^{-1}$
$\hat{\mathbf{V}}_{\mathbf{NO}}$	maximum specific nitrate uptake rate	moles-(N)· mole-(biomass as C)$^{-1}\cdot hr^{-1}$
$\hat{\mathbf{V}}_{\mathbf{P}}$	maximum specific phosphate uptake rate	moles-(P)· mole-(biomass as C)$^{-1}\cdot hr^{-1}$
X_{CPO}	concentration of carbon-accumulating phototrophic biomass	moles-(biomass as C)$\cdot L^{-1}$
X_{PG}	concentration of stored polyglucose (PG)	moles-(PG as C)$\cdot L^{-1}$

Table 6.8 - Continued

Parameter	Description	Units
X_{TAG}	concentration of stored triacylglycerol (TAG)	moles-(TAG as C)·L^{-1}
X_{TSS}	total suspended solids concentration	g-(TSS)·m^{-3}
X_{VSS}	volatile suspended solids concentration	g-(VSS)·m^{-3}

Chapter 7
Conclusions and Engineering Significance

7.1. Overview

The overarching goal of this dissertation is to advance the sustainability of wastewater treatment systems, the primary barrier between society's waste and the aquatic environment. This work began with the identification of barriers to the implementation of resource recovery systems, and the development of a planning and design process to address social factors that are often neglected in the design and implementation of wastewater infrastructure (Chapter 3; [24]). Fundamental to this approach is the concept of place-based solutions, or the need to incorporate locality-specific considerations in the design of wastewater infrastructure. A key challenge in the development of such solutions is the diversity of stakeholder perspectives within and across projects; a challenge that may be overcome through the use of qualitative tools to elucidate stakeholder values and communicate sustainability concepts to a broad audience (Chapter 4; [252]). To address environmental, economic, and performance factors, a quantitative sustainability assessment framework was developed using LCA, present worth analysis, and a WWTP simulator (Chapter 5). Finally, metabolic and pseudo-mechanistic models were developed for phototrophic microorganisms to enable their evaluation as an emerging energy recovery technology in wastewater management (Chapter 6).

7.2. Quantitative Sustainable Design Framework

One of the unique contributions of this work is in the integration of state of the art tools to create a framework for sustainability assessments of wastewater treatment systems. Specifically, the quantitative framework is the first to simultaneously address economic, environmental, and performance factors to enable both the creation and evaluation of sustainable design concepts for wastewater systems. By integrating existing tools from the literature rather than developing a new, independent sustainability metric, this framework can continue to evolve by incorporating advancements made by researchers

for the improvement of individual tools contributing to the larger framework. As an example, future studies contributing to more accurate life cycle inventories of WWTPs (as in [130]) or characterization factors (as in [328]) can be incorporated to improve the environmental assessment. As the body of LCA literature continues to advance, this framework could be adapted to include spatial scale more explicitly [329], which is a key challenge facing LCA [330]. By building the performance assessment on tools from industry (GPS-X^{TM}) coupled with an uncertainty assessment approach from the literature, this framework may also continue to take advantage of advancements in WWTP modeling and design approaches that explicitly characterize uncertainty. Cost assessments, as well, can be updated as unit prices change and improved correlations are developed, or they can be replaced with proprietary costing methods used by individual design firms. Beyond the structure of the framework and its ability to adapt to advancements in research and practice, additional contributions of this work stem from the questions it can be used to answer.

7.3. Integrated WWTP Management

Although the case study evaluated in Chapter 5 was for a single WWTP, this framework offers exciting opportunities to develop designs and evaluate policy alternatives at a larger (e.g., watershed) scale. In the Chesapeake Bay, for example, regulatory agencies are pursuing policies to protect the Bay from excessive nutrient loads and the resulting ecosystem damage [21]. The Environmental Protection Agency and its Bay partners have imposed strict effluent nitrogen and phosphorus limits (as wasteload allocations) on facilities deemed to be “significant” dischargers of these nutrients, which includes 483 wastewater treatment plants across 6 states and the District of Columbia [21]. These policies vary by state or district, and have been expected to result in a minimum cost of $3.36 to $3.96 billion in WWTP upgrades [21]. Although the implementation of a viable nutrient trading market may facilitate some level of efficiency improvement (shuttling money to WWTPs that can achieve the greatest reductions in mass of nutrients discharged per dollar spent), the framework presented in this dissertation creates opportunities to more proactively evaluate policy alternatives for the watershed.

If the end goal is to protect the Bay, coupling Bay models with the framework presented in Chapter 5 can facilitate stakeholder engagement and create the opportunity to achieve coordinated upgrades of WWTPs to reduce costs and advance Bay restoration.

This research would likely lead to a number of policy questions requiring attention, including how best to distribute costs and other upgrade burdens across utilities and across states. Researchers could pursue optimal solutions (e.g., minimization of costs subject to a Bay nutrient loading constraint), and develop an understanding of what incentive structures would be needed for utilities, state-level regulators, and other stakeholders to buy-in to such proposals. Research into policy and incentive structures would undoubtedly require the engagement of social scientists, and would benefit from an integration of the planning and design concepts introduced in Chapters 3 and 4 of this dissertation.

7.4. The Role of Research in Design

In this dissertation, process design (Chapter 5) has been achieved using a standardized approach that relies on liberal use of empirical knowledge and safety factors [6, 54] – an approach affirmed by effluent water quality and process reliability at WWTPs across the globe. It is clear, however, that the environmental impacts of WWTPs extend beyond receiving waters, and social factors are playing an increasingly important role as utilities are compelled to recover resources from wastewater. As awareness of these issues continues to rise, it is reasonable to question what role these emerging factors should play in the design of wastewater treatment systems in the 21st century.

The application of new metrics to design evaluation (such as LCA integrated with cost and social factors) imposes a driving force to rethink the way we design treatment systems. That is not to say we should compromise our current objectives of protecting public health and water quality, but rather we should push and pull designs in new ways to better understand the tensions and synergies among current and emerging goals for sustainability. Although the quantitative sustainable design framework was applied to a case study comparing two conceptual designs of a WWTP (Chapter 5), the integrated assessment tool also lends itself to the evaluation of design alternatives across their decision space (where *decision space* is defined as all possible combinations of design parameters). This capability creates opportunities for exciting new insights in the comparison between robust and optimized WWTP designs, and will make inroads in the quantification of trade-offs among these and other design philosophies.

Sustainability research offers us the opportunity to view design through a new lens, providing motivation to pursue innovative designs that may simultaneously improve

WWTP characteristics in multiple dimensions. This research should not be done in a vacuum, as locality-specific factors (including social factors) will influence system sustainability. By coupling quantitative design endeavors with the larger planning and design process proposed in Chapter 3, designers may be better equipped to develop novel designs that will advance their system's sustainability. This work will require the recognition that sustainable design is not equivalent to life cycle design, and that the recovery of resources is not inherently sustainable.

7.5. Emerging Technologies in Wastewater Management

A central element of this dissertation work has been the transition from viewing wastewater as a hazard that must be mitigated to a renewable resource that may provide a net benefit for communities [30]. As stakeholders consider which design approach or technologies are most appropriate for them, the quantitative sustainable design framework may offer valuable insight into the relative sustainability of emerging technologies. To evaluate a given technology, however, designers must be able to develop a conceptual design and model its performance. In order to demonstrate this process, this dissertation also included the development of a metabolic model with corresponding stoichiometric and kinetic expressions for the use of phototrophic microorganisms for energy recovery (Chapter 6).

The contributions of this phototrophic process model extend beyond opportunities for comparative sustainability assessments of this emerging technology, and will also enable designers to gain insight into factors influencing competition between phototrophs and wastewater-relevant chemotrophs, and inform the design of photobioreactors and bioprocesses that may achieve selective pressures and enrich for target functions (e.g., lipid accumulation). Ultimately, these advancements may contribute to a transition away from reliance on aerobic chemotrophs and help overcome key barriers to the economic and environmental sustainability of using phototrophs for energy recovery from wastewater.

Appendix A

Supporting Information for a New Planning and Design Paradigm to Achieve Sustainable Resource Recovery from Wastewater

Table A.1. Proposed *Guiding Principles* for the design of sustainable resource recovery systems (RRS) applied to water. Inspired by [331].

Category	Characteristics of a Sustainable RRS	Related Discussions from the Water, Wastewater, and Sustainability Literature
environmental	will not generate waste	[332, 333]
	will be net energy positive or neutral	[11, 39, 193, 334, 335]
	will not deplete water resources nor alter natural hydrological processes	[29, 192, 336, 337]
	will achieve responsible nutrient management and contribute to soil fertility	[29, 37, 222, 332, 338, 339]
	will not consume non-renewable or non-recoverable resources	[333]
	will not contribute to global warming	[39, 41, 340, 341]
ecological	will not diminish ecosystem health	[29, 192, 336, 337]
	will not reduce biodiversity nor threaten individual species	[29, 192, 342, 343]
economic	will have lifecycle costs that are affordable to all stakeholders	[46, 211, 344-346]
	will contribute to the economic development of the municipality and beyond	[344, 345]
social	will provide access to safe drinking water and appropriate sanitation for all	[43, 44]
	will protect public health	[43, 344]
	will be understood and accepted by all stakeholders	[40, 46, 347, 348]
	will not disproportionately impact a segment of the population	[70, 331]
	will apportion costs equitably and in proportion to benefits received	[203, 331, 346]
functional	will be flexible and adaptable	[210, 227, 344]
	will be reliable and resilient	[15, 227, 336]
	will be manageable and safe for operational staff	[345]

Note: A discussion of competing factors at various spatial scales (e.g., household objectives and external influences versus city objectives and external influences) can be found elsewhere [344, 349]. It is important to note that the Guiding Principles identified in Table A1 are an idealized set of goals for resource recovery systems, and will not all be achieved simultaneously by a given project. Instead, they are meant to do exactly what their name indicates – *guide* stakeholders as they undergo the process of elucidating their own locality- and project-specific definition of sustainability and identification of specific sustainability targets (see [201] for a discussion of sustainability *goals* and *targets*).

Table A.2. Challenges for and future technologies in resource recovery systems (RRS).

Challenge	Current Technology	Technology of the Future
energy and climate	• In 2000 the energy required to treat and convey drinking water in the U.S. had a typical range of 0.37 kWh/m^3 and 0.48 kWh/m^3 for surface and groundwater freshwater sources, respectively [354]. In Southern California, these values are up to 10× higher because of energy requirements for source water conveyance [355]. • Typical range for wastewater treatment energy requirements is 30-105 kWh per person-equivalent per year [11, 41, 253, 356]. Aeration accounts for roughly half of on-site electricity consumption [54, 74, 253]. • Of the total U.S. greenhouse gas emissions in 2007 (7,150 Tg CO_2 equivalents), 15.8 Tg CO_2 equivalents (eq.) were associated with CH_4 production and 4.9***** Tg CO_2 eq. were associated with N_2O production from domestic wastewater treatment (data from [357]).	• Water reuse and urban green design will minimize the conveyance of water by matching the geographic location of supply with the location of demand. Indirect potable reuse will be utilized to minimize the transportation of water between watersheds. • Wastewater treatment will be achieved using energy recovery technologies (e.g., methane- and biofuel-generating treatments, microbial fuel cells) with reduced reliance on energy-intensive aeration. Decentralized wastewater management will facilitate heat energy recovery. • The water industry will not be a major contributor of greenhouse gas emissions globally as systems approach energy neutrality and minimize fugitive emissions (e.g., CH_4 and N_2O) during both conveyance and treatment.
water	• Water is treated to potable quality (regardless of end-use) and distributed from central locations to support one-time use. • Recent estimates suggest roughly 0.6% of non-agricultural water consumption is reused in Europe [358] and 7.4% of wastewater is reused in the U.S. [359]. • Pathogen removal is primarily based on indicator organisms specific to the end-use (e.g., for drinking water – total coliform; for wastewater effluent – total coliform, fecal coliform, and MS2 coliphage) [54].	• Direct non-potable reuse will be achieved in water stressed regions using decentralized infrastructure. Water and wastewater infrastructure will be adaptable to achieve indirect or direct water reuse as climate change increases the prevalence of drought-prone regions. • The level of water treatment will match end-use requirements. • Culture-independent detection methods will allow for rapid and comprehensive monitoring of indicator organisms and emerging pathogens. • Address emerging chemicals of concern (e.g., pharmaceuticals) through technology implementation and upstream management (reduced use, source control).
nutrients and materials	• Nutrient management strategies in the wastewater industry are based primarily on removal to minimize impacts on receiving bodies of water. • Nitrogen in wastewater is oxidized aerobically and, where required, removed as dinitrogen gas (often with the addition of an exogenous electron donor). Phosphorus is chemically precipitated and land-filled or captured biologically and land-filled or land-applied. Land-application of enhanced biological phosphorus removal biosolids reduces allowable application rates and economic viability of the practice [11].	• Nutrient management strategies will focus on opportunities for recovery and reuse. • Integrated water management systems will decouple the water and nutrient metabolisms of cities to enhance the aquatic environment and assist food production [192]. • Source-separation of waste streams (including urine) will allow for efficient recovery of nutrients [350] and will reduce the need for nitrification and denitrification at the wastewater treatment plant [351]. • Bioelectrochemical systems (BES) may be utilized for the production of high-value products during wastewater treatment [352].

*****EPA estimates for N_2O production during domestic wastewater treatment are based on data from a wastewater treatment plant that did not perform nitrification or denitrification [353]. N_2O production would likely be significantly higher for biological nutrient removal processes.

Appendix B
Design Assumptions for Quantitative Sustainable Design

Both the Standard and Seasonal designs were developed using the following steps:

1. The acceptable MLSS concentration was determined based on existing secondary clarifiers.
2. A design SRT was selected.
3. The required mass of biomass in system and wastage rate were determined based on substrate removal and design SRT.
4. The ANA/ANX/AER volumes were determined based on mass of biomass in system, acceptable MLSS concentration, and relative SRTs (ANA:ANX:AER). Note that the final zones were placed in existing on-site tankage, and new tankage was constructed for preceding zones as needed.
5. Aeration equipment was sized based on steady-state simulations and the use of peaking factors.
6. Denitrification filters were sized based on selected hydraulic loading rates.
7. Pumping rates were selected based on assumptions of reactor and clarifier performance (internal recycle, RAS, WAS, primary sludge, ISB RAS, ISB WAS, denitrification filter backwash).
8. Pumps were sized.

Table B1. Characteristics of Standard and Seasonal Designs.

Reactor	Standard Design	Seasonal Design
Anaerobic [m^3]	3,116	3,142
Anoxic 1 [m^3]	2,493	4,714
Aerobic 1 [m^3]	28,990	24,545
Anoxic 2 [m^3]	3,739	4,714
Aerobic 2 [m^3]	2,167	2,167
Total Volume [m^3]	40,504	39,281
Denit Filter Area [m^2]	515	588
Airflow Requirements at Steady State and 28 °C [$m^3 \cdot d^{-1}$]	517,982 (AER1A) 154,108 (AER1B) 0 (ANX2) 35,343 (AER2) TOTAL: 707,500	525,935 (AER1A) 189,644 (AER1B) 0 (ANX2) 48,924 (AER2) **TOTAL: 764,500**
Airflow Requirements at Steady State and 17.9 °C [$m^3 \cdot d^{-1}$]	530,442 (AER1A) 224,274 (AER1B) 0 (ANX2) 52,789 (AER2) **TOTAL: 807,500**	431,560 (AER1A) 224,412 (AER1B) 65,533 (ANX2) 25,711 (AER2) TOTAL: 747,200

Table B.2. Solids residence times (SRTs) used for design.

Secondary Treatment Process			Standard Design		Seasonal Design	
			Winter	Summer	Winter	Summer
			5 Bard		A2O	5 Bard
SRT (d)	ANA		1	0.7	1	0.7
	ANX	ANX1	0.8	0.56	1.5	1.05
		ANX2	1.2	0.84	–	1.05
	AER	AER1	9.3	6.5	7.9	5.6
		SWING	–	–	1.5	–
		AER2	0.7	0.5	0.6	0.4
Denitrification Filter Loading			4.0		3.5	

Primary clarifiers and primary solids pump station. Three 120 foot diameter primary clarifiers were designed with a side water depth of 12 ft. These primary clarifiers have a surface overflow rate of 1,150 $gal \cdot d^{-1} \cdot ft^{-2}$ at the average annual flow (24 MGD, plus steady-state recycle and ISB streams leading to a total flow of 26.3 MGD) with one train out of service. An acceptable surface overflow rate (930 $gal \cdot d^{-1} \cdot ft^{-2}$) was also confirmed under maximum monthly flow conditions (29 MGD, max month from last 8 years, plus recycle streams leading to a total flow of 31.6 MGD) with all trains in service. It was assumed that the primary clarifiers would achieve roughly 55% TSS removal with an underflow solids concentration of 3%.

Secondary clarifiers and RAS/WAS pump station. Two sets of clarifiers already exist onsite. Units 1, 2, and 3 are 130 ft in diameter with a side water depth of 16 ft and a RAS pumping capacity of 4 MGD per unit. Units 7, 8, and 9 are 90 ft in diameter with a

side water depth of 12.5 ft and a RAS pumping capacity of 1.33 MGD per unit. Sufficient WAS pumping capacity exists onsite. As a result, no construction costs were included for WAS pumping. RAS pumping rates were calculated at the design SRT of 13 days with a MLSS of 3,100 mg-(TSS)·L^{-1} and an underflow solids concentration of 8,000 mg-(TSS)·L^{-1}. The pumping capacity installed was 1.5x the required pumping rate. Additional RAS pumping was added as needed to achieve the required installed capacity with one 130 ft clarifier out of service under average flow conditions (12 MGD existing RAS pumping capacity).

The maximum target MLSS was selected using Figure B.1 for a maximum solids loading rate (SLR) of 20-25 lbs·ft^{-2}·d^{-1} and a likely underflow solids concentration (X_U) of 8,000-10,000 mg-(TSS)·L^{-1}. When examining the two cases (maximum month with all units in service or average month with one unit out of service), the average flow with one unit out of service resulted in a higher SLR. Based on these results, a maximum MLSS concentration of 3,100 mg·L^{-1} was selected for design.

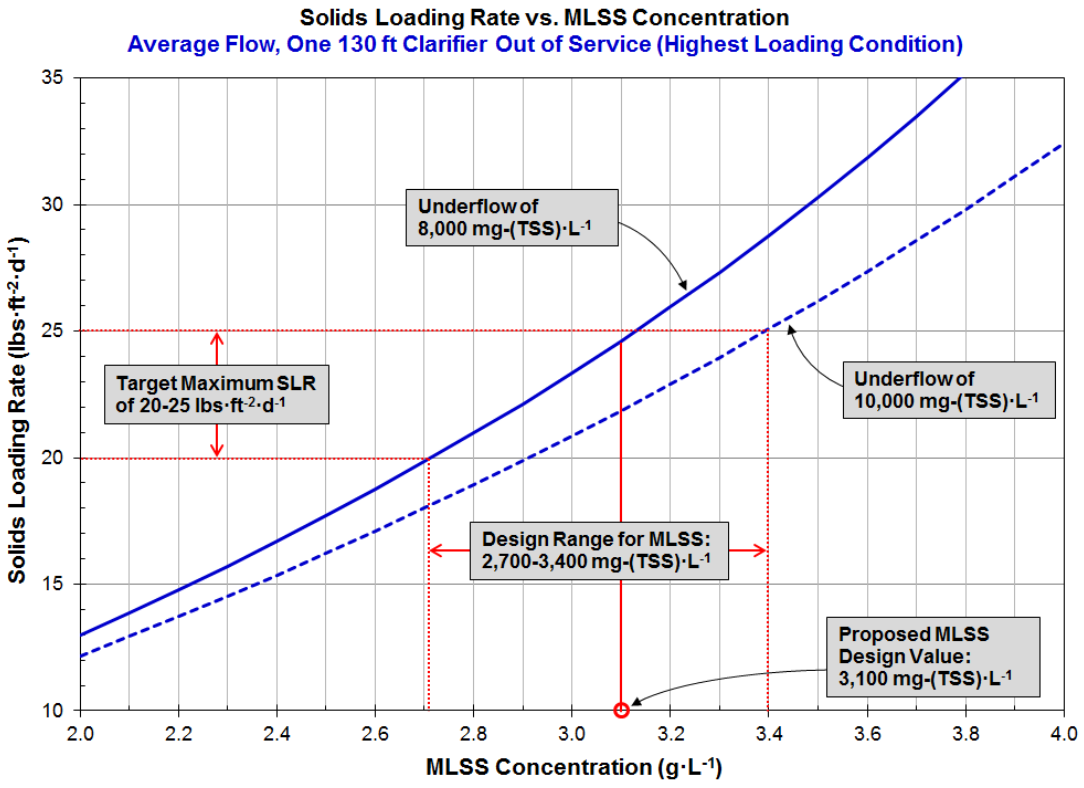

Figure B.1. Design range for MLSS based on a maximum target solids loading rate (SLR) of 20-25 lbs·ft^{-2}·d^{-1}.

Secondary treatment biological reactors. Due to space limitations at the Chesapeake-Elizabeth WWTP, it is estimated that the maximum length of new reactors (including walls and baffles) for the secondary treatment system is 192 ft. Existing aeration tanks are constructed as 12 parallel trains. For all new tankage, 6 parallel trains have been designed and will precede existing tankage. Modifications may be made to existing tankage to achieve anoxic conditions as needed.

Denitrification filters. Downflow denitrification filters were designed as a total of 12 columns, assuming that 2 would be out of service under design flow. It was assumed that water backwash pumping would be at a rate of 10 $gal \cdot min^{-1} \cdot ft^{-2}$ for 15 minutes once a day.

Disinfection. It was assumed that the existing disinfection system would remain unchanged.

ISB Treatment System. The ISB Treatment System (ISBTS) was designed as a single PFR (HRT of 4 hours) with an ISBTS SRT of 4 days. Expected ISB flow is assumed to be 1 MGD with WAS flow on the order of 0.2-0.4 MGD (based on steady state GPS-X simulations).

Primary sludge thickening. There are two existing gravity thickeners onsite which will be used for primary sludge thickening. Given the anticipated primary solids flow rate of roughly 100,000 $gal \cdot d^{-1}$, the hydraulic loading rate with one gravity thickener out of service would be roughly 26 $gal \cdot ft^{-2} \cdot d^{-1}$, significantly below the typical design range of 380-760 $gal \cdot ft^{-2} \cdot d^{-1}$. Secondary clarifier effluent was recycled and mixed with primary solids raise surface overflow rates to typical design values.

WAS thickening. Gravity belt thickeners (GBTs) were designed to operate at the same frequency as the centrifuges (22.7 hours a day, 7 days a week). It is assumed that no solids storage exists immediately upstream or downstream of the GBTs, requiring GBT operation whenever secondary solids are wasted. GBTs were designed such that the maximum hydraulic loading is no more than 150 $gal \cdot m^{-1} \cdot min^{-1}$ with all units in service and no more than 200 $gal \cdot m^{-1} \cdot min^{-1}$ with one unit out of service.

Dewatering. The Chesapeake-Elizabeth WWTP has three existing centrifuges – only one is typically in operation at any given time. The expected loading to centrifuges is on

the order of 0.03-0.15 MGD (current loading averages 0.44 MGD, minimum month of 0.23 MGD and maximum month of 0.70 MGD), with influent solids concentrations a factor of 5 times more concentrated than the centrifuges currently see (current influent solids average 1.2% solids). Despite fluctuations in loading, centrifuges operated on average 22.7 +/- 0.7 hrs per day, every day of the year, in recent years. It is assumed that the same schedule will be followed, despite the significant reduction in solids and hydraulic loading.

Multiple Hearth Incinerator. There are two existing multiple hearth incinerators at the Chesapeake-Elizabeth WWTP. Only one incinerator is typically in operation at any given time, with an operational schedule that matches the dewatering unit process (22.7 +/- 0.7 hrs per day, every day of the year). It is assumed that the same schedule will be followed, despite the significant reduction in wet sludge loading.

Aeration equipment sizing. To be able to quantify the aeration energy required under dynamic and uncertain conditions, the aeration requirements are predicted by GPS-X assuming as "airflow at standard conditions" and using DO controllers set to 2 mg-$(O_2)\cdot L^{-1}$ in each aerobic basin. Although these estimates of aeration requirements may not be as accurate as hand calculations, this will provide consistency in dynamic estimates for aeration energy requirements. For design purposes, the blower and air header sizing will be based on the steady state aeration requirement from GPS-X multiplied by 1.5. This value (1.5*steady state aeration) will then be used to determine the number of fine bubble diffusers, assuming 1.9 scfm per diffuser.

Internal recycle pumping rate. The internal recycle pumping rate (from AER1 to ANX1 in the 5-stage Bardenpho process; from AER to ANX in the A2O process) were set to 2x forward flow through the biological process (~27.3 MGD) based on steady state simulations at the design annual average raw influent hydraulic load of 24 MGD. The installed pumping capacity was 1.5x this design pumping rate.

Appendix C
Ecoinvent Materials and Processes Used for Life Cycle Assessment

Construction Inventory Materials & Processes

Zimmermann [German]		Zimmermann [translated]		Doka		Foley		Guest	
Input-Materialien	**Input Materials**		**Construction Materials**		**Construction Process**	**Construction Materials**		**Construction Materials**	
Beton (ohne Armierungseisen)	Concrete (without rebar)		concrete, exacting, at plant			Readymix Concrete		Concrete, exacting, at plant/CH U	
Stahl unlegiert	Unalloyed steel		reinforcing steel, at plant			Steel, Blastscope Port Hamilton		Reinforcing steel, at plant/RER U	
Wasser	Water		tap water, at user			Water (delivered)		Tap water, at user/RER U	
Aluminium 0% Rec.	Aluminium 0% Rec. (recycled)		aluminium, production mix, cast alloy, at plant			Aluminium, primary, rec. NEI emission estimates		Aluminium, production mix, cast alloy, at plant/RER U	
Kalkstein	Limestone		limestone crushed, washed			Limestone (calcite)		Limestone, crushed, washed/CH U	
Stahl hochlegiert	High-alloy steel		chromium steel 1838, at plant			Chromium Steel 18% Cr 8% Ni		Chromium steel 1896, at plant/RER U	
Glas (Flach-) unbeschichtet	Glass (Flat, uncoated)		glass fibre, at plant			PA6 30% glass fibre		Flat glass, uncoated at plant/RER U	
Kupfer	Copper		copper, at plant			Copper		Copper, primary, at refinery/RNA U	
Kunststoff EPDM	EPDM Rubber		synthetic rubber, at plant			EPDM (synthetic) Rubber		Synthetic rubber, at plant/RER U	
Mineralwolle	Mineral wool		rock wool mat, packed, at plant			Mineral Wool (Rock Wool)		Rock wool, packed, at plant/CH U	
Chemikalien organisch	Organic chemicals		chemicals organic, at plant			Chemicals - Organic (use LDPE as a proxy)		Chemicals organic, at plant/GLO U	
Bitumen from refinery CH	Bitumen from refinery - Switzerland		bitumen, at refinery			Bitumen		Bitumen, at refinery/CH U	
Chemikalien anorganisch	Inorganic Chemicals		chemicals inorganic, at plant			Chemicals - inorganic (use Phosphoric Acid as proxy)		Chemicals inorganic, at plant/GLO U	
PE (LD)	Polyethylene (low-density)		polyethylene, LDPE, granulate, at plant			Low Density Polyethylene (LDPE)		Polyethylene, LDPE, granulate, at plant/RER U	
PE (HD)	Polyethylene (high-density)		polyethylene, HDPE, granulate, at plant			High Density Polyethylene (HDPE)		Polyethylene, HDPE, granulate, at plant/RER U	
						EPDM (synthetic) Rubber			
						Polypropylene			
						Hollow Fibre Membrane, HDPE			
						Steel, Blastscope Port Hamilton			
						Mass of Electric Motors			
						Mass of Pumps, Mixers, Compressors, etc.			
Transporte/Bauprozesse/Energieträger	**Construction Process**		**Construction Process**			**Construction Process**		**Construction Process**	
Aushub Hydraulikbagger	Hydraulic excavator digging		excavation, hydraulic digger			Excavation, hydraulic digger/RER U			
Transport LKW 28 t	Transport truck 28 tonne		transport, lorry 28t			Transport, Articulated Truck 28/60 (Freight)		Transport, lorry >28t, fleet average/CH U	
Strom Mittelspannung, Bezug in CH	Current Medium Voltage - reference in Switzerland		electricity, medium voltage, at grid			Electricity, East Australian HV Average Mix		Electricity, low voltage, at grid/US U	
			transport, freight, rail			Transport, Rail (Bulk Transport)		Transport, freight, rail, diesel/US U	
			extrusion			Extrusion of PET		Extrusion, plastic pipes/RER U	
						Transport, Articulated Truck 28/60 (Urban)			
						Transport, Articulated Truck 28/60 (50% rural)			
Abfälle	**Waste**		**Construction Waste**			**Construction Waste**		**Construction Waste**	
Abfälle in Inertstoffdeponie	Waste in inert material landfill							Disposal, inert waste, 5% water, to inert material landfill/CH U	
Beton in Inertstoffdeponie	Concrete in inert material landfill							Disposal, concrete, 5% water, to inert material landfill/CH U	
Bitumen in Reaktorndeponie	Bitumen in sanitary landfill							Disposal, bitumen, 1.4% water, to sanitary landfill/CH U	
Glas in Inertstoffdeponie	Glass in inert material landfill							Disposal, glass, 0% water, to inert material landfill/CH U	
Kunststoffe in KVA	Plastics to municipal waste incinerator							Disposal, polyethylene, 0.4% water, to municipal incineration/CH U	
Stahl in Inertstoffdeponie	Steel in inert material landfill							Disposal, steel, 0% water, to inert material landfill/CH U	
Zimmermann, P., Doka, G., Huber, F., Labhardt, A., Ménard, M. Ökoinventare von Entsorgungsprozessen: Grundlagen zur Integration der Entsorgung in Ökobilanzen. ESU-Reihe, 1996. Gruppe Energie-Stoffe-Umwelt ESU, Laboratorium für Energiesysteme, Institut für Energietechnik, ETH Zürich, Switzerland, 1996.			Doka, G. Life Cycle Inventories of Waste Treatment Services. ecoinvent report No. 13. Swiss Centre for Life Cycle Inventories, Dübendorf, 2009.			Foley, J., de Haas, D., Hartley, K., Lant, P., Comprehensive life cycle inventories of alternative wastewater treatment systems. Water Research 2010, 44, (5), 1654-1666.		Guest, JS. Dissertation. 2012.	

Operation Inventory Materials & Processes

Operation Materials
Acetic acid, 98% in H2O, at plant/RER U
Methanol, at plant/GLO U
Iron (III) chloride, 40% in H2O, at plant/CH U
Natural gas, at consumer/RNA U
Methyl methacrylate, at plant/RER U
Operation Processes
Electricity, hard coal, at power plant/US U
Electricity, oil, at power plant/GB U
Electricity, natural gas, at power plant/US U
Electricity, nuclear, at power plant/US U
Electricity, hydropower, at power plant/GB U
Electricity, at wind power plant/RER U
Disposal, digester sludge, to municipal incineration/CH U

Appendix D

Probability Density Functions for Model Parameters for Quantitative Sustainable Design

Reproduced from Table 5.1:

Table D.1. Input uncertainty for model parameters

ID	Parameter	Distribution	Minimum & Maximum (uniform) or Average & Standard Deviation (normal)	Units
1	dry weather influent flow	uniform	18 (min); 23 (max)	MGD
2	rainfall	empirical [b,c]	NA	MGD
3	influent BOD_5	normal [b]	243 (avg); 19 (stdev)	$mg \cdot L^{-1}$
4	influent BOD:TKN ratio [d]	normal [b]	5.7 (avg); 0.79 (stdev)	$mg\text{-}(BOD_5) \cdot L^{-1}$ per $mg\text{-}(N) \cdot L^{-1}$
5	influent BOD:TP ratio [e]	normal [b]	41 (avg); 2.5 (stdev)	$mg\text{-}(BOD_5) \cdot L^{-1}$ per $mg\text{-}(P) \cdot L^{-1}$
6	nitrifier maximum specific growth rate [f]	uniform	0.77 (min); 0.92 (max)	d^{-1}
7	oxygen half saturation coefficient for heterotrophs	uniform [g]	0.1 (min); 0.3 (max)	$mg\text{-}(COD) \cdot L^{-1}$
8	ammonium half saturation coefficient for AOB	uniform [g]	0.5 (min); 1.5 (max)	$mg\text{-}(N) \cdot L^{-1}$
9	temperature	uniform [b]	12 (min); 28 (max)	°C

[a] The plant experiences roughly 1 MGD of influent from rain events on average. The values for dry weather influent flow exclude flow from rain events, which were simulated as a separate, independent parameter.

[b] Observed distribution based on HRSD data.

[c] Empirical distribution characterized by HRSD data. See Supporting Information for additional details.

[d] Influent ammonium was set to 74% of the influent TKN concentration based on the median value of HRSD data.

[e] Influent soluble phosphorus was set to 80% of the influent TP concentration; no data from HRSD was available for soluble phosphorus.

[f] AOB and nitrite oxidizing bacteria (NOB) decay were fixed at 0.17 d^{-1}, and NOB maximum specific growth rate was set to 0.1 d^{-1} greater than the AOB maximum specific growth rate based on this default assumption in GPS-X™.

[g] Distribution and values are consistent with assumption in [126].

D.1. Dry Weather Influent Flow

Although the average annual design flow for the plant is 24 MGD, it rarely sees flows that high. The average dry weather flow is roughly 18 MGD and the average daily total influent flow (i.e., with wet days) is 19 MGD. Here we distinguish between the dry weather municipal wastewater flow (which we assume contains all of the contaminants) and additional flow resulting from rain events (which we assume has no contaminants and only dilutes the wastewater contaminants).

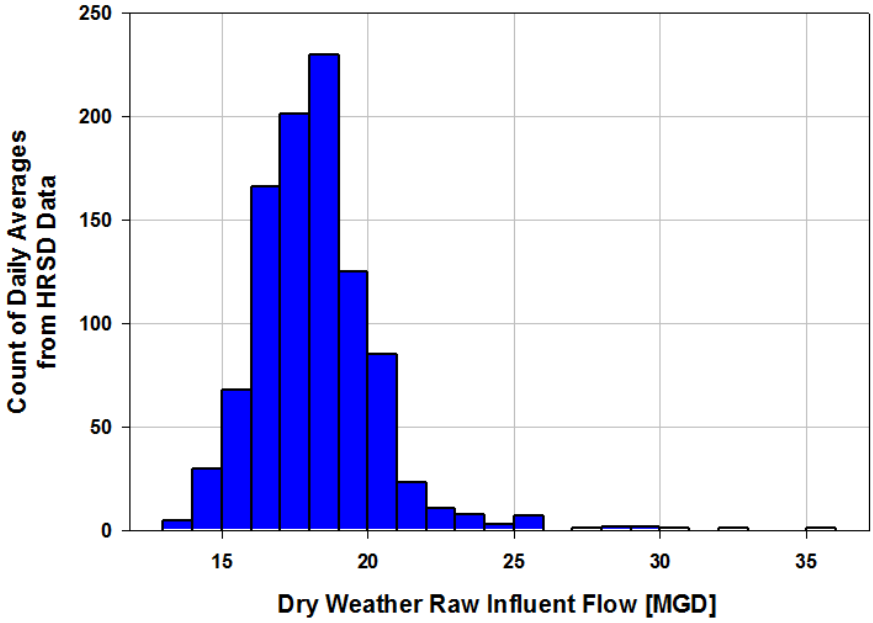

Figure D.1. Histogram of HRSD data for dry weather raw influent flow.

The dry weather influent to the plant will be assumed to have a uniform distribution from 18 MGD to 23 MGD. Note that 23 MGD – with 1 MGD of average influent from rainfall – is at the design value of 24 MGD. This flow rate does not include the 1 MGD from the incinerator scrubber blowdown. Also note that the population in the Hampton Roads metropolitan area has experienced the lowest population growth in Virginia over the last 7 years (http://hamptonroadsperforms.org/indicators/economy/net-migration.php).

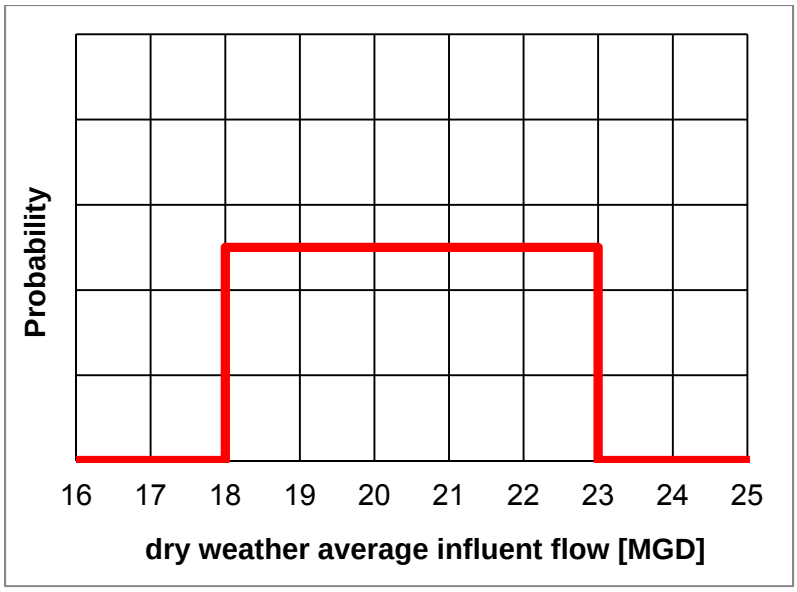

Figure D.2. Probability density function for dry weather raw influent flow.

The diurnal was established from dry weather hourly flows from 2005-2010 (970 days). The weekday and weekend diurnals were tightly clustered amongst themselves.

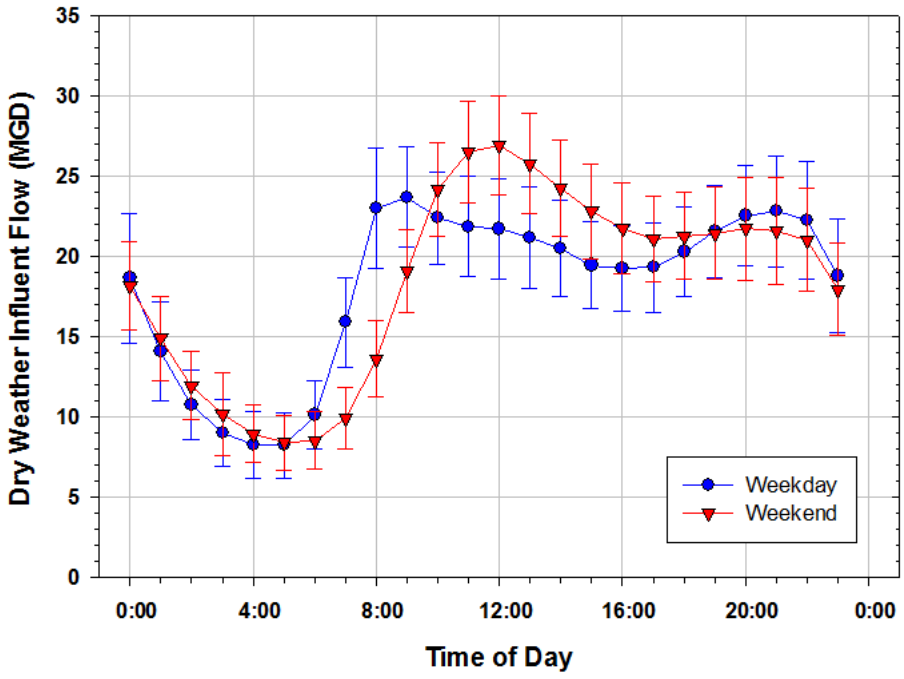

Figure D.3. Weekday and weekend dry weather diurnal flow based on HRSD data.

These weekday and weekend values were each normalized to total 1 MGD – these are the weekday and weekend unit vectors for hourly flow. To generate a weekday and weekend diurnal for the influent time series, these unit vectors are multiplied by the "dry weather influent flow" (one of the uncertain parameters specified in the LHS simulation set).

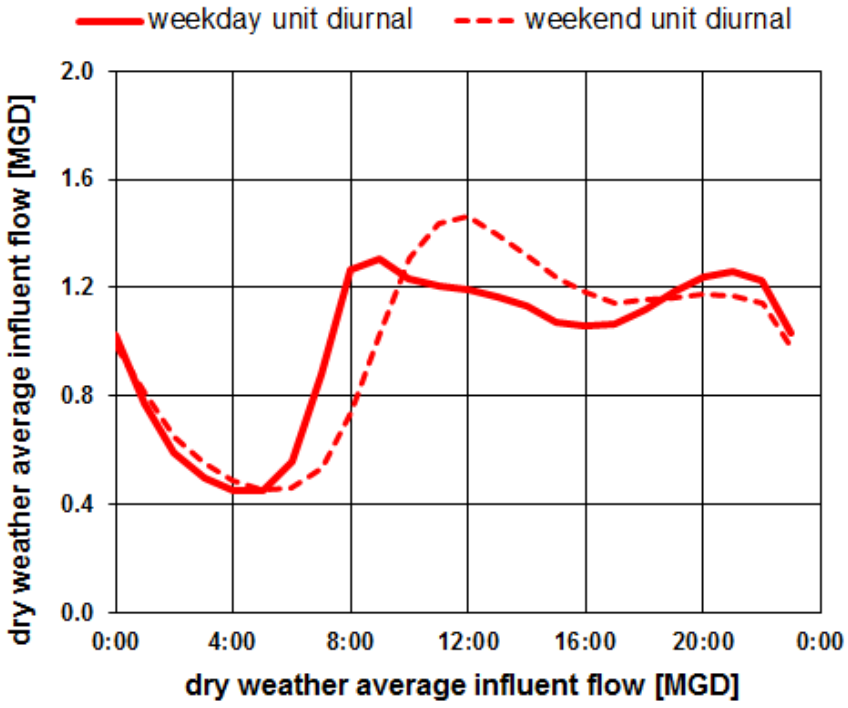

Figure D.4. Unit diurnal flow used in simulations.

D.2. Rainfall

Rainfall data was used to estimate the additional flow into the plant from rain events. Any daily reported flow data that included a "rainfall" value greater than 0 inches was classified as having had a "rain event". The distribution of rainfall intensity from HRSD data indicates that the vast majority of rain events very small.

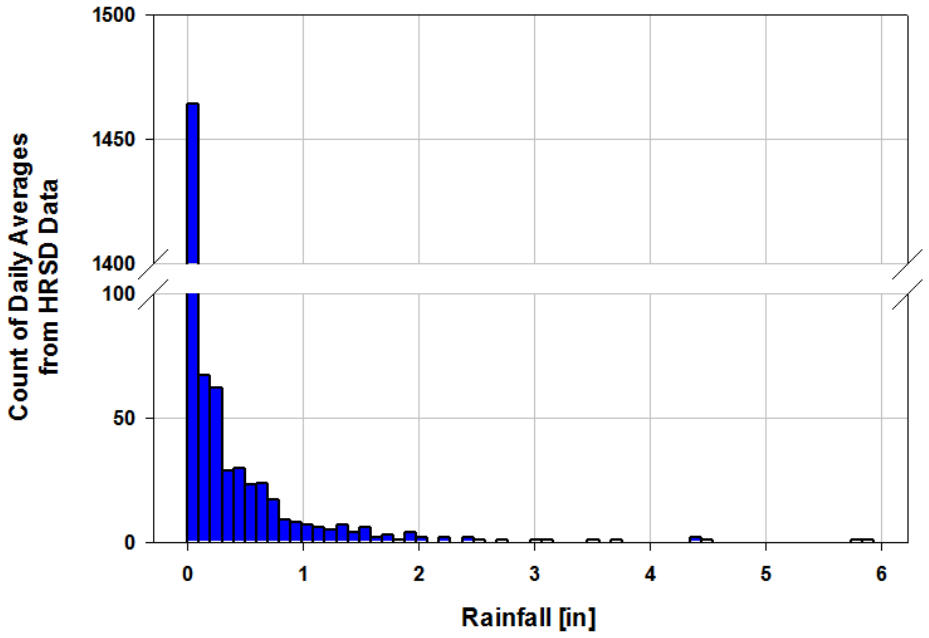

Figure D.5. Histogram of HRSD data for rain events.

Rain events will be assumed occur on 41% of days (consistent with HRSD data) and to have the same trend in magnitude of rainfall (see histogram below). This will be achieved using a Matlab code that can use data to define a new probability distribution function.

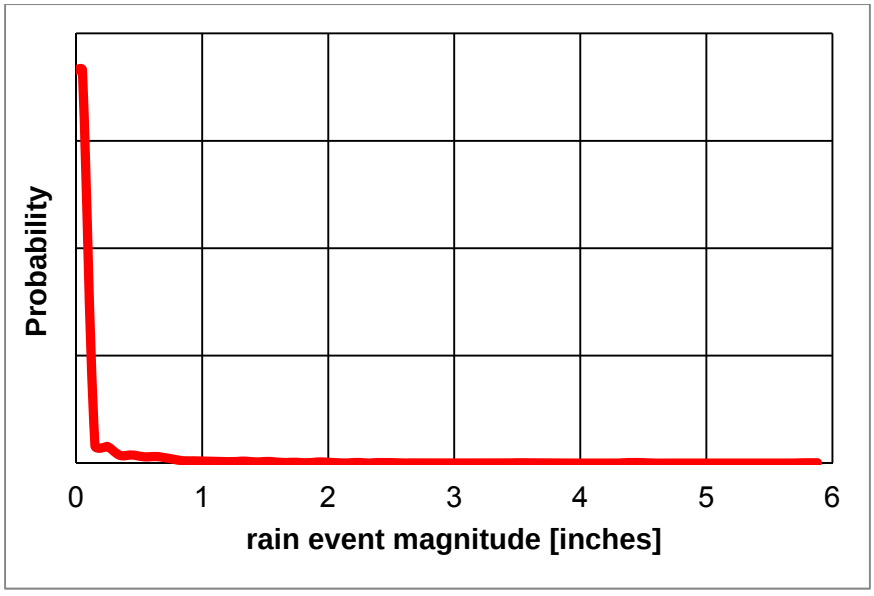

Figure D.6. Probability density function for rain events.

The volume of influent resulting from a given rain event was estimated using HRSD data. Average dry weather diurnal curves were established for each day of the week (weekdays were very similar to one another, and Saturday and Sunday were very similar). All days with rain events greater than 0.3 inches were then used to compare the total flow on the day of the rain event to the corresponding average dry flow for that day. The difference between the rain event day's flow and the dry weather flow was used to determine the estimate the resulting increase in influent volume for a given rainfall.

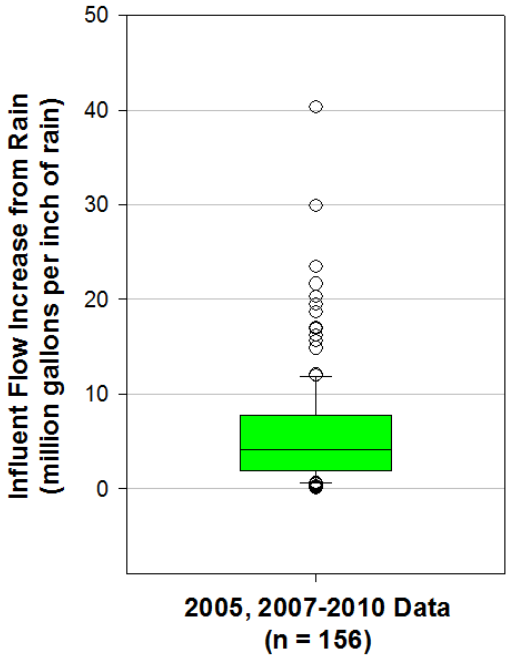

Figure D.7. HRSD data for influent flow increase per inch of rain.

The median value was 4.1 million gallons of additional influent flow per 1 inch of rainfall. This value was then used to adjust average monthly observed concentrations of influent BOD_5, TKN, and TP to dry weather concentrations by assuming the same BOD5, TKN, and TP mass loading would have arrived at the WWTP with less flow in the absence of rain events. This approach estimated that rainfall was responsible for roughly 2% of the influent flow on average.

Hydrographs were constructed by comparing hourly flows on days with intense rain events (greater than 0.6 inches) to dry weather diurnals for that particular day of the week. Three normalized hydrographs (each totaling 1 million gallons of rainwater) can be seen in the figure below.

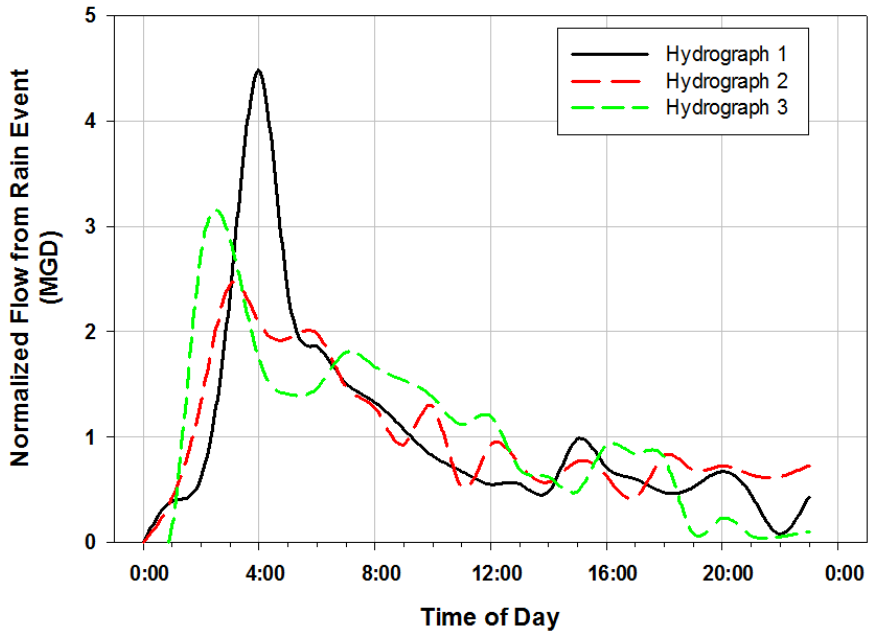

Figure D.8. Normalized hydrographs (sum to 1 MGD) based on hourly HRSD data.

For simulations, only hydrograph 3 will be used. For a given day, the intensity of its rain event (determined by the rainfall value in the LHS-generated simulation set) will be multiplied by the hydrograph to distribute the influent flow from rainwater over a single 24 hour period. The start of the 24 hour period over which the rain falls will be randomly selected (it will begin between 0:00 and 23:00 on the day to which the rain event was assigned), and the resulting hydrograph will be added to the influent flow diurnal. Concentrations of constituents (BOD_5, TKN, NH_4^+, TP, PO_4^{3-}) will be adjusted to ensure the desired dry weather loading (from the LHS simulation set) is achieved.

D.3. Influent BOD_5

Monthly averages of influent BOD_5 from 2003-2010 have ranged from 162-292 g-(BOD_5)·m^{-3} with a median of 239 g-(BOD_5)·m^{-3}. With rainfall corrections (removing the flow from rainfall and assuming the BOD load is unchanged), these values become 168-294 g-(BOD_5)·m^{-3} with a median of 243 g-(BOD_5)·m^{-3}.

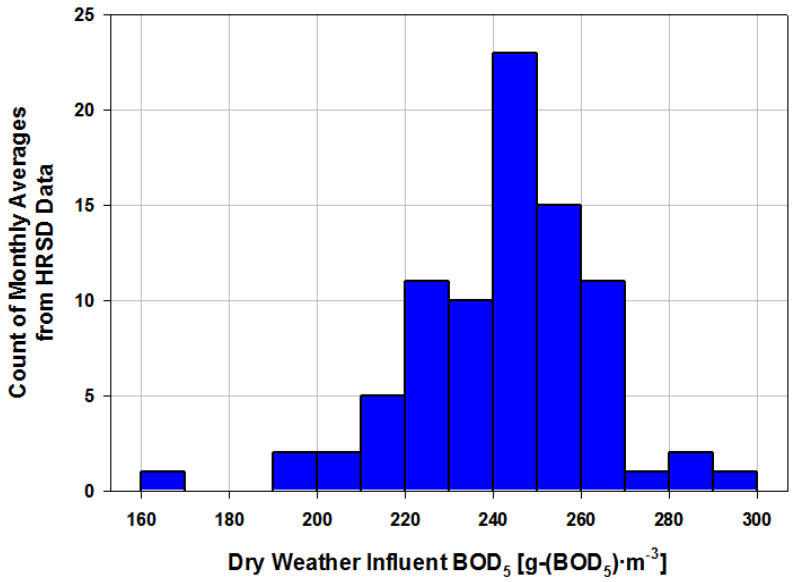

Figure D.9. Histogram of dry weather influent BOD_5 data.

The influent dry weather BOD5 was assumed to have a normal distribution centered at 243 g-$(BOD_5)\cdot m^{-3}$.

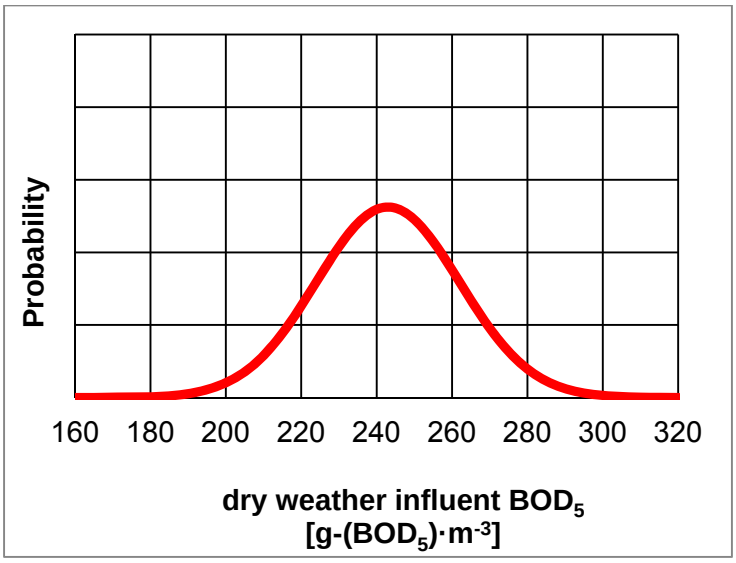

Figure D.10. Probability density function for dry weather influent BOD_5.

D.4. Influent BOD:TKN Ratio

Monthly averages of influent TKN from December 2004 through 2010 have ranged from 29-57 g-$(N)\cdot m^{-3}$ with a median of 41 g-$(N)\cdot m^{-3}$. With rainfall corrections (removing the

flow from rainfall and assuming the TKN load is unchanged), these values become 30-57 g-(N)·m^{-3} with a median of 42 g-(N)·m^{-3}.

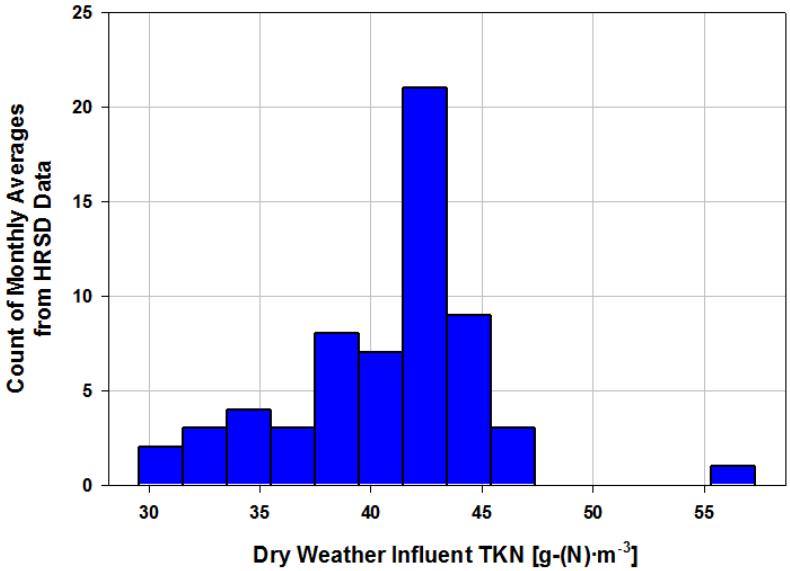

Figure D.11. Histogram of HRSD data for dry weather influent TKN.

Originally, we were considering assigning the influent dry weather TKN a normal distribution centered at 42 g-(TKN)·m^{-3}. However, the variation in influent TKN does not vary entirely independently of BOD_5.

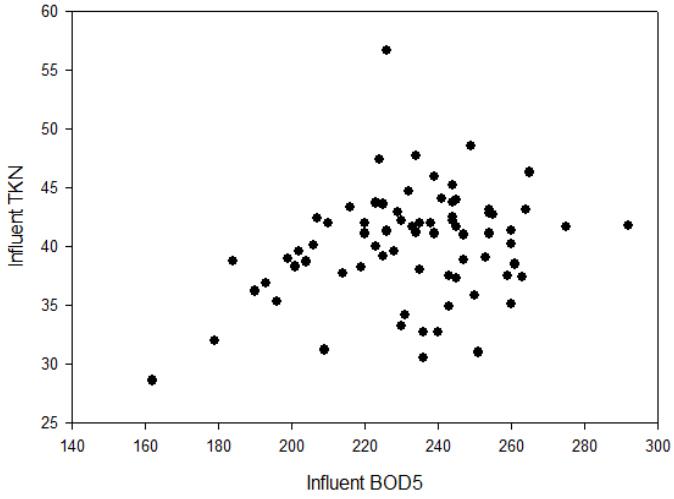

Figure D.12. Scatter plot of influent BOD_5 and TKN.

As we examine the typical ratio of TKN to BOD_5, we can see that TKN is not entirely independent. As such, we varied it according to the distribution from the BOD_5/TKN histogram below.

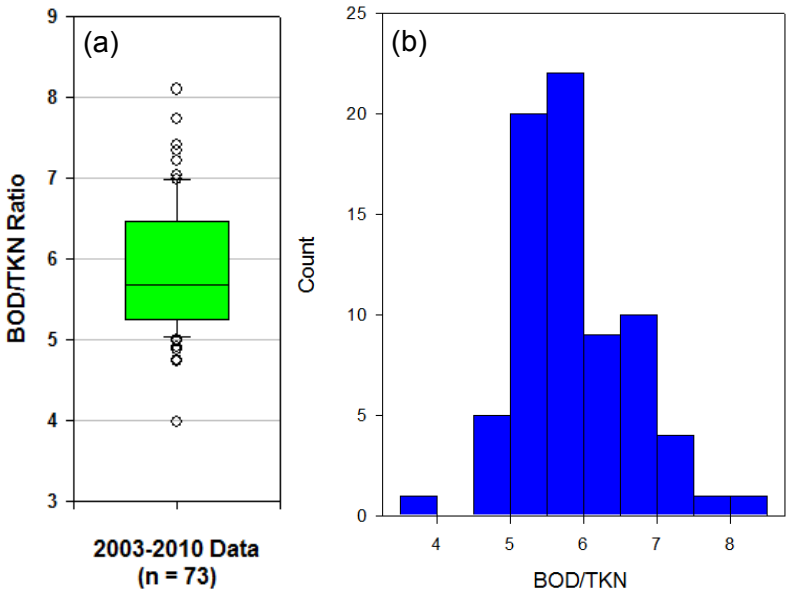

Figure D.13. Plots of HRSD data for influent BOD_5:TKN ratio.

Although the relative fraction of ammonium:TKN varies (see histogram and box and whisker plot below), it will be assumed that ammonium is always 74% of the influent TKN (equivalent to the median and mean values from the available data).

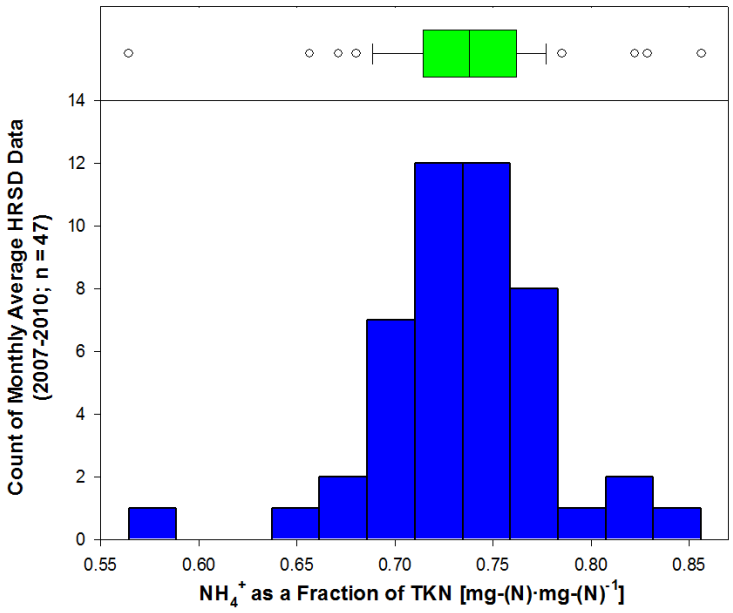

Figure D.14. Plots of HRSD data for influent ammonium:TKN ratio.

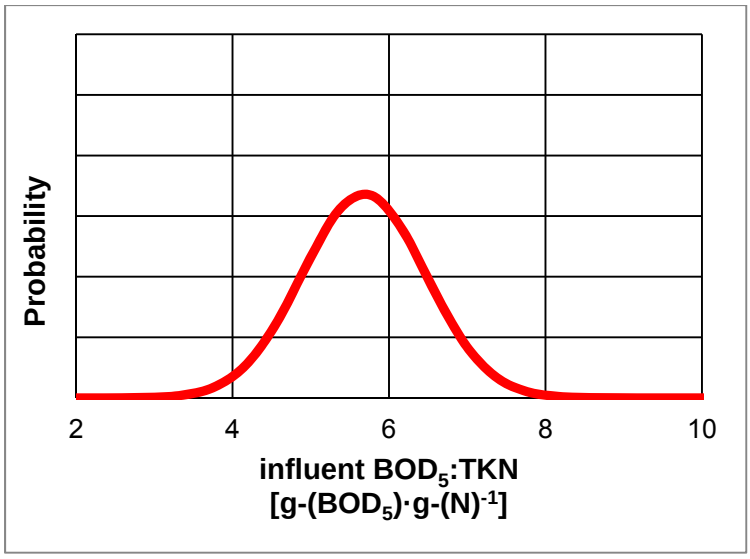

Figure D.15. Probability density function for influent BOD_5:TKN ratio.

D.5. Influent BOD:TP Ratio

Monthly averages of influent TP from 2003-2010 have ranged from 4.0-7.1 g-(P)·m^{-3} with a median of 6.0 g-(P)·m^{-3}. With rainfall corrections (removing the flow from rainfall and assuming the TP load is unchanged), these values become 4.1-7.3 g-(P)·m^{-3} with a median of 6.1 g-(P)·m^{-3}.

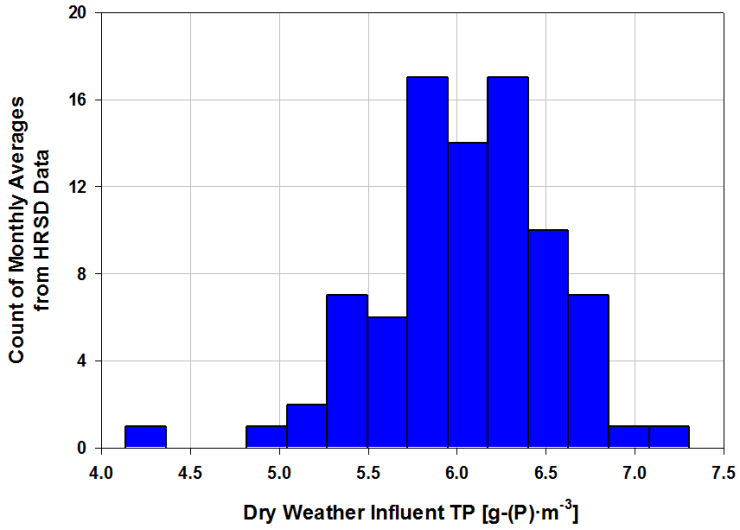

Figure D.16. Histogram of HRSD data for dry weather influent TP.

However, influent TP does not vary independently of BOD_5.

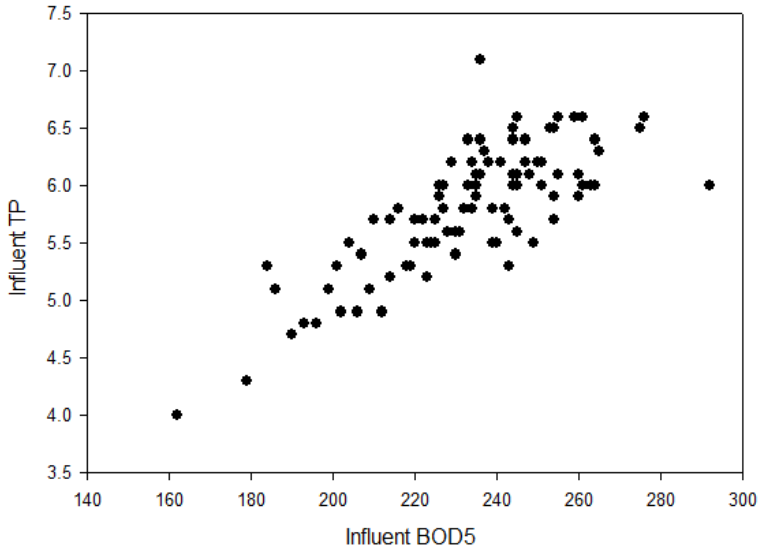

Figure D.17. Scatter plot of influent BOD_5 vs influent TP.

Typical ratios of BOD_5 to TP can be seen in the figures below.

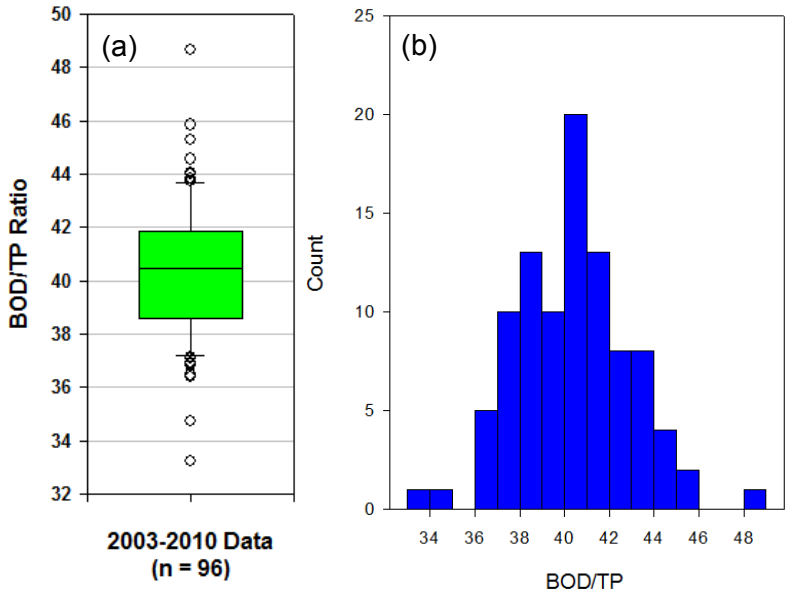

Figure D.18. Plots of HRSD data for BOD_5:TP ratio.

Instead of varying TP independently of BOD_5, we will vary it according to the distribution from the BOD_5/TP histogram above.

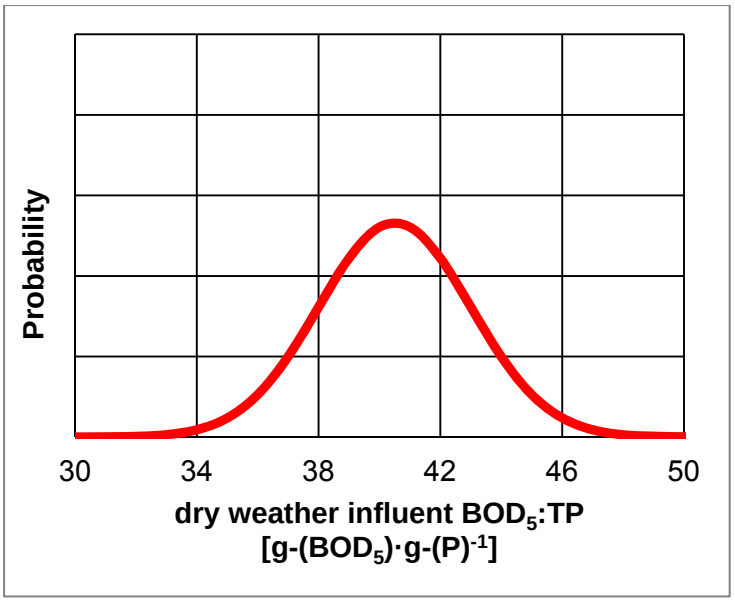

Figure D.19. Probability density function for influent BOD_5:TP ratio.

No data is available for the relative fraction of soluble phosphate:TP. It is assumed that the soluble phosphate concentration is always 80% of influent TP.

D.6. Nitrifier Maximum Specific Growth Rate

In acknowledgement of published work on uncertainty in wastewater modeling (Sin et al. 2011; Benedetti et al. 2008), we have also included this as an uncertain parameter. Since we are now using the Mantis2 model because we wanted to include NO_2^- as a state variable (in case we wanted to use this value for N_2O estimates), AOB and NOB are separate. For this study, we assume AOB and NOB decay rates are constant, and we allow the difference between AOB maximum specific growth and decay to range from 0.60-0.75 d^{-1} with a uniform distribution (note that decay is fixed at 0.17 d^{-1}). We assume that the NOB decay rate is the same as AOB, and the NOB maximum specific growth rate is always 0.1 d^{-1} greater than AOB.

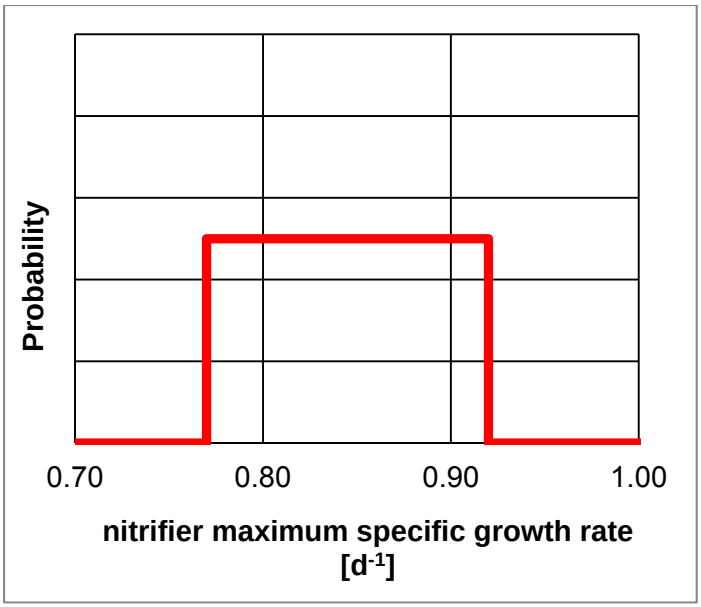

Figure D.20. Probability density function for nitrifier maximum specific growth rate.

D.7. Oxygen Half Saturation Coefficient for Heterotrophs

In acknowledgement of published work on uncertainty in wastewater modeling [124, 126], we have also included this as an uncertain parameter. This value will have an average of 0.2 g-(COD)·m^{-3} with a uniform distribution and a range of 0.10-0.30 g-(COD)·m^{-3} (consistent with [124]).

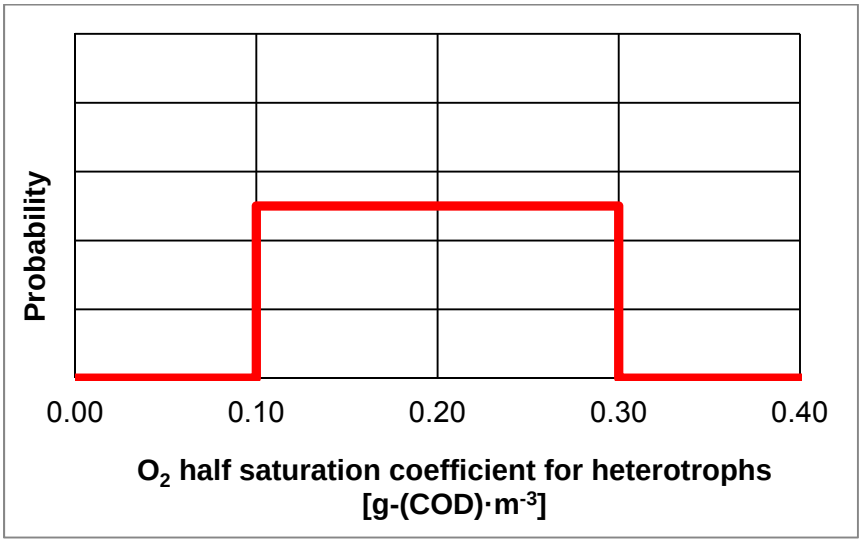

Figure D.21. Probability density function for O_2 half saturation coefficientfor heterotrophs.

D.8. Ammonium Half Saturation Coefficient for AOB

In acknowledgement of published work on uncertainty in wastewater modeling (Sin et al. 2011), we have also included this as an uncertain parameter. This value will have an average of 1.0 g-(N)·m^{-3} with a uniform distribution and a range of 0.5-1.5 g-(N)·m^{-3} (consistent with [124]).

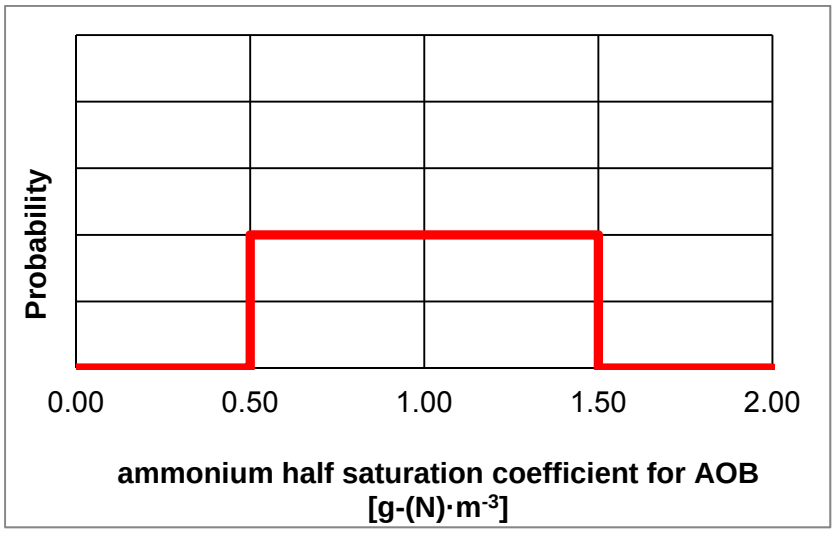

Figure D.22. Probability density function for ammonium half saturation coefficient for AOB.

D.9. Temperature

Based on monthly average data from 2003-2010, the minimum month influent temperature was 13°C, the maximum month was 28°C, and the median and mean were 21°C. In fact, raw influent temperature had a relatively uniform distribution from 2003-2010.

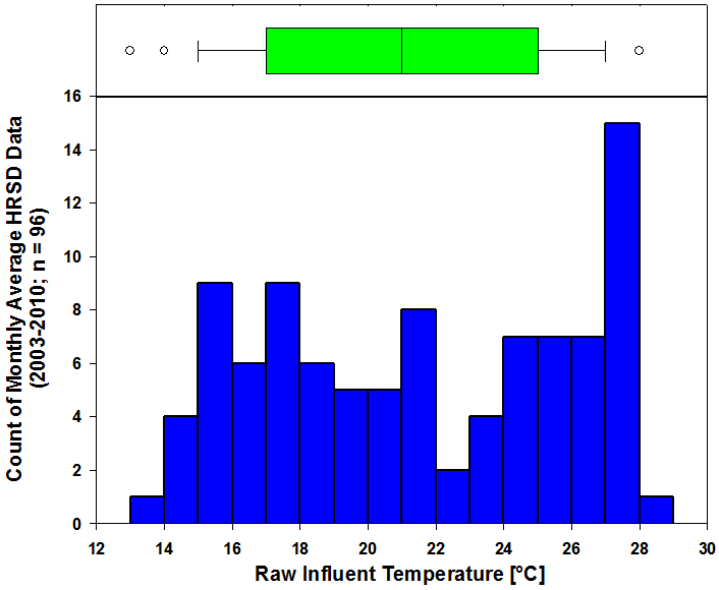

Figure D.23. Plots of HRSD data for influent wastewater temperature.

It was assumed that temperature did not change through the plant, and mixed liquor temperature would be the same as influent temperature.

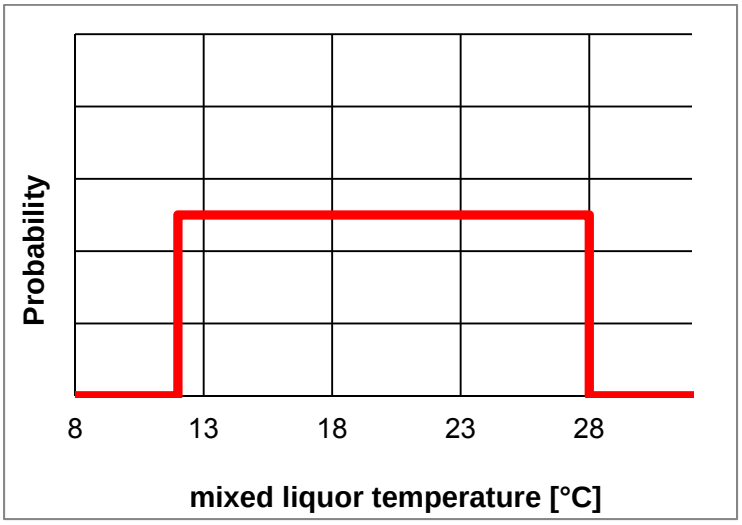

Figure D.24. Probability density function for mixed liquor temperature.

Appendix E

Sensitivity Analysis Results for Quantitative Sustainable Design

Reproduced from Table 5.2:

Table E.1. Sensitivity analysis overview.

Parameter	Default Value	Likely Minimum Value	Likely Maximum Value
Life Cycle Inventory			
Energy Source – Fraction Supplied by Coal [a]	0.342 [b]	0.141 [c]	0.632 [c]
N_2O Emission Factor – In WWTP [kg-(N_2O-N)·kg-(N denitrified)$^{-1}$]	0.005 [d]	0.0002 [e]	0.0059 [e]
N_2O Emission Factor – In Effluent [kg-(N_2O-N)·kg-(N in effluent)$^{-1}$]	0.005 [d]	0.005 [f]	0.046 [g]
Construction Multiplication Factor per m^3 Concrete – All Individual Materials & Processes	1x Fahner factor [h]	0.5x Fahner factor	4x Fahner factor
Cost Analysis			
Electricity Unit Cost [$·kWh^{-1}]	0.065 [h]	0.06	0.10

[a] Any changes to the coal fraction were compensated for with increase or decrease in the fraction electricity from nuclear power. The balance of electricity replaced by (or in place of) coal was assumed to be nuclear.
[b] Fraction based on 2010 data for the Commonwealth of Virginia [267].
[c] 25th percentile (likely minimum) and 75th percentile (likely maximum) of coal fractions by state for 2010 [267].
[d] [264]
[e] [256, 268]
[f] [256, 264]
[g] [256, 269]
[h] Factors developed in [263], and used by others (e.g., [130, 260])
[i] HRSD current pricing.

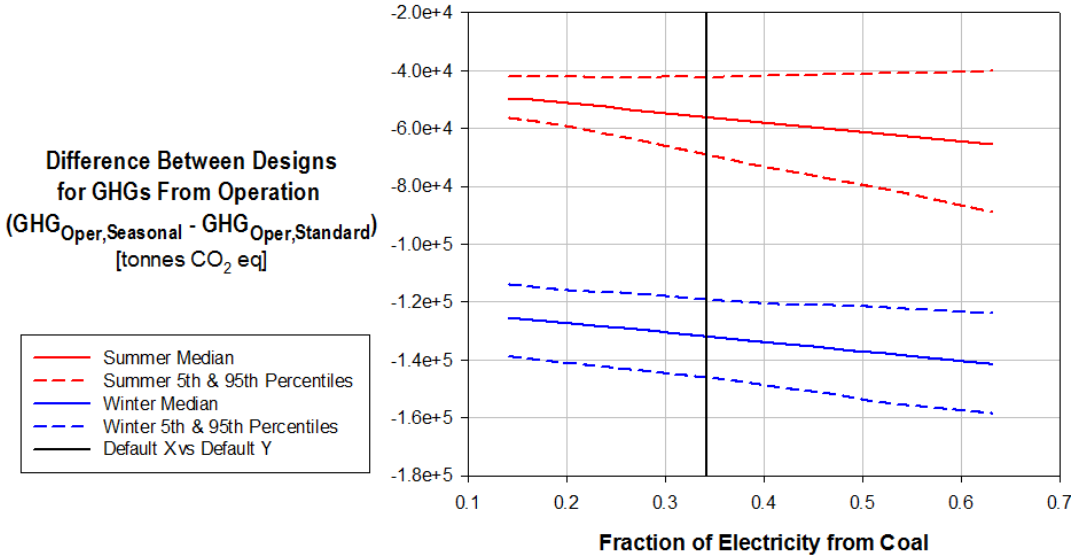

Figure E.1. Sensitivity of the difference in operational greenhouse gas emissions to the fraction of electricity provided by coal (black vertical line is default value of 0.342).

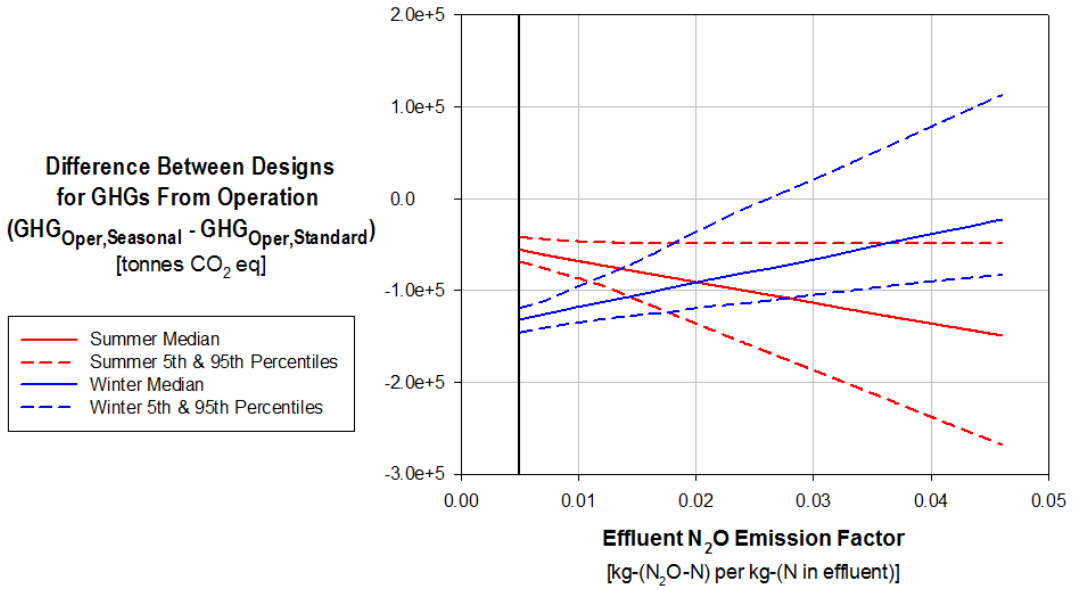

Figure E.2. Sensitivity of the difference in operational greenhouse gas emissions to the effluent N_2O emission factor (black vertical line is default value of 0.005).

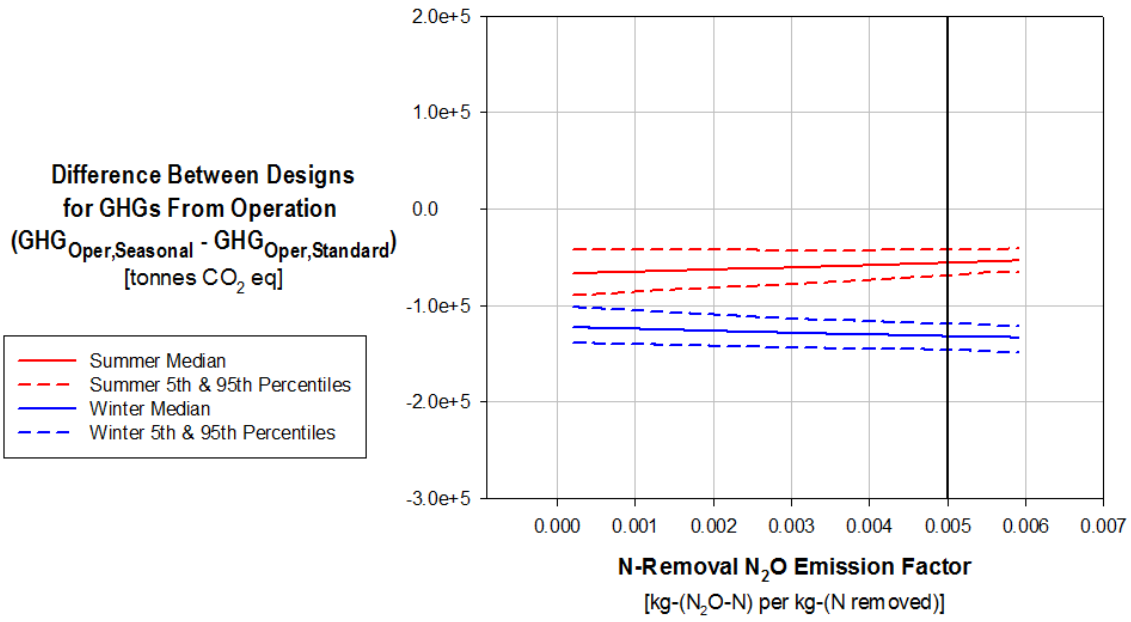

Figure E.3. Sensitivity of the difference in operational greenhouse gas emissions to the denitrification N_2O emission factor (black vertical line is default value of 0.005).

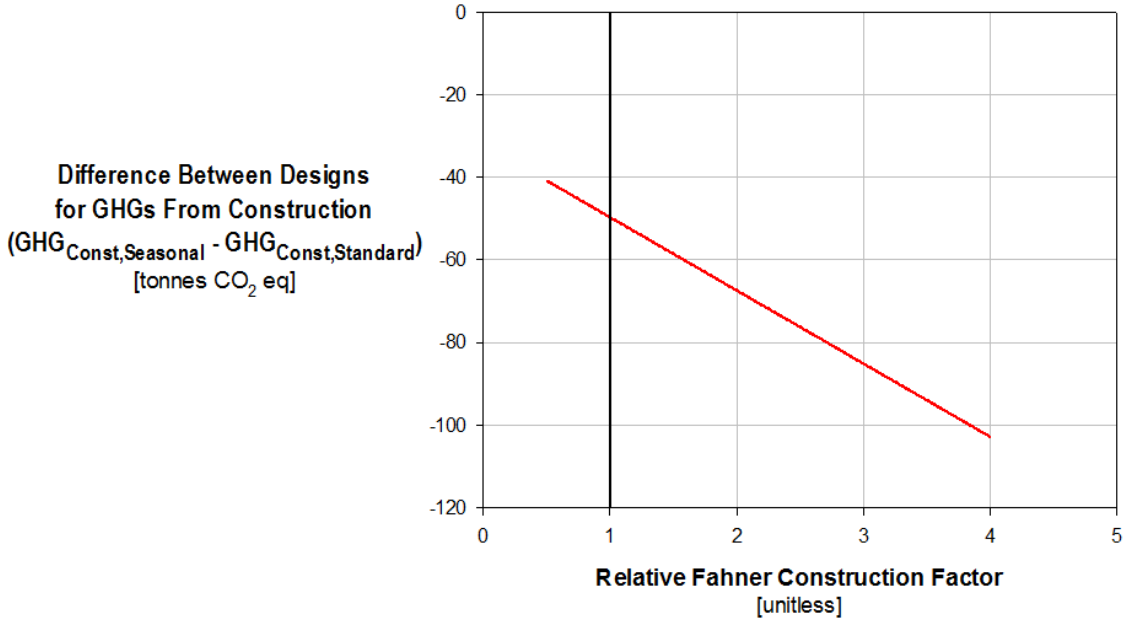

Figure E.4. Sensitivity of the difference in construction greenhouse gas emissions to the relative Fahner construction factor (black vertical line is default value of 1.0).

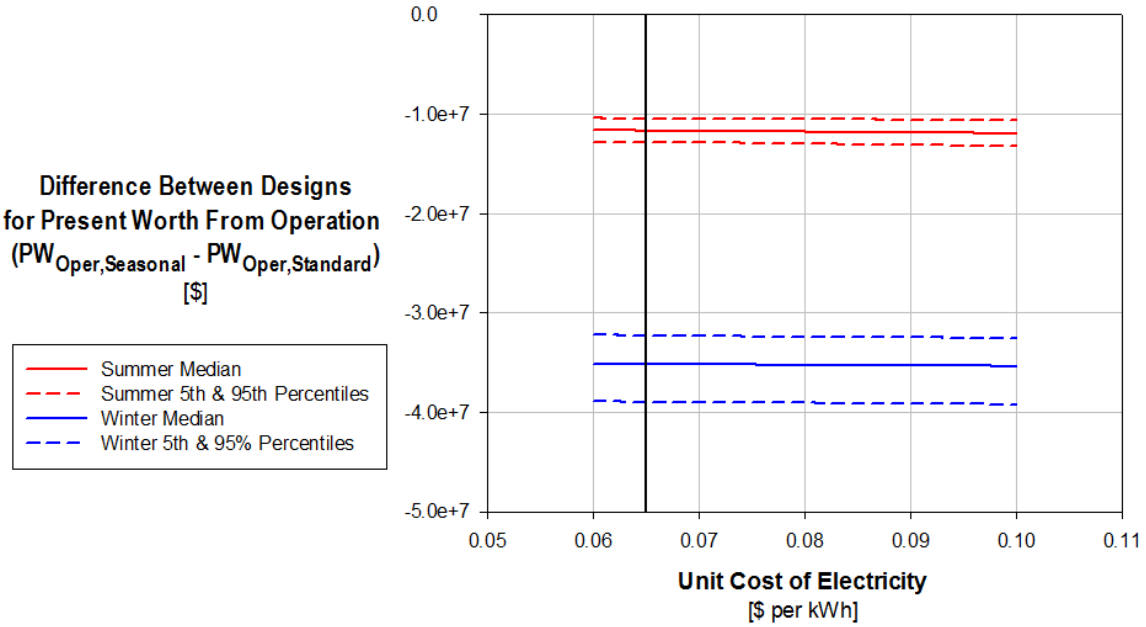

Figure E.5. Sensitivity of the present worth of operation to the unit cost of electricity.

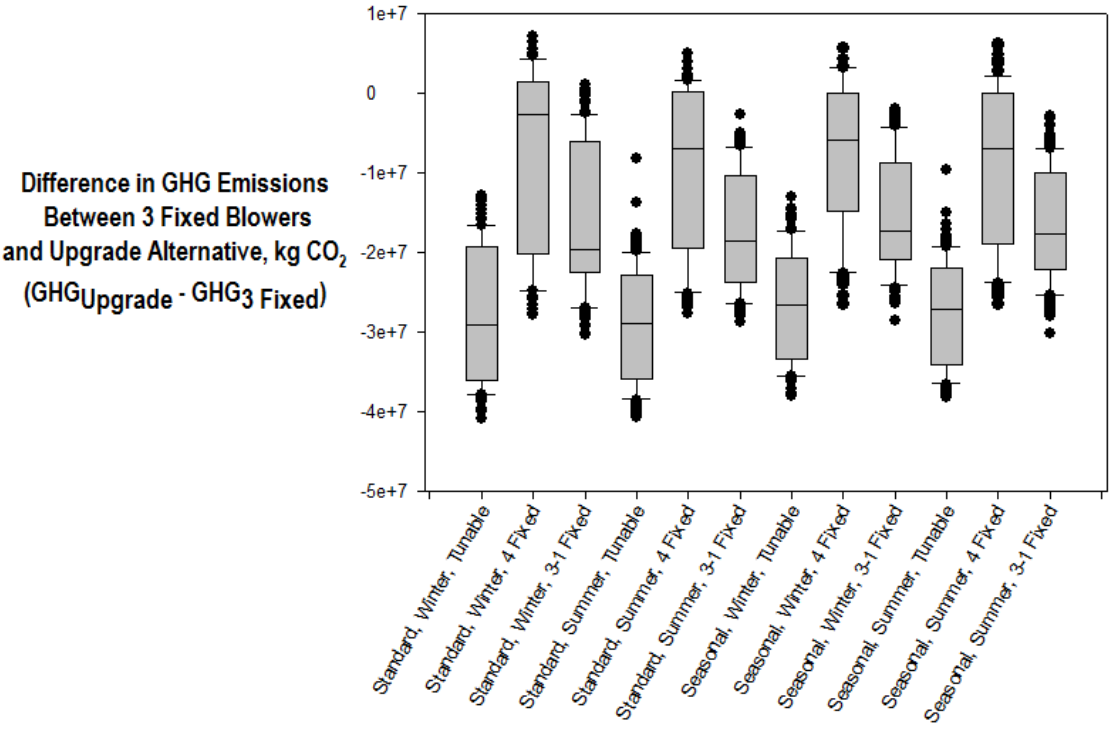

Figure E.6. Sensitivity of the difference in operational greenhouse gas emissions to the choice of blowers. Options are 3 fixed blowers (equal sized; default), tunable blowers, 4 fixed blowers (equal sized), and 4 fixed blowers (3 large, 1 small).

Appendix F
Relationships Derived from CAPDET and CapdetWorks™ for Quantitative Sustainable Design

Note: Figures below are compiled outputs from CapdetWorks™ simulations. Best-fit lines were used in the MATLAB codes for cost and life cycle environmental impact assessments.

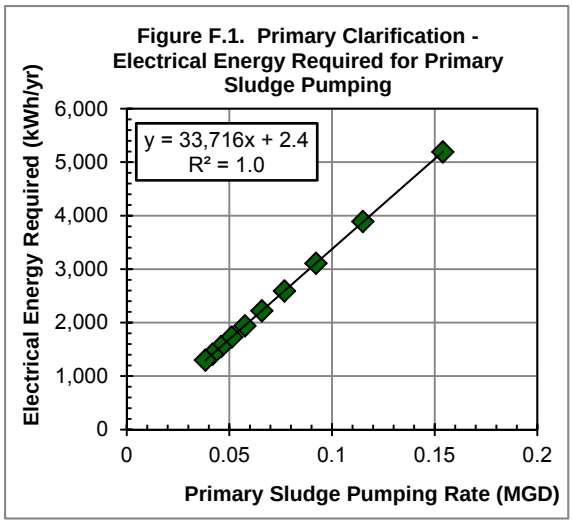

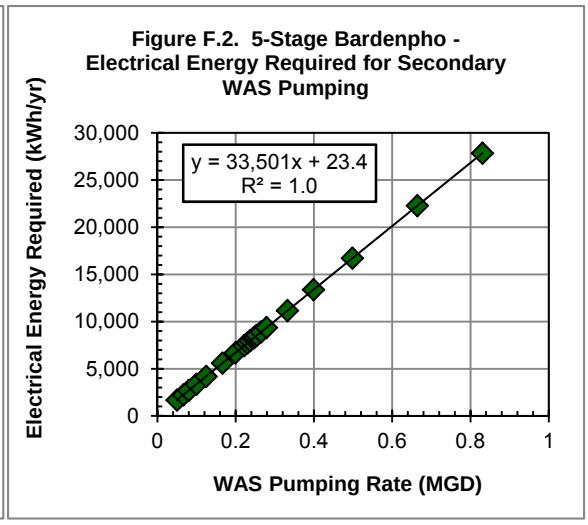

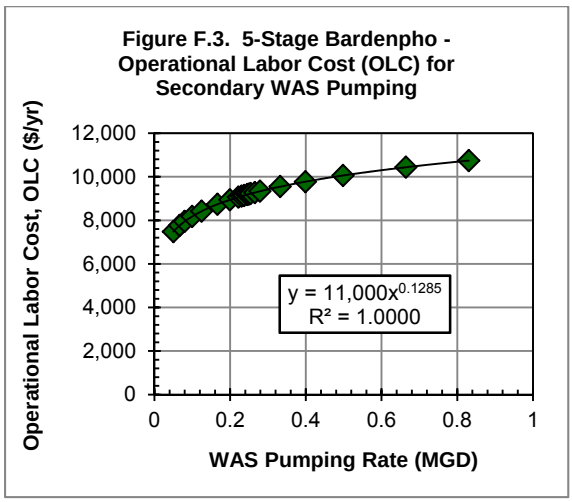

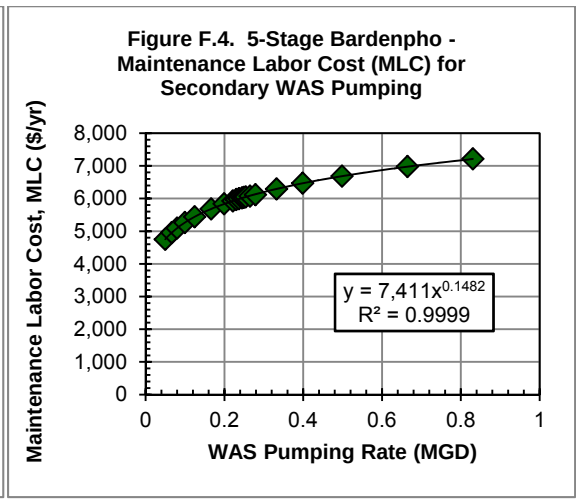

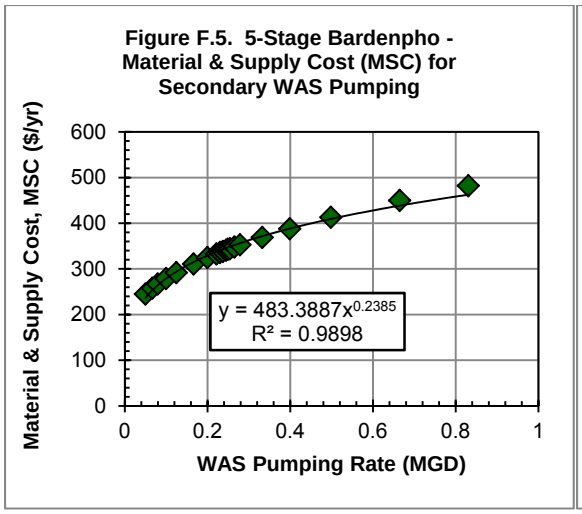

Figure F.5. 5-Stage Bardenpho - Material & Supply Cost (MSC) for Secondary WAS Pumping

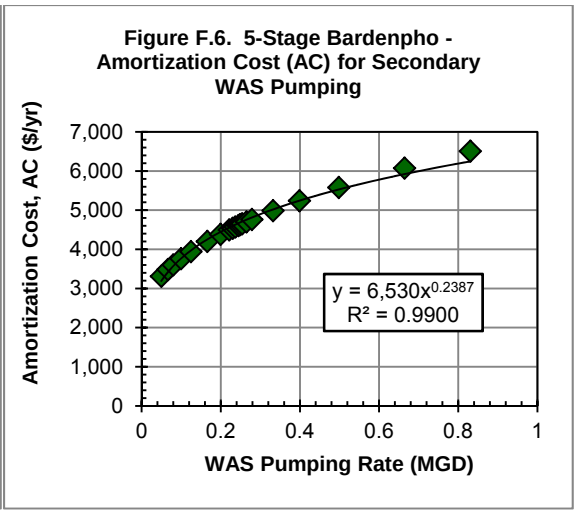

Figure F.6. 5-Stage Bardenpho - Amortization Cost (AC) for Secondary WAS Pumping

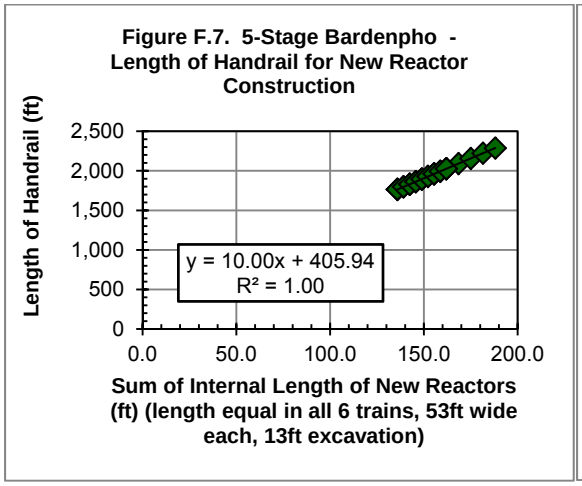

Figure F.7. 5-Stage Bardenpho - Length of Handrail for New Reactor Construction

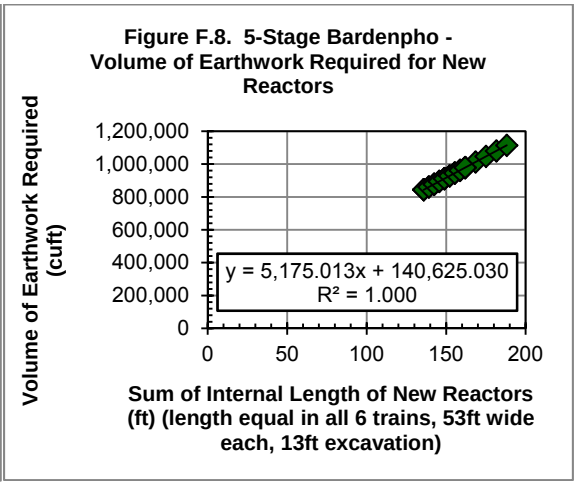

Figure F.8. 5-Stage Bardenpho - Volume of Earthwork Required for New Reactors

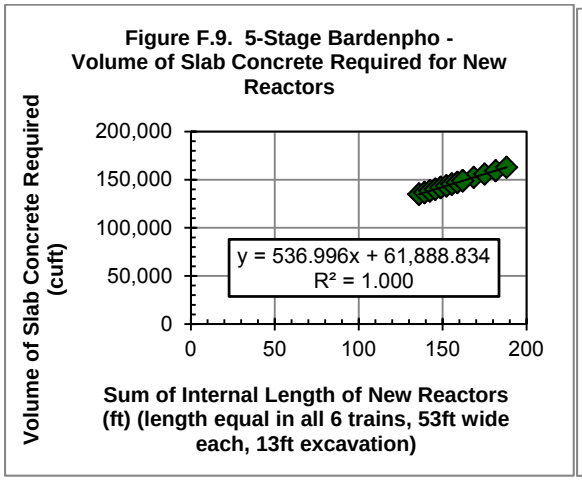

Figure F.9. 5-Stage Bardenpho - Volume of Slab Concrete Required for New Reactors

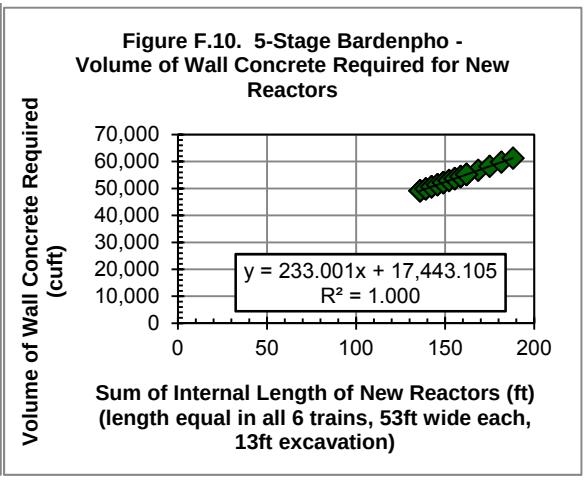

Figure F.10. 5-Stage Bardenpho - Volume of Wall Concrete Required for New Reactors

Figure F.11. 5-Stage Bardenpho - Electrical Energy Required for RAS Pumping

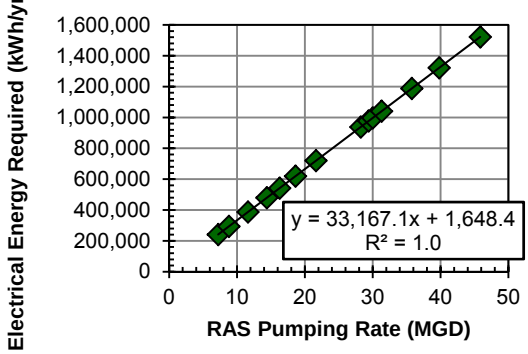

Figure F.12. 5-Stage Bardenpho - Operational Labor Cost (OLC) for RAS Pumping

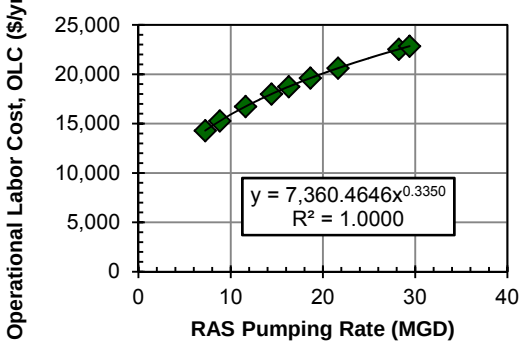

Figure F.13. 5-Stage Bardenpho - Maintenance Labor Cost (MLC) for RAS Pumping

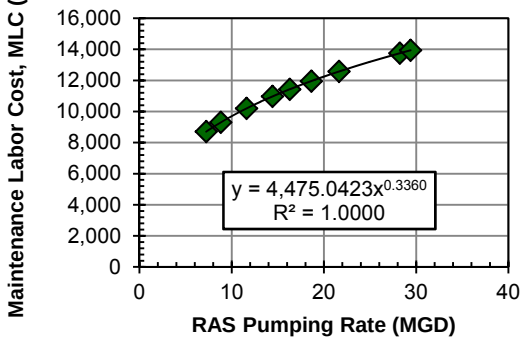

Figure F.14. 5-Stage Bardenpho - Material & Supply Cost (MSC) for RAS Pumping

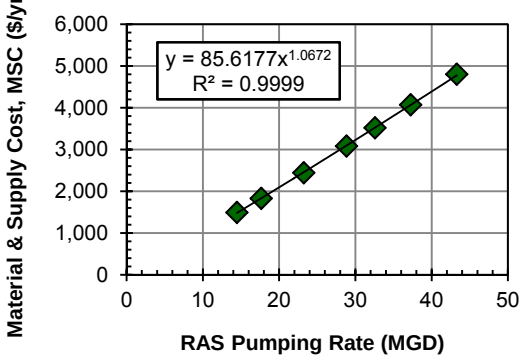

Figure F.15. 5-Stage Bardenpho - Amortization Cost (AC) for RAS Pumping

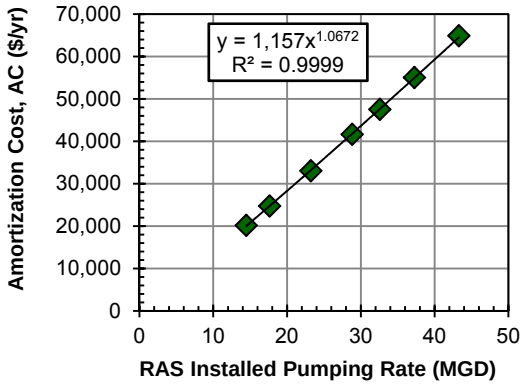

Figure F.16. 5-Stage Bardenpho - Electrical Energy Required for Internal Recycle Pumping

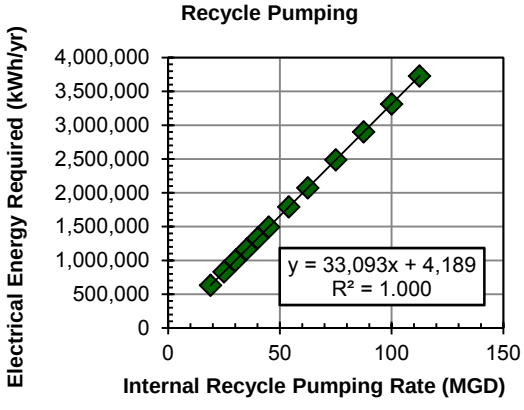

Figure F.17. 5-Stage Bardenpho - Operational Labor Cost (OLC) for Internal Recycle Pumping

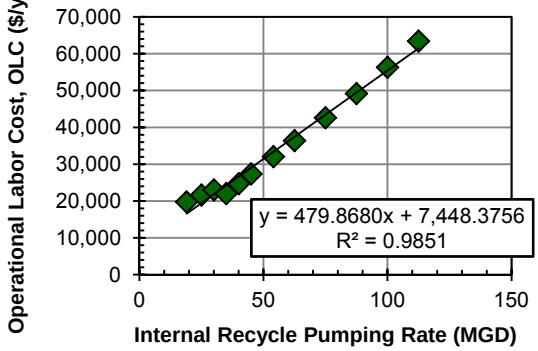

Figure F.18. 5-Stage Bardenpho - Maintenance Labor Cost (MLC) for Internal Recycle Pumping

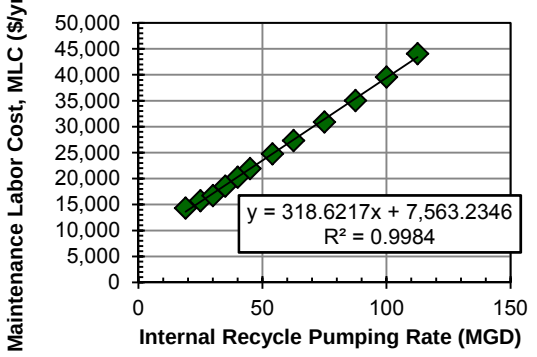

Figure F.19. 5-Stage Bardenpho - Construction & Equipment Cost (CEC) for Internal Recycle Pumping

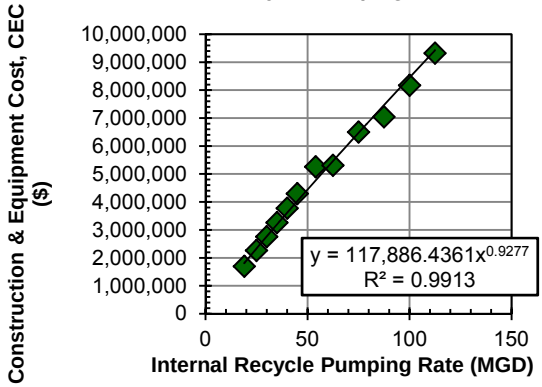

Figure F.20. 5-Stage Bardenpho - Material & Supply Cost (MSC) for Internal Recycle Pumping

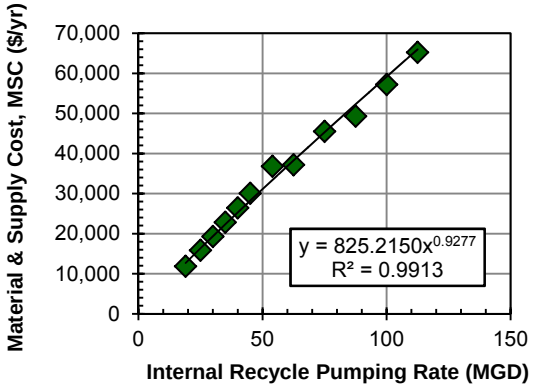

Figure F.21. 5-Stage Bardenpho - Amortization Cost (AC) for Internal Recycle Pumping

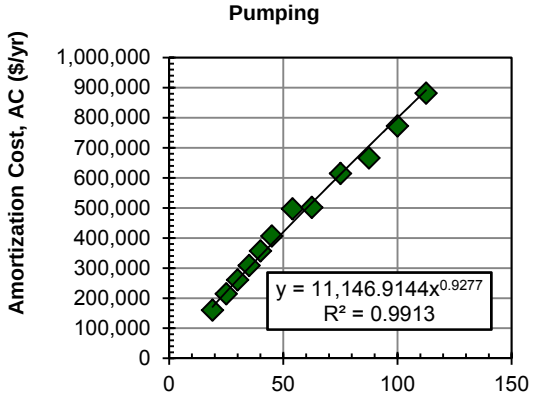

Figure F.22. 5-Stage Bardenpho - Volume of Earthwork Required for Internal Recycle Pumping

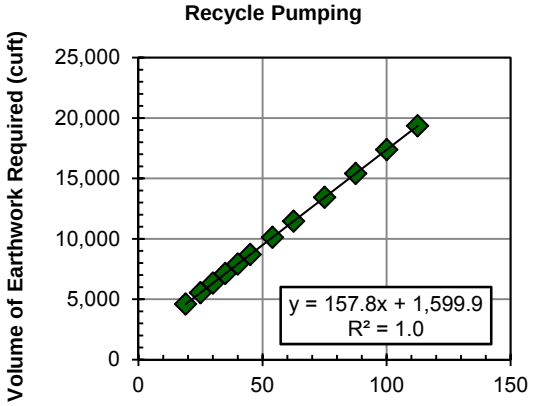

Figure F.23. 5-Stage Bardenpho - Area of Pump Building for Internal Recycle Pumping

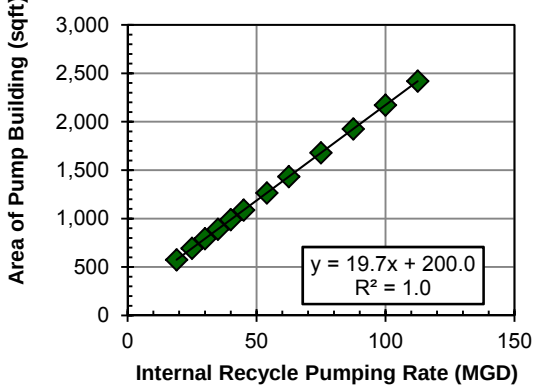

Figure F.24. 5-Stage Bardenpho - Construction & Equipment Cost (CEC) for RAS Pumping

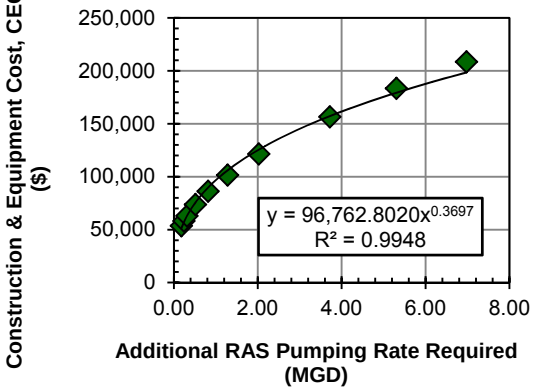

Figure F.25. Blower System - Amortization Cost (AC)

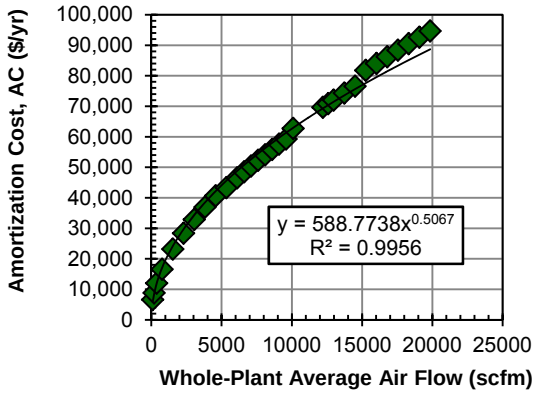

Figure F.26. Blower System - Construction & Equipment Cost (CEC)

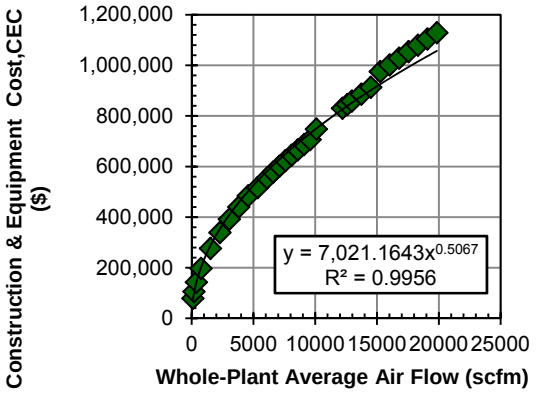

Figure F.27. Denitrification Filter - Electrical Energy Required Backwash Pumping (estimated based on all other pumping/energy data)

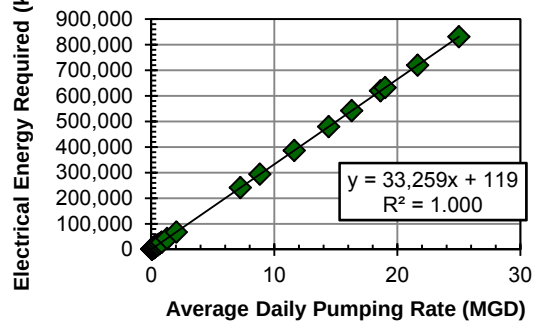

Figure F.28. Denitrification Filter - Area of Pump Building for Backwash Pumping

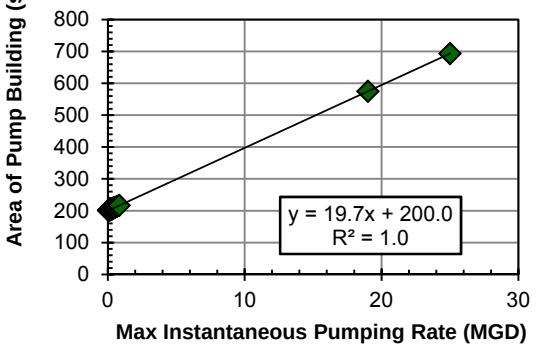

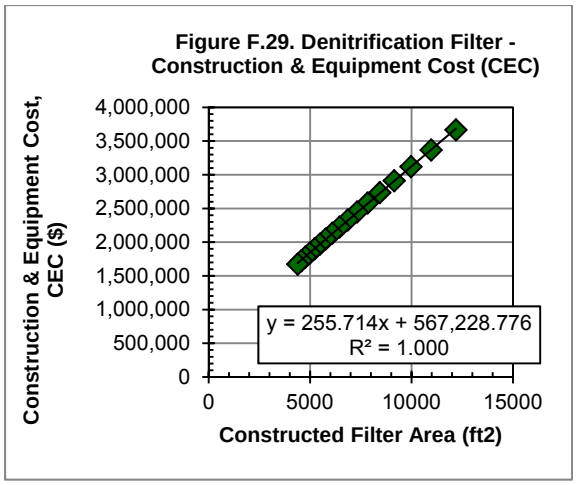
Figure F.29. Denitrification Filter - Construction & Equipment Cost (CEC)
Construction & Equipment Cost, CEC ($)
4,000,000
3,500,000
3,000,000
2,500,000
2,000,000
1,500,000
1,000,000
500,000
0
y = 255.714x + 567,228.776
R² = 1.000
0
5000
10000
15000
Constructed Filter Area (ft2)

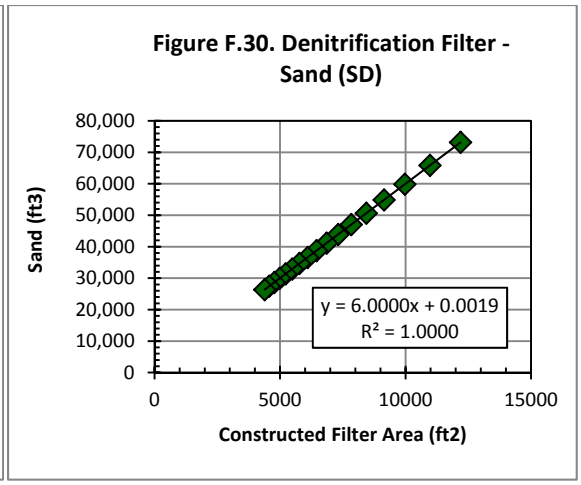
Figure F.30. Denitrification Filter - Sand (SD)
Sand (ft3)
80,000
70,000
60,000
50,000
40,000
30,000
20,000
10,000
0
y = 6.0000x + 0.0019
R² = 1.0000
0
5000
10000
15000
Constructed Filter Area (ft2)

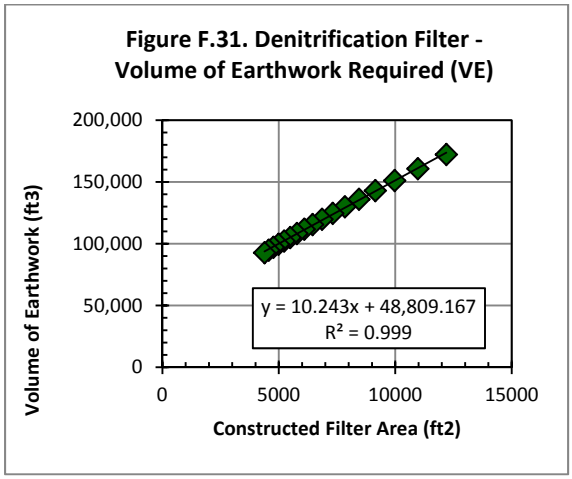
Figure F.31. Denitrification Filter - Volume of Earthwork Required (VE)
Volume of Earthwork (ft3)
200,000
150,000
100,000
50,000
0
y = 10.243x + 48,809.167
R² = 0.999
0
5000
10000
15000
Constructed Filter Area (ft2)

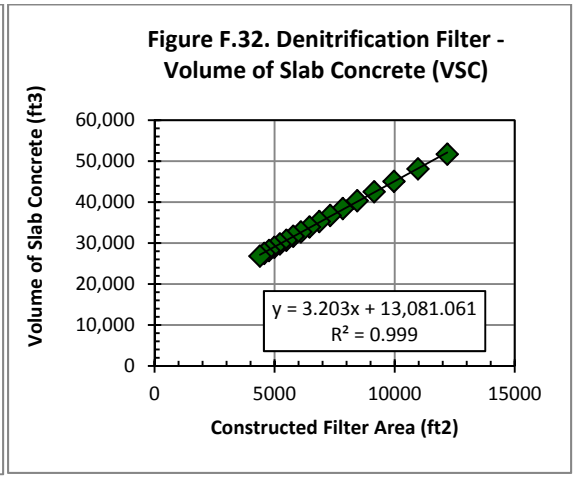
Figure F.32. Denitrification Filter - Volume of Slab Concrete (VSC)
Volume of Slab Concrete (ft3)
60,000
50,000
40,000
30,000
20,000
10,000
0
y = 3.203x + 13,081.061
R² = 0.999
0
5000
10000
15000
Constructed Filter Area (ft2)

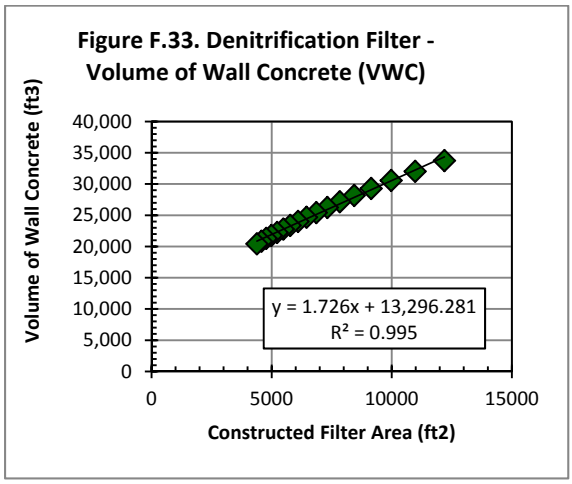
Figure F.33. Denitrification Filter - Volume of Wall Concrete (VWC)
Volume of Wall Concrete (ft3)
40,000
35,000
30,000
25,000
20,000
15,000
10,000
5,000
0
y = 1.726x + 13,296.281
R² = 0.995
0
5000
10000
15000
Constructed Filter Area (ft2)

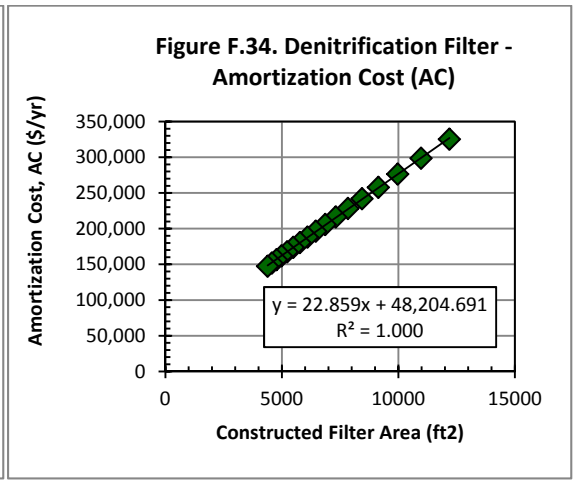
Figure F.34. Denitrification Filter - Amortization Cost (AC)
Amortization Cost, AC ($/yr)
350,000
300,000
250,000
200,000
150,000
100,000
50,000
0
y = 22.859x + 48,204.691
R² = 1.000
0
5000
10000
15000
Constructed Filter Area (ft2)

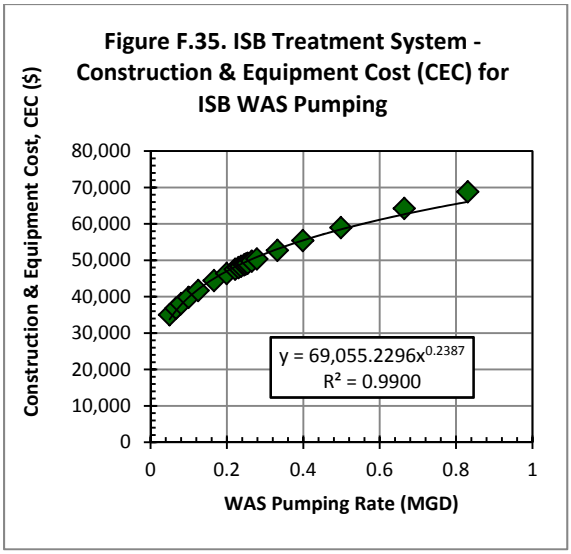
Figure F.35. ISB Treatment System - Construction & Equipment Cost (CEC) for ISB WAS Pumping
Construction & Equipment Cost, CEC ($)
80,000
70,000
60,000
50,000
40,000
30,000
20,000
10,000
0
0
0.2
0.4
0.6
0.8
1
WAS Pumping Rate (MGD)
y = 69,055.2296x^0.2387
R² = 0.9900

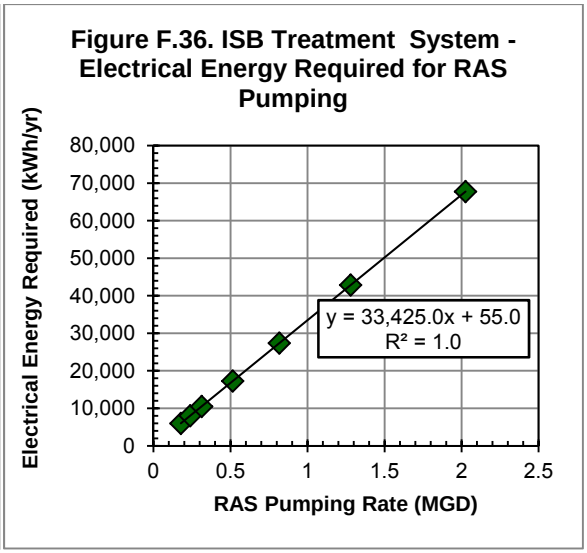
Figure F.36. ISB Treatment System - Electrical Energy Required for RAS Pumping
Electrical Energy Required (kWh/yr)
80,000
70,000
60,000
50,000
40,000
30,000
20,000
10,000
0
0
0.5
1
1.5
2
2.5
RAS Pumping Rate (MGD)
y = 33,425.0x + 55.0
R² = 1.0

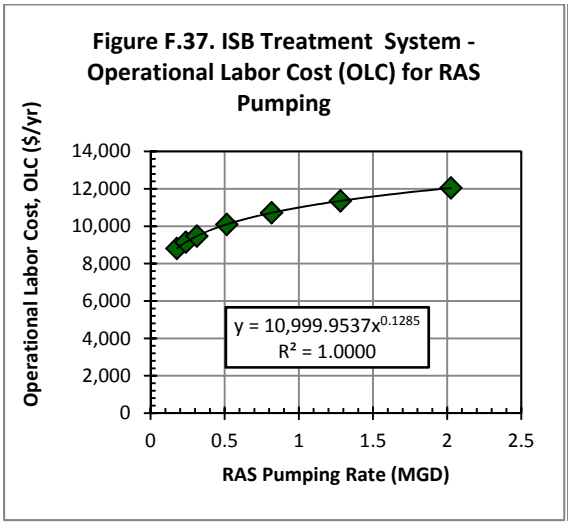
Figure F.37. ISB Treatment System - Operational Labor Cost (OLC) for RAS Pumping
Operational Labor Cost, OLC ($/yr)
14,000
12,000
10,000
8,000
6,000
4,000
2,000
0
0
0.5
1
1.5
2
2.5
RAS Pumping Rate (MGD)
y = 10,999.9537x^0.1285
R² = 1.0000

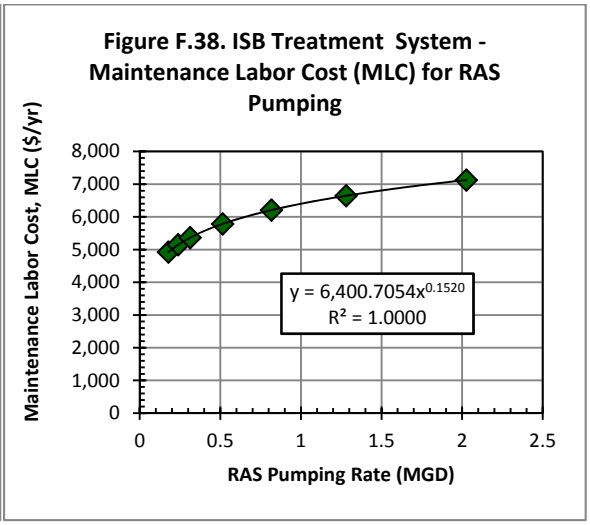
Figure F.38. ISB Treatment System - Maintenance Labor Cost (MLC) for RAS Pumping
Maintenance Labor Cost, MLC ($/yr)
8,000
7,000
6,000
5,000
4,000
3,000
2,000
1,000
0
0
0.5
1
1.5
2
2.5
RAS Pumping Rate (MGD)
y = 6,400.7054x^0.1520
R² = 1.0000

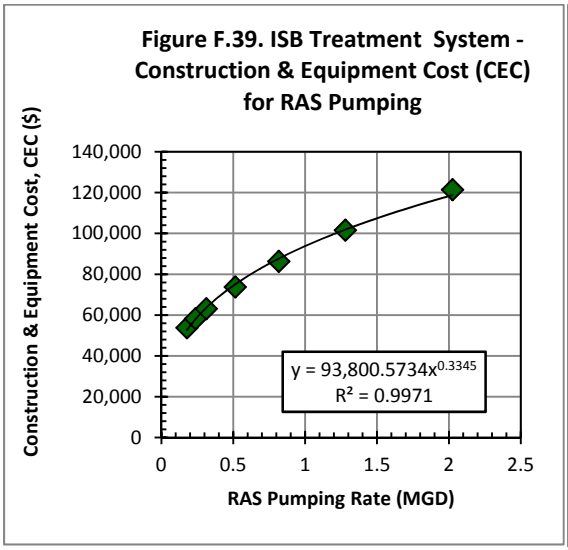
Figure F.39. ISB Treatment System - Construction & Equipment Cost (CEC) for RAS Pumping
Construction & Equipment Cost, CEC ($)
140,000
120,000
100,000
80,000
60,000
40,000
20,000
0
0
0.5
1
1.5
2
2.5
RAS Pumping Rate (MGD)
y = 93,800.5734x^0.3345
R² = 0.9971

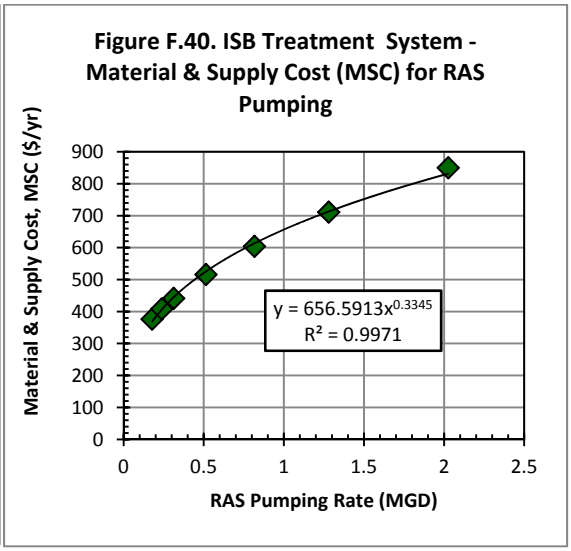
Figure F.40. ISB Treatment System - Material & Supply Cost (MSC) for RAS Pumping
Material & Supply Cost, MSC ($/yr)
900
800
700
600
500
400
300
200
100
0
0
0.5
1
1.5
2
2.5
RAS Pumping Rate (MGD)
y = 656.5913x^0.3345
R² = 0.9971

Figure F.41. ISB Treatment System - Amortization Cost (AC) for RAS Pumping

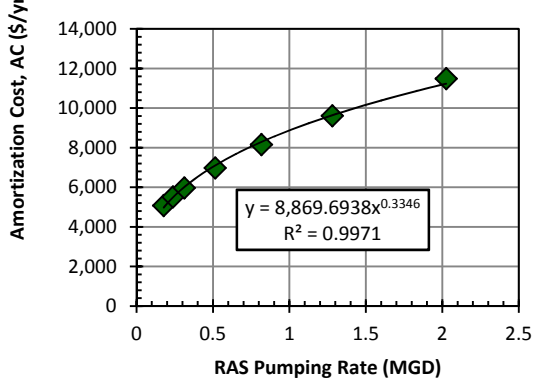

Figure F.42. ISB Treatment System - Volume of Earthwork Required for RAS Pumping

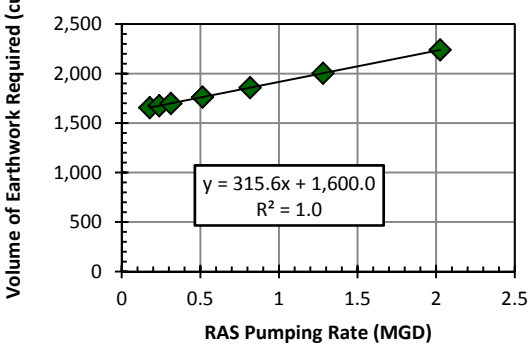

Figure F.43. ISB Treatment System - Area of Pump Building for RAS Pumping

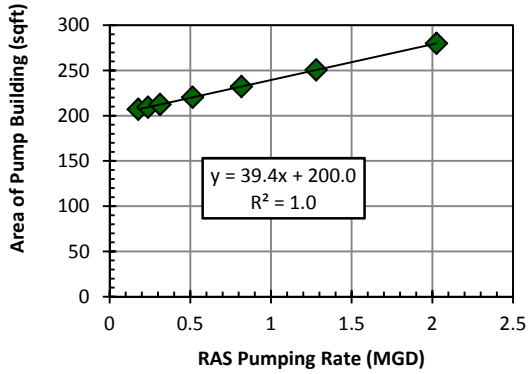

Figure F.44. ISB Treatment System - Area of Pump Building for WAS Pumping

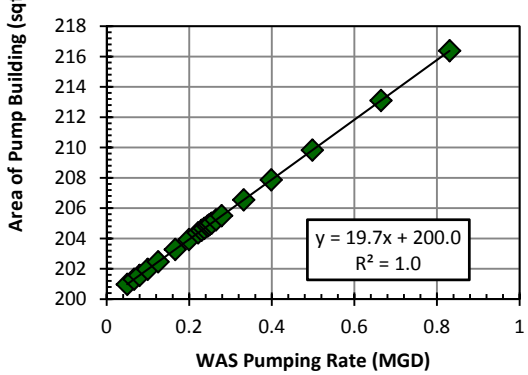

Figure F.45. ISB Treatment System - Volume of Earthwork Required for WAS Pumping

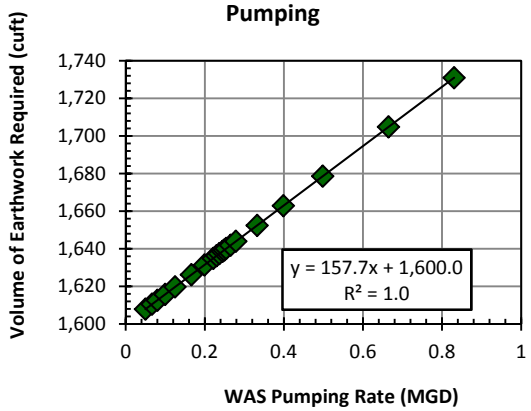

Figure F.46. WAS Thickening - Operational Labor Cost (OLC) for GBTs

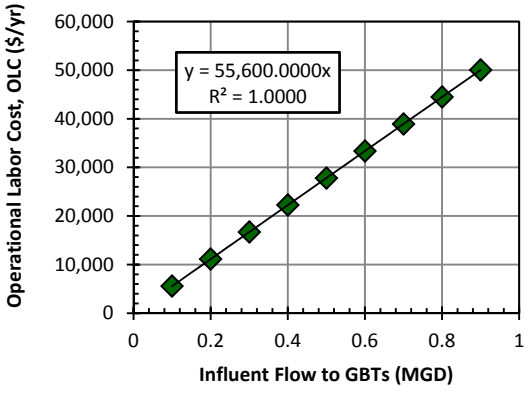

Figure F.47. WAS Thickening - Maintenance Labor Cost (MLC) for GBTs

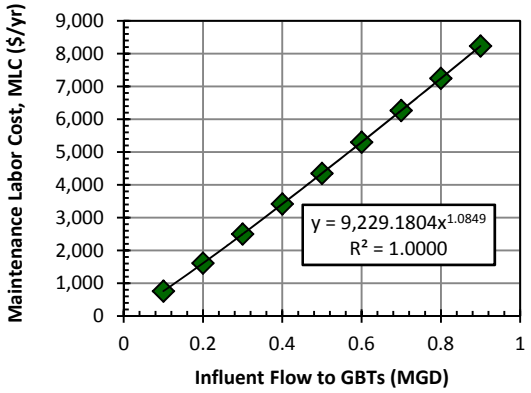

Figure F.48. WAS Thickening - Electrical Energy Required (EE) for GBTs

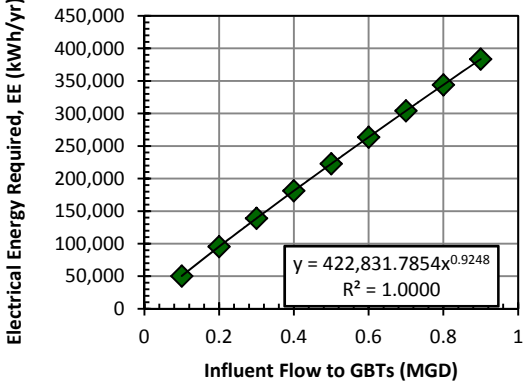

Figure F.49. Dewatering System - Operational Labor Cost (OLC) for Centrifuges

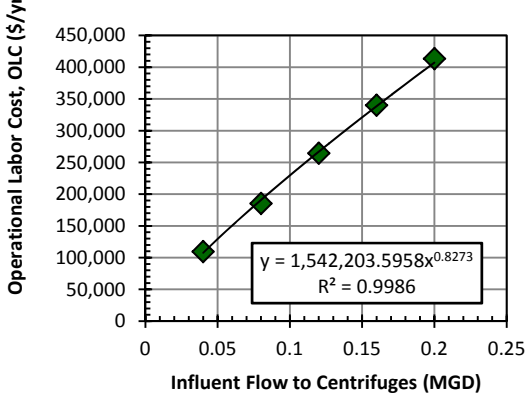

Figure F.50. Dewatering System - Maintenance Labor Cost (MLC) for Centrifuges

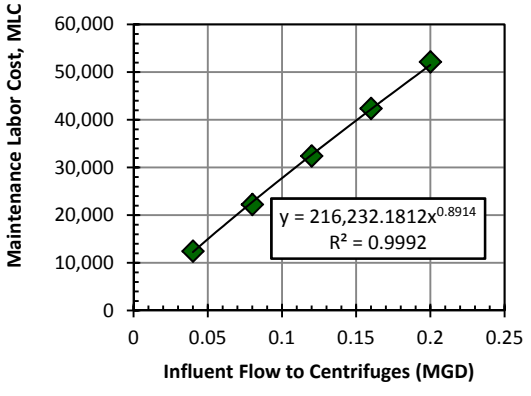

Figure F.51. Dewatering System - Material & Supply Cost (MSC) for Centrifuges

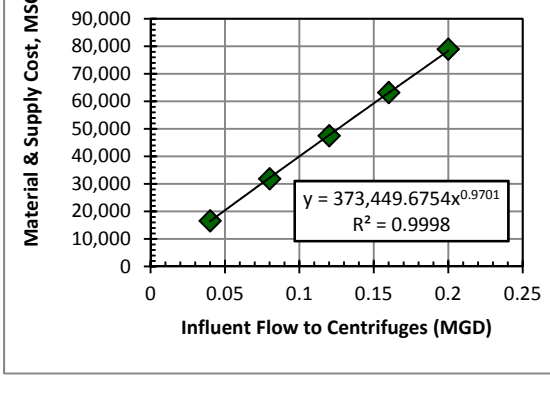

Figure F.52. Dewatering System - Amortization Cost (AC) for Centrifuges

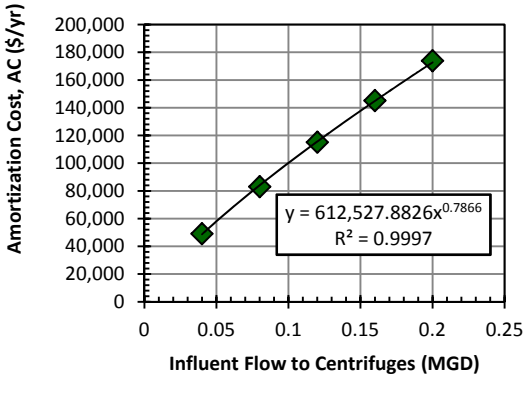

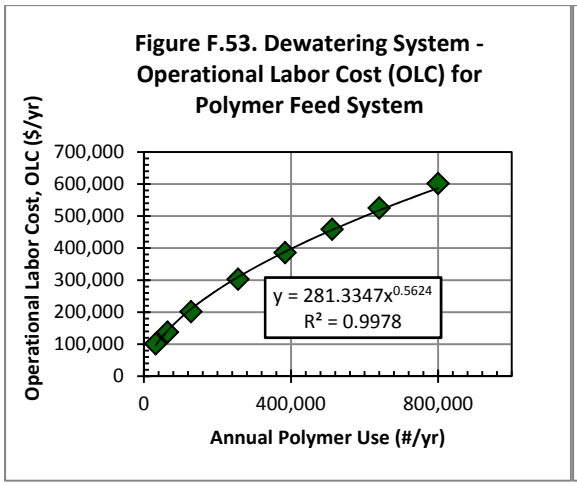
Figure F.53. Dewatering System - Operational Labor Cost (OLC) for Polymer Feed System
Operational Labor Cost, OLC ($/yr)
700,000
600,000
500,000
400,000
300,000
200,000
100,000
0
0
400,000
800,000
Annual Polymer Use (#/yr)
y = 281.3347x^0.5624
R² = 0.9978

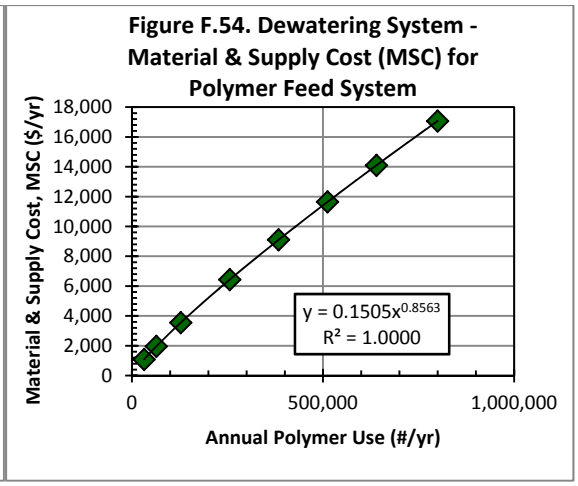
Figure F.54. Dewatering System - Material & Supply Cost (MSC) for Polymer Feed System
Material & Supply Cost, MSC ($/yr)
18,000
16,000
14,000
12,000
10,000
8,000
6,000
4,000
2,000
0
0
500,000
1,000,000
Annual Polymer Use (#/yr)
y = 0.1505x^0.8563
R² = 1.0000

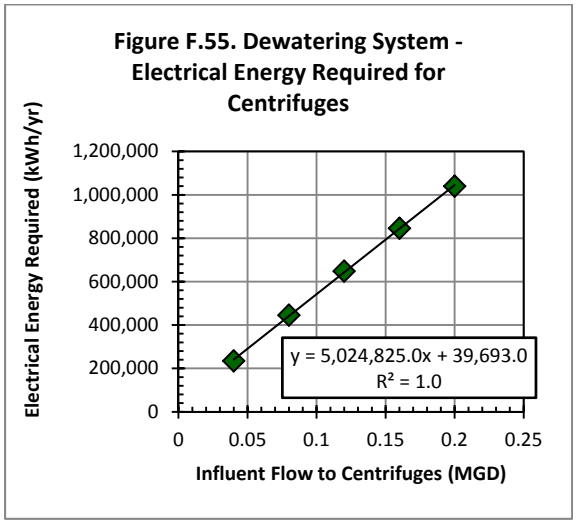
Figure F.55. Dewatering System - Electrical Energy Required for Centrifuges
Electrical Energy Required (kWh/yr)
1,200,000
1,000,000
800,000
600,000
400,000
200,000
0
0
0.05
0.1
0.15
0.2
0.25
Influent Flow to Centrifuges (MGD)
y = 5,024,825.0x + 39,693.0
R² = 1.0

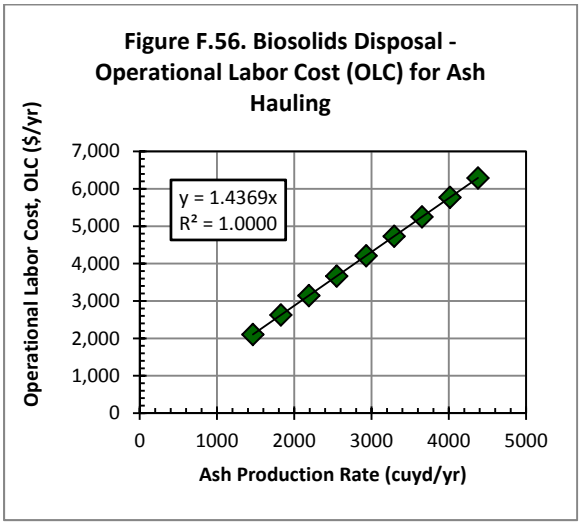
Figure F.56. Biosolids Disposal - Operational Labor Cost (OLC) for Ash Hauling
Operational Labor Cost, OLC ($/yr)
7,000
6,000
5,000
4,000
3,000
2,000
1,000
0
0
1000
2000
3000
4000
5000
Ash Production Rate (cuyd/yr)
y = 1.4369x
R² = 1.0000

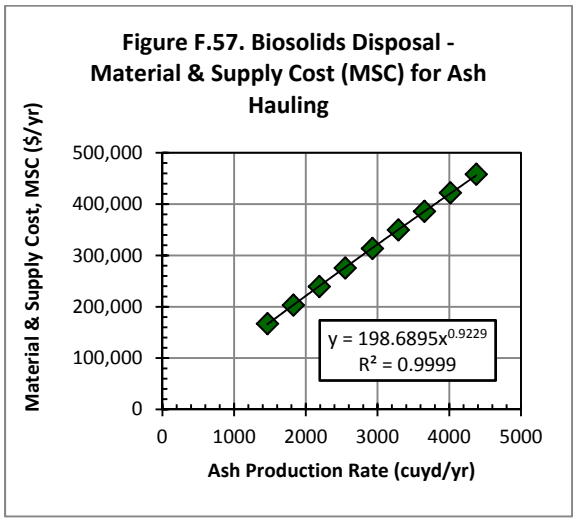
Figure F.57. Biosolids Disposal - Material & Supply Cost (MSC) for Ash Hauling
Material & Supply Cost, MSC ($/yr)
500,000
400,000
300,000
200,000
100,000
0
0
1000
2000
3000
4000
5000
Ash Production Rate (cuyd/yr)
y = 198.6895x^0.9229
R² = 0.9999

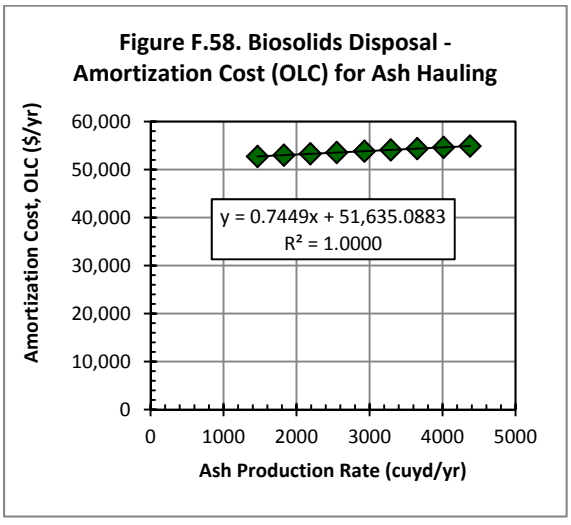
Figure F.58. Biosolids Disposal - Amortization Cost (OLC) for Ash Hauling
Amortization Cost, OLC ($/yr)
60,000
50,000
40,000
30,000
20,000
10,000
0
0
1000
2000
3000
4000
5000
Ash Production Rate (cuyd/yr)
y = 0.7449x + 51,635.0883
R² = 1.0000

Appendix G
MATLAB Code for GPS-X™ Simulations and Preliminary Data Analysis for Quantitative Sustainable Design

```
function std_vs_seas_dynamic_10_26_2011(configuration)
warning('SEASONAL WWTP CONFIGURATION. Make sure temperature setting matches setting at top of m-file.  You are about to evaluate a WWTP configuration defined within this m-file. The configuration name you entered must match the configuration name and location in the m-file. If you need to modify a different configuration, you must change the .m file code. The outputs of this file can be used for LCA and cost analysis.');

tic % Starts a timer to count how long it takes to execute this m-file.


% SECTION 1.1
% IMPORTANT INPUTS TO THIS SCRIPT - The following are a list of items you
% will want to check before running new simulations:
%   A. file names of all input/output files - Section 1.2 & 2.1
%   B. output file headers - Section 1.3, and these headers should match the
%   values in Section XX.XX
%   C. parameters for uncertainty analysis - Section 2.1 should correspond
%   with raw LHS data file aa_raw_lhs_data_file.txt.  There needs to be an
%   "elseif" statement for every parameter, they need to be listed in the
%   "strmatch" function, and they need to be assigned a "parameter_set"
%   value below the column identification.
%   D. You must have your configuration built in GPS-X and have identified
%   the file input controllers.
%   D. You must have a .xec file in the same folder as the configuration.
%   The .xec file should say one of two things.  For a steady state
%   simulation, it should say: "START" (return) "STEADY" (return) "EXIT".
%   For a dynamic simulation it should say: "STEADY" (return) "TSTOP 14 d"
%   (return) "START" (return) "EXIT".


% SECTION 1.2
% DEFINE ALL FILENAMES - Identify names of .dat and .out files based on
% configuration's name (e.g., config_1_5bard).  Creates three .dat files
% that are input file controllers for GPS-X: "decision" for decision
% variables, "parameters" for kinetic and stoichiometric model parameters,
% and "influent" for influent.  The .out file is for data output from
% GPS-X, and the fourth .dat file (datastoragefilename) is for data output
% from this script.
volumefileextension = '_volume_2006_01_01.dat';
volumefilename = strcat(configuration, volumefileextension);
constantpumpingfileextension = '_constantpumping_2006_01_01.dat';
constantpumpingfilename = strcat(configuration, constantpumpingfileextension);
variablepumpingfileextension = '_variablepumping_2006_01_01.dat';
variablepumpingfilename = strcat(configuration, variablepumpingfileextension);
influentfileextension = '_influent_2006_01_01.dat';
influentfilename = strcat(configuration, influentfileextension);
kineticsfileextension = '_kinetics_2006_01_01.dat';
kineticsfilename = strcat(configuration, kineticsfileextension);
dissolvedoxygenfileextension = '_o2_2006_01_01.dat';
dissolvedoxygenfilename = strcat(configuration, dissolvedoxygenfileextension);
outfileextension = '_Default Scenario_2006_1_1.out'; %  (formerly '_Default_2006_1_1.out')
outfilename=strcat(configuration, outfileextension);
gpsxdatastoragefileextension = '.dat';
gpsxdatastoragefilename=strcat('_gpsx_output_', configuration, gpsxdatastoragefileextension);

% SECTION 1.3
```

```
% CREATE DATA STORAGE FILE - this is for the data you want to extract from
% this script. Creates a file with header info (line11), and then every line
% after that will be data appended to the file after each run of the loop.
% All data you want to collect must have a header in line11 and a
% corresponding value at the end of the script in line12. Note that the use
% of 'w' in the fid command below wipes the data file clean and adds the
% header line11.
line11 = sprintf('lhs_set \t config \t season \t actual_srt_d (d) \t rec_capacity (m3/d) \t
volume_ana (m3) \t volume_anx1 (m3) \t volume_aer1 (m3) \t volume_anx2 (m3) \t volume_aer2 (m3)
\t qconisbwas_capacity (m3/d) \t qconisbwas_operation (m3/d) \t qprimover_avg (m3/d) \t
qconras_operation (m3/d) \t qconras_capacity (m3/d) \t qconrctrwas_capacity (m3/d) \t
qconrctrwas_operation (m3/d) \t average_mlss (g/m3) \t tn_rctr_loading_avg (gN/d) \t
qprimunder_avg (m3/d) \t xrctraeff_avg (g/m3) \t xlrctrbeff1_avg (g/m3) \t xlrctrceff1_avg (g/m3)
\t snhlrctrceff2_conc_avg (g/m3) \t qsecforward_max (m3/d) \t qsecforward_avg (m3/d) \t
snoalrctrceff2_conc_avg (g/m3) \t qairstandlrctreff_max (m3/d) \t qairstandlrctreff_avg (m3/d) \t
qcentinf_avg (m3/d) \t xcentinf_conc_avg (g/m3) \t qcentcake_avg (m3/d) \t xcentcake_conc_avg
(g/m3) \t xisbwas_avg (g/m3) \t qfiltereff_avg (m3/d) \t scodsecforward_conc_avg (g/m3) \t
tnrctrwas_mass_removal_avg (gN/d) \t stpfiltereff_conc_avg (gP/m3) \t sndfiltereff_conc_avg
(gN/m3) \t tneff_conc_avg (gN/m3) \t n2o_emissions_aer_avg_chandran (gN2O-N/d) \t
scodsecforward_max (g/m3) \t stpfiltereff_max (gP/m3) \t snoafiltereff_max (gN/m3) \t
snoafiltereff_conc_avg (gN/m3) \t tneff_max (gN/m3) \t qconisbras_capacity (m3/d) \t
qconisbras_operation (m3/d) \t n2o_emissions_anx_avg_chandran (gN2O-N/d) \t
denit_backwash_flow_avg (m3/d) \t internal_rec_operation_avg (m3/d) \t qconmeohrctrc_avg (m3/d)
\t qconmeohdf_avg (m3/d) \t qair_tunableblowers_delivered (m3/d) \t qair_3fixedblowers_delivered
(m3/d) \t qair_4fixedblowers_delivered (m3/d) \t qair_3_1_fixedblowers_delivered (m3/d) \t
blower_exceeded_time_fraction (fraction of time points)');
datastorageheader = {line11}; % if 2 header lines, write as: {line11; line##};
fid=fopen(gpsxdatastoragefilename,'w');
for row = 1:1 %1:2 if 2 row header
  fprintf(fid, '%s \r\n', datastorageheader{row,:});
end
fclose(fid);

% SECTION 1.4
% DEFINE GPS-X OUTPUT FILE CHARACTERISTICS - In order to import data from
% the GPS-X output file (outfilename), the following variables need to be
% defined (tab delimited and 2 header lines).
DELIMITER = '\t';
HEADERLINES = 3; % NOTE:  this value needs to be "2" if doing a steady
                 % state simulation so that the data imported is from the
                 % 3rd row (steady state results). For dynamic simulations,
                 % start importing data at row 4 (so call top 3 rows
                 % "headers".

% SECTION 2.1
% DEFINE BASE INPUTS FOR UNCERTAIN PARAMETERS AS UNIT VECTORS - For all
% parameters that are either uncertainy or that will vary with time, a
% times series is required.

    % SECTION 2.1.1
    % DIURNAL - The shape of the diurnal is based on the "highest hour
    % flow report" which reports that highest flows at a given hour of the
    % day at the Chesapeake-Elizabeth WWTP for each month from January 2003
    % through December 2010. In other words, January 2004 has 24 flow rates
    % listed, one rate for each hour of the day (0:00, 1:00, ..., 23:00).
    % The flow rate listed for 1:00 is the highest 1 AM flowrate observed
```

```
% during that month. This was the best available data. The diurnal is
% written as a unit vector (the average daily flow is 1.0) so that an
% hourly flow rate can be achieved by multiplying this matrix by an
% average daily flow rate.
hours_of_day = [0;1;2;3;4;5;6;7;8;9;10;11;12;13;14;15;16;17;18;19;...
    20;21;22;23];
diurnal_time_series = hours_of_day/24;
simulation_timepoints = 240; % 10days *24.  NOTE:  The number of days
% you intend to simulate must match the days indicated in the .XEC
% file (e.g., "TSTOP 10 d").
startup_timepoints = 72; %3*24
weekday_diurnal_unit_load = [1.028081; 0.775268; 0.591862; 0.497774;...
    0.454289; 0.453293; 0.557713; 0.876288; 1.267858; 1.305163; ...
    1.233389; 1.203805; 1.196441; 1.165673; 1.130172; 1.071942; ...
    1.060145; 1.063789; 1.118169; 1.187538; 1.242161; 1.258034; ...
    1.226251; 1.034900]; % Averages 1. Multiply by average daily
    % flow to get hourly influent flow in units of volume/time.
weekend_diurnal_unit_load = [0.985293; 0.808421; 0.648304; 0.552911; ...
    0.485395; 0.455655; 0.463152; 0.537771; 0.739582; 1.036052; ...
    1.311503; 1.439822; 1.463094; 1.400234; 1.319489; 1.238696; ...
    1.182107; 1.144136; 1.156531; 1.164861; 1.178922; 1.170495; ...
    1.142960; 0.974612]; % Averages 1. Multiply by average daily
    % flow to get hourly influent flow in units of volume/time.
hydrograph_1_unit_load = [0.00000; 0.39110; 0.61910; 2.36085; ...
    4.47858; 2.36751; 1.86352; 1.50708; 1.32931; 1.07376; 0.82087; ...
    0.67510; 0.54888; 0.55821; 0.47999; 0.98220; 0.71554; 0.60266; ...
    0.47377; 0.52221; 0.67021; 0.45421; 0.07467; 0.43066]; % Averages
    % 1 million gallons over the course of 24 hours. Multiply by
    % volume of rainwater to get increase in hourly influent flow in
    % MGD.
hydrograph_2_unit_load = [0.00000; 0.42625; 1.34324; 2.45268; ...
    2.08500; 1.93537; 1.98361; 1.47614; 1.28122; 0.92437; 1.29402; ...
    0.51436; 0.92410; 0.74129; 0.57141; 0.76760; 0.63205; 0.41936; ...
    0.82423; 0.68556; 0.72658; 0.64008; 0.62447; 0.72702]; % Averages
    % 1 million gallons over the course of 24 hours. Multiply by
    % volume of rainwater to get increase in hourly influent flow in
    % MGD.
hydrograph_3_unit_load = [0.00000; 0.15912; 2.75319; 2.87720; ...
    1.73846; 1.40973; 1.45730; 1.80243; 1.66825; 1.53768; 1.38152; ...
    1.11545; 1.20075; 0.69551; 0.62268; 0.48063; 0.92320; 0.83888; ...
    0.80804; 0.08530; 0.23027; 0.06269; 0.05222; 0.09951]; % Averages
    % 1 million gallons over the course of 24 hours. Multiply by
    % volume of rainwater to get increase in hourly influent flow in
    % MGD.  Note that only this hydrograph is used for Fall 2011
    % simulations.

qconinf_base = 87064; % m3/d.  Assumes 23 MGD of dry weather base flow
% (excludes average of 1 MGD of rain totalling 24 MGD design flow).
simulation_time_series = zeros(simulation_timepoints,1);
simulation_diurnal_unit_load = zeros(simulation_timepoints,1);
for days = 0:9;
    start_row = 1+days*24;
    end_row = start_row + 23;
    simulation_time_series(start_row:end_row,1) = diurnal_time_series + days;
    if days <=2
        simulation_diurnal_unit_load(start_row:end_row,1) = weekday_diurnal_unit_load;
```

```
        else % later might be able to use unidcdf to select a random
             % simulation day to begin the weekend.  For now, simply pick
             % simulation days 7 and 8 (days 6 and 7 in code) for weekend.
             if days <=5
                 simulation_diurnal_unit_load(start_row:end_row,1) = weekday_diurnal_unit_load;
             elseif days >=8
                 simulation_diurnal_unit_load(start_row:end_row,1) = weekday_diurnal_unit_load;
             else
                 simulation_diurnal_unit_load(start_row:end_row,1) = weekend_diurnal_unit_load;
             end
        end
    end

    % SECTION 2.1.2
    % BASE LOADINGS ACROSS DIURNAL - It is assumed that nutrient loads (in
    % units of mass per time) follow the same patterns as the typical
    % diurnal. In other words, for the "base case" diurnal, the
    % concentrations of various influent constituents are constant over
    % the course of the day. These loadings profiles will not change, and
    % will only increase uniformly or decrease uniformly based on
    % assumptions of the actual average influent concentration at 23 MGD
    % (87064 m3/d) of dry weather flow. Changes to average flow rates will
    % affect concentrations uniformly, but rainfall will change
    % concentrations non-uniformly to maintain the same mass loading over
    % time.
    bodconinf_base_concentration = 243; % dry weather, g/m3
    bodconinf_base_concentration_series = zeros(simulation_timepoints,1);
    bodconinf_base_concentration_series(:,1) = bodconinf_base_concentration;
    tknconinf_base_concentration = 42; % dry weather, g-N/m3
    tknconinf_base_concentration_series = zeros(simulation_timepoints,1);
    tknconinf_base_concentration_series(:,1) = tknconinf_base_concentration;
    tpconinf_base_concentration = 6.1; % dry weather, g-P/m3
    tpconinf_base_concentration_series = zeros(simulation_timepoints,1);
    tpconinf_base_concentration_series(:,1) = tpconinf_base_concentration;
    % CONVERT TO MASS LOADINGS - Multiply concentrations (g/m3) by base
    % case flow rates (m3/d) by hour to get a mass loading per hour (g/d).
    simulation_diurnal_base_flow = qconinf_base*simulation_diurnal_unit_load;
    bodconinf_base_loading = bodconinf_base_concentration_series.*simulation_diurnal_base_flow;
    tknconinf_base_loading = tknconinf_base_concentration_series.*simulation_diurnal_base_flow;
    tpconinf_base_loading = tpconinf_base_concentration_series.*simulation_diurnal_base_flow;

% SECTION 2.2
% IMPORT LATIN HYPERCUBE SAMPLING PARAMETER SET - Use seperate LHS m-files
% to generate datasets of equal size (e.g., if you want to do 500
% simulations, you need 500 values for each parameter). Use the appropriate
% LHS script for a given probability distribution function:  use latin_hs.m
% for normal distributions and lhsu.m for uniform distributions. Assemble
% all of these LHS values into a single Excel file where each column is one
% parameter's values, and where the first row ONLY is the name of the
% parameter (e.g., muh) and all other rows are values to use in
% simulations.  If you plan to run 500 simulations with uncertainty around
% 6 parameters, that means you need a 501x6 matrix. Save the Excel file as
% a .txt with the following name:  aa_raw_lhs_data_file.txt. The code below
% creates a 1-column vector for each parameter with the vector's name being
% the text you put in row 1 of each column.
% NOTE:  Confirm that all parameter names are NOT existing functions in
```

```
% Matlab.  For example, do NOT use "mu" as a parameter name, because it
% means something else in Matlab.

aa_raw_lhs_data_filename = 'aa_raw_lhs_data_file.txt';
    rawlhsdata = importdata(aa_raw_lhs_data_filename);
    number_of_parameters = length(rawlhsdata.colheaders);
    for i = 1:size(rawlhsdata.colheaders,2)
       columnheader = rawlhsdata.colheaders{i};
        parameter_number = strmatch(columnheader,strvcat('munhconrctreff', 'khsoconrctreff',↙
'kalsnhconrctreff', 'bodconinf', 'bod_to_tkn', 'bod_to_tp', 'qconinf', 'rainfall_day1',↙
'rainfall_day2', 'rainfall_day3', 'rainfall_day4', 'rainfall_day5', 'rainfall_day6',↙
'rainfall_day7', 'temp', 'rainstart_day1', 'rainstart_day2', 'rainstart_day3', 'rainstart_day4',↙
'rainstart_day5', 'rainstart_day6', 'rainstart_day7', 'lhs_set'),'exact');
        if (parameter_number <= 1)
            col_munhconrctreff = i;
        elseif (parameter_number <= 2)
            col_khsoconrctreff = i;
        elseif (parameter_number <= 3)
            col_kalsnhconrctreff = i;
        elseif (parameter_number <= 4)
            col_bodconinf = i;
        elseif (parameter_number <= 5)
            col_bod_to_tkn = i;
        elseif (parameter_number <= 6)
            col_bod_to_tp = i;
        elseif (parameter_number <=7)
            col_qconinf = i;
        elseif (parameter_number <= 8)
            col_rainfall_day1 = i;
        elseif (parameter_number <= 9)
            col_rainfall_day2 = i;
        elseif (parameter_number <= 10)
            col_rainfall_day3 = i;
        elseif (parameter_number <= 11)
            col_rainfall_day4 = i;
        elseif (parameter_number <= 12)
            col_rainfall_day5 = i;
        elseif (parameter_number <= 13)
            col_rainfall_day6 = i;
        elseif (parameter_number <= 14)
            col_rainfall_day7 = i;
        elseif (parameter_number <= 15)
            col_temp = i;
        elseif (parameter_number <= 16)
            col_rainstart_day1 = i;
        elseif (parameter_number <= 17)
            col_rainstart_day2 = i;
        elseif (parameter_number <= 18)
            col_rainstart_day3 = i;
        elseif (parameter_number <= 19)
            col_rainstart_day4 = i;
        elseif (parameter_number <= 20)
            col_rainstart_day5 = i;
        elseif (parameter_number <= 21)
            col_rainstart_day6 = i;
        elseif (parameter_number <= 22)
```

```
            col_rainstart_day7 = i;
        elseif (parameter_number <= 23)
            col_lhs_set = i;
        else
           warning('aa_raw_lhs_data_file column header not identified');
        end
    end
    munhconrctreff_parameter_set = rawlhsdata.data(:,col_munhconrctreff);
    khsoconrctreff_parameter_set = rawlhsdata.data(:,col_khsoconrctreff);
    ka1snhconrctreff_parameter_set = rawlhsdata.data(:,col_ka1snhconrctreff);
    bodconinf_parameter_set = rawlhsdata.data(:,col_bodconinf);
    bod_to_tkn_parameter_set = rawlhsdata.data(:,col_bod_to_tkn);
    bod_to_tp_parameter_set = rawlhsdata.data(:,col_bod_to_tp);
    qconinf_parameter_set = rawlhsdata.data(:,col_qconinf);
    rainfall_day1_parameter_set = rawlhsdata.data(:,col_rainfall_day1);
    rainfall_day2_parameter_set = rawlhsdata.data(:,col_rainfall_day2);
    rainfall_day3_parameter_set = rawlhsdata.data(:,col_rainfall_day3);
    rainfall_day4_parameter_set = rawlhsdata.data(:,col_rainfall_day4);
    rainfall_day5_parameter_set = rawlhsdata.data(:,col_rainfall_day5);
    rainfall_day6_parameter_set = rawlhsdata.data(:,col_rainfall_day6);
    rainfall_day7_parameter_set = rawlhsdata.data(:,col_rainfall_day7);
    temp_parameter_set = rawlhsdata.data(:,col_temp);
    rainstart_day1_parameter_set = rawlhsdata.data(:,col_rainstart_day1);
    rainstart_day2_parameter_set = rawlhsdata.data(:,col_rainstart_day2);
    rainstart_day3_parameter_set = rawlhsdata.data(:,col_rainstart_day3);
    rainstart_day4_parameter_set = rawlhsdata.data(:,col_rainstart_day4);
    rainstart_day5_parameter_set = rawlhsdata.data(:,col_rainstart_day5);
    rainstart_day6_parameter_set = rawlhsdata.data(:,col_rainstart_day6);
    rainstart_day7_parameter_set = rawlhsdata.data(:,col_rainstart_day7);
    lhs_set = rawlhsdata.data(:,col_lhs_set);

    tknconinf_parameter_set = bodconinf_parameter_set./bod_to_tkn_parameter_set;
    tpconinf_parameter_set = bodconinf_parameter_set./bod_to_tp_parameter_set;

    number_of_simulations = length(munhconrctreff_parameter_set);
% SECTION 2.3
% PROCESS DESIGN OUTSIDE OF LOOP - Any parameters that are
% universal to all simulations being performed, set them here. This
% prevents Matlab from having to re-run these calculations every time it
% runs through the loop. For example, if the reactor sizes are fixed for a
% given set of simulations, the reactor size calculations can be placed
% here.  If they are adjusted from loop to loop, they should be placed
% below the start of the loop in Section 2.3.

    % SECTION 2.3.1
    % TARGET DESIGN VALUES INFLUENCING DECISION VARIABLES
    int_rec_ratio = 2;  % Internal recycle flow rate ratio to forward flow.
                        % Value *100% of forward flow. Acceptable range
                        % is 2-4 (which is 200-400% of forward flow).

    % Set volume-dictating SRT values (winter design SRT) for "Standard" and
    % "Seasonal" designs.
    % STANDARD DESIGN
    srt_dv_ana_standard = 1;     % Anaerobic SRT in days. Acceptable range is 0.5-2d.
    srt_dv_anx_standard = 2;     % Anoxic SRT in days. Acceptable range is 1-3d.
    srt_dv_aer_standard = 10;     % Aerobic SRT in days. Acceptable range is 8-12d.
```

```
    v_ratio_anx_standard = 1.5;  % Ratio of Anoxic 2 volume to Anoxic 1 volume.
    srttarget_standard = srt_dv_ana_standard + srt_dv_anx_standard + srt_dv_aer_standard;   %↙
Total SRT in days.
    denit_filter_area_standard = 515; % m2; assumes 4 gpm/ft2 loading at typical flow of 26.6 MGD↙
with 10 of 12 units in service (all 12 units in service can also handle max month of 31.6 MGD).
    % SEASONAL DESIGN
    srt_dv_ana_seasonal = 1;     % Anaerobic SRT in days. Acceptable range is 0.5-2d.
    srt_dv_anx_seasonal = 1.5;     % Anoxic SRT in days. Acceptable range is 1-3d.
    srt_dv_aer_seasonal = 10;     % Aerobic SRT in days. Acceptable range is 8-12d.
    v_ratio_anx_seasonal = 1;  % Ratio of Anoxic 2 volume to Anoxic 1 volume.
    srttarget_seasonal = srt_dv_ana_seasonal + srt_dv_anx_seasonal + srt_dv_aer_seasonal;   %↙
Total SRT in days.
    denit_filter_area_seasonal = 588; % m2; assumes 3.5 gpm/ft2 loading at typical flow of 26.6↙
MGD with 10 of 12 units in service (all 12 units in service can also handle max month of 31.6↙
MGD).
    % both designs
    mlsstarget = 3100;  % Target MLSS concentration in g-(tss)/m3.
    xconsecundertarget = 8000;  % Target MLSS concentration of secondary
                                % clarifier underflow g-(tss)/m3.
    isbmlsstarget = 4500;   % Anticipated MLSS concentration for ISB treatment
                            % system in g-(tss)/m3 based on GPS-X simulations.
    isbxconsecundertarget = 10000;  % Target MLSS concentration of ISB
                                    % treatment system secondary clarifier
                                    % underflow g-(tss)/m3.
    q_isb = 3785.41;    % ISB flow in m3/d.
    new_reactor_max_interior_length = 188; % ft
    old_reactor_max_interior_length = 144.3; % ft
    ft_per_meter = 3.28083;
    reactor_depth_meters = 15/ft_per_meter;
    new_reactor_width_meters = (53*6)/ft_per_meter;
    old_reactor_width_meters = (25*12)/ft_per_meter;

    % SECTION 2.3.2
    % DESIGN CALCULATIONS TO ACHIEVE TARGET MLSS AND SRT
    % NOTE:  The values used in these calculations are the assumptions a
    % designer would make in the design of the system. The uncertainty
    % imposed around these values are used for simulations to evaluate how
    % the design would perform if some of these values are not entirely
    % accurate.
    % Source: Grady Jr. CPL, Daigger GT, Love NG, Filipe CDM. 2011. Biological
    %         Wastewater Treatment. Boca Raton, FL: CRC Press. 1022 p.
    qrctrinf = 104000; % Was 103464 for a q_inf of 90850 m3/d
                    % (this value includes rain). 12,614 m3/d in ISB, solids
                    % handling, denit backwash, etc., recycle flows.
    rec_design = qrctrinf*int_rec_ratio;  % Summer internal recycle flow in m3/d.
    rec_capacity = 1.5*rec_design;
    qconwinterrec_design = rec_design; % Winter internal recycle flow for
    % Seasonal design in m3/d.
    qconwinterrec_capacity = 1.5*qconwinterrec_design;
    xtss = mlsstarget;
    yieldhettss = 0.529; % Assumed yield of OHO in gTSS/gCOD. (was 0.49682)
    yieldpaotss = 0.508; % Assumed yield of PAO in gTSS/gCOD. (was 0.49682)
    i_o_xbt = 1.258; % Assumed COD per biomass TSS in gCOD/gTSS.
    bhet = 0.24; % Assumed lysis rate for OHO in d-1. (was 0.175)
    bpao = 0.077; % Assumed lysis rate for PAO in d-1. (was 0.0875)
    fd = 0.207; % Assumed inert fraction of decay products in gCOD/gCOD.
```

```
            % Converted from GPS-X value using GDLF EQN 3.68.(was 0.229)
    yieldauttss = 0.190779; % Assumed yield of autotrophs in gTSS/gN.
    baut = 0.132; % Assumed lysis rate for autotrophs in d-1. (was 0.15)
    xio_t = 37; % Assumed inert and inorganic solids (TSS0-VSS0+nbVSS) in
                % g-TSS/m3. (was 37)

    subdegraded_standard = (1.724*0.72*bodconinf_base_concentration)*(qconinf_base/qrctrinf); %
    subdegraded_seasonal = (1.724*0.72*bodconinf_base_concentration)*(qconinf_base/qrctrinf); %

    %subdegraded = (0.75*bodconinf_base_concentration + 90)*(qconinf_base/qrctrinf); % Assumed
biological substrate degradation
                % (SS0 + XS0 - SS) in g-COD/m3. (greater than influent BOD
                % because of methanol for denitrification)
    nr_het_standard = 0.087*((1+(fd*bhet*srttarget_standard))*yieldhettss*i_o_xbt)/
(1+bhet*srttarget_standard);
    nr_het_seasonal = 0.087*((1+(fd*bhet*srttarget_seasonal))*yieldhettss*i_o_xbt)/
(1+bhet*srttarget_seasonal);
    sna_predict_standard = 32.7 - nr_het_standard*(subdegraded_standard);  % Assumed
concentration of
                                                % ammonia nitrified in gN/m3.
    sna_predict_seasonal = 32.7 - nr_het_seasonal*(subdegraded_seasonal);
    snh_predict = 0.5; % Assumed effluent ammonium in gN/m3.
    solidswastage_design_standard = qrctrinf*(xio_t + ((1 + (fd*bhet*srttarget_standard))
*yieldhettss ...
        *subdegraded_standard/(1 + bhet*srttarget_standard)) + ((1 +
(fd*baut*srttarget_standard)) ...
        *yieldauttss*(sna_predict_standard - snh_predict)/(1 + baut*srttarget_standard)));
    solidswastage_design_seasonal = qrctrinf*(xio_t + ((1 + (fd*bhet*srttarget_seasonal))
*yieldhettss ...
        *subdegraded_seasonal/(1 + bhet*srttarget_seasonal)) + ((1 +
(fd*baut*srttarget_seasonal)) ...
        *yieldauttss*(sna_predict_seasonal - snh_predict)/(1 + baut*srttarget_seasonal)));
    % Grady et al. Equation 11.20

    qconrctrwas_design_standard = solidswastage_design_standard/xconsecundertarget;
    qconrctrwas_design_seasonal = solidswastage_design_seasonal/xconsecundertarget;
    qconrctrwas_capacity_standard = 1.5*qconrctrwas_design_standard;
    qconrctrwas_capacity_seasonal = 1.5*qconrctrwas_design_seasonal;

    qconras_design_standard = ((mlsstarget*qrctrinf)-
(xconsecundertarget*qconrctrwas_design_standard)) ...
        /(xconsecundertarget - mlsstarget);
    qconras_design_seasonal = ((mlsstarget*qrctrinf)-
(xconsecundertarget*qconrctrwas_design_seasonal)) ...
        /(xconsecundertarget - mlsstarget);
    qconras_capacity_standard = 1.5*qconras_design_standard;
    qconras_capacity_seasonal = 1.5*qconras_design_seasonal;

    qconsecunder_design_standard = qconrctrwas_design_standard + qconras_design_standard;
    qconsecunder_design_seasonal = qconrctrwas_design_seasonal + qconras_design_seasonal;
    qconsecunder_capacity_standard = 1.5*qconsecunder_design_standard;
    qconsecunder_capacity_seasonal = 1.5*qconsecunder_design_seasonal;

    qconisbwas_design_standard = qconrctrwas_design_standard*(8000/10000);
    qconisbwas_design_seasonal = qconrctrwas_design_seasonal*(8000/10000);
    qconisbwas_capacity_standard = 1.5*qconisbwas_design_standard;
```

```
    qconisbwas_capacity_seasonal = 1.5*qconisbwas_design_seasonal;

    qconisbras_design_standard = ((isbmlsstarget*(q_isb + qconrctrwas_design_standard)) ...
        - (isbxconsecundertarget*qconisbwas_design_standard))/(isbxconsecundertarget ...
        - isbmlsstarget);
    qconisbras_design_seasonal = ((isbmlsstarget*(q_isb + qconrctrwas_design_seasonal)) ...
        - (isbxconsecundertarget*qconisbwas_design_seasonal))/(isbxconsecundertarget ...
        - isbmlsstarget);
    qconisbras_capacity_standard = 1.5*qconisbras_design_standard;
    qconisbras_capacity_seasonal = 1.5*qconisbras_design_seasonal;

    qconisbsecunder_design_standard = qconisbwas_design_standard + qconisbras_design_standard;
    qconisbsecunder_design_seasonal = qconisbwas_design_seasonal + qconisbras_design_seasonal;
    qconisbsecunder_capacity_standard = 1.5*qconisbsecunder_design_standard;
    qconisbsecunder_capacity_seasonal = 1.5*qconisbsecunder_design_seasonal;

    volumetotal_standard = (srttarget_standard*solidswastage_design_standard)/(mlsstarget);
    volume_ana_standard = volumetotal_standard*(srt_dv_ana_standard/srttarget_standard);
    volume_anx_standard = volumetotal_standard*(srt_dv_anx_standard/srttarget_standard);
    volume_anx1_standard = volume_anx_standard/(1 + v_ratio_anx_standard);
    volume_anx2_standard = volume_anx_standard - volume_anx1_standard;
    volume_aer_standard = volumetotal_standard*(srt_dv_aer_standard/srttarget_standard);
    volume_aer2_standard = (0.5/24)*qrctrinf;
    volume_aer1_standard = volume_aer_standard - volume_aer2_standard;

    volumetotal_seasonal = (srttarget_seasonal*solidswastage_design_seasonal)/(mlsstarget);
    volume_ana_seasonal = volumetotal_seasonal*(srt_dv_ana_seasonal/srttarget_seasonal);
    volume_anx_seasonal = volumetotal_seasonal*(srt_dv_anx_seasonal/srttarget_seasonal);
    volume_anx1_seasonal = volume_anx_seasonal; % only anoxic zone under winter A2O mode.
    volume_anx2_seasonal = volume_anx1_seasonal*v_ratio_anx_seasonal;
    volume_aer_seasonal = volumetotal_seasonal*(srt_dv_aer_seasonal/srttarget_seasonal);
    volume_aer2_seasonal = (0.5/24)*qrctrinf;
    volume_aer1_seasonal = volume_aer_seasonal - volume_aer2_seasonal - volume_anx2_seasonal; %↙
ANX2 operates as aerobic zone in winter A2O mode.

    % SECTION 2.3.3
    % FINAL DESIGN CALCULATIONS (makes assumption that ANX 2, AER 2, and
    % part of AER 1 are in existing reactor basins; all other reactors are
    % new construction).

    l_aer2_ft_standard = (volume_aer2_standard/(reactor_depth_meters ...
        *old_reactor_width_meters))*ft_per_meter;
    l_anx2_ft_standard = (volume_anx2_standard/(reactor_depth_meters ...
        *old_reactor_width_meters))*ft_per_meter;
    l_aer1b_ft_standard = old_reactor_max_interior_length - l_aer2_ft_standard -↙
l_anx2_ft_standard;
    l_aer1a_ft_standard = ((volume_aer1_standard - ((l_aer1b_ft_standard/ft_per_meter) ...
        *old_reactor_width_meters*reactor_depth_meters))...
        /(reactor_depth_meters*new_reactor_width_meters))*ft_per_meter;
    l_anx1_ft_standard = (volume_anx1_standard/(reactor_depth_meters ...
        *new_reactor_width_meters))*ft_per_meter;
    l_ana_ft_standard = (volume_ana_standard/(reactor_depth_meters ...
        *new_reactor_width_meters))*ft_per_meter;
    volume_aer1b_standard = (l_aer1b_ft_standard/ft_per_meter)↙
*old_reactor_width_meters*reactor_depth_meters;
    volume_aer1a_standard = volume_aer1_standard - volume_aer1b_standard;
```

```
    l_aer2_ft_seasonal = (volume_aer2_seasonal/(reactor_depth_meters ...
        *old_reactor_width_meters))*ft_per_meter;
    l_anx2_ft_seasonal = (volume_anx2_seasonal/(reactor_depth_meters ...
        *old_reactor_width_meters))*ft_per_meter;
    l_aer1b_ft_seasonal = old_reactor_max_interior_length - l_aer2_ft_seasonal -↙
l_anx2_ft_seasonal;
    l_aer1a_ft_seasonal = ((volume_aer1_seasonal - ((l_aer1b_ft_seasonal/ft_per_meter) ...
        *old_reactor_width_meters*reactor_depth_meters))...
        /(reactor_depth_meters*new_reactor_width_meters))*ft_per_meter;
    l_anx1_ft_seasonal = (volume_anx1_seasonal/(reactor_depth_meters ...
        *new_reactor_width_meters))*ft_per_meter;
    l_ana_ft_seasonal = (volume_ana_seasonal/(reactor_depth_meters ...
        *new_reactor_width_meters))*ft_per_meter;
    volume_aer1b_seasonal = (l_aer1b_ft_seasonal/ft_per_meter)↙
*old_reactor_width_meters*reactor_depth_meters;
    volume_aer1a_seasonal = volume_aer1_seasonal - volume_aer1b_seasonal;

% SECTION 3.1
% LOOP START - The purpose of using Matlab for this work is to be able to
% run GPS-X simulations many times and collect the data. Below this point
% are the loops that define the GPS-X simulations that will be run. If you
% are enumerating a decision space, you can just make these nested "for"
% loops with a loop for each decision variable. For example, to run across
% a range of aerobic SRTs and internal recycle ratios, you might use loops
% like this:  "for int_rec_ratio = 2:0.2:4; a return, and then
% for srt_dv_aer = 8:0.5:12;" where the notation means (min:stepsize:max).
% This will run every combination of internal recycle ratio (from 2 to 4
% in steps of 0.2) and aerobic SRT (from 8 to 12 in steps of 0.5). Instead,
% this "dynamic simulation" file will take a matrix of inputs of uncertain
% parameters (e.g., peaking factor, influent TKN, decay rate) generated via
% Latin Hypercube Sampling (LHS), and generate files for kinetics and
% stoichiometry and a time series file for influent.


for sim_set = 1:number_of_simulations;
    % FIXED VALUES - Kinetic parameters.
    munhconrctreff_sim_value = munhconrctreff_parameter_set(sim_set,1);
    khsoconrctreff_sim_value = khsoconrctreff_parameter_set(sim_set,1);
    ka1snhconrctreff_sim_value = ka1snhconrctreff_parameter_set(sim_set,1);
    % TIME-DEPENDENT VALUES - Influent composition and flow.
    bodconinf_sim_value = bodconinf_parameter_set(sim_set,1);
    tknconinf_sim_value = tknconinf_parameter_set(sim_set,1);
    tpconinf_sim_value = tpconinf_parameter_set(sim_set,1);
    qconinf_sim_value = qconinf_parameter_set(sim_set,1);
    rainfall_day1_sim_value = rainfall_day1_parameter_set(sim_set,1);
    rainfall_day2_sim_value = rainfall_day2_parameter_set(sim_set,1);
    rainfall_day3_sim_value = rainfall_day3_parameter_set(sim_set,1);
    rainfall_day4_sim_value = rainfall_day4_parameter_set(sim_set,1);
    rainfall_day5_sim_value = rainfall_day5_parameter_set(sim_set,1);
    rainfall_day6_sim_value = rainfall_day6_parameter_set(sim_set,1);
    rainfall_day7_sim_value = rainfall_day7_parameter_set(sim_set,1);
    temp_sim_value = temp_parameter_set(sim_set,1);
    rainstart_day1_sim_value = rainstart_day1_parameter_set(sim_set,1);
    rainstart_day2_sim_value = rainstart_day2_parameter_set(sim_set,1);
```

```
    rainstart_day3_sim_value = rainstart_day3_parameter_set(sim_set,1);
    rainstart_day4_sim_value = rainstart_day4_parameter_set(sim_set,1);
    rainstart_day5_sim_value = rainstart_day5_parameter_set(sim_set,1);
    rainstart_day6_sim_value = rainstart_day6_parameter_set(sim_set,1);
    rainstart_day7_sim_value = rainstart_day7_parameter_set(sim_set,1);
    lhs_sim_value = lhs_set(sim_set,1);

    % SECTION 3.2
    % FILE INPUT CONTROLLER CALCULATIONS - Prepare matrices for GPS-X
    % time series file input controllers and other file input controllers
    % requireing calculations.
    for config = 1:2;

        if (config==1);
            design = 'standard';
            volume_ana = volume_ana_standard;
            volume_anx1 = volume_anx1_standard;
            volume_aer1a = volume_aer1a_standard;
            volume_aer1b = volume_aer1b_standard;
            volume_anx2 = volume_anx2_standard;
            volume_aer2 = volume_aer2_standard;
            afiltereff = denit_filter_area_standard;

        elseif (config==2);
            design = 'seasonal';
            volume_ana = volume_ana_seasonal;
            volume_anx1 = volume_anx1_seasonal;
            volume_aer1a = volume_aer1a_seasonal;
            volume_aer1b = volume_aer1b_seasonal;
            volume_anx2 = volume_anx2_seasonal;
            volume_aer2 = volume_aer2_seasonal;
            afiltereff = denit_filter_area_seasonal;
        else
            warning('Configuration type not identified - Standard vs. Seasonal. Unknown which
file input controllers to generate.');
        end

    volume_total = volume_ana + volume_anx1 + volume_aer1a + volume_aer1b + volume_anx2 +
volume_aer2;

    % CREATE REACTOR VOLUME FILE INPUT CONTROLLER
    line21 = sprintf('t \t vmrctraeff \t vlconrctrbeff(1) \t vlconrctrbeff(2) \t vlconrctrbeff(3)
\t vlconrctrceff(1) \t vlconrctrceff(2) \t afiltereff');
    line22 = sprintf('d \t m3 \t m3 \t m3 \t m3 \t m3 \t m3 \t m2');
    line23 = sprintf('%d \t %d \t %d \t %d \t %d \t %d \t %d \t %d', ...
            -2, volume_ana, volume_anx1, volume_aer1a, volume_aer1b, ...
            volume_anx2, volume_aer2, afiltereff);
    rctr_volume_var = {line21; line22; line23};
    fid=fopen(volumefilename,'w');
        for row = 1:3
            fprintf(fid, '%s \r\n', rctr_volume_var{row,:});
        end
    fclose(fid);

    % SECTION 3.2.1
    % ADJUSTED PUMPING RATES BASED ON ALTERED INFLUENT - Need to adjust
```

```
    % pumping rate file input controller so the correct SRT is actually
    % achieved.
    qrctrinf_operation = 1.057*qconinf_sim_value + 9619; % Was anticipated average reactor
                    % influent in m3/d based on steady state GPS-X
                    % simulations. (was 1.057*qconinf_sim_value + 9619)


    % subdegraded_operation = (0.75*bodconinf_sim_value + 90)*↙
(qconinf_sim_value/qrctrinf_operation); % Assumed biological substrate
                    % degradation (SS0 + XS0 - SS) in g-COD/m3. Was 142
                    % for a BOD influent of 236 g/m3. (was 0.63bodconinf
                    % plus some value)
% JSGXX - consider revisiting subdegraded_operation estimate because no
% methanol added in winter to suspended culture.
    if (config==1)
        subdegraded_operation = (1.72414*0.77*bodconinf_sim_value)*↙
(qconinf_sim_value/qrctrinf_operation);% (0.75*bodconinf_sim_value + 94)*↙
(qconinf_sim_value/qrctrinf_operation); % Assumed biological substrate
                    % degradation (SS0 + XS0 - SS) in g-COD/m3. Was 142
                    % for a BOD influent of 236 g/m3. (was 0.63bodconinf
                    % plus some value)
        if (temp_sim_value > 18)
            srttarget_operation = 0.7*srttarget_standard;
        elseif (temp_sim_value <= 18)
            srttarget_operation = srttarget_standard;
        end
    elseif (config==2)
        if (temp_sim_value > 18)
            subdegraded_operation = (1.72414*0.77*bodconinf_sim_value)*↙
(qconinf_sim_value/qrctrinf_operation);% (0.75*bodconinf_sim_value + 94)*↙
(qconinf_sim_value/qrctrinf_operation); % Assumed biological substrate
                    % degradation (SS0 + XS0 - SS) in g-COD/m3. Was 142
                    % for a BOD influent of 236 g/m3. (was 0.63bodconinf
                    % plus some value)
            srttarget_operation = 0.7*srttarget_seasonal;
        elseif (temp_sim_value <= 18)
            subdegraded_operation = (1.72414*0.77*bodconinf_sim_value)*↙
(qconinf_sim_value/qrctrinf_operation);% (0.75*bodconinf_sim_value + 84)*↙
(qconinf_sim_value/qrctrinf_operation); % Assumed biological substrate
                    % degradation (SS0 + XS0 - SS) in g-COD/m3. Was 142
                    % for a BOD influent of 236 g/m3. (was 0.63bodconinf
                    % plus some value)
            srttarget_operation = srttarget_seasonal;
        end
    else
        warning('Configuration type not identified - Standard vs. Seasonal. Unknown which file↙
input controllers to generate.');
    end

    nr_het_operation = 0.087*((1+(fd*bhet*srttarget_operation))*yieldhettss*i_o_xbt)/↙
(1+bhet*srttarget_operation);
    sna_predict_operation = 32.7 - nr_het_operation*(subdegraded_operation); % Assumed
                    % concentration of ammonia nitrified in gN/m3.
    solidswastage_operation = qrctrinf_operation*(xio_t + ((1 + (fd*bhet*srttarget_operation))↙
*yieldhettss ...
        *subdegraded_operation/(1 + bhet*srttarget_operation)) + ((1 +↙
```

```
(fd*baut*srttarget_operation)) ...
        *yieldauttss*(sna_predict_operation - snh_predict)/(1 + baut*srttarget_operation)));

    mlss_operation = solidswastage_operation*srttarget_operation/(volume_total);
    xsecunder_operation = mlss_operation*(xconsecundertarget/mlsstarget);

    qconrctrwas_operation = solidswastage_operation/xsecunder_operation;

    qconras_operation = ((mlss_operation*qrctrinf_operation)-
(xsecunder_operation*qconrctrwas_operation)) ...
        /(xsecunder_operation - mlss_operation);
    qconsecunder_operation = qconrctrwas_operation + qconras_operation;
    qconisbwas_operation = qconrctrwas_operation*(8000/10000);
    qconisbras_operation = ((isbmlsstarget*(q_isb + qconrctrwas_operation)) ...
        - (isbxconsecundertarget*qconisbwas_operation))/(isbxconsecundertarget ...
        - isbmlsstarget);
    qconisbsecunder_operation = qconisbwas_operation + qconisbras_operation;

    % SECTION 3.2.3
    % FLOW
    inf_from_rain = 15558; % Median influent increase (m3) per inch of rain.
    % No rain events will occur on days 1-3 of the dynamic simulation
    % (which means 0.0-2.99 days) because the model reaches steady-state
    % with diurnal flow during that time.  Can make this random with this
    % approach: unidrnd(simulation_timepoints - startup_timepoints)
    rain_event_day1 = hydrograph_3_unit_load*(rainfall_day1_sim_value ...
        *inf_from_rain);
    rain_event_day1_start_row = rainstart_day1_sim_value + 3*24;
    rain_event_day1_end_row = rain_event_day1_start_row + length(hydrograph_3_unit_load) - 1;
    rain_day1_sim_series_adjustment = zeros(simulation_timepoints,1);
    rain_day1_sim_series_adjustment(rain_event_day1_start_row:rain_event_day1_end_row,1) =
rain_event_day1;

    rain_event_day2 = hydrograph_3_unit_load*(rainfall_day2_sim_value ...
        *inf_from_rain);
    rain_event_day2_start_row = rainstart_day2_sim_value + 4*24;
    rain_event_day2_end_row = rain_event_day2_start_row + length(hydrograph_3_unit_load) - 1;
    rain_day2_sim_series_adjustment = zeros(simulation_timepoints,1);
    rain_day2_sim_series_adjustment(rain_event_day2_start_row:rain_event_day2_end_row,1) =
rain_event_day2;

    rain_event_day3 = hydrograph_3_unit_load*(rainfall_day3_sim_value ...
        *inf_from_rain);
    rain_event_day3_start_row = rainstart_day3_sim_value + 5*24;
    rain_event_day3_end_row = rain_event_day3_start_row + length(hydrograph_3_unit_load) - 1;
    rain_day3_sim_series_adjustment = zeros(simulation_timepoints,1);
    rain_day3_sim_series_adjustment(rain_event_day3_start_row:rain_event_day3_end_row,1) =
rain_event_day3;

    rain_event_day4 = hydrograph_3_unit_load*(rainfall_day4_sim_value ...
        *inf_from_rain);
    rain_event_day4_start_row = rainstart_day4_sim_value + 6*24;
    rain_event_day4_end_row = rain_event_day4_start_row + length(hydrograph_3_unit_load) - 1;
    rain_day4_sim_series_adjustment = zeros(simulation_timepoints,1);
    rain_day4_sim_series_adjustment(rain_event_day4_start_row:rain_event_day4_end_row,1) =
rain_event_day4;
```

```
    rain_event_day5 = hydrograph_3_unit_load*(rainfall_day5_sim_value ...
        *inf_from_rain);
    rain_event_day5_start_row = rainstart_day5_sim_value + 7*24;
    rain_event_day5_end_row = rain_event_day5_start_row + length(hydrograph_3_unit_load) - 1;
    rain_day5_sim_series_adjustment = zeros(simulation_timepoints,1);
    rain_day5_sim_series_adjustment(rain_event_day5_start_row:rain_event_day5_end_row,1) =↙
rain_event_day5;

    rain_event_day6 = hydrograph_3_unit_load*(rainfall_day6_sim_value ...
        *inf_from_rain);
    rain_event_day6_start_row = rainstart_day6_sim_value + 8*24;
    rain_event_day6_end_row = rain_event_day6_start_row + length(hydrograph_3_unit_load) - 1;
    rain_day6_sim_series_adjustment = zeros(simulation_timepoints,1);
    rain_day6_sim_series_adjustment(rain_event_day6_start_row:rain_event_day6_end_row,1) =↙
rain_event_day6;

    rain_event_day7 = hydrograph_3_unit_load*(rainfall_day7_sim_value ...
        *inf_from_rain);
    rain_event_day7_start_row = rainstart_day7_sim_value + 9*24;
    rain_event_day7_end_row = rain_event_day7_start_row + length(hydrograph_3_unit_load) - 1;
    if (rain_event_day7_end_row > simulation_timepoints)
        rain_event_day7_end_row_corrected = simulation_timepoints; % To prevent having extra rows↙
in rain file beyond simulation set.
    else
        rain_event_day7_end_row_corrected = rain_event_day7_end_row;
    end
    rain_day7_sim_series_adjustment = zeros(simulation_timepoints,1);
    for rain_event_day7_row = rain_event_day7_start_row:rain_event_day7_end_row_corrected;
        rain_day7_sim_series_adjustment(rain_event_day7_row,1) = rain_event_day7↙
(rain_event_day7_row - rain_event_day7_start_row + 1);
    end

    rain_sim_series_adjustment = rain_day1_sim_series_adjustment ...
        + rain_day2_sim_series_adjustment + rain_day3_sim_series_adjustment ...
        + rain_day4_sim_series_adjustment + rain_day5_sim_series_adjustment ...
        + rain_day6_sim_series_adjustment + rain_day7_sim_series_adjustment;

    wastewater_flow_sim_series = qconinf_sim_value*simulation_diurnal_unit_load;
    qconinf_sim_series = wastewater_flow_sim_series + rain_sim_series_adjustment;
    % BOD
    bodconinf_sim_series = (bodconinf_sim_value ...
         /bodconinf_base_concentration).*(bodconinf_base_loading ...
         ./qconinf_sim_series);
    % TKN
    tknconinf_sim_series = (tknconinf_sim_value ...
         /tknconinf_base_concentration).*(tknconinf_base_loading ...
         ./qconinf_sim_series);
    % TP
    tpconinf_sim_series = (tpconinf_sim_value ...
         /tpconinf_base_concentration).*(tpconinf_base_loading ...
         ./qconinf_sim_series);
    % Other parameters will be directly tied to the LHS outputs above.
    % Specifically, NOB max specific growth rate is assumed to 0.1 d-1
    % faster than AOB max specific growth rate, influent soluble
    % phosphorus is assumed to be 60% of total phosphorus,
```

```
    % and influent ammonium is 73.7% of influent TKN.
    % MUNO2
    muno2conrctreff_sim_value = munhconrctreff_sim_value + 0.1;
    % SNH
    snhinf_sim_value = tknconinf_sim_value*0.737;
    snhinf_sim_series = tknconinf_sim_series.*0.737;
    % TP
    spinf_sim_value = tpconinf_sim_value*0.8;
    spinf_sim_series = tpconinf_sim_series.*0.8;
    % Acetate (needs to be included because if BOD dips too low without
    % decreasing influent acetate, then you get a negative SSINF.
    sacinf_sim_value = bodconinf_sim_value*0.1;
    sacinf_sim_series = bodconinf_sim_series.*0.1;
    % Colloidal substrate also needs to be included to avoid negative
    % SSINF.
    scolinf_sim_value = bodconinf_sim_value*0.16667;
    scolinf_sim_series = bodconinf_sim_series.*0.16667;

    % Internal Recycle
    internal_rec_operation = zeros(simulation_timepoints,1);
    for internal_recycle_hour = 1:simulation_timepoints;
        target_rec_operation = (qconinf_sim_series(internal_recycle_hour,1) + 12614)↙
*int_rec_ratio;
        % The 12,614 m3/d is from ISB, solids handling, denit backwash,
        % etc., recycle flows.
        if (target_rec_operation <= rec_capacity)
            internal_rec_operation(internal_recycle_hour,1) = target_rec_operation;
        else
            internal_rec_operation(internal_recycle_hour,1) = rec_capacity;
        end
        warning('Configuration type not identified - Standard vs. Seasonal. Unknown which file↙
input controllers to generate.');
    end

    % Set methanol dosing for ANX2 and denit filters.
    % ANX2 dosing will target the addition of 34 mg-(BOD5)/L, which tends
    % to remove about 4 mg-N/L in steady-state simulations.  Methanol has a
    % density of 792,000 mg/L, with a COD of 1.50 g-COD/g-MeOH, which
    % results in a COD content of 1,190,000 mg-COD/L.

    % NOTE:  GPS-X was not allowing for the growth of methylotrophic bacteria because
    % of a convergence issue.  Switched to acetate to be able to run
    % simulations.  This is not always expected to be a problem, but it
    % occured with the Mantis2 model with our plant configuration.
    % Hydromantis will look into the convergence issue.

    % Set acetate dosing for ANX2 and denit filters.
    % ANX2 dosing will target the addition of 25 mg-(BOD5)/L.  Acetate has
    % a density of 1,049,000 mg/L, with a COD of 1.07 g-COD/g-HAc, which
    % results in a COD content of 1,122,000 mg-COD/L.

        qconmeohrctrc = zeros(simulation_timepoints,1);
        qconmeohdf = zeros(simulation_timepoints,1);
%         meoh_concentration = 1188000; % g-COD/m3
        meoh_hac_concentration = 1122000; % g-COD/m3
```

```
    if (config==1); % Standard design is inflexible
        rec_operation = internal_rec_operation;
        qconwinterrec_operation = zeros(simulation_timepoints,1);
        setpsolrctrceff1 = 0;
        meoh_addition_anx2_target = 42; % g-COD/m3
        meoh_addition_df_target = 22; % g-COD/m3; for loading df at 4 gpm/ft2.
        % Dosing to second anoxic zone and denit filter.
        for qmeoh_hour = 1:simulation_timepoints
            forward_flow_to_anx2 = (qconinf_sim_series(qmeoh_hour,1) + 12614) +↙
qconras_operation; % 12,614 m3/d in ISB, solids
                    % handling, denit backwash, etc., recycle flows
            qconmeohrctrc(qmeoh_hour,1) =↙
meoh_addition_anx2_target*forward_flow_to_anx2/meoh_hac_concentration;
            forward_flow_to_df = (qconinf_sim_series(qmeoh_hour,1) + 3785);
            qconmeohdf(qmeoh_hour,1) =↙
meoh_addition_df_target*forward_flow_to_df/meoh_hac_concentration;
        end

    elseif (config==2); % Seasonal design has seasonal flexibility
        if (temp_sim_value > 18)
            rec_operation = internal_rec_operation;
            qconwinterrec_operation = zeros(simulation_timepoints,1);
            setpsolrctrceff1 = 0;
            meoh_addition_anx2_target = 30; % g-COD/m3
            meoh_addition_df_target = 22; % g-COD/m3; for loading df at 4 gpm/ft2.
            % Dosing to second anoxic zone and denit filter.
            for qmeoh_hour = 1:simulation_timepoints
                forward_flow_to_anx2 = (qconinf_sim_series(qmeoh_hour,1) + 12614) +↙
qconras_operation; % 12,614 m3/d in ISB, solids
                        % handling, denit backwash, etc., recycle flows
                qconmeohrctrc(qmeoh_hour,1) =↙
meoh_addition_anx2_target*forward_flow_to_anx2/meoh_hac_concentration;
                forward_flow_to_df = (qconinf_sim_series(qmeoh_hour,1) + 3785);
                qconmeohdf(qmeoh_hour,1) =↙
meoh_addition_df_target*forward_flow_to_df/meoh_hac_concentration;
            end
        elseif (temp_sim_value <= 18)
            rec_operation = zeros(simulation_timepoints,1);
            qconwinterrec_operation = internal_rec_operation;
            setpsolrctrceff1 = 2;
            meoh_addition_anx2_target = 0; % g-COD/m3
            meoh_addition_df_target = 30; % g-COD/m3; for loading df at 3.5 gpm/ft2.
            % Dosing to second anoxic zone and denit filter.
            for qmeoh_hour = 1:simulation_timepoints
                forward_flow_to_anx2 = (qconinf_sim_series(qmeoh_hour,1) + 12614) +↙
qconras_operation; % 12,614 m3/d in ISB, solids
                        % handling, denit backwash, etc., recycle flows
                qconmeohrctrc(qmeoh_hour,1) =↙
meoh_addition_anx2_target*forward_flow_to_anx2/meoh_hac_concentration; % goes to zero because↙
target is 0 for A2O operation.
                forward_flow_to_df = (qconinf_sim_series(qmeoh_hour,1) + 3785);
                qconmeohdf(qmeoh_hour,1) =↙
meoh_addition_df_target*forward_flow_to_df/meoh_hac_concentration;
            end
        else
            warning('Temperature not understood.  Unclear if operation is during winter or↙
```

```
summer.');
        end
    else
        warning('Configuration type not identified - Standard vs. Seasonal. Unknown which file
input controllers to generate.');
    end

    forward_flow_to_anx2_steady = (qconinf_sim_value + 12614) + qconras_operation;
    qconmeohrctrc_steady =
meoh_addition_anx2_target*forward_flow_to_anx2_steady/meoh_hac_concentration;
    forward_flow_to_df_steady = qconinf_sim_value + 3785;
    qconmeohdf_steady = meoh_addition_df_target*forward_flow_to_df_steady/meoh_hac_concentration;
    qconwinterrec_operation_steady = sum(qconwinterrec_operation)/length
(qconwinterrec_operation);
    rec_operation_steady = sum(rec_operation)/length(rec_operation);

% Add denit filter backwash - flow rate at 2.5x qinf sim value
denit_backwash_rate = 10; % gpm/ft2 for 15 min a day
    if (config==1); % Standard design is inflexible
        df_loading = 4; % gpm/ft2
    elseif (config==2); % Seasonal design has seasonal flexibility
        if (temp_sim_value > 18)
            df_loading = 4; % gpm/ft2
        elseif (temp_sim_value <= 18)
            df_loading = 3.5; % gpm/ft2
        end
    end
denit_backwash_flow = (denit_backwash_rate/df_loading)*(qconinf_sim_value + 3785);
bwflowfiltereff = denit_backwash_flow;

% SECTION 3.3
% GENERATE FILE INPUT CONTROLLERS

    % SECTION 3.3.4
    % DISSOLVED OXYGEN SETPOINT FILE INPUT CONTROLLER AND TEMP
    line71 = sprintf('t \t setpsolrctrceff(1) \t temp \t airtemp');
    line72 = sprintf('d \t - \t - \t -');
    line73 = sprintf('%d \t %d \t %d \t %d', -2, setpsolrctrceff1, temp_sim_value,
temp_sim_value);
    dissolvedoxygen_var = {line71; line72; line73};
    fid=fopen(dissolvedoxygenfilename,'w');
    for row = 1:3
        fprintf(fid, '%s \r\n', dissolvedoxygen_var{row,:});
    end
    fclose(fid);

% Meaning of "rec" changed in GPS-X file from original
% config_1_5bard.  "rec" now means basin 3 to 1 in Reactor B.
% Also added a new pumped flow in this code.  Careful with this when making
% changes.

    % SECTION 3.3.1
    % CREATE PUMPING FILE INPUT CONTROLLER
    line31 = sprintf('t \t qconrctrwas \t qconsecunder \t qconisbwas \t qconisbsecunder \t
bwflowfiltereff');
    line32 = sprintf('d \t m3/d \t m3/d \t m3/d \t m3/d \t m3/d \t m3/d');
```

```
    line33 = sprintf('%d \t %d \t %d \t %d \t %d \t %d', ...
        -2, qconrctrwas_operation, qconsecunder_operation, qconisbwas_operation, ...
        qconisbsecunder_operation, bwflowfiltereff);
    constant_rctr_pumping_var = {line31; line32; line33};
    fid=fopen(constantpumpingfilename,'w');
        for row = 1:3
            fprintf(fid, '%s \r\n', constant_rctr_pumping_var{row,:});
        end
    fclose(fid);

    % VARIABLE PUMPING - Generate this file input controller
    % in 2 parts. First, create the file with 3 headers. Then append the
    % time points line-by-line.
    line311 = sprintf('t \t rec \t qconwinterrec \t qconmeohrctrc \t qconmeohdf');
    line321 = sprintf('d \t m3/d \t m3/d \t m3/d \t m3/d');
    line331 = sprintf('%d \t %d \t %d \t %d \t %d', ...
        -2, rec_operation_steady, qconwinterrec_operation_steady, qconmeohrctrc_steady, ...
        qconmeohdf_steady);
    variable_rctr_pumping_var = {line311; line321; line331};
    fid=fopen(variablepumpingfilename,'w');

    for row = 1:3
        fprintf(fid, '%s \r\n', variable_rctr_pumping_var{row,:});
    end
    fclose(fid);
    fid=fopen(variablepumpingfilename,'a');
    for row = 1:simulation_timepoints
        line341 = sprintf('%d \t %d \t %d \t %d \t %d', ...
            simulation_time_series(row,1), rec_operation(row,1), ...
            qconwinterrec_operation(row,1), qconmeohrctrc(row,1), ...
            qconmeohdf(row,1));
        fprintf(fid, '%s \r\n', line341);
    end
    fclose(fid);

    % SECTION 3.3.2
    % KINETIC PARAMETER FILE INPUT CONTROLLER
    line41 = sprintf('t \t munhconrctraeff \t khsoconrctraeff \t ka1snhconrctraeff \t
muno2conrctraeff \t munhconrctrbeff \t khsoconrctrbeff \t ka1snhconrctrbeff \t muno2conrctrbeff
\t munhconrctrceff \t khsoconrctrceff \t ka1snhconrctrceff \t muno2conrctrceff');
    line42 = sprintf('d \t 1/d \t gCOD/m3 \t gN/m3 \t - \t 1/d \t gCOD/m3 \t gN/m3 \t - \t 1/d \t
gCOD/m3 \t gN/m3 \t -');
    line43 = sprintf('%d \t %d \t %d \t %d \t %d \t %d \t %d \t %d \t %d \t %d \t %d \t %
d', -2, munhconrctreff_sim_value, ...
            khsoconrctreff_sim_value, ka1snhconrctreff_sim_value, ...
            muno2conrctreff_sim_value, munhconrctreff_sim_value, ...
            khsoconrctreff_sim_value, ka1snhconrctreff_sim_value, ...
            muno2conrctreff_sim_value, munhconrctreff_sim_value, ...
            khsoconrctreff_sim_value, ka1snhconrctreff_sim_value, ...
            muno2conrctreff_sim_value);
    kinetics_var = {line41; line42; line43};
    fid=fopen(kineticsfilename,'w');
    for row = 1:3
        fprintf(fid, '%s \r\n', kinetics_var{row,:});
    end
    fclose(fid);
```

```
    % SECTION 3.3.3
    % INFLUENT FILE INPUT CONTROLLER - Generate this file input controller
    % in 2 parts. First, create the file with 3 headers. Then append the
    % time points line-by-line.
    line51 = sprintf('t \t qconinf \t bodconinf \t tknconinf \t spinf \t snhinf \t tpconinf \t↙
sacinf \t scolinf');
    line52 = sprintf('d \t m3/d \t g/m3 \t gN/m3 \t gP/m3 \t gN/m3 \t gP/m3 \t gCOD/m3 \t↙
gCOD/m3');
    line53 = sprintf('%d \t %d \t %d \t %d \t %d \t %d \t %d \t %d \t %d', ...
        -2, qconinf_sim_value, bodconinf_sim_value, tknconinf_sim_value, ...
        spinf_sim_value, snhinf_sim_value, tpconinf_sim_value, sacinf_sim_value,↙
scolinf_sim_value);
    influent_var = {line51; line52; line53};
    fid=fopen(influentfilename,'w');
    for row = 1:3
        fprintf(fid, '%s \r\n', influent_var{row,:});
    end
    fclose(fid);

    fid=fopen(influentfilename,'a');
    for row = 1:simulation_timepoints
        line54 = sprintf('%d \t %d \t %d \t %d \t %d \t %d \t %d \t %d \t %d', ...
            simulation_time_series(row,1), qconinf_sim_series(row,1), ...
            bodconinf_sim_series(row,1), tknconinf_sim_series(row,1), ...
            spinf_sim_series(row,1), snhinf_sim_series(row,1), ...
            tpconinf_sim_series(row,1), sacinf_sim_series(row,1), scolinf_sim_series(row,1));
        fprintf(fid, '%s \r\n', line54);
    end
    fclose(fid);



% SECTION 3.4
% RUN GPS-X SIMULATIONS - Launch GPS-X in batch mode and collect
% data after the simulation finishes. Note that the .xec file (which
% must be in the same folder as the configuration and this script)
% tells GPS-X what to do with the configuration (e.g., run a dynamic
% simulation and then exit the program). The "!" makes this script wait
% for GPS-X to close before it continues, which it needs to do to get
% the data that GPS-X outputs. The "-1" tells GPS-X to open a specific
    !"C:\Program Files (x86)\GPS-X60\bin\gpsx.exe" -1 "C:↙
\Users\jsguest\Dropbox\Active\__Sustainable_Design\Matlab_Code\Trial_27_October_26_2011_Op_Flex\c↙
onfig_2_seasonal.lyt"

% SECTION 3.5
% ACQUIRE DATA GENERATED BY GPS-X - GPS-X will output any data that you
% have told it to "save" using a table or graph in the simulation
% space. The script below first identifies which column each set of
% data is in (e.g., which column of the .out file is effluent ammonium
% in?), then collects that data.


    fid=fopen(outfilename,'r');
```

```
        outfileheader = textscan(fid, '%s %s %s %s %s %s %s %s %s %s %s %s %s %s %s %s %s %s %s %
s %s %s %s %s %s %s %s %s %s %s %s %s %s %s %s %s %s %s %s %s %s %s %s %s %s %s %s %s', 1); % %*s
means skip this value (may be used for the first column in steady state simulations)
    fclose(fid);
    for i=1:48
        columnheader = outfileheader{1,i};
        out_parameter_number = strmatch(columnheader,strvcat
('t','qinf','xrctraeff','qprimover','tnprimover','qprimunder','xlrctrbeff(1)','xlrctrbeff
(2)','xlrctrbeff(3)','solrctrbeff(1)','solrctrbeff(2)','solrctrbeff(3)','snhlrctrbeff
(2)','snhlrctrbeff(3)','snoilrctrbeff(1)','snoilrctrbeff(2)','snoilrctrbeff(3)','snoalrctrbeff
(1)','qairstandlrctrbeff(2)','qairstandlrctrbeff
(3)','qcentinf','xcentinf','qcentcake','xcentcake','xlrctrceff(1)','xlrctrceff(2)','solrctrceff
(1)','solrctrceff(2)','snhlrctrceff(2)','snoilrctrceff(1)','snoilrctrceff(2)','snoalrctrceff
(1)','snoalrctrceff(2)','qairstandlrctrceff
(2)','xsecunder','xisbwas','qsecforward','scodsecforward','tnrctrwas','qfiltereff','stpfiltereff'
,'snhfiltereff','sndfiltereff','snoifiltereff','snoafiltereff', 'snoalrctrbeff(2)', 'snhlrctrceff
(1)', 'qairstandlrctrceff(1)'),'exact');
        if (out_parameter_number <= 1)
            col_time = i;
        elseif (out_parameter_number <= 2)
            col_qinf = i;
        elseif (out_parameter_number <= 3)
            col_xrctraeff = i;
        elseif (out_parameter_number <= 4)
            col_qprimover = i;
        elseif (out_parameter_number <= 5)
            col_tnprimover = i;
        elseif (out_parameter_number <= 6)
            col_qprimunder = i;
        elseif (out_parameter_number <= 7)
            col_xlrctrbeff1 = i;
        elseif (out_parameter_number <= 8)
            col_xlrctrbeff2 = i;
        elseif (out_parameter_number <= 9)
            col_xlrctrbeff3 = i;
        elseif (out_parameter_number <= 10)
            col_solrctrbeff1 = i;
        elseif (out_parameter_number <= 11)
            col_solrctrbeff2 = i;
        elseif (out_parameter_number <= 12)
            col_solrctrbeff3 = i;
        elseif (out_parameter_number <= 13)
            col_snhlrctrbeff2 = i;
        elseif (out_parameter_number <= 14)
            col_snhlrctrbeff3 = i;
        elseif (out_parameter_number <= 15)
            col_snoilrctrbeff1 = i;
        elseif (out_parameter_number <= 16)
            col_snoilrctrbeff2 = i;
        elseif (out_parameter_number <= 17)
            col_snoilrctrbeff3 = i;
        elseif (out_parameter_number <= 18)
            col_snoalrctrbeff1 = i;
        elseif (out_parameter_number <= 19)
            col_qairstandlrctrbeff2 = i;
        elseif (out_parameter_number <= 20)
```

```
        col_qairstandlrctrbeff3 = i;
    elseif (out_parameter_number <= 21)
        col_qcentinf = i;
    elseif (out_parameter_number <= 22)
        col_xcentinf = i;
    elseif (out_parameter_number <= 23)
        col_qcentcake = i;
    elseif (out_parameter_number <= 24)
        col_xcentcake = i;
    elseif (out_parameter_number <= 25)
        col_xlrctrceff1 = i;
    elseif (out_parameter_number <= 26)
        col_xlrctrceff2 = i;
    elseif (out_parameter_number <= 27)
        col_solrctrceff1 = i;
    elseif (out_parameter_number <= 28)
        col_solrctrceff2 = i;
    elseif (out_parameter_number <= 29)
        col_snhlrctrceff2 = i;
    elseif (out_parameter_number <= 30)
        col_snoilrctrceff1 = i;
    elseif (out_parameter_number <= 31)
        col_snoilrctrceff2 = i;
    elseif (out_parameter_number <= 32)
        col_snoalrctrceff1 = i;
    elseif (out_parameter_number <= 33)
        col_snoalrctrceff2 = i;
    elseif (out_parameter_number <= 34)
        col_qairstandlrctrceff2 = i;
    elseif (out_parameter_number <= 35)
        col_xsecunder = i;
    elseif (out_parameter_number <= 36)
        col_xisbwas = i;
    elseif (out_parameter_number <= 37)
        col_qsecforward = i;
    elseif (out_parameter_number <= 38)
        col_scodsecforward = i;
    elseif (out_parameter_number <= 39)
        col_tnrctrwas = i;
    elseif (out_parameter_number <= 40)
        col_qfiltereff = i;
    elseif (out_parameter_number <= 41)
        col_stpfiltereff = i;
    elseif (out_parameter_number <= 42)
        col_snhfiltereff = i;
    elseif (out_parameter_number <= 43)
        col_sndfiltereff = i;
    elseif (out_parameter_number <= 44)
        col_snoifiltereff = i;
    elseif (out_parameter_number <= 45)
        col_snoafiltereff = i;
    elseif (out_parameter_number <= 46)
        col_snoalrctrbeff2 = i;
    elseif (out_parameter_number <= 47)
        col_snhlrctrceff1 = i;
    elseif (out_parameter_number <= 48)
```

```
            col_qairstandlrctrceff1 = i;

        else
            warning('.out file column header not identified');
        end
    end

    dynamic_data = importdata(outfilename, DELIMITER, HEADERLINES);
    data_timepoints = length(dynamic_data.data) - 1; % Note:  The "-1" was added because the time↙
point for day 10 appears twice.  This makes sure that time point is not counted twice.
    data_collection_start = (20*startup_timepoints/24) + 1; % Note:  .DAT files were created with↙
1 hour time steps.  .OUT files are created with 0.05 day time steps.

    time_over_time = dynamic_data.data(data_collection_start:data_timepoints,col_time);
    qinf_over_time = dynamic_data.data(data_collection_start:data_timepoints,col_qinf);
    xrctraeff_over_time = dynamic_data.data(data_collection_start:data_timepoints,col_xrctraeff);
    qprimover_over_time = dynamic_data.data(data_collection_start:data_timepoints,col_qprimover);
    tnprimover_over_time = dynamic_data.data(data_collection_start:data_timepoints,↙
col_tnprimover);
    qprimunder_over_time = dynamic_data.data(data_collection_start:data_timepoints,↙
col_qprimunder);
    xlrctrbeff1_over_time = dynamic_data.data(data_collection_start:data_timepoints,↙
col_xlrctrbeff1);
    xlrctrbeff2_over_time = dynamic_data.data(data_collection_start:data_timepoints,↙
col_xlrctrbeff2);
    xlrctrbeff3_over_time = dynamic_data.data(data_collection_start:data_timepoints,↙
col_xlrctrbeff3);
    solrctrbeff1_over_time = dynamic_data.data(data_collection_start:data_timepoints,↙
col_solrctrbeff1);
    solrctrbeff2_over_time = dynamic_data.data(data_collection_start:data_timepoints,↙
col_solrctrbeff2);
    solrctrbeff3_over_time = dynamic_data.data(data_collection_start:data_timepoints,↙
col_solrctrbeff3);
    snhlrctrbeff2_over_time = dynamic_data.data(data_collection_start:data_timepoints,↙
col_snhlrctrbeff2);
    snhlrctrbeff3_over_time = dynamic_data.data(data_collection_start:data_timepoints,↙
col_snhlrctrbeff3);
    snoilrctrbeff1_over_time = dynamic_data.data(data_collection_start:data_timepoints,↙
col_snoilrctrbeff1);
    snoilrctrbeff2_over_time = dynamic_data.data(data_collection_start:data_timepoints,↙
col_snoilrctrbeff2);
    snoilrctrbeff3_over_time = dynamic_data.data(data_collection_start:data_timepoints,↙
col_snoilrctrbeff3);
    snoalrctrbeff1_over_time = dynamic_data.data(data_collection_start:data_timepoints,↙
col_snoalrctrbeff1);
    qairstandlrctrbeff2_over_time = dynamic_data.data(data_collection_start:data_timepoints,↙
col_qairstandlrctrbeff2);
    qairstandlrctrbeff3_over_time = dynamic_data.data(data_collection_start:data_timepoints,↙
col_qairstandlrctrbeff3);
    qcentinf_over_time = dynamic_data.data(data_collection_start:data_timepoints,col_qcentinf);
    xcentinf_over_time = dynamic_data.data(data_collection_start:data_timepoints,col_xcentinf);
    qcentcake_over_time = dynamic_data.data(data_collection_start:data_timepoints,col_qcentcake);
    xcentcake_over_time = dynamic_data.data(data_collection_start:data_timepoints,col_xcentcake);
    xlrctrceff1_over_time = dynamic_data.data(data_collection_start:data_timepoints,↙
col_xlrctrceff1);
    xlrctrceff2_over_time = dynamic_data.data(data_collection_start:data_timepoints,↙
```

```
col_xlrctrceff2);
    solrctrceff1_over_time = dynamic_data.data(data_collection_start:data_timepoints,↙
col_solrctrceff1);
    solrctrceff2_over_time = dynamic_data.data(data_collection_start:data_timepoints,↙
col_solrctrceff2);
    snhlrctrceff2_over_time = dynamic_data.data(data_collection_start:data_timepoints,↙
col_snhlrctrceff2);
    snoilrctrceff1_over_time = dynamic_data.data(data_collection_start:data_timepoints,↙
col_snoilrctrceff1);
    snoilrctrceff2_over_time = dynamic_data.data(data_collection_start:data_timepoints,↙
col_snoilrctrceff2);
    snoalrctrceff1_over_time = dynamic_data.data(data_collection_start:data_timepoints,↙
col_snoalrctrceff1);
    snoalrctrceff2_over_time = dynamic_data.data(data_collection_start:data_timepoints,↙
col_snoalrctrceff2);
    qairstandlrctrceff2_over_time = dynamic_data.data(data_collection_start:data_timepoints,↙
col_qairstandlrctrceff2);
    xsecunder_over_time = dynamic_data.data(data_collection_start:data_timepoints,col_xsecunder);
    xisbwas_over_time = dynamic_data.data(data_collection_start:data_timepoints,col_xisbwas);
    qsecforward_over_time = dynamic_data.data(data_collection_start:data_timepoints,↙
col_qsecforward);
    scodsecforward_over_time = dynamic_data.data(data_collection_start:data_timepoints,↙
col_scodsecforward);
    tnrctrwas_over_time = dynamic_data.data(data_collection_start:data_timepoints,col_tnrctrwas);
    qfiltereff_over_time = dynamic_data.data(data_collection_start:data_timepoints,↙
col_qfiltereff);
    stpfiltereff_over_time = dynamic_data.data(data_collection_start:data_timepoints,↙
col_stpfiltereff);
    snhfiltereff_over_time = dynamic_data.data(data_collection_start:data_timepoints,↙
col_snhfiltereff);
    sndfiltereff_over_time = dynamic_data.data(data_collection_start:data_timepoints,↙
col_sndfiltereff);
    snoifiltereff_over_time = dynamic_data.data(data_collection_start:data_timepoints,↙
col_snoifiltereff);
    snoafiltereff_over_time = dynamic_data.data(data_collection_start:data_timepoints,↙
col_snoafiltereff);

    snoalrctrbeff2_over_time = dynamic_data.data(data_collection_start:data_timepoints,↙
col_snoalrctrbeff2);
    snhlrctrceff1_over_time = dynamic_data.data(data_collection_start:data_timepoints,↙
col_snhlrctrceff1);
    qairstandlrctrceff1_over_time = dynamic_data.data(data_collection_start:data_timepoints,↙
col_qairstandlrctrceff1);


% SECTION 3.6
% CONVERT DYNAMIC DATA TO RELEVANT VALUES FOR PERFORMANCE, ECONOMIC,
% AND ENVIRONMENTAL ASSESSMENTS - Rather than sending all dynamic data
% from every simulation (which would result in 5,600,000 data points
% for an LHS set with 500 simulations), the data is consolidated as
% much as possible here. First, below is a list of how each parameter's
% dataset is used. Note "FWA" means "flow weighted average".

%     time: used only to convert flows into masses or volumes.
%     qinf: recorded but unused.
%     qprimover: used with tnprimover to calculate N loading to biological
```

```
%       reactor (required if N2O is calucated via emissions factors).
%     tnprimover: used with qprimover to calculate N loading to biological
%       reactor (required if N2O is calucated via emissions factors).
%     qprimunder: used for primary clarifier sludge pumping electricity
%       use (average value).
%     xrctraeff: used for SRT calculations (average value), for
%       construction cost equations and for mixing energy
%       equations in ANA/ANX zones (averaged value).
%     xlrctrbeff1: same as explanation for xrctraeff.
%     xlrctrbeff2: same as explanation for xrctraeff.
%     xlrctrbeff3: same as explanation for xrctraeff.
%   xlrctrbeff4
%     xlrctrceff1: same as explanation for xrctraeff.
%     xlrctrceff2: same as explanation for xrctraeff.
%     solrctrbeff1: used for N2O emissions calculations using Chandran
%       Regression Model. Dynamic values used for N2O emissions
%       predictions.
%     solrctrbeff2: same as explanation for solrctrbeff1.
%     solrctrbeff3: same as explanation for solrctrbeff1.
%   solrctrbeff4
%     solrctrceff1: same as explanation for solrctrbeff1.
%     solrctrceff2: same as explanation for solrctrbeff1.
%     snhlrctrbeff2: same as explanation for solrctrbeff1.
%     snhlrctrbeff3: same as explanation for solrctrbeff1.
%   snhlrctrbeff4
%   snhlrctrceff1
%     snhlrctrceff2: same as explanation for solrctrbeff1. May also be used
%       to correct for excessive NH4+ release in denitrification filters.
%     snoilrctrbeff1: same as explanation for solrctrbeff1.
%     snoilrctrbeff2: same as explanation for solrctrbeff1.
%     snoilrctrbeff3: same as explanation for solrctrbeff1.
%   snoilrctrbeff4
%     snoilrctrceff1: same as explanation for solrctrbeff1.
%     snoilrctrceff2: same as explanation for solrctrbeff1.
%     snoalrctrbeff1: same as explanation for solrctrbeff1.
%   snoalrctrbeff2
%     snoalrctrceff1: same as explanation for solrctrbeff1.
%     snoalrctrceff2: coupled with qsecforward, used for calculations
%       related to denitrification filter design (max values) and operation
%       costs and environmental impacts (FWA).
%     qairstandlrctrbeff2: used for blower sizing (max value) and blower
%       energy consumption and maintenance (average value).
%     qairstandlrctrbeff3: used for blower sizing (max value) and blower
%       energy consumption and maintenance (average value).
%   qairstandlrctrbeff4
%   qairstandlrctrceff1
%     qairstandlrctrceff2: same as explanation for qairstandlrctrbeff2.
%     qcentinf: used for costing and energy equations associated with
%       solids dewatering (average value).
%     xcentinf: used for polymer cost and use equations (FWA value).
%     qcentcake: used for incinerator energy consumption and ash production
%       (average value).
%     xcentcake: same as explanation for qcentcake (FWA value).
%     xsecunder: used with qconrctrwas for SRT calculation (average value
%       because flow rate does not change).
%     xisbwas: used for polymer consumption estimates (average value
```

```
%       because flow rate does not change).
%     qsecforward: coupled with snoalrctrceff2, used for calculations
%       related to denitrification filter design (max values) and operation
%       costs and environmental impacts (FWA).
%     scodsecforward: assumed to represent effluent sCOD. Converted to
%       units of mass per year with qfiltereff.
%     tnrctrwas: used with qconrctrwas to calculate N loss as biomass from
%       reactor (required if N2O is calucated via emissions factors).
%     qfiltereff: used for chlorine and aquatic emissions (average value).
%     stpfiltereff: used for effluent TP quantification (FWA value).
%     snhfiltereff: used for effluent NH4+ quantification (FWA value).
%     sndfiltereff: used for effluent SND quantification (FWA value).
%     snoifiltereff: used for effluent NO2- quantification (FWA value).
%     snoafiltereff: used for effluent NO3- quantification (FWA value)
%       and for methanol calculations (FWA value).

%   SECTION 3.6.1
%   DATA CONSOLIDATION - Calculate maximum values, mass flows, and flow
%   weighted average concentrations as needed.
    qinf_avg = sum(qinf_over_time)/length(qinf_over_time); % [m3/d]
    qprimover_avg = sum(qprimover_over_time)/length(qprimover_over_time); % [m3/d]
    tn_rctr_loading_over_time = qprimover_over_time.*tnprimover_over_time; % [gN/d]
    tn_rctr_loading_avg = sum(tn_rctr_loading_over_time)/length(tn_rctr_loading_over_time); %↙
[gN/d]
    qprimunder_avg = sum(qprimunder_over_time)/length(qprimunder_over_time); % [m3/d]
    xrctraeff_max = max(xrctraeff_over_time); % [g/m3]
    xrctraeff_avg = sum(xrctraeff_over_time)/length(xrctraeff_over_time); % [g/m3]
    xlrctrbeff1_max = max(xlrctrbeff1_over_time); % [g/m3]
    xlrctrbeff1_avg = sum(xlrctrbeff1_over_time)/length(xlrctrbeff1_over_time); % [g/m3]
    xlrctrbeff2_max = max(xlrctrbeff2_over_time); % [g/m3]
    xlrctrbeff2_avg = sum(xlrctrbeff2_over_time)/length(xlrctrbeff2_over_time); % [g/m3]
    xlrctrbeff3_max = max(xlrctrbeff3_over_time); % [g/m3]
    xlrctrbeff3_avg = sum(xlrctrbeff3_over_time)/length(xlrctrbeff3_over_time); % [g/m3]
    xlrctrceff1_max = max(xlrctrceff1_over_time); % [g/m3]
    xlrctrceff1_avg = sum(xlrctrceff1_over_time)/length(xlrctrceff1_over_time); % [g/m3]
    xlrctrceff2_max = max(xlrctrceff2_over_time); % [g/m3]
    xlrctrceff2_avg = sum(xlrctrceff2_over_time)/length(xlrctrceff2_over_time); % [g/m3]
    snhlrctrceff2_mass_avg = sum(snhlrctrceff2_over_time.*qinf_over_time) ...
        ./length(snhlrctrceff2_over_time); % [g/d]
    snhlrctrceff2_conc_avg = snhlrctrceff2_mass_avg/qinf_avg; % [g/m3]
    qsecforward_max = max(qsecforward_over_time); % [m3/d]
    qsecforward_avg = sum(qsecforward_over_time) ...
        /length(qsecforward_over_time); % [m3/d]
    snoalrctrceff2_max = max(snoalrctrceff2_over_time); % [g/m3]
    snoalrctrceff2_mass_avg = sum(snoalrctrceff2_over_time ...
        .*qsecforward_over_time)./length(snoalrctrceff2_over_time); % [g/d]
    snoalrctrceff2_conc_avg = snoalrctrceff2_mass_avg/qsecforward_avg; % [g/m3]
    qairstandlrctreff_over_time = qairstandlrctrbeff2_over_time +↙
qairstandlrctrbeff3_over_time...
        + qairstandlrctrceff1_over_time + qairstandlrctrceff2_over_time; % [m3/d]
    qairstandlrctreff_max = max(qairstandlrctreff_over_time); % [m3/d]
    qairstandlrctreff_avg = sum(qairstandlrctreff_over_time) ...
        /length(qairstandlrctreff_over_time); % [m3/d]
    qcentinf_avg = sum(qcentinf_over_time)/length(qcentinf_over_time); % [m3/d]
    xcentinf_mass_avg = sum(xcentinf_over_time.*qcentinf_over_time) ...
        ./length(xcentinf_over_time); % [g/d]
```

```
    xcentinf_conc_avg = xcentinf_mass_avg/qcentinf_avg; % [g/m3]
    qcentcake_avg = sum(qcentcake_over_time)/length(qcentcake_over_time); % [m3/d]
    xcentcake_mass_avg = sum(xcentcake_over_time.*qcentcake_over_time) ...
        ./length(xcentcake_over_time); % [g/d]
    xcentcake_conc_avg = xcentcake_mass_avg/qcentcake_avg; % [g/m3]
    xsecunder_avg = sum(xsecunder_over_time)/length(xsecunder_over_time); % [g/m3]
    xisbwas_avg = sum(xisbwas_over_time)/length(xisbwas_over_time); % [g/m3]
    qfiltereff_avg = sum(qfiltereff_over_time)/length(qfiltereff_over_time); % [m3/d]
    scodsecforward_max = max(scodsecforward_over_time); % [g/m3]
    scodsecforward_mass_avg = sum(scodsecforward_over_time ...
        .*qfiltereff_over_time)/length(scodsecforward_over_time); % [g/d]
    scodsecforward_conc_avg = scodsecforward_mass_avg/qfiltereff_avg; % [g/m3]
    tnrctrwas_mass_removal_over_time = qconrctrwas_operation*tnrctrwas_over_time; % [gN/d]
    tnrctrwas_mass_removal_avg = sum(tnrctrwas_mass_removal_over_time) ...
        /length(tnrctrwas_mass_removal_over_time); % [gN/d]
    stpfiltereff_max = max(stpfiltereff_over_time); % [gP/m3]
    stpfiltereff_mass_avg = sum(stpfiltereff_over_time ...
        .*qfiltereff_over_time)/length(stpfiltereff_over_time); % [gP/d]
    stpfiltereff_conc_avg = stpfiltereff_mass_avg/qfiltereff_avg; % [gP/m3]
    snhfiltereff_max = max(snhfiltereff_over_time); % [gN/m3]
    snhfiltereff_mass_avg = sum(snhfiltereff_over_time ...
        .*qfiltereff_over_time)/length(snhfiltereff_over_time); % [gN/d]
    sndfiltereff_max = max(sndfiltereff_over_time); % [gN/m3]
    sndfiltereff_mass_avg = sum(sndfiltereff_over_time ...
        .*qfiltereff_over_time)/length(sndfiltereff_over_time); % [gN/d]
    sndfiltereff_conc_avg = sndfiltereff_mass_avg/qfiltereff_avg; % [gN/m3]
    snoifiltereff_max = max(snoifiltereff_over_time); % [gN/m3]
    snoifiltereff_mass_avg = sum(snoifiltereff_over_time ...
        .*qfiltereff_over_time)/length(snoifiltereff_over_time); % [gN/d]
    snoafiltereff_max = max(snoafiltereff_over_time); % [gN/m3]
    snoafiltereff_mass_avg = sum(snoafiltereff_over_time ...
        .*qfiltereff_over_time)/length(snoafiltereff_over_time); % [gN/d]
    snoafiltereff_conc_avg = snoafiltereff_mass_avg/qfiltereff_avg; % [gN/m3]
    tnfiltereff_max = max(snhfiltereff_over_time + sndfiltereff_over_time ...
        + snoifiltereff_over_time + snoafiltereff_over_time); % [gN/m3]
    tnfiltereff_mass_avg = snhfiltereff_mass_avg + sndfiltereff_mass_avg ...
        + snoifiltereff_mass_avg + snoafiltereff_mass_avg; % [gN/d]
    tnfiltereff_conc_avg = tnfiltereff_mass_avg/qfiltereff_avg; % [gN/m3]
    % Just in case GPS-X is overpredicting how much ammonia is released in
    % the denit filters, also calculate effluent TN in this way:
    tneff_max = tnfiltereff_max;    %     tneff_max = max(snhlrctrceff2_over_time +↙
sndfiltereff_over_time ...
        %         + snoifiltereff_over_time + snoafiltereff_over_time); % [gN/m3]
    tneff_mass_avg = tnfiltereff_mass_avg;    %     tneff_mass_avg = snhlrctrceff2_mass_avg +↙
sndfiltereff_mass_avg ...
        %         + snoifiltereff_mass_avg + snoafiltereff_mass_avg; % [gN/d]
    tneff_conc_avg =  tnfiltereff_conc_avg;   %     tneff_conc_avg =↙
tneff_mass_avg/qfiltereff_avg; % [gN/m3]

    if (config==1);
        biomass_in_system_g = (xrctraeff_avg*volume_ana_standard) ...
            + (xlrctrbeff1_avg*volume_anx1_standard) + (xlrctrbeff2_avg*volume_aer1a_standard)↙
...
            + (xlrctrbeff3_avg*volume_aer1b_standard) + (xlrctrceff1_avg*volume_anx2_standard) +↙
(xlrctrceff2_avg*volume_aer2_standard);
        average_mlss = biomass_in_system_g/(volumetotal_standard); % [g/m3]
```

```
    elseif (config==2);
        biomass_in_system_g = (xrctraeff_avg*volume_ana_seasonal) ...
            + (xlrctrbeff1_avg*volume_anx1_seasonal) + (xlrctrbeff2_avg*volume_aer1a_seasonal)...
            + (xlrctrbeff3_avg*volume_aer1b_seasonal) + (xlrctrceff1_avg*volume_anx2_seasonal) +...
(xlrctrceff2_avg*volume_aer2_seasonal);
        average_mlss = biomass_in_system_g/(volumetotal_seasonal); % [g/m3]
    else
            warning('Configuration type not identified - Standard vs. Seasonal. Unknown which...
volumes to use in SRT calculation.');
    end

    % Calculate SRT
    biomass_wastage_g_per_d = (xsecunder_avg*qconrctrwas_operation);
    actual_srt_d = biomass_in_system_g/biomass_wastage_g_per_d;









    % AERATION BY CONFIGURATION - Note that aeration energy is linear with
    % delivered airflow.  Therefore, only the average airflow is needed.
    % qairstandlrctreff_over_time changed for Standard design blowers;


aeration_capacity_standard = 807500*1.5; % [m3/d] based on steady state simulations of Standard...
design under summer (28C) and winter (17.9C) conditions - max aeration demand was 807,500 m3/d in...
summer.
aeration_capacity_seasonal = 764500*1.5; % [m3/d] based on steady state simulations of Seasonal...
design under summer (28C) and winter (17.9C) conditions - max aeration demand was 764,500 m3/d in...
winter.

% Blower capacity check

blower_capacity_check = zeros(length(qairstandlrctreff_over_time),1);

for check_hour = 1:length(qairstandlrctreff_over_time);
    if (config==1)
        if (qairstandlrctreff_over_time(check_hour,1) <= aeration_capacity_standard)
            blower_capacity_check(check_hour,1) = 0;
        else
            blower_capacity_check(check_hour,1) = 1;
        end
    else
        if (qairstandlrctreff_over_time(check_hour,1) <= aeration_capacity_seasonal)
            blower_capacity_check(check_hour,1) = 0;
        else
            blower_capacity_check(check_hour,1) = 1;
        end
    end
end
```

```
blower_exceeded_time_fraction = sum(blower_capacity_check)/length(blower_capacity_check);

% We will calculate the impact of fully tunable vs. constant speed blowers
% for both designs just so we have the data.

    % Fully tunable blowers
    qair_tunableblowers_delivered = qairstandlrctreff_avg;

    % Fixed blowers - 3 equally-sized constant speed blowers, easily turned on/off.
    qair_3fixedblowers_over_time = zeros(length(qairstandlrctreff_over_time),1);
    for air_time_3blower = 1:length(qairstandlrctreff_over_time);
        if (config==1)
                if (qairstandlrctreff_over_time(air_time_3blower,1) <=↙
1*aeration_capacity_standard/3);
                qair_3fixedblowers_over_time(air_time_3blower,1) =↙
1*aeration_capacity_standard/3;
            elseif (qairstandlrctreff_over_time(air_time_3blower,1) <=↙
2*aeration_capacity_standard/3);
                qair_3fixedblowers_over_time(air_time_3blower,1) =↙
2*aeration_capacity_standard/3;
            else
                qair_3fixedblowers_over_time(air_time_3blower,1) =↙
3*aeration_capacity_standard/3;
            end
        else
            if (qairstandlrctreff_over_time(air_time_3blower,1) <=↙
1*aeration_capacity_seasonal/3);
                qair_3fixedblowers_over_time(air_time_3blower,1) =↙
1*aeration_capacity_seasonal/3;
            elseif (qairstandlrctreff_over_time(air_time_3blower,1) <=↙
2*aeration_capacity_seasonal/3);
                qair_3fixedblowers_over_time(air_time_3blower,1) =↙
2*aeration_capacity_seasonal/3;
            else
                qair_3fixedblowers_over_time(air_time_3blower,1) =↙
3*aeration_capacity_seasonal/3;
            end
        end
    end
    qair_3fixedblowers_delivered = sum(qair_3fixedblowers_over_time)/length↙
(qair_3fixedblowers_over_time);

    % Fixed blowers - 4 equally-sized constant speed blowers, easily turned on/off.
    qair_4fixedblowers_over_time = zeros(length(qairstandlrctreff_over_time),1);
    for air_time_4blower = 1:length(qairstandlrctreff_over_time);
        if (config==1)
            if (qairstandlrctreff_over_time(air_time_4blower,1) <=↙
1*aeration_capacity_standard/4);
                qair_4fixedblowers_over_time(air_time_4blower,1) =↙
1*aeration_capacity_standard/4;
            elseif (qairstandlrctreff_over_time(air_time_4blower,1) <=↙
2*aeration_capacity_standard/4);
                qair_4fixedblowers_over_time(air_time_4blower,1) =↙
2*aeration_capacity_standard/4;
            elseif (qairstandlrctreff_over_time(air_time_4blower,1) <=↙
```

```
3*aeration_capacity_standard/4);
                qair_4fixedblowers_over_time(air_time_4blower,1) =↙
3*aeration_capacity_standard/4;
            else
                qair_4fixedblowers_over_time(air_time_4blower,1) =↙
4*aeration_capacity_standard/4;
            end
        else
            if (qairstandlrctreff_over_time(air_time_4blower,1) <=↙
1*aeration_capacity_seasonal/4);
                qair_4fixedblowers_over_time(air_time_4blower,1) =↙
1*aeration_capacity_seasonal/4;
            elseif (qairstandlrctreff_over_time(air_time_4blower,1) <=↙
2*aeration_capacity_seasonal/4);
                qair_4fixedblowers_over_time(air_time_4blower,1) =↙
2*aeration_capacity_seasonal/4;
            elseif (qairstandlrctreff_over_time(air_time_4blower,1) <=↙
3*aeration_capacity_seasonal/4);
                qair_4fixedblowers_over_time(air_time_4blower,1) =↙
3*aeration_capacity_seasonal/4;
            else
                qair_4fixedblowers_over_time(air_time_4blower,1) =↙
4*aeration_capacity_seasonal/4;
            end
        end
    end
    qair_4fixedblowers_delivered = sum(qair_4fixedblowers_over_time)/length↙
(qair_4fixedblowers_over_time);

    % Fixed blowers - 3 equally-sized, 1 small constant speed blowers,
    % easily turned on/off.  The small blower is 1/2 the size of the large
    % blowers.  Therefore, each of the three large blowers can handle
    % 28.57 percent of the airflow capacity, while the small blower can
    % handle 14.29 percent of the airflow capacity.
    qair_3_1_fixedblowers_over_time = zeros(length(qairstandlrctreff_over_time),1);
    small_blower_fraction = 0.1429;
    large_blower_fraction = 0.2857;
    blower_combo_1 = small_blower_fraction;
    blower_combo_2 = large_blower_fraction;
    blower_combo_3 = small_blower_fraction + large_blower_fraction;
    blower_combo_4 = 2*large_blower_fraction;
    blower_combo_5 = (2*large_blower_fraction) + small_blower_fraction;
    blower_combo_6 = 3*large_blower_fraction;
    blower_combo_7 = (3*large_blower_fraction) + small_blower_fraction;

    for air_time_3_1_blower = 1:length(qairstandlrctreff_over_time);
        if (config==1)
            if (qairstandlrctreff_over_time(air_time_3_1_blower,1) <=↙
blower_combo_1*aeration_capacity_standard);
                qair_3_1_fixedblowers_over_time(air_time_3_1_blower,1) =↙
blower_combo_1*aeration_capacity_standard;
            elseif (qairstandlrctreff_over_time(air_time_3_1_blower,1) <=↙
blower_combo_2*aeration_capacity_standard);
                qair_3_1_fixedblowers_over_time(air_time_3_1_blower,1) =↙
blower_combo_2*aeration_capacity_standard;
            elseif (qairstandlrctreff_over_time(air_time_3_1_blower,1) <=↙
```

```
blower_combo_3*aeration_capacity_standard);
                qair_3_1_fixedblowers_over_time(air_time_3_1_blower,1) =↙
blower_combo_3*aeration_capacity_standard;
            elseif (qairstandlrctreff_over_time(air_time_3_1_blower,1) <=↙
blower_combo_4*aeration_capacity_standard);
                qair_3_1_fixedblowers_over_time(air_time_3_1_blower,1) =↙
blower_combo_4*aeration_capacity_standard;
            elseif (qairstandlrctreff_over_time(air_time_3_1_blower,1) <=↙
blower_combo_5*aeration_capacity_standard);
                qair_3_1_fixedblowers_over_time(air_time_3_1_blower,1) =↙
blower_combo_5*aeration_capacity_standard;
            elseif (qairstandlrctreff_over_time(air_time_3_1_blower,1) <=↙
blower_combo_6*aeration_capacity_standard);
                qair_3_1_fixedblowers_over_time(air_time_3_1_blower,1) =↙
blower_combo_6*aeration_capacity_standard;
            else (qairstandlrctreff_over_time(air_time_3_1_blower,1) <=↙
blower_combo_7*aeration_capacity_standard);
                qair_3_1_fixedblowers_over_time(air_time_3_1_blower,1) =↙
blower_combo_7*aeration_capacity_standard;
            end
        else
            if (qairstandlrctreff_over_time(air_time_3_1_blower,1) <=↙
blower_combo_1*aeration_capacity_seasonal);
                qair_3_1_fixedblowers_over_time(air_time_3_1_blower,1) =↙
blower_combo_1*aeration_capacity_seasonal;
            elseif (qairstandlrctreff_over_time(air_time_3_1_blower,1) <=↙
blower_combo_2*aeration_capacity_seasonal);
                qair_3_1_fixedblowers_over_time(air_time_3_1_blower,1) =↙
blower_combo_2*aeration_capacity_seasonal;
            elseif (qairstandlrctreff_over_time(air_time_3_1_blower,1) <=↙
blower_combo_3*aeration_capacity_seasonal);
                qair_3_1_fixedblowers_over_time(air_time_3_1_blower,1) =↙
blower_combo_3*aeration_capacity_seasonal;
            elseif (qairstandlrctreff_over_time(air_time_3_1_blower,1) <=↙
blower_combo_4*aeration_capacity_seasonal);
                qair_3_1_fixedblowers_over_time(air_time_3_1_blower,1) =↙
blower_combo_4*aeration_capacity_seasonal;
            elseif (qairstandlrctreff_over_time(air_time_3_1_blower,1) <=↙
blower_combo_5*aeration_capacity_seasonal);
                qair_3_1_fixedblowers_over_time(air_time_3_1_blower,1) =↙
blower_combo_5*aeration_capacity_seasonal;
            elseif (qairstandlrctreff_over_time(air_time_3_1_blower,1) <=↙
blower_combo_6*aeration_capacity_seasonal);
                qair_3_1_fixedblowers_over_time(air_time_3_1_blower,1) =↙
blower_combo_6*aeration_capacity_seasonal;
            else (qairstandlrctreff_over_time(air_time_3_1_blower,1) <=↙
blower_combo_7*aeration_capacity_seasonal);
                qair_3_1_fixedblowers_over_time(air_time_3_1_blower,1) =↙
blower_combo_7*aeration_capacity_seasonal;
            end
        end
    end
    qair_3_1_fixedblowers_delivered = sum(qair_3_1_fixedblowers_over_time)/length↙
(qair_3_1_fixedblowers_over_time);

% CALCULATE PUMPING AVERAGES
```

```
denit_backwash_flow_avg = denit_backwash_flow*0.25/24; % [m3/d]
internal_rec_operation_avg = sum(internal_rec_operation)/length(internal_rec_operation); % [m3/d]

% CALCULATE MeOH AVERAGES
qconmeohrctrc_avg = sum(qconmeohrctrc)/length(qconmeohrctrc); % [m3/d]
qconmeohdf_avg = sum(qconmeohdf)/length(qconmeohdf); % [m3/d]


%   SECTION 3.6.2
%   CALCULATION OF N2O EMISSIONS USING THE CHANDRAN REGRESSION MODEL -
%   Nitrous oxide emissions are estimated in one of two ways. Either based
%   on a fixed emissions factor (e.g., 0.005 kgN2O-N released per kg-N
%   removed via denitrification), or with an equation derived out of
%   correlations in data from several full-scale WWTPs. The latter approach
%   is implemented here, while the former approach (emissions factors) may
%   be implemented in the LCA-COST m-file as only average N removals are
%   required for that approach.
%   Source: Ahn JH, Kim S, Park H, Rahm B, Pagilla K, Chandran K. 2010. N2O
%       emissions from activated sludge processes, 2008-2009: results of a
%       national monitoring survey in the United States. Environ. Sci.
%       Technol. 44(12):4505-4511.

%   NOTE: The equations presented here are not the same as in Ahn et al.
%   2010. Through personal communications with the corresponding and first
%   authors, it came to my (JSG) attention that the equations presented in
%   the manuscript were incorrect. The following equations are correct:
%   AEROBIC ZONE N2O EMISSIONS:
%   ln(N2O emissions) = 6.1 + 1.0*ln(ammonium) + 0.60*ln(nitrite) ...
%       + 0.59*ln(DO) + 0.18*ln(ammonium)*ln(nitrite)
%   ANOXIC ZONE N2O EMISSIONS:
%   ln(N2O emissions) = -1.2 + 0.67*ln(DO)*ln(nitrite)
%   UNITS:
%       N2O emissions = [gN2O-N/day per 0.13 m2 of reactor surface area]
%                       (0.13 m2 is the area of the SEIFC sampler)
%       ammonium = [gN/m3]
%       nitrite = [gN/m3]
%       DO = [gO2/m3]

%   ADDITIONAL NOTE: When performing the multivariate linear regression,
%   the authors also performed a listwise deletion for any data point that
%   had a value of "zero" for any of the values (ammonium, nitrite, or DO).
%   This was anticipated since an "ln(0)" is undefined. However, it means
%   that the model (as it exists) cannot be used in this methodology
%   because very low values of any of the parameters (ammonium, nitrite, or
%   DO) will significantly skew the results. In order to make it work, the
%   data from Ahn et al. 2010 was re-analyzed by adding a term within
%   the ln() to enable the equation to function if ammonium, nitrite, or DO
%   measurements were zero (or very low). The new coefficients were solved
%   for by minimizing the sum of squares. Original R2 values were 0.576 for
%   aerobic predictions and 0.292 for anoxic predictions. R2 values for
%   modified equations (which now include all data) were 0.530 for aerobic
%   zones, and the minimization of the sum of squares resulted in a
%   recommended fixed emission. For the time being, an emission factor will
%   be used instead.
%   AEROBIC ZONE N2O EMISSIONS (MODIFIED):
%   ln(N2O emissions) = 5.82 + 1.03*ln(ammonium + 0.17) ...
```

```
%       + 1.12*ln(nitrite + 0.17) + 0.82*ln(DO + 0.17) ...
%       + 0.23*ln(ammonium + 0.17)*ln(nitrite + 0.17)
%   ANOXIC ZONE N2O EMISSIONS (MODIFIED):
%   total N2O emissions [gN2O-N] = 0.005*(total N denitrified)
%   NOTE:  In MATLAB, "log()" calculates the "natural log".
%   For final implementation, I've switched back to the Chandran model
%   directly, since we switched to the Mantis2 biological model in GPS-X to
%   allow for nitrite modeling.

%   Aerobic Zones (not all aerobic all year)
    ln_aer1a_n2o_over_time = 6.1 + 1.0*log(snhlrctrbeff2_over_time) ...
        + 0.60*log(snoilrctrbeff2_over_time) ...
        + 0.59*log(solrctrbeff2_over_time) ...
        + 0.18*(log(snhlrctrbeff2_over_time) ...
        .*log(snoilrctrbeff2_over_time)); % [gN2O-N/((0.13 m2)(day))]
    ln_aer1b_n2o_over_time = 6.1 + 1.0*log(snhlrctrbeff3_over_time) ...
        + 0.60*log(snoilrctrbeff3_over_time) ...
        + 0.59*log(solrctrbeff3_over_time) ...
        + 0.18*(log(snhlrctrbeff3_over_time) ...
        .*log(snoilrctrbeff3_over_time)); % [gN2O-N/((0.13 m2)(day))]
    ln_swing_n2o_over_time = 6.1 + 1.0*log(snhlrctrceff1_over_time) ...
        + 0.60*log(snoilrctrceff1_over_time) ...
        + 0.59*log(solrctrceff1_over_time) ...
        + 0.18*(log(snhlrctrceff1_over_time) ...
        .*log(snoilrctrceff1_over_time)); % [gN2O-N/((0.13 m2)(day))]
    ln_aer2_n2o_over_time = 6.1 + 1.0*log(snhlrctrceff2_over_time) ...
        + 0.60*log(snoilrctrceff2_over_time) ...
        + 0.59*log(solrctrceff2_over_time) ...
        + 0.18*(log(snhlrctrceff2_over_time) ...
        .*log(snoilrctrceff2_over_time)); % [gN2O-N/((0.13 m2)(day))]
%   Total N2O Emissions from Aerobic Zones
    n2o_emissions_aer1a_over_time = exp(ln_aer1a_n2o_over_time); % [gN2O-N/((0.13 m2)(day))]
    n2o_emissions_aer1b_over_time = exp(ln_aer1b_n2o_over_time); % [gN2O-N/((0.13 m2)(day))]
    n2o_emissions_aer2_over_time = exp(ln_aer2_n2o_over_time); % [gN2O-N/((0.13 m2)(day))]

    if (setpsolrctrceff1==0)
        n2o_emissions_swing_over_time = 0; % AEROBIC EMISSIONS [gN2O-N/((0.13 m2)(day))]
    else
        n2o_emissions_swing_over_time = exp(ln_swing_n2o_over_time); % AEROBIC EMISSIONS [gN2O-N/↙
((0.13 m2)(day))]
    end

%   Anoxic Zones (not all anoxic all year)
    ln_anx1_n2o_over_time = -1.2 + 0.67*(log(solrctrbeff1_over_time) ...
        .*log(snoilrctrbeff1_over_time)); % [gN2O-N/((0.13 m2)(day))]
    ln_anx2_n2o_over_time = -1.2 + 0.67*(log(solrctrceff1_over_time) ...
        .*log(snoilrctrceff1_over_time)); % [gN2O-N/((0.13 m2)(day))]

    %   Total N2O Emissions from Anoxic Zones
    n2o_emissions_anx1_over_time = exp(ln_anx1_n2o_over_time); % [gN2O-N/((0.13 m2)(day))]

    if (setpsolrctrceff1==0)
        n2o_emissions_anx2_over_time = exp(ln_anx2_n2o_over_time); % ANOXIC EMISSIONS [gN2O-N/↙
((0.13 m2)(day))]
    else
        n2o_emissions_anx2_over_time = 0; % ANOXIC EMISSIONS [gN2O-N/((0.13 m2)(day))]
```

```
    end

    if (config==1);
        sa_anx1_m2 = (l_anx1_ft_standard/ft_per_meter)*new_reactor_width_meters; % [m2]
        sa_aer1a_m2 = (l_aer1a_ft_standard/ft_per_meter)*new_reactor_width_meters; % [m2]
        sa_aer1b_m2 = (l_aer1b_ft_standard/ft_per_meter)*old_reactor_width_meters; % [m2]
        sa_anx2_m2 = (l_anx2_ft_standard/ft_per_meter)*old_reactor_width_meters; % [m2]
        sa_aer2_m2 = (l_aer2_ft_standard/ft_per_meter)*old_reactor_width_meters; % [m2]
    elseif (config==2);
        sa_anx1_m2 = (l_anx1_ft_seasonal/ft_per_meter)*new_reactor_width_meters; % [m2]
        sa_aer1a_m2 = (l_aer1a_ft_seasonal/ft_per_meter)*new_reactor_width_meters; % [m2]
        sa_aer1b_m2 = (l_aer1b_ft_seasonal/ft_per_meter)*old_reactor_width_meters; % [m2]
        sa_anx2_m2 = (l_anx2_ft_seasonal/ft_per_meter)*old_reactor_width_meters; % [m2]
        sa_aer2_m2 = (l_aer2_ft_seasonal/ft_per_meter)*old_reactor_width_meters; % [m2]
    else
            warning('Configuration type not identified - Standard vs. Seasonal. Unknown which
surface areas to use for N2O calculations.');
    end

    n2o_emissions_aer_over_time = (n2o_emissions_swing_over_time/0.13) ...
        *sa_anx2_m2 + (n2o_emissions_aer1a_over_time/0.13) ...
        *sa_aer1a_m2 + (n2o_emissions_aer1b_over_time/0.13)*sa_aer1b_m2 ...
        + (n2o_emissions_aer2_over_time/0.13)*sa_aer2_m2; % [gN2O-N/d]
    n2o_emissions_anx_over_time = (n2o_emissions_anx1_over_time/0.13) ...
        *sa_anx1_m2 + (n2o_emissions_anx2_over_time/0.13)*sa_anx2_m2; % [gN2O-N/d]

    n2o_emissions_aer_avg_chandran = sum(n2o_emissions_aer_over_time) ...
        /length(n2o_emissions_aer_over_time); % [gN2O-N/d]
    n2o_emissions_anx_avg_chandran = sum(n2o_emissions_anx_over_time) ...
        /length(n2o_emissions_anx_over_time); % [gN2O-N/d]

%   Calculation of N2O emissions from ANX zones will be done in LCA-cost
%   m-file using emissions factors and calculations of TN removed via
%   denitrification.


% SECTION 3.7
% APPEND SIMULATION SUMMARY DATA TO FILE FOR LATER USE - Data will be
% output to a .dat file to be later imported and used by a separate
% m-file to run cost analyses, LCA, and summarize the performance
% results.

    if (config==1);
        volume_ana = volume_ana_standard;
        volume_anx1 = volume_anx1_standard;
        volume_aer1 = volume_aer1_standard;
        volume_anx2 = volume_anx2_standard;
        volume_aer2 = volume_aer2_standard;
        qconisbwas_capacity = qconisbwas_capacity_standard;
        qconras_capacity = qconras_capacity_standard;
        qconrctrwas_capacity = qconrctrwas_capacity_standard;
        qconisbras_capacity = qconisbras_capacity_standard;
    elseif (config==2);
        volume_ana = volume_ana_seasonal;
        volume_anx1 = volume_anx1_seasonal;
        volume_aer1 = volume_aer1_seasonal;
```

```
        volume_anx2 = volume_anx2_seasonal;
        volume_aer2 = volume_aer2_seasonal;
        qconisbwas_capacity = qconisbwas_capacity_seasonal;
        qconras_capacity = qconras_capacity_seasonal;
        qconrctrwas_capacity = qconrctrwas_capacity_seasonal;
        qconisbras_capacity = qconisbras_capacity_seasonal;
    else
            warning('Configuration type not identified - Standard vs. Seasonal. Unknown↙
configuration - do not know which data to output.');
    end

%   Data that needs to be output:
    output0001 = lhs_sim_value;
    output0002 = config;
    if (temp_sim_value <= 18)
        output0003 = 'Winter';
    else
        output0003 = 'Summer';
    end

    output01 = actual_srt_d; % [d]
    output02 = rec_capacity; % [m3/d]  Note: This represents either internal recycle, since one↙
is on at a time.
    output03 = volume_ana; % [m3]
    output04 = volume_anx1; % [m3]
    output05 = volume_aer1; % [m3]
    output06 = volume_anx2; % [m3]
    output07 = volume_aer2; % [m3]
    output08 = qconisbwas_capacity; % [m3/d]
    output09 = qconisbwas_operation; % [m3/d]
    output10 = qprimover_avg; % [m3/d]
    output11 = qconras_operation; % [m3/d]
    output12 = qconras_capacity; % [m3/d]
    output13 = qconrctrwas_capacity; % [m3/d]
    output14 = qconrctrwas_operation; % [m3/d]
    output15 = average_mlss; % [g/m3]
    output16 = tn_rctr_loading_avg; % [gN/d]
    output17 = qprimunder_avg; % [m3/d]
    output18 = xrctraeff_avg; % [g/m3]
    output19 = xlrctrbeff1_avg; % [g/m3]
    output20 = xlrctrceff1_avg; % [g/m3]
    output21 = snhlrctrceff2_conc_avg; % [g/m3]
    output22 = qsecforward_max; % [m3/d]
    output23 = qsecforward_avg; % [m3/d]
    output24 = snoalrctrceff2_conc_avg; % [g/m3]
    output25 = qairstandlrctreff_max; % [m3/d]
    output26 = qairstandlrctreff_avg; % [m3/d]
    output27 = qcentinf_avg; % [m3/d]
    output28 = xcentinf_conc_avg; % [g/m3]
    output29 = qcentcake_avg; % [m3/d]
    output30 = xcentcake_conc_avg; % [g/m3]
    output31 = xisbwas_avg; % [g/m3]
    output32 = qfiltereff_avg; % [m3/d]
    output33 = scodsecforward_conc_avg; % [g/m3]
    output34 = tnrctrwas_mass_removal_avg; % [gN/d]
    output35 = stpfiltereff_conc_avg; % [gP/m3]
```

```
    output36 = sndfiltereff_conc_avg; % [gN/m3]
    output37 = tneff_conc_avg; % [gN/m3]
    output38 = n2o_emissions_aer_avg_chandran; % [gN2O-N/d]
%   Additional data that may be of interest later:
    output39 = scodsecforward_max; % [g/m3]
    output40 = stpfiltereff_max; % [gP/m3]
    output41 = snoafiltereff_max; % [gN/m3]
    output42 = snoafiltereff_conc_avg; % [gN/m3]
    output43 = tneff_max; % [gN/m3]
    output44 = qconisbras_capacity; % [m3/d]
    output45 = qconisbras_operation; % [m3/d]
    output46 = n2o_emissions_anx_avg_chandran; % [gN2O-N/d]

    output47 = denit_backwash_flow_avg; % [m3/d]
    output48 = internal_rec_operation_avg; % [m3/d]
    output49 = qconmeohrctrc_avg; % [m3/d]
    output50 = qconmeohdf_avg; % [m3/d]
    output51 = qair_tunableblowers_delivered; % [m3/d]
    output52 = qair_3fixedblowers_delivered; % [m3/d]
    output53 = qair_4fixedblowers_delivered; % [m3/d]
    output54 = qair_3_1_fixedblowers_delivered; % [m3/d]
    output55 = blower_exceeded_time_fraction; % [fraction of time points]


line12 = sprintf('%d \t %d \t %s \t %d \t %d \t %d \t %d \t %d \t %d \t %d \t %d \t %d \t %d \t %
d \t %d \t %d \t %d \t %d \t %d \t %d \t %d \t %d \t %d \t %d \t %d \t %d \t %d \t %d \t %d \t %d
\t %d \t %d \t %d \t %d \t %d \t %d \t %d \t %d \t %d \t %d \t %d \t %d \t %d \t %d \t %d \t %d
\t %d \t %d \t %d \t %d \t %d \t %d \t %d \t %d \t %d \t %d \t %d \t %d \t %d \t %d \t %d', ...
        output0001, output0002, output0003, output01, output02, output03, output04, output05,
output06, ...
        output07, output08, output09, output10, output11, output12, ...
        output13, output14, output15, output16, output17, output18, ...
        output19, output20, output21, output22, output23, output24, ...
        output25, output26, output27, output28, output29, output30, ...
        output31, output32, output33, output34, output35, output36, ...
        output37, output38, output39, output40, output41, output42, ...
        output43, output44, output45, output46, output47, output48, ...
        output49, output50, output51, output52, output53, output54, ...
        output55);

fid=fopen(gpsxdatastoragefilename,'a');
fprintf(fid, '%s \r\n', line12);
% Note: Normally we use "fclose(fid)" to close the file. However, it
% appears that the files aren't fully closed with this command. As a
% result, if the script runs and has to access files more than a total of
% 511 times (the max number of files that can be open), the code will stop
% running. Now use fclose('all') at the end of each loop run.
fclose('all');
end
end
% SECTION 4.1
% END LOOP AND END SCRIPT
toc % Stops timer and reports in command window how long it took to
    % execute this m-file.
end
```

Appendix H
MATLAB Code for LCA and Cost Analysis for Quantitative Sustainable Design

```
function sustain_design_lca_cost_11_08_2011(inputdatafilename)
warning('Input file name without file extension (i.e., do not type ".txt"). Note that the
"Season" column of the GPS-X data must be converted. "Winter" should become "12" and "Summer"
should become "28". This simplifies data extraction (MATLAB has some difficulties with strings).
All cost and LCA equations are based on flow ranges expected at a 24 MGD WWTP, with assumptions
about which processes are new/modified/untouched.');

% The purpose of this m-file is to to quantify the costs and sources
% of environmental impacts associated with the construction and operation
% of an upgrade of the Hampton Roads Sanitation District (HRSD)
% Chesapeake-Elizabeth Wastewater Treatment Plant (WWTP). The equations
% below are specifically for an upgrade that includes secondary treatment
% via a 5-stage Bardenpho or A2O processes, and the system boundaries
% discussed in the corresponding manuscript (Guest et al., in preparation).

tic % Starts a timer to count how many seconds it takes to execute this m-file.

% SECTION 1.1
% DEFINE ALL FILENAMES - Identify names of .dat files based on input data
% file name (input by user) and name of file you want Matlab to output with
% processed data. Creates one .dat file (processeddatafilename) for the
% data output from this script.
inputdatafileextension = '.txt';
processeddatafileextension = '.dat';
processeddatafilename = strcat('_processed', inputdatafilename, processeddatafileextension);

% SECTION 1.2
% CREATE DATA STORAGE FILE - this is for the data you want to extract from
% this script. Creates a file with header info (line61), and then every line
% after that will be data appended to the file after each run of the loop.
% All data you want to collect must have a header in line61 and a
% corresponding value at the end of the script in line62. Note that the use
% of 'w' in the fid command below wipes the data file clean and adds the
% header line21.
% CNSTR = Construction Phase; OPER = Operation Phase; PW = Present Worth
line61 = sprintf('lhs_set \t config \t season \t Actual SRT (d) \t PW ($) \t PW CNSTR ($) \t PW
OPER ($) \t PW Blower CNSTR ($) \t PW Blower OPER ($) \t CNSTR ACID (H moles) \t CNSTR CARCIN (kg
benz) \t CNSTR ECOTOX (kg 24D) \t CNSTR EUTR (kg N) \t CNSTR GHG (kg CO2) \t CNSTR NON-CARC (kg
tolue) \t CNSTR OZONE (kg CFC) \t CNSTR RESPIR (kg PM) \t CNSTR SMOG (g NOx) \t OPER ACID (H
moles) \t OPER CARCIN (kg benz) \t OPER ECOTOX (kg 24D) \t OPER EUTR (kg N) \t OPER GHG (kg CO2)
\t OPER NON-CARC (kg tolue) \t OPER OZONE (kg CFC) \t OPER RESPIR (kg PM) \t OPER SMOG (g NOx) \t
Eff TN (g/m3) \t IR (x qprimover \t Additional PW Tunable ($) \t Additional PW 3-Fixed ($) \t
Additional PW 4-Fixed ($) \t Additional PW 3-1 Fixed ($) \t Additional GHG Tunable (kg CO2) \t
Additional GHG 3-Fixed (kg CO2) \t Additional GHG 4-Fixed (kg CO2) \t Additional GHG 3-1 Fixed
(kg CO2) \t Lifetime Electricity (kWh) \t Lifetime Effluent Nitrogen (kg-N) \t Lifetime N
Denitrified (kg-N) \t Concrete (m3) \t Internal Recycle Capital Cost at 1.15x ($) \t
total_acetate_(kg) \t qairstandlrctreff_avg (m3/d)');
processeddataheader = {line61}; % if 2 header lines, write as: {line21; line##};
fid=fopen(processeddatafilename,'w');
for row = 1:1 %1:2 if 2 row header
  fprintf(fid, '%s \r\n', processeddataheader{row,:});
end
fclose(fid);

% SECTION 1.3
% DEFINE NUMERICAL CONVERSIONS - The GPS-X file outputs are in SI units
```

```
% (e.g., m3/d), while the calculations below are in U.S. units (e.g.,
% million gallons per day).
ft_per_meter = 3.28083;
m3_per_cuft = 0.02831685;
gal_per_m3 = 264.1721;
lbs_per_g = 0.0022046;
mg_per_m3 = gal_per_m3*(10^-6);
mgd_per_gpd = (10^-6);
lbs_mg_per_mg_L = 8.3454;
sand_lbs_per_cuft = 92.6;
kg_per_lb = 0.4535924;
mj_per_1000cuft_ng = 1055.056; % final number is 1055.056 MJ per 1,000 cuft
kg_per_gal_fo = 3.634; % kg of fuel oil per gallon of fuel oil, assumes 960 kg/m3
scfm_per_mgd = 92.83;
g_per_m3_hac = 1049000; % g/m3
g_per_m3_meoh = 792000; % g/m3

% SECTION 1.4
% DEFINE UNIT COSTS AND OTHER KEY ASSUMPTIONS - The unit costs below will
% be used.  These units costs may be built into any equations and values
% that do not have a "*(unit cost)" term, and should not be changed without
% confirming that they are not embedded in any equations without the
% "*(unit cost)" term.
unit_elec = 0.065;        % Electricity, $/kWh; number supplied by C.B. Bott (HRSD↙
Representative).
unit_meoh = 1.54;         % Methanol, $/#; was 0.5, but source unclear. New source for MeOH and↙
HAc is http://www.icis.com/chemicals/channel-info-chemicals-a-z/ (accessed 11/10/2011, 11:28 AM)
unit_hac = 0.68;        % Acetate, $/#; Source for MeOH and HAc is http://www.icis.↙
com/chemicals/channel-info-chemicals-a-z/ (accessed 11/10/2011, 11:28 AM)
unit_hypo = 0.475;       % Hypochlorite,    $/#
unit_poly = 1.296;       % Polymer, $/#
unit_fecl3 = 0.36;      % Ferric Chloride, $/#
unit_oil = 2.22;         % Fuel Oil,    $/gal
unit_gas = 7.25;        % Natural Gas, $/1,000 cuft; number supplied by C.B. Bott (HRSD↙
Representative).
unit_operator = 25;     % Operator labor rate, $/hr
unit_diffus = 50;        % Standard 2 scfm Fine Bubble Diffuser, $/unit
unit_head = 14000;       % Standard 550 scfm Swing Arm Diffuser, $/unit
unit_mix = 8950;         % 5 HP Vertical Turbine Mixer, $/unit
unit_excavat = 0.29628;  % Excavation, $/cuft
unit_wall = 18.518;      % Wall Concrete, $/cuft
unit_slab = 12.963;      % Slab Concrete, $/cuft
unit_crane = 200;        % Crane Rental, $/hr
unit_hand = 75;          % Hand Rail, $/ft
unit_land = 0;           % Land Costs, $/acre; HRSD already owns the land.
unit_conlab = 32;        % Construction Labor Rate, $/hr
unit_headtime = 25;      % Labor Required for Air Header Installation, person-hr/header
unit_cranetime = 0.1;    % Crane Time Requirement per Installation Labor, crane-hr/person-hr
cepcip = 738.8;         % Pipe Cost Index (CEPCIP)
pmincaer = 0.10;        % Other Costs for Aerobic Equipment (PMINCaer), fraction of equipment↙
cost  (e.g., 0.10 = 10%)
pmincan = 23;           % Other Costs for Anaerobic/Anoxic Equipment (PMINCana-anx),  % of↙
equipment cost
cf = 0.11;              % Correction Factor, fraction of total bare construction cost (TBCC), (e.↙
g., 0.11 = 11%)
interest = 0.08;        % Interest as a fraction (0.08 = 8% interest)
```

```
% SECTION 1.5
% KEY ASSUMPTIONS -
elec_grid_loss = 0.07; % assumes 7% of electricity generated at the power plant is lost before it gets to the end user.
xlrctr_mixer_sizing = 3600; % assumes the mixers must be able to mix MLSS up to at least 3,600 mg-TSS/L.
aeration_capacity_standard = 807500*1.5; % [m3/d] based on steady state simulations of Standard design under summer (28C) and winter (17.9C) conditions - max aeration demand was 807,500 m3/d in summer.
aeration_capacity_seasonal = 764500*1.5; % [m3/d] based on steady state simulations of Seasonal design under summer (28C) and winter (17.9C) conditions - max aeration demand was 764,500 m3/d in winter.
new_reactor_max_interior_length_ft = 188; %ft
old_reactor_max_interior_length_ft = 144.3; %ft
reactor_depth_ft = 15; %ft
reactor_depth_meters = reactor_depth_ft/ft_per_meter;
new_reactor_trains = 6;
old_reactor_trains = 12;
new_reactor_width_ft = 53*new_reactor_trains; % ft
new_reactor_width_meters = new_reactor_width_ft/ft_per_meter;
old_reactor_width_ft = 25*old_reactor_trains; % ft
old_reactor_width_meters = old_reactor_width_ft/ft_per_meter;



df_backwash_gpm_per_ft2 = 10; % gpm/ft2 for 15 min a day
denit_filter_area_standard_m2 = 515; % m2
denit_filter_area_seasonal_m2 = 588; % m2

unit_dual_internal_recycle_for_config1 = 1;
unit_dual_internal_recycle_for_config2 = 1.15; % Assumes that having the
    % ability to pull internal recycle from 2 different locations (AER1b
    % OR AER2) costs 15% more than if it were only from 1 location (AER1b).
    % This is an additional cost incurred by the operationally flexible
    % design.
unit_blower_tunable = 1.15; % Assumes a blower with better turn-up/turn-down capacity costs 15% more than a standard blower.
unit_blower_4fixed = 1.05;
unit_blower_3_1_fixed = 1.08;
unit_blower_standard = 1.0;

cl_dose = 42.1; % lbs of Cl2 per MG
py_dose_gbt = 0.004; % lbs of polymer per lb of TSS
py_dose_cent = 0.02; % lbs of polymer per lb of TSS
meoh_per_no3 = 2.333; % lbs of MeOH required per lb of NO3-N; based on 3.5 kg-COD/kg-N
fo_dose_inc = 2.8; % gal of fuel oil per ton of TSS incinerated
ng_dose_inc = 6.4; % 1,000 cuft of natural gas per ton TSS
ap_by_inc = 0.344; % cuyd of ash produced per ton of TSS incinerated
scfm_per_diffuser = 1.9; % design air flow in scfm per diffuser
scfm_per_header = 365; % design air flow in scfm per air header
q_ras_existing_capacity = 12; % MGD of existing RAS pumping capacity
plant_lifetime = 40; % years - this assumption (40 yrs) is embedded in amortization equations
dc_profit = 0.15; % profit for design/construction firms on direct costs
ic_ratio = 0.36; % indirect costs relative to direct costs
land_costs = 0;
```

```
construction_period = 3; % years
qconisb = 3785.41; % m3/d, not tied to anything except final LCA calcs
present_worth_factor = ((((1 + interest)^plant_lifetime) - 1)/interest)*(1/((1 + interest)
^plant_lifetime));

% N2O Assumptions
ef_n2o_effluent = 0.005; % N2O emission factor in effluent [gN2O-N/(g-N in effluent)]
ef_n2o_wwt = 0.005; % N2O emission factor in denit zones [gN2O-N/(g-N
    % denitrified)]

% SECTION 1.6
% IMPORT GPS-X DATA - GPS-X data from the simulation MATLAB code is output
% with a total of 58 columns and a row for each simulation run.  For the
% Latin Hypercube Sampling set of 500 (i.e., there are 500 combinations of
% parameters input to the simulator), there are 1,000 simulations (1
% simulation per configuration; 2 configurations).  This means that the
% typical output will be a matrix with 58 columns and 1,001 rows (1,000
% simulations plus the header row).
DELIMITER = '\t';
HEADERLINES = 1;

gpsx_data_filename = strcat(inputdatafilename, inputdatafileextension);
gpsxdata = importdata(gpsx_data_filename);
number_of_columns = length(gpsxdata.colheaders);
% Note:  Although the approach below (the "for" loop with string matching)
% is not the quickest way to extract the data, it does ensure that the
% columns from the data file are correctly matched with the variable names
% in this code.
for i = 1:number_of_columns
    columnheader = gpsxdata.colheaders{i};
    data_number = strmatch(columnheader,strvcat('lhs_set',' config ',...
        ' season ',' actual_srt_d (d) ',' rec_capacity (m3/d) ',...
        ' volume_ana (m3) ',' volume_anx1 (m3) ',' volume_aer1 (m3) ',...
        ' volume_anx2 (m3) ',' volume_aer2 (m3) ',...
        ' qconisbwas_capacity (m3/d) ',' qconisbwas_operation (m3/d) ',...
        ' qprimover_avg (m3/d) ',' qconras_operation (m3/d) ',...
        ' qconras_capacity (m3/d) ',' qconrctrwas_capacity (m3/d) ',...
        ' qconrctrwas_operation (m3/d) ',' average_mlss (g/m3) ',...
        ' tn_rctr_loading_avg (gN/d) ',' qprimunder_avg (m3/d) ',...
        ' xrctraeff_avg (g/m3) ',' xlrctrbeff1_avg (g/m3) ',...
        ' xlrctrceff1_avg (g/m3) ',' snhlrctrceff2_conc_avg (g/m3) ',...
        ' qsecforward_max (m3/d) ',' qsecforward_avg (m3/d) ',...
        ' snoalrctrceff2_conc_avg (g/m3) ',...
        ' qairstandlrctreff_max (m3/d) ',...
        ' qairstandlrctreff_avg (m3/d) ',' qcentinf_avg (m3/d) ',...
        ' xcentinf_conc_avg (g/m3) ',' qcentcake_avg (m3/d) ',...
        ' xcentcake_conc_avg (g/m3) ',' xisbwas_avg (g/m3) ',...
        ' qfiltereff_avg (m3/d) ',' scodsecforward_conc_avg (g/m3) ',...
        ' tnrctrwas_mass_removal_avg (gN/d) ',' stpfiltereff_conc_avg (gP/m3) ',...
        ' sndfiltereff_conc_avg (gN/m3) ',' tneff_conc_avg (gN/m3) ',...
        ' n2o_emissions_aer_avg_chandran (gN2O-N/d) ',' scodsecforward_max (g/m3) ',...
        ' stpfiltereff_max (gP/m3) ',' snoafiltereff_max (gN/m3) ',...
        ' snoafiltereff_conc_avg (gN/m3) ',' tneff_max (gN/m3) ',...
        ' qconisbras_capacity (m3/d) ',' qconisbras_operation (m3/d) ',...
        ' n2o_emissions_anx_avg_chandran (gN2O-N/d) ',...
        ' denit_backwash_flow_avg (m3/d) ',' internal_rec_operation_avg (m3/d) ',...
```

```
        ' qconmeohrctrc_avg (m3/d) ',' qconmeohdf_avg (m3/d) ',...
        ' qair_tunableblowers_delivered (m3/d) ',' qair_3fixedblowers_delivered (m3/d) ',...
        ' qair_4fixedblowers_delivered (m3/d) ',' qair_3_1_fixedblowers_delivered (m3/d) ',...
        ' blower_exceeded_time_fraction (fraction of time points) '),'exact');
    if (data_number <= 1)
        col_lhs_set = i;
    elseif (data_number <= 2)
        col_config = i;
    elseif (data_number <= 3)
        col_season = i;
    elseif (data_number <= 4)
        col_actual_srt_d = i;
    elseif (data_number <= 5)
        col_rec_capacity = i;
    elseif (data_number <= 6)
        col_volume_ana = i;
    elseif (data_number <= 7)
        col_volume_anx1 = i;
    elseif (data_number <= 8)
        col_volume_aer1 = i;
    elseif (data_number <= 9)
        col_volume_anx2 = i;
    elseif (data_number <= 10)
        col_volume_aer2 = i;
    elseif (data_number <= 11)
        col_qconisbwas_capacity = i;
    elseif (data_number <= 12)
        col_qconisbwas_operation = i;
    elseif (data_number <= 13)
        col_qprimover_avg = i;
    elseif (data_number <= 14)
        col_qconras_operation = i;
    elseif (data_number <= 15)
        col_qconras_capacity = i;
    elseif (data_number <= 16)
        col_qconrctrwas_capacity = i;
    elseif (data_number <= 17)
        col_qconrctrwas_operation = i;
    elseif (data_number <= 18)
        col_average_mlss = i;
    elseif (data_number <= 19)
        col_tn_rctr_loading_avg = i;
    elseif (data_number <= 20)
        col_qprimunder_avg = i;
    elseif (data_number <= 21)
        col_xrctraeff_avg = i;
    elseif (data_number <= 22)
        col_xlrctrbeff1_avg = i;
    elseif (data_number <= 23)
        col_xlrctrceff1_avg = i;
    elseif (data_number <= 24)
        col_snh1rctrceff2_conc_avg = i;
    elseif (data_number <= 25)
        col_qsecforward_max = i;
    elseif (data_number <= 26)
        col_qsecforward_avg = i;
```

```
elseif (data_number <= 27)
    col_snoalrctrceff2_conc_avg = i;
elseif (data_number <= 28)
    col_qairstandlrctreff_max = i;
elseif (data_number <= 29)
    col_qairstandlrctreff_avg = i;
elseif (data_number <= 30)
    col_qcentinf_avg = i;
elseif (data_number <= 31)
    col_xcentinf_conc_avg = i;
elseif (data_number <= 32)
    col_qcentcake_avg = i;
elseif (data_number <= 33)
    col_xcentcake_conc_avg = i;
elseif (data_number <= 34)
    col_xisbwas_avg = i;
elseif (data_number <= 35)
    col_qfiltereff_avg = i;
elseif (data_number <= 36)
    col_scodsecforward_conc_avg = i;
elseif (data_number <= 37)
    col_tnrctrwas_mass_removal_avg = i;
elseif (data_number <= 38)
    col_stpfiltereff_conc_avg = i;
elseif (data_number <= 39)
    col_sndfiltereff_conc_avg = i;
elseif (data_number <= 40)
    col_tneff_conc_avg = i;
elseif (data_number <= 41)
    col_n2o_emissions_aer_avg_chandran = i;
elseif (data_number <= 42)
    col_scodsecforward_max = i;
elseif (data_number <= 43)
    col_stpfiltereff_max = i;
elseif (data_number <= 44)
    col_snoafiltereff_max = i;
elseif (data_number <= 45)
    col_snoafiltereff_conc_avg = i;
elseif (data_number <= 46)
    col_tneff_max = i;
elseif (data_number <= 47)
    col_qconisbras_capacity = i;
elseif (data_number <= 48)
    col_qconisbras_operation = i;
elseif (data_number <= 49)
    col_n2o_emissions_anx_avg_chandran = i;
elseif (data_number <= 50)
    col_denit_backwash_flow_avg = i;
elseif (data_number <= 51)
    col_internal_rec_operation_avg = i;
elseif (data_number <= 52)
    col_qconmeohrctrc_avg = i;
elseif (data_number <= 53)
    col_qconmeohdf_avg = i;
elseif (data_number <= 54)
    col_qair_tunableblowers_delivered = i;
```

```
    elseif (data_number <= 55)
        col_qair_3fixedblowers_delivered = i;
    elseif (data_number <= 56)
        col_qair_4fixedblowers_delivered = i;
    elseif (data_number <= 57)
        col_qair_3_1_fixedblowers_delivered = i;
    elseif (data_number <= 58)
        col_blower_exceeded_time_fraction = i;
    else
       warning('gpsx_data_filename column header not identified');
    end
end

lhs_set_parameter_set = gpsxdata.data(:,col_lhs_set);
config_parameter_set = gpsxdata.data(:,col_config);
season_parameter_set = gpsxdata.data(:,col_season);
actual_srt_d_parameter_set = gpsxdata.data(:,col_actual_srt_d);
rec_capacity_parameter_set = gpsxdata.data(:,col_rec_capacity);
volume_ana_parameter_set = gpsxdata.data(:,col_volume_ana);
volume_anx1_parameter_set = gpsxdata.data(:,col_volume_anx1);
volume_aer1_parameter_set = gpsxdata.data(:,col_volume_aer1);
volume_anx2_parameter_set = gpsxdata.data(:,col_volume_anx2);
volume_aer2_parameter_set = gpsxdata.data(:,col_volume_aer2);
qconisbwas_capacity_parameter_set = gpsxdata.data(:,col_qconisbwas_capacity);
qconisbwas_operation_parameter_set = gpsxdata.data(:,col_qconisbwas_operation);
qprimover_avg_parameter_set = gpsxdata.data(:,col_qprimover_avg);
qconras_operation_parameter_set = gpsxdata.data(:,col_qconras_operation);
qconras_capacity_parameter_set = gpsxdata.data(:,col_qconras_capacity);
qconrctrwas_capacity_parameter_set = gpsxdata.data(:,col_qconrctrwas_capacity);
qconrctrwas_operation_parameter_set = gpsxdata.data(:,col_qconrctrwas_operation);
average_mlss_parameter_set = gpsxdata.data(:,col_average_mlss);
tn_rctr_loading_avg_parameter_set = gpsxdata.data(:,col_tn_rctr_loading_avg);
qprimunder_avg_parameter_set = gpsxdata.data(:,col_qprimunder_avg);
xrctraeff_avg_parameter_set = gpsxdata.data(:,col_xrctraeff_avg);
xlrctrbeff1_avg_parameter_set = gpsxdata.data(:,col_xlrctrbeff1_avg);
snhlrctrceff2_conc_avg_parameter_set = gpsxdata.data(:,col_snhlrctrceff2_conc_avg);
qsecforward_max_parameter_set = gpsxdata.data(:,col_qsecforward_max);
qsecforward_avg_parameter_set = gpsxdata.data(:,col_qsecforward_avg);
snoalrctrceff2_conc_avg_parameter_set = gpsxdata.data(:,col_snoalrctrceff2_conc_avg);
qairstandlrctreff_max_parameter_set = gpsxdata.data(:,col_qairstandlrctreff_max);
qairstandlrctreff_avg_parameter_set = gpsxdata.data(:,col_qairstandlrctreff_avg);
qcentinf_avg_parameter_set = gpsxdata.data(:,col_qcentinf_avg);
xcentinf_conc_avg_parameter_set = gpsxdata.data(:,col_xcentinf_conc_avg);
qcentcake_avg_parameter_set = gpsxdata.data(:,col_qcentcake_avg);
xcentcake_conc_avg_parameter_set = gpsxdata.data(:,col_xcentcake_conc_avg);
xisbwas_avg_parameter_set = gpsxdata.data(:,col_xisbwas_avg);
qfiltereff_avg_parameter_set = gpsxdata.data(:,col_qfiltereff_avg);
scodsecforward_conc_avg_parameter_set = gpsxdata.data(:,col_scodsecforward_conc_avg);
tnrctrwas_mass_removal_avg_parameter_set = gpsxdata.data(:,col_tnrctrwas_mass_removal_avg);
stpfiltereff_conc_avg_parameter_set = gpsxdata.data(:,col_stpfiltereff_conc_avg);
sndfiltereff_conc_avg_parameter_set = gpsxdata.data(:,col_sndfiltereff_conc_avg);
tneff_conc_avg_parameter_set = gpsxdata.data(:,col_tneff_conc_avg);
n2o_emissions_aer_avg_chandran_parameter_set = gpsxdata.data(:,↙
col_n2o_emissions_aer_avg_chandran);
scodsecforward_max_parameter_set = gpsxdata.data(:,col_scodsecforward_max);
stpfiltereff_max_parameter_set = gpsxdata.data(:,col_stpfiltereff_max);
```

```
snoafiltereff_max_parameter_set = gpsxdata.data(:,col_snoafiltereff_max);
snoafiltereff_conc_avg_parameter_set = gpsxdata.data(:,col_snoafiltereff_conc_avg);
tneff_max_parameter_set = gpsxdata.data(:,col_tneff_max);
qconisbras_capacity_parameter_set = gpsxdata.data(:,col_qconisbras_capacity);
qconisbras_operation_parameter_set = gpsxdata.data(:,col_qconisbras_operation);
n2o_emissions_anx_avg_chandran_parameter_set = gpsxdata.data(:,↙
col_n2o_emissions_anx_avg_chandran);
denit_backwash_flow_avg_parameter_set = gpsxdata.data(:,col_denit_backwash_flow_avg);
internal_rec_operation_avg_parameter_set = gpsxdata.data(:,col_internal_rec_operation_avg);
qconmeohrctrc_avg_parameter_set = gpsxdata.data(:,col_qconmeohrctrc_avg);
qconmeohdf_avg_parameter_set = gpsxdata.data(:,col_qconmeohdf_avg);
qair_tunableblowers_delivered_parameter_set = gpsxdata.data(:,col_qair_tunableblowers_delivered);
qair_3fixedblowers_delivered_parameter_set = gpsxdata.data(:,col_qair_3fixedblowers_delivered);
qair_4fixedblowers_delivered_parameter_set = gpsxdata.data(:,col_qair_4fixedblowers_delivered);
qair_3_1_fixedblowers_delivered_parameter_set = gpsxdata.data(:,↙
col_qair_3_1_fixedblowers_delivered);
blower_exceeded_time_fraction_parameter_set = gpsxdata.data(:,col_blower_exceeded_time_fraction);

number_of_simulations = length(actual_srt_d_parameter_set);

% SECTION 1.8
% PREPARE VECTORS FOR DATA OUTPUT FROM THIS CODE SO THAT SUMMARY
% CALCULATIONS (E.G., COMPARING CONFIGURATIONS 1 AND 2) CAN ALSO BE MADE.
lhs_set_output_set = zeros(number_of_simulations,2);
config_output_set = zeros(number_of_simulations,2);
season_output_set = zeros(number_of_simulations,2);
actual_srt_d_output_set = zeros(number_of_simulations,2);
present_worth_output_set = zeros(number_of_simulations,2);
present_worth_construction_output_set = zeros(number_of_simulations,2);
present_worth_operation_output_set = zeros(number_of_simulations,2);
present_worth_blower_construction_output_set = zeros(number_of_simulations,2);
present_worth_blower_operation_output_set = zeros(number_of_simulations,2);
construction_acidification_output_set = zeros(number_of_simulations,2);
construction_carcinogenics_output_set = zeros(number_of_simulations,2);
construction_ecotoxicity_output_set = zeros(number_of_simulations,2);
construction_eutrophication_output_set = zeros(number_of_simulations,2);
construction_global_warming_output_set = zeros(number_of_simulations,2);
construction_noncarcinogenics_output_set = zeros(number_of_simulations,2);
construction_ozone_depletion_output_set = zeros(number_of_simulations,2);
construction_respiratory_output_set = zeros(number_of_simulations,2);
construction_smog_output_set = zeros(number_of_simulations,2);
operation_acidification_output_set = zeros(number_of_simulations,2);
operation_carcinogenics_output_set = zeros(number_of_simulations,2);
operation_ecotoxicity_output_set = zeros(number_of_simulations,2);
operation_eutrophication_output_set = zeros(number_of_simulations,2);
operation_global_warming_output_set = zeros(number_of_simulations,2);
operation_noncarcinogenics_output_set = zeros(number_of_simulations,2);
operation_ozone_depletion_output_set = zeros(number_of_simulations,2);
operation_respiratory_output_set = zeros(number_of_simulations,2);
operation_smog_output_set = zeros(number_of_simulations,2);
tneff_conc_avg_output_set = zeros(number_of_simulations,2);
ir_ratio_output_set = zeros(number_of_simulations,2);

additional_pw_tunable_output_set = zeros(number_of_simulations,2);
additional_pw_3fixed_output_set = zeros(number_of_simulations,2);
additional_pw_4fixed_output_set = zeros(number_of_simulations,2);
```

```
additional_pw_3_1_fixed_output_set = zeros(number_of_simulations,2);
additional_ghg_tunable_output_set = zeros(number_of_simulations,2);
additional_ghg_3fixed_output_set = zeros(number_of_simulations,2);
additional_ghg_4fixed_output_set = zeros(number_of_simulations,2);
additional_ghg_3_1_fixed_output_set = zeros(number_of_simulations,2);


% SECTION 2.1
% "FOR" LOOP FOR LCA AND COST ASSESSMENT OF INDIVIDUAL SIMULATIONS
for k = 1:number_of_simulations
    lhs_set = lhs_set_parameter_set(k,1);
    config = config_parameter_set(k,1);
    season = season_parameter_set(k,1);
    if (season == 12)
        season_type = 'Winter';
    elseif (season == 28)
        season_type = 'Summer';
    end
    actual_srt_d = actual_srt_d_parameter_set(k,1);
    rec_capacity = rec_capacity_parameter_set(k,1);
    volume_ana = volume_ana_parameter_set(k,1);
    volume_anx1 = volume_anx1_parameter_set(k,1);
    volume_aer1 = volume_aer1_parameter_set(k,1);
    volume_anx2 = volume_anx2_parameter_set(k,1);
    volume_aer2 = volume_aer2_parameter_set(k,1);
    qconisbwas_capacity = qconisbwas_capacity_parameter_set(k,1);
    qconisbwas_operation = qconisbwas_operation_parameter_set(k,1);
    qprimover_avg = qprimover_avg_parameter_set(k,1);
    qconras_operation = qconras_operation_parameter_set(k,1);
    qconras_capacity = qconras_capacity_parameter_set(k,1);
    qconrctrwas_capacity = qconrctrwas_capacity_parameter_set(k,1);
    qconrctrwas_operation = qconrctrwas_operation_parameter_set(k,1);
    average_mlss = average_mlss_parameter_set(k,1);
    tn_rctr_loading_avg = tn_rctr_loading_avg_parameter_set(k,1);
    qprimunder_avg = qprimunder_avg_parameter_set(k,1);
    xrctraeff_avg = xrctraeff_avg_parameter_set(k,1);
    xlrctrbeff1_avg = xlrctrbeff1_avg_parameter_set(k,1);
    snhlrctrceff2_conc_avg = snhlrctrceff2_conc_avg_parameter_set(k,1);
    qsecforward_max = qsecforward_max_parameter_set(k,1);
    qsecforward_avg = qsecforward_avg_parameter_set(k,1);
    snoalrctrceff2_conc_avg = snoalrctrceff2_conc_avg_parameter_set(k,1);
    qairstandlrctreff_max = qairstandlrctreff_max_parameter_set(k,1);
    qairstandlrctreff_avg = qairstandlrctreff_avg_parameter_set(k,1);
    qcentinf_avg = qcentinf_avg_parameter_set(k,1);
    xcentinf_conc_avg = xcentinf_conc_avg_parameter_set(k,1);
    qcentcake_avg = qcentcake_avg_parameter_set(k,1);
    xcentcake_conc_avg = xcentcake_conc_avg_parameter_set(k,1);
    xisbwas_avg = xisbwas_avg_parameter_set(k,1);
    qfiltereff_avg = qfiltereff_avg_parameter_set(k,1);
    scodsecforward_conc_avg = scodsecforward_conc_avg_parameter_set(k,1);
    tnrctrwas_mass_removal_avg = tnrctrwas_mass_removal_avg_parameter_set(k,1);
    stpfiltereff_conc_avg = stpfiltereff_conc_avg_parameter_set(k,1);
    sndfiltereff_conc_avg = sndfiltereff_conc_avg_parameter_set(k,1);
    tneff_conc_avg = tneff_conc_avg_parameter_set(k,1);
    n2o_emissions_aer_avg_chandran = n2o_emissions_aer_avg_chandran_parameter_set(k,1);
    scodsecforward_max = scodsecforward_max_parameter_set(k,1);
```

```
    stpfiltereff_max = stpfiltereff_max_parameter_set(k,1);
    snoafiltereff_max = snoafiltereff_max_parameter_set(k,1);
    snoafiltereff_conc_avg = snoafiltereff_conc_avg_parameter_set(k,1);
    tneff_max = tneff_max_parameter_set(k,1);
    qconisbras_capacity = qconisbras_capacity_parameter_set(k,1);
    qconisbras_operation = qconisbras_operation_parameter_set(k,1);
    n2o_emissions_anx_avg_chandran = n2o_emissions_anx_avg_chandran_parameter_set(k,1);
    denit_backwash_flow_avg = denit_backwash_flow_avg_parameter_set(k,1);
    internal_rec_operation_avg = internal_rec_operation_avg_parameter_set(k,1);
    qconmeohrctrc_avg = qconmeohrctrc_avg_parameter_set(k,1);
    qconmeohdf_avg = qconmeohdf_avg_parameter_set(k,1);
    qair_tunableblowers_delivered = qair_tunableblowers_delivered_parameter_set(k,1);
    qair_3fixedblowers_delivered = qair_3fixedblowers_delivered_parameter_set(k,1);
    qair_4fixedblowers_delivered = qair_4fixedblowers_delivered_parameter_set(k,1);
    qair_3_1_fixedblowers_delivered = qair_3_1_fixedblowers_delivered_parameter_set(k,1);
    blower_exceeded_time_fraction = blower_exceeded_time_fraction_parameter_set(k,1);

    % Note:  In the configuration evaluated, MeOH was actually acetate.
    % The reason for this was that methanol was not degrading properly in
    % the GPS-X simulations and methylotrophs weren't growing, so we switched
    % to acetate addition for denitrification in the ANX2 zone and on the denit
    % filters.
    qconhacrctrc_avg = qconmeohrctrc_avg;
    qconhacdf_avg = qconmeohdf_avg;

    if (stpfiltereff_conc_avg >= 0.7)
        stp_precipitated = stpfiltereff_conc_avg - 0.7;
        stpfiltereff_conc = 0.7;
    else
        stp_precipitated = 0;
        stpfiltereff_conc = stpfiltereff_conc_avg;
    end

    fraction_p_precipitated = stp_precipitated/stpfiltereff_conc_avg;
    fecl3_addition = -2.25*log10(1-fraction_p_precipitated); % [g/m3] Based on Figure 6-14 on↙
page 506 of Metcalf & Eddy.
    fecl3_addition_lbs_per_mgd = fecl3_addition*lbs_mg_per_mg_L;

% SECTION 2.2
% CONFIGURATION-SPECIFIC CALCULATIONS
    if (config == 1)
        unit_dual_internal_recycle = unit_dual_internal_recycle_for_config1;
        qairstandlrctreff_blower_capacity_m3d = aeration_capacity_standard;
        df_loading = 4; % gpm/ft2
        denit_filter_area_m2 = denit_filter_area_standard_m2;  % m2
    elseif (config == 2)
        unit_dual_internal_recycle = unit_dual_internal_recycle_for_config2; % Cost, VE, BA↙
factor for adding piping to pull internal recycle from AER1b or from AER2 (rather than just from↙
AER1b).
        qairstandlrctreff_blower_capacity_m3d = aeration_capacity_seasonal;
        denit_filter_area_m2 = denit_filter_area_seasonal_m2;  % m2
        if (season == 28)
            df_loading = 4; % gpm/ft2
        elseif (season == 12)
            df_loading = 3.5; % gpm/ft2
        else
```

```
            warning('Unknown season. Names "summer" and "winter" are only known seasons for this
code.');
        end
    else
        warning('Unknown design type. Names "seasonal" and "standard" are only known types for
this code. Stop the run - this code will not give usable data.');
    end

% SECTION 2.3
% SIZING CALCULATIONS
eqn_df_size_ft2 = denit_filter_area_m2*(ft_per_meter^2);  % sqft
l_anx2_m = (volume_anx2/(reactor_depth_meters ...
    *old_reactor_width_meters));
l_aer2_m = (volume_aer2/(reactor_depth_meters ...
    *old_reactor_width_meters));
l_aer1b_m = (old_reactor_max_interior_length_ft/ft_per_meter) - l_aer2_m - l_anx2_m;
l_aer1a_m = ((volume_aer1 - (l_aer1b_m*old_reactor_width_meters...
    *reactor_depth_meters))/(reactor_depth_meters*new_reactor_width_meters));
l_anx1_m = (volume_anx1/(reactor_depth_meters ...
    *new_reactor_width_meters));
l_ana_m = (volume_ana/(reactor_depth_meters ...
    *new_reactor_width_meters));
volume_aer1b = l_aer1b_m*old_reactor_width_meters*reactor_depth_meters;
volume_aer1a = volume_aer1 - volume_aer1b;
eqn_df_bwip_capacity_mgd = (1/12)*eqn_df_size_ft2*df_backwash_gpm_per_ft2*(24*60)*mgd_per_gpd; %
MGD pumping rate required to backwash a single denit filter at a time
ir_ratio = internal_rec_operation_avg/qprimover_avg;

% SECTION 2.4
% CONVERSIONS TO U.S. UNITS
qairstandlrctreff_blower_capacity_mgd = qairstandlrctreff_blower_capacity_m3d*mg_per_m3;

qconrctrwas_capacity_mgd = qconrctrwas_capacity*mg_per_m3; % Note:  this value is not used
because HRSD has sufficient WAS pumping on site.  No additional WAS pumps will need to be
purchased.
qconras_capacity_mgd = qconras_capacity*mg_per_m3;
qconisbwas_capacity_mgd = qconisbwas_capacity*mg_per_m3;
qconisbras_capacity_mgd = qconisbras_capacity*mg_per_m3;
denit_backwash_flow_avg_mgd = denit_backwash_flow_avg*mg_per_m3; % MGD
l_ana_ft = l_ana_m*ft_per_meter;
l_anx1_ft = l_anx1_m*ft_per_meter;
l_aer1a_ft = l_aer1a_m*ft_per_meter;
l_aer1b_ft = l_aer1b_m*ft_per_meter;
l_anx2_ft = l_anx2_m*ft_per_meter;
l_aer2_ft = l_aer2_m*ft_per_meter;

qconras_operation_mgd = qconras_operation*mg_per_m3;
q_primunder_mgd = qprimunder_avg*mg_per_m3;
q_internal_operation_mgd = internal_rec_operation_avg*mg_per_m3;
q_internal_capacity_mgd = rec_capacity*mg_per_m3;
qconrctrwas_operation_mgd = qconrctrwas_operation*mg_per_m3;
qcentinf_avg_mgd = qcentinf_avg*mg_per_m3;
qfiltereff_avg_mgd = qfiltereff_avg*mg_per_m3;
qsecforward_max_mgd = qsecforward_max*mg_per_m3; % Unused now that denit filters are pre-
designed.
qsecforward_avg_mgd = qsecforward_avg*mg_per_m3;
```

```
qcentcake_avg_mgd = qcentcake_avg*mg_per_m3;
qconisbras_operation_mgd = qconisbras_operation*mg_per_m3;
qconisbwas_operation_mgd = qconisbwas_operation*mg_per_m3;
qair_tunableblowers_delivered_mgd = qair_tunableblowers_delivered*mg_per_m3;
qair_3fixedblowers_delivered_mgd = qair_3fixedblowers_delivered*mg_per_m3;
qair_4fixedblowers_delivered_mgd = qair_4fixedblowers_delivered*mg_per_m3;
qair_3_1_fixedblowers_delivered_mgd = qair_3_1_fixedblowers_delivered*mg_per_m3;

% SECTION XX
% INTERMEDIATE ENERGY CALCULATIONS
    if (config == 1)
        unit_blower = unit_blower_standard;
        qairstandlrctreff_delivered_mgd = qair_3fixedblowers_delivered_mgd;
        eqn_stbcr_ee_an = (0.004718)*(xlrctrbeff1_avg^0.298)*((((l_ana_ft + l_anx1_ft)↙
*reactor_depth_ft*new_reactor_width_ft) + (l_anx2_ft*reactor_depth_ft*old_reactor_width_ft))/133.↙
68)*0.85*365.25;
        % eqn_stbcr_ee_an = (0.00475 hp/1,000 gal)*(0.9778^0.3)...
        % *((MLSS, mg/L)^0.298)*[(LANA + LANX1, ft)*(15 ft)*(53 ft)...
        % *(6 trains in service) + (LANX2, ft)*(15 ft)*(25 ft)...
        % *(12 trains in service)]*(1,000 gal/133.68 cuft)*(0.85 kW/hp)...
        % *(24 hrs/day)*(365.25 days/year)
    elseif (config == 2)
        unit_blower = unit_blower_standard;  % Cost factor for buying a blower and control system↙
capable of supplying only the required airflow.
        qairstandlrctreff_delivered_mgd = qair_3fixedblowers_delivered_mgd;
        if (season == 28)
            eqn_stbcr_ee_an = (0.004718)*(xlrctrbeff1_avg^0.298)*((((l_ana_ft + l_anx1_ft)↙
*reactor_depth_ft*new_reactor_width_ft) + (l_anx2_ft*reactor_depth_ft*old_reactor_width_ft))/133.↙
68)*0.85*365.25;
        elseif (season == 12)
            eqn_stbcr_ee_an = (0.004718)*(xlrctrbeff1_avg^0.298)*((((l_ana_ft + l_anx1_ft)↙
*reactor_depth_ft*new_reactor_width_ft))/133.68)*0.85*365.25;
        end

    else
        warning('Unknown blower type.');
    end

eqn_stbcr_ee_aer = (qairstandlrctreff_delivered_mgd)*scfm_per_mgd*241.6; % conversions of↙
scfm_per_mgd scfm/MGD, and 241.6 kWh/yr/scfm


% SECTION 3.1
% ------------------ SOURCES OF ENVIRONMENTAL IMPACTS ---------------------

% Ferric Chloride Use [#/yr]
eqn_df_fecl3 = qsecforward_avg_mgd*fecl3_addition_lbs_per_mgd*365.25;

% SECTION 3.1.1
% ------- VOLUME OF EARTHWORK (VE), ALL IN UNITS OF "CUFT"
% Note:  For RAS, WAS, and Internal Recycle pumping, all best fit equations
% are linear with an intercept at 1,600 cuft.  This value was not included
% for each individual set of pumping as there would be a significant amount
% of earthwork overlap for RAS/WAS and RAS/IR lines.  As such, only one
% 1,600 cuft was included for the secondary treatment process pumping and
% one 1,600 cuft was included for the ISB Treatment System pumping.
```

```
eqn_pc_ve = 782000; % primary clarifier
eqn_psp_ve = 1610; % primary sludge pumping
eqn_sc_ve = 0; % secondary clarifier
eqn_stbnr_ve = (5175)*(l_ana_ft + l_anx1_ft + l_aer1a_ft) + (140625); % 5-stage Bardenpho, new reactors
eqn_stber_ve = 0; % 5-stage Bardenpho, existing reactors
eqn_stbcr_ve = 0; % 5-stage Bardenpho, combined (new + existing) reactors
eqn_stbras_ve = 0; % 5-stage Bardenpho, RAS pumping
eqn_stbir_ve = ((158)*(q_internal_capacity_mgd))*unit_dual_internal_recycle + (1600); % 5-stage Bardenpho, internal recycle pumping
eqn_stbwas_ve = 0; % 5-stage Bardenpho, WAS pumping
eqn_blo_ve = 0; % blowers
eqn_df1_ve = (10.2)*eqn_df_size_ft2 + (48809); % denitrification filters - configuration 1
eqn_cct_ve = 0; % chlorine contact tank
eqn_isbpfr_ve = 72137; % incinerator scrubber blowdown TS plug flow reactor
eqn_isbras_ve = (316)*qconisbras_capacity_mgd + (1600); % incinerator scrubber blowdown TS RAS pumping
eqn_isbsc_ve = 13805; % incinerator scrubber blowdown TS secondary clarification
eqn_isbwas_ve = (158)*qconisbwas_capacity_mgd; % incinerator scrubber blowdown TS WAS pumping, "+1,600 cuft" omitted.
eqn_gt_ve = 0; % gravity thickners for primary solids
eqn_gbt_ve = 0; % gravity belt thickeners for secondary solids
eqn_cent_ve = 0; % centrifuges
eqn_poly_ve = 0; % polymer feed system
eqn_inc_ve = 0; % incinerator
eqn_ah_ve = 0; % ash hauling

% SECTION 3.1.2
% ------- VOLUME OF SLAB CONCRETE (VSC), ALL IN UNITS OF "CUFT"
eqn_pc_vsc = 34600;  % primary clarifier
eqn_psp_vsc = 0;  % primary sludge pumping
eqn_sc_vsc = 0;  % secondary clarifier
eqn_stbnr_vsc = (537.0)*(l_ana_ft + l_anx1_ft + l_aer1a_ft) + (61889);  % 5-stage Bardenpho, new reactors
eqn_stber_vsc = 0;  % 5-stage Bardenpho, existing reactors
eqn_stbcr_vsc = 0;  % 5-stage Bardenpho, combined (new + existing) reactors
eqn_stbras_vsc = 0;  % 5-stage Bardenpho, RAS pumping
eqn_stbir_vsc = 0;  % 5-stage Bardenpho, internal recycle pumping
eqn_stbwas_vsc = 0;  % 5-stage Bardenpho, WAS pumping
eqn_blo_vsc = 0;  % blowers
eqn_df1_vsc = (3.20)*eqn_df_size_ft2 + (13081);  % denitrification filters - configuration 1
eqn_cct_vsc = 0;  % chlorine contact tank
eqn_isbpfr_vsc = 6313;  % incinerator scrubber blowdown TS plug flow reactor
eqn_isbras_vsc = 0;  % incinerator scrubber blowdown TS RAS pumping
eqn_isbsc_vsc = 2720;  % incinerator scrubber blowdown TS secondary clarification
eqn_isbwas_vsc = 0;  % incinerator scrubber blowdown TS WAS pumping
eqn_gt_vsc = 0;  % gravity thickners for primary solids
eqn_gbt_vsc = 0;  % gravity belt thickeners for secondary solids
eqn_cent_vsc = 0;  % centrifuges
eqn_poly_vsc = 0;  % polymer feed system
eqn_inc_vsc = 0;  % incinerator
eqn_ah_vsc = 0;  % ash hauling

% SECTION 3.1.3
% ------- VOLUME OF WALL CONCRETE (VWC), ALL IN UNITS OF "CUFT"
eqn_pc_vwc = 16900;  % primary clarifier
```

```
eqn_psp_vwc = 0;  % primary sludge pumping
eqn_sc_vwc = 0;  % secondary clarifier
eqn_stbnr_vwc = (233.0)*(l_ana_ft + l_anx1_ft + l_aer1a_ft) + (17443);  % 5-stage Bardenpho, new reactors
eqn_stber_vwc = 10200;  % 5-stage Bardenpho, existing reactors - new baffles
eqn_stbcr_vwc = 0;  % 5-stage Bardenpho, combined (new + existing) reactors
eqn_stbras_vwc = 0;  % 5-stage Bardenpho, RAS pumping
eqn_stbir_vwc = 0;  % 5-stage Bardenpho, internal recycle pumping
eqn_stbwas_vwc = 0;  % 5-stage Bardenpho, WAS pumping
eqn_blo_vwc = 0;  % blowers
eqn_df1_vwc = (1.73)*eqn_df_size_ft2 + (13296);  % denitrification filters - configuration 1
eqn_cct_vwc = 0;  % chlorine contact tank
eqn_isbpfr_vwc = 5652;  % incinerator scrubber blowdown TS plug flow reactor
eqn_isbras_vwc = 0;  % incinerator scrubber blowdown TS RAS pumping
eqn_isbsc_vwc = 4858;  % incinerator scrubber blowdown TS secondary clarification
eqn_isbwas_vwc = 0;  % incinerator scrubber blowdown TS WAS pumping
eqn_gt_vwc = 0;  % gravity thickners for primary solids
eqn_gbt_vwc = 0;  % gravity belt thickeners for secondary solids
eqn_cent_vwc = 0;  % centrifuges
eqn_poly_vwc = 0;  % polymer feed system
eqn_inc_vwc = 0;  % incinerator
eqn_ah_vwc = 0;  % ash hauling

% SECTION 3.1.4
% ------- BUILDING AREA (BA), ALL IN UNITS OF "SQFT"
% Note:  For RAS, WAS, and Internal Recycle pumping, all best fit equations
% are linear with an intercept at 200 sqft.  This value was not included
% for each individual set of pumping as there would be a significant amount
% of building sharing for RAS/WAS/IR pumps.  As such, only one
% 200 sqft was included for the secondary treatment process pumping and
% one 200 sqft was included for the ISB Treatment System pumping.
eqn_pc_ba = 0;  % primary clarifier
eqn_psp_ba = 202;  % primary sludge pumping
eqn_sc_ba = 0;  % secondary clarifier
eqn_stbnr_ba = 0;  % 5-stage Bardenpho, new reactors
eqn_stber_ba = 0;  % 5-stage Bardenpho, existing reactors
eqn_stbcr_ba = 0;  % 5-stage Bardenpho, combined (new + existing) reactors
eqn_stbras_ba = 0;  % 5-stage Bardenpho, RAS pumping
eqn_stbir_ba = ((19.7)*(q_internal_capacity_mgd))*unit_dual_internal_recycle + (200);  % 5-stage Bardenpho, internal recycle pumping
eqn_stbwas_ba = 0;  % 5-stage Bardenpho, WAS pumping
eqn_blo_ba = 0;  % blowers
eqn_df1_ba = (19.7)*eqn_df_bwip_capacity_mgd + 200;  % denitrification filters - configuration 1
eqn_cct_ba = 0;  % chlorine contact tank
eqn_isbpfr_ba = 0;  % incinerator scrubber blowdown TS plug flow reactor
eqn_isbras_ba = (39.4)*qconisbras_capacity_mgd + (200);  % incinerator scrubber blowdown TS RAS pumping
eqn_isbsc_ba = 0;  % incinerator scrubber blowdown TS secondary clarification
eqn_isbwas_ba = (19.7)*qconisbwas_capacity_mgd;  % incinerator scrubber blowdown TS WAS pumping;
"+ 200 sqft" omitted.
eqn_gt_ba = 0;  % gravity thickners for primary solids
if qconisbwas_capacity_mgd < 0.288;
    eqn_gbt_ba = 2860; % two 1m GBTs, gravity belt thickeners for secondary solids
elseif qconisbwas_capacity_mgd < 0.576;
    eqn_gbt_ba = 3250; % two 2m GBTs, gravity belt thickeners for secondary solids
elseif qconisbwas_capacity_mgd < 1.152;
```

```
    eqn_gbt_ba = 3575; % three 2m GBTs, gravity belt thickeners for secondary solids
else
    eqn_gbt_ba = 3900; % four 2m GBTs, gravity belt thickeners for secondary solids
end
eqn_cent_ba = 0;  % centrifuges
eqn_poly_ba = 0;  % polymer feed system
eqn_inc_ba = 0;  % incinerator
eqn_ah_ba = 0;  % ash hauling

% SECTION 3.1.5
% ------- ELECTRICAL ENERGY (EE), ALL IN UNITS OF "KWH/YR"
eqn_pc_ee = 13100;  % primary clarifier
eqn_psp_ee = (33716)*q_primunder_mgd + 2.4;  % primary sludge pumping
eqn_sc_ee = 19654;  % secondary clarifier
eqn_stbnr_ee = 0;  % 5-stage Bardenpho, new reactors
eqn_stber_ee = 0;  % 5-stage Bardenpho, existing reactors
eqn_stbcr_ee = eqn_stbcr_ee_an;  % 5-stage Bardenpho, combined (new + existing) reactors
eqn_stbras_ee = (33167)*qconras_operation_mgd + (1648);  % 5-stage Bardenpho, RAS pumping
eqn_stbir_ee = (33093)*(q_internal_operation_mgd) + (4189);  % 5-stage Bardenpho, internal↙
recycle pumping
eqn_stbwas_ee = (33501)*qconrctrwas_operation_mgd + 23.4;  % 5-stage Bardenpho, WAS pumping
eqn_blo_ee = eqn_stbcr_ee_aer;  % blowers (energy attributed to aerobic reactors)
eqn_df1_ee = (33259)*denit_backwash_flow_avg_mgd + 119;  % denitrification filters -↙
configuration 1
eqn_cct_ee = 157550;  % chlorine contact tank
eqn_isbpfr_ee = 200920;  % incinerator scrubber blowdown TS plug flow reactor
eqn_isbras_ee = (33425)*qconisbras_operation_mgd + (55);  % incinerator scrubber blowdown TS RAS↙
pumping
eqn_isbsc_ee = 7852;  % incinerator scrubber blowdown TS secondary clarification
eqn_isbwas_ee = (33501)*qconisbwas_operation_mgd + (23.4);  % incinerator scrubber blowdown TS↙
WAS pumping
eqn_gt_ee = 8890;  % gravity thickners for primary solids
eqn_gbt_ee = (422832)*(qconisbwas_operation_mgd^0.9248);  % gravity belt thickeners for secondary↙
solids
eqn_cent_ee = (5024825)*qcentinf_avg_mgd + (39693);  % centrifuges
eqn_poly_ee = 0;  % polymer feed system
eqn_inc_ee = 242055;  % incinerator
eqn_ah_ee = 0;  % ash hauling

% Additional blower calculations
eqn_blo_ee_tunable = (qair_tunableblowers_delivered_mgd)*scfm_per_mgd*241.6;
eqn_blo_ee_3fixed = (qair_3fixedblowers_delivered_mgd)*scfm_per_mgd*241.6;
eqn_blo_ee_4fixed = (qair_4fixedblowers_delivered_mgd)*scfm_per_mgd*241.6;
eqn_blo_ee_3_1_fixed = (qair_3_1_fixedblowers_delivered_mgd)*scfm_per_mgd*241.6;

% SECTION 3.1.6
% ------- CHLORINE (CL), ALL IN UNITS OF "LBS/YR"
eqn_pc_cl = 0;  % primary clarifier
eqn_psp_cl = 0;  % primary sludge pumping
eqn_sc_cl = 0;  % secondary clarifier
eqn_stbnr_cl = 0;  % 5-stage Bardenpho, new reactors
eqn_stber_cl = 0;  % 5-stage Bardenpho, existing reactors
eqn_stbcr_cl = 0;  % 5-stage Bardenpho, combined (new + existing) reactors
eqn_stbras_cl = 0;  % 5-stage Bardenpho, RAS pumping
eqn_stbir_cl = 0;  % 5-stage Bardenpho, internal recycle pumping
eqn_stbwas_cl = 0;  % 5-stage Bardenpho, WAS pumping
```

```
eqn_blo_cl = 0;  % blowers
eqn_df1_cl = 0;  % denitrification filters - configuration 1
eqn_cct_cl = qfiltereff_avg_mgd*cl_dose*365.25;  % chlorine contact tank
eqn_isbpfr_cl = 0;  % incinerator scrubber blowdown TS plug flow reactor
eqn_isbras_cl = 0;  % incinerator scrubber blowdown TS RAS pumping
eqn_isbsc_cl = 0;  % incinerator scrubber blowdown TS secondary clarification
eqn_isbwas_cl = 0;  % incinerator scrubber blowdown TS WAS pumping
eqn_gt_cl = 0;  % gravity thickners for primary solids
eqn_gbt_cl = 0;  % gravity belt thickeners for secondary solids
eqn_cent_cl = 0;  % centrifuges
eqn_poly_cl = 0;  % polymer feed system
eqn_inc_cl = 0;  % incinerator
eqn_ah_cl = 0;  % ash hauling

% SECTION 3.1.7
% ------- POLYMER (PY), ALL IN UNITS OF "LBS/YR"
eqn_pc_py = 0;  % primary clarifier
eqn_psp_py = 0;  % primary sludge pumping
eqn_sc_py = 0;  % secondary clarifier
eqn_stbnr_py = 0;  % 5-stage Bardenpho, new reactors
eqn_stber_py = 0;  % 5-stage Bardenpho, existing reactors
eqn_stbcr_py = 0;  % 5-stage Bardenpho, combined (new + existing) reactors
eqn_stbras_py = 0;  % 5-stage Bardenpho, RAS pumping
eqn_stbir_py = 0;  % 5-stage Bardenpho, internal recycle pumping
eqn_stbwas_py = 0;  % 5-stage Bardenpho, WAS pumping
eqn_blo_py = 0;  % blowers
eqn_df1_py = 0;  % denitrification filters - configuration 1
eqn_cct_py = 0;  % chlorine contact tank
eqn_isbpfr_py = 0;  % incinerator scrubber blowdown TS plug flow reactor
eqn_isbras_py = 0;  % incinerator scrubber blowdown TS RAS pumping
eqn_isbsc_py = 0;  % incinerator scrubber blowdown TS secondary clarification
eqn_isbwas_py = 0;  % incinerator scrubber blowdown TS WAS pumping
eqn_gt_py = 0;  % gravity thickners for primary solids
eqn_gbt_py = qconisbwas_operation_mgd*xisbwas_avg*lbs_mg_per_mg_L*py_dose_gbt*365.25;    %
gravity belt thickeners for secondary solids
eqn_cent_py = 0;  % centrifuges
eqn_poly_py = qcentinf_avg_mgd*xcentinf_conc_avg*lbs_mg_per_mg_L*py_dose_cent*365.25;  % polymer
feed system
eqn_inc_py = 0;  % incinerator
eqn_ah_py = 0;  % ash hauling

% SECTION 3.1.8
% ------- SAND (SD), ALL IN UNITS OF "LBS"
eqn_pc_sd = 0;  % primary clarifier
eqn_psp_sd = 0;  % primary sludge pumping
eqn_sc_sd = 0;  % secondary clarifier
eqn_stbnr_sd = 0;  % 5-stage Bardenpho, new reactors
eqn_stber_sd = 0;  % 5-stage Bardenpho, existing reactors
eqn_stbcr_sd = 0;  % 5-stage Bardenpho, combined (new + existing) reactors
eqn_stbras_sd = 0;  % 5-stage Bardenpho, RAS pumping
eqn_stbir_sd = 0;  % 5-stage Bardenpho, internal recycle pumping
eqn_stbwas_sd = 0;  % 5-stage Bardenpho, WAS pumping
eqn_blo_sd = 0;  % blowers
eqn_df1_sd = sand_lbs_per_cuft*eqn_df_size_ft2*6;  % denitrification filters
eqn_cct_sd = 0;  % chlorine contact tank
eqn_isbpfr_sd = 0;  % incinerator scrubber blowdown TS plug flow reactor
```

```
eqn_isbras_sd = 0;  % incinerator scrubber blowdown TS RAS pumping
eqn_isbsc_sd = 0;  % incinerator scrubber blowdown TS secondary clarification
eqn_isbwas_sd = 0;  % incinerator scrubber blowdown TS WAS pumping
eqn_gt_sd = 0;  % gravity thickners for primary solids
eqn_gbt_sd = 0;  % gravity belt thickeners for secondary solids
eqn_cent_sd = 0;  % centrifuges
eqn_poly_sd = 0;  % polymer feed system
eqn_inc_sd = 0;  % incinerator
eqn_ah_sd = 0;  % ash hauling

% SECTION 3.1.9
% ------- METHANOL (MEOH), ALL IN UNITS OF "LBS/YR"
% NOTE:  This is actually acetate.  Methanol was not degrading properly in
% the GPS-X simulations and methylotrophs weren't growing, so we switched
% to acetate addition for denitrification in the ANX2 zone and on the denit
% filters.
eqn_pc_hac = 0;  % primary clarifier
eqn_psp_hac = 0;  % primary sludge pumping
eqn_sc_hac = 0;  % secondary clarifier
eqn_stbnr_hac = 0;  % 5-stage Bardenpho, new reactors
eqn_stber_hac = 0;  % 5-stage Bardenpho, existing reactors
eqn_stbcr_hac = qconhacrctrc_avg*g_per_m3_hac*lbs_per_g*365.25; % m3/d * g/m3 * lbs/g * d/yr
eqn_stbras_hac = 0;  % 5-stage Bardenpho, RAS pumping
eqn_stbir_hac = 0;  % 5-stage Bardenpho, internal recycle pumping
eqn_stbwas_hac = 0;  % 5-stage Bardenpho, WAS pumping
eqn_blo_hac = 0;  % blowers
eqn_df1_hac = qconhacdf_avg*g_per_m3_hac*lbs_per_g*365.25; % m3/d * g/m3 * lbs/g * d/yr  %↙
denitrification filters
eqn_cct_hac = 0;  % chlorine contact tank
eqn_isbpfr_hac = 0;  % incinerator scrubber blowdown TS plug flow reactor
eqn_isbras_hac = 0;  % incinerator scrubber blowdown TS RAS pumping
eqn_isbsc_hac = 0;  % incinerator scrubber blowdown TS secondary clarification
eqn_isbwas_hac = 0;  % incinerator scrubber blowdown TS WAS pumping
eqn_gt_hac = 0;  % gravity thickners for primary solids
eqn_gbt_hac = 0;  % gravity belt thickeners for secondary solids
eqn_cent_hac = 0;  % centrifuges
eqn_poly_hac = 0;  % polymer feed system
eqn_inc_hac = 0;  % incinerator
eqn_ah_hac = 0;  % ash hauling

% SECTION 3.1.10
% ------- FUEL OIL (FO), ALL IN UNITS OF "GAL/YR"
eqn_pc_fo = 0;  % primary clarifier
eqn_psp_fo = 0;  % primary sludge pumping
eqn_sc_fo = 0;  % secondary clarifier
eqn_stbnr_fo = 0;  % 5-stage Bardenpho, new reactors
eqn_stber_fo = 0;  % 5-stage Bardenpho, existing reactors
eqn_stbcr_fo = 0;  % 5-stage Bardenpho, combined (new + existing) reactors
eqn_stbras_fo = 0;  % 5-stage Bardenpho, RAS pumping
eqn_stbir_fo = 0;  % 5-stage Bardenpho, internal recycle pumping
eqn_stbwas_fo = 0;  % 5-stage Bardenpho, WAS pumping
eqn_blo_fo = 0;  % blowers
eqn_df1_fo = 0;  % denitrification filters - configuration 1
eqn_cct_fo = 0;  % chlorine contact tank
eqn_isbpfr_fo = 0;  % incinerator scrubber blowdown TS plug flow reactor
eqn_isbras_fo = 0;  % incinerator scrubber blowdown TS RAS pumping
```

```
eqn_isbsc_fo = 0;  % incinerator scrubber blowdown TS secondary clarification
eqn_isbwas_fo = 0;  % incinerator scrubber blowdown TS WAS pumping
eqn_gt_fo = 0;  % gravity thickners for primary solids
eqn_gbt_fo = 0;  % gravity belt thickeners for secondary solids
eqn_cent_fo = 0;  % centrifuges
eqn_poly_fo = 0;  % polymer feed system
eqn_inc_fo = qcentcake_avg_mgd*xcentcake_conc_avg*(lbs_mg_per_mg_L/2000)*fo_dose_inc*365.25;  %↙
incinerator; "fo_dose_inc" is in units of gallons per 2,000 lbs of dry solids.
eqn_ah_fo = 0;  % ash hauling

% SECTION 3.1.11
% ------- NATURAL GAS (NG), ALL IN UNITS OF "1,000 CUFT/YR"
eqn_pc_ng = 0;  % primary clarifier
eqn_psp_ng = 0;  % primary sludge pumping
eqn_sc_ng = 0;  % secondary clarifier
eqn_stbnr_ng = 0;  % 5-stage Bardenpho, new reactors
eqn_stber_ng = 0;  % 5-stage Bardenpho, existing reactors
eqn_stbcr_ng = 0;  % 5-stage Bardenpho, combined (new + existing) reactors
eqn_stbras_ng = 0;  % 5-stage Bardenpho, RAS pumping
eqn_stbir_ng = 0;  % 5-stage Bardenpho, internal recycle pumping
eqn_stbwas_ng = 0;  % 5-stage Bardenpho, WAS pumping
eqn_blo_ng = 0;  % blowers
eqn_df1_ng = 0;  % denitrification filters - configuration 1
eqn_cct_ng = 0;  % chlorine contact tank
eqn_isbpfr_ng = 0;  % incinerator scrubber blowdown TS plug flow reactor
eqn_isbras_ng = 0;  % incinerator scrubber blowdown TS RAS pumping
eqn_isbsc_ng = 0;  % incinerator scrubber blowdown TS secondary clarification
eqn_isbwas_ng = 0;  % incinerator scrubber blowdown TS WAS pumping
eqn_gt_ng = 0;  % gravity thickners for primary solids
eqn_gbt_ng = 0;  % gravity belt thickeners for secondary solids
eqn_cent_ng = 0;  % centrifuges
eqn_poly_ng = 0;  % polymer feed system
eqn_inc_ng = qcentcake_avg_mgd*xcentcake_conc_avg*(lbs_mg_per_mg_L/2000)*ng_dose_inc*365.25;  %↙
incinerator; "ng_dose_inc" is in units of gallons per 2,000 lbs of dry solids.
eqn_ah_ng = 0;  % ash hauling

% SECTION 3.1.12
% ------- ASH PRODUCED (AP), ALL IN UNITS OF "CUYD/YR"
eqn_pc_ap = 0;  % primary clarifier
eqn_psp_ap = 0;  % primary sludge pumping
eqn_sc_ap = 0;  % secondary clarifier
eqn_stbnr_ap = 0;  % 5-stage Bardenpho, new reactors
eqn_stber_ap = 0;  % 5-stage Bardenpho, existing reactors
eqn_stbcr_ap = 0;  % 5-stage Bardenpho, combined (new + existing) reactors
eqn_stbras_ap = 0;  % 5-stage Bardenpho, RAS pumping
eqn_stbir_ap = 0;  % 5-stage Bardenpho, internal recycle pumping
eqn_stbwas_ap = 0;  % 5-stage Bardenpho, WAS pumping
eqn_blo_ap = 0;  % blowers
eqn_df1_ap = 0;  % denitrification filters - configuration 1
eqn_cct_ap = 0;  % chlorine contact tank
eqn_isbpfr_ap = 0;  % incinerator scrubber blowdown TS plug flow reactor
eqn_isbras_ap = 0;  % incinerator scrubber blowdown TS RAS pumping
eqn_isbsc_ap = 0;  % incinerator scrubber blowdown TS secondary clarification
eqn_isbwas_ap = 0;  % incinerator scrubber blowdown TS WAS pumping
eqn_gt_ap = 0;  % gravity thickners for primary solids
eqn_gbt_ap = 0;  % gravity belt thickeners for secondary solids
```

```
eqn_cent_ap = 0;  % centrifuges
eqn_poly_ap = 0;  % polymer feed system
eqn_inc_ap = qcentcake_avg_mgd*xcentcake_conc_avg*(lbs_mg_per_mg_L/2000)*ap_by_inc*365.25;  %↙
incinerator; "ap_by_inc" is in units of gallons per 2,000 lbs of dry solids.
eqn_ah_ap = 0;  % ash hauling

% SECTION 3.2
% ------------------ INTERMEDIATE COST CALCULATIONS -----------------------
eqn_stbnr_cost_e = eqn_stbnr_ve*unit_excavat;
eqn_stbnr_cost_cw = eqn_stbnr_vwc*unit_wall;
eqn_stber_cost_cw = eqn_stber_vwc*unit_wall;
eqn_stbnr_cost_cs = eqn_stbnr_vsc*unit_slab;
eqn_stbnr_cost_hr = (10.0*(l_ana_ft + l_anx1_ft + l_aer1a_ft) + 406)*unit_hand;

eqn_stbcr_cost_d = ((qairstandlrctreff_blower_capacity_mgd*scfm_per_mgd)/scfm_per_diffuser)↙
*unit_diffus; % conversions of scfm_per_mgd scfm/MGD
eqn_stbcr_cost_h = ((qairstandlrctreff_blower_capacity_mgd*scfm_per_mgd)/scfm_per_header)↙
*unit_head; % cost of air headers
eqn_stbcr_imh_aer = ((qairstandlrctreff_blower_capacity_mgd*scfm_per_mgd)/scfm_per_header)↙
*unit_headtime; % construction labor (person-hrs) for header installation
eqn_stbcr_ch_aer = eqn_stbcr_imh_aer*unit_cranetime; % crane-hours required for air equipment↙
installation
eqn_stbcr_cost_ap = 1.2*28.59*(((qairstandlrctreff_blower_capacity_mgd)*scfm_per_mgd*20/6)^0.↙
8085)*(cepcip/241); % 20/6 is diffused air correction used by Hydromantis
eqn_stbcr_iec_aer = ((eqn_stbcr_cost_d + eqn_stbcr_cost_h)*(1 + pmincaer)) +↙
(eqn_stbcr_imh_aer*unit_conlab) + (eqn_stbcr_ch_aer*unit_crane);

eqn_stbnr_hp_anam = (0.00475/133.68)*(1.197^0.3)*(xlrctr_mixer_sizing^0.298)*(l_ana_ft*15*53); %↙
total horsepower of mixers in each anerobic zone
eqn_stbnr_hp_anx1m = (0.00475/133.68)*(1.197^0.3)*(xlrctr_mixer_sizing^0.298)*(l_anx1_ft*15*53);↙
% total horsepower of mixers in each anoxic 1 zone
eqn_stber_hp_anx2m = (0.00475/133.68)*(1.197^0.3)*(xlrctr_mixer_sizing^0.298)*(l_anx2_ft*15*25);↙
% total horsepower of mixers in each anoxic 2 zone
eqn_stbnr_n_anam = (eqn_stbnr_hp_anam/5.0)*6; % Number of Mixers Required for Anaerobic Zones
eqn_stbnr_n_anx1m = (eqn_stbnr_hp_anx1m/5.0)*6; % Number of Mixers Required for Anoxic 1 Zones
eqn_stber_n_anx2m = (eqn_stber_hp_anx2m/5.0)*12; % Number of Mixers Required for Anoxic 2 Zones
eqn_stbnr_rsx_mana = 0.67 + 0.067*(eqn_stbnr_hp_anam/eqn_stbnr_n_anam); % cost ratio, will be↙
fixed since number of mixers has been made continuous (not discrete)
eqn_stbnr_rsx_manx1 = 0.67 + 0.067*(eqn_stbnr_hp_anx1m/eqn_stbnr_n_anx1m);
eqn_stber_rsx_manx2 = 0.67 + 0.067*(eqn_stber_hp_anx2m/eqn_stber_n_anx2m);
eqn_stbnr_cost_m = ((eqn_stbnr_n_anam*eqn_stbnr_rsx_mana) +↙
(eqn_stbnr_n_anx1m*eqn_stbnr_rsx_manx1))*unit_mix; % Total Purchase Cost of Mixers for new↙
reactors ($)
eqn_stber_cost_m = (eqn_stber_n_anx2m*eqn_stber_rsx_manx2)*unit_mix; % Total Purchase Cost of↙
Mixers for existing reactors ($)
eqn_stbnr_imh_an = (61.3 + (0.18*(eqn_stbnr_hp_anam/eqn_stbnr_n_anam)))*eqn_stbnr_n_anam + (61.3↙
+ (0.18*(eqn_stbnr_hp_anx1m/eqn_stbnr_n_anx1m)))*eqn_stbnr_n_anx1m; % Labor for Anaerobic/Anoxic↙
Equipment Installation (person-hrs)
eqn_stber_imh_an = (61.3 + (0.18*(eqn_stber_hp_anx2m/eqn_stber_n_anx2m)))*eqn_stber_n_anx2m;
eqn_stbnr_ch_an = eqn_stbnr_imh_an*unit_cranetime; % Crane Rental time for Anaerobic/Anoxic↙
Equipment Installation
eqn_stber_ch_an = eqn_stber_imh_an*unit_cranetime; % Crane Rental time for Anaerobic/Anoxic↙
Equipment Installation
eqn_stbnr_iec_an = (eqn_stbnr_cost_m*(1 + pmincan)) + (eqn_stbnr_imh_an*unit_conlab) +↙
(eqn_stbnr_ch_an*unit_crane);
eqn_stber_iec_an = (eqn_stber_cost_m*(1 + pmincan)) + (eqn_stber_imh_an*unit_conlab) +↙
```

```
(eqn_stber_ch_an*unit_crane);

eqn_stber_ac_cost_e = 0; % DELETED eqn_stber_ac_cost_e = (787350)*unit_excavat; % Unobserved Cost of Earthwork to Replace Existing Reactors
eqn_stber_ac_cost_cw = 0; % DELETED eqn_stber_ac_cost_cw = (72700)*unit_wall; % Unobserved Cost of Concrete Walls to Replace Existing Reactors
eqn_stber_ac_cost_cs = 0; % DELETED eqn_stber_ac_cost_cs = (127890)*unit_slab; % Unobserved Cost of Concrete Slab to Replace Existing Reactors
eqn_stber_ac_cost_hr = 0; % DELETED eqn_stber_ac_cost_hr = (2660)*unit_hand; % Unobserved Cost of Handrails to Replace Existing Reactors

eqn_stbnr_ic_str = (eqn_stbnr_cost_e + eqn_stbnr_cost_cw + eqn_stbnr_cost_cs + eqn_stbnr_cost_hr)*(1 + cf); % Initial Cost of Structure
eqn_stber_ic_str = (eqn_stber_ac_cost_e + eqn_stber_ac_cost_cw + eqn_stber_ac_cost_cs + eqn_stber_ac_cost_hr)*(1 + cf); % Unobserved initial cost of existing structure
eqn_stbcr_ic_h = (eqn_stbcr_cost_h*(1 + pmincaer) + (eqn_stbcr_imh_aer*unit_conlab) + (eqn_stbcr_ch_aer*unit_crane))*(1 + cf); % Initial Cost of Headers (for amortization calcs)
eqn_stbcr_ic_d = (eqn_stbcr_cost_d)*(1 + pmincaer)*(1 + cf); % Initial Cost of diffusers (for amortization calcs)
eqn_stbcr_ic_ap = eqn_stbcr_cost_ap*(1 + cf); % Initial cost of air piping (for amortization calcs)
eqn_stbnr_ic_m = ((eqn_stbnr_cost_m*(1 + pmincan)) + (eqn_stbnr_imh_an*unit_conlab) + (eqn_stbnr_ch_an*unit_crane))*(1 + cf); % initial cost of mixers (for amortization calcs)
eqn_stber_ic_m = ((eqn_stber_cost_m*(1 + pmincan)) + (eqn_stber_imh_an*unit_conlab) + (eqn_stber_ch_an*unit_crane))*(1 + cf); % initial cost of mixers (for amortization calcs)
eqn_stbnr_rc_str = eqn_stbnr_ic_str*(1/((1 + interest)^40)); % Replacement Cost of Structure
eqn_stber_rc_str = eqn_stber_ic_str*(1/((1 + interest)^40)); % Replacement Cost of Structure
eqn_stbcr_rc_h = eqn_stbcr_ic_h*(1/((1 + interest)^40)); % Replacement Cost of headers
eqn_stbcr_rc_d = eqn_stbcr_ic_d*((1/((1 + interest)^10)) + (1/((1 + interest)^20)) + (1/((1 + interest)^30)) + (1/((1 + interest)^40))); % Replacement Cost of diffusers
eqn_stbcr_rc_ap = eqn_stbcr_ic_ap*(1/((1 + interest)^40)); % Replacement Cost of air piping
eqn_stbnr_rc_m = eqn_stbnr_ic_m*((1/((1 + interest)^20)) + (1/((1 + interest)^40))) ; % Replacement Cost of mixers
eqn_stber_rc_m = eqn_stber_ic_m*((1/((1 + interest)^20)) + (1/((1 + interest)^40))) ; % Replacement Cost of mixers

eqn_stbnr_ac_str = (eqn_stbnr_ic_str + eqn_stbnr_rc_str)*((interest/(((1 + interest)^40) - 1)) + interest); % amortization cost of structure
eqn_stber_ac_str = (eqn_stber_ic_str + eqn_stber_rc_str)*((interest/(((1 + interest)^40) - 1)) + interest); % amortization cost of structure
eqn_stbcr_ac_h = (eqn_stbcr_ic_h + eqn_stbcr_rc_h)*((interest/(((1 + interest)^40) - 1)) + interest); % amortization cost of air headers
eqn_stbcr_ac_d = (eqn_stbcr_ic_d + eqn_stbcr_rc_d)*((interest/(((1 + interest)^40) - 1)) + interest); % amortization cost of diffusers
eqn_stbcr_ac_ap = (eqn_stbcr_ic_ap + eqn_stbcr_rc_ap)*((interest/(((1 + interest)^40) - 1)) + interest); % amortization cost of air piping
eqn_stbnr_ac_m = (eqn_stbnr_ic_m + eqn_stbnr_rc_m)*((interest/(((1 + interest)^40) - 1)) + interest); % amortization cost of mixers
eqn_stber_ac_m = (eqn_stber_ic_m + eqn_stber_rc_m)*((interest/(((1 + interest)^40) - 1)) + interest); % amortization cost of mixers


% SECTION 3.3
% ------------------ SOURCES OF COSTS -----------------------------------

% SECTION 3.3.1
```

```
% ------- CONSTRUCTION & EQUIPMENT COST (CEC), ALL IN UNITS OF "$"
eqn_pc_cec = 1680000;  % primary clarifier
eqn_psp_cec = 39200;  % primary sludge pumping
eqn_sc_cec = 0;  % secondary clarifier
eqn_stbnr_cec = 0;  % 5-stage Bardenpho, new reactors
eqn_stber_cec = 0;  % 5-stage Bardenpho, existing reactors
eqn_stbcr_cec = (eqn_stbnr_cost_e + eqn_stbnr_cost_cw + eqn_stbnr_cost_cs + eqn_stbnr_cost_hr +↙
eqn_stbcr_cost_ap ...
    + eqn_stbcr_iec_aer + eqn_stbnr_iec_an + eqn_stber_cost_cw + eqn_stber_iec_an)*(1 + cf);  %↙
5-stage Bardenpho, combined (new + existing) reactors
eqn_stbras_cec = (96763)*((qconras_capacity_mgd - q_ras_existing_capacity)^0.3697);  % 5-stage↙
Bardenpho, RAS pumping
eqn_stbir_cec = ((117886)*(q_internal_capacity_mgd^0.9277))*unit_dual_internal_recycle;  % 5-↙
stage Bardenpho, internal recycle pumping
eqn_stbwas_cec = 0;  % 5-stage Bardenpho, WAS pumping
eqn_blo_cec = ((7021)*(((qairstandlrctreff_blower_capacity_mgd)*scfm_per_mgd)^0.5067))↙
*unit_blower;  % blowers
eqn_df1_cec = (255.7)*eqn_df_size_ft2 + (567229);  % denitrification filters - configuration 1
eqn_cct_cec = 0;  % chlorine contact tank
eqn_isbpfr_cec = 357130;  % incinerator scrubber blowdown TS plug flow reactor
eqn_isbras_cec = (93800)*(qconisbras_capacity_mgd^0.3345);  % incinerator scrubber blowdown TS↙
RAS pumping
eqn_isbsc_cec = 404840;  % incinerator scrubber blowdown TS secondary clarification
eqn_isbwas_cec = (69055)*(qconisbwas_capacity_mgd^0.2387);  % incinerator scrubber blowdown TS↙
WAS pumping
eqn_gt_cec = 0;  % gravity thickners for primary solids
if qconisbwas_capacity_mgd < 0.288;
    eqn_gbt_cec = 1149780; % two 1m GBTs, gravity belt thickeners for secondary solids
elseif qconisbwas_capacity_mgd < 0.576;
    eqn_gbt_cec = 1302300; % two 2m GBTs, gravity belt thickeners for secondary solids
elseif qconisbwas_capacity_mgd < 1.152;
    eqn_gbt_cec = 1836500; % three 2m GBTs, gravity belt thickeners for secondary solids
else
    eqn_gbt_cec = 2370700; % four 2m GBTs, gravity belt thickeners for secondary solids
end
eqn_cent_cec = 0;  % centrifuges
eqn_poly_cec = 0;  % polymer feed system
eqn_inc_cec = 0;  % incinerator
eqn_ah_cec = 0;  % ash hauling

% Additional blower calculations - Capital costs are by capacity.
eqn_blo_cec_tunable = ((7021)*(((qairstandlrctreff_blower_capacity_mgd)*scfm_per_mgd)^0.5067))↙
*unit_blower_tunable;
eqn_blo_cec_3fixed = ((7021)*(((qairstandlrctreff_blower_capacity_mgd)*scfm_per_mgd)^0.5067))↙
*unit_blower_standard;
eqn_blo_cec_4fixed = ((7021)*(((qairstandlrctreff_blower_capacity_mgd)*scfm_per_mgd)^0.5067))↙
*unit_blower_4fixed;
eqn_blo_cec_3_1_fixed = ((7021)*(((qairstandlrctreff_blower_capacity_mgd)*scfm_per_mgd)^0.5067))↙
*unit_blower_3_1_fixed;

% SECTION 3.3.2
% ------- OPERATIONAL LABOR COST COST (OLC), ALL IN UNITS OF "$/YR"
eqn_pc_olc = 41800;  % primary clarifier
eqn_psp_olc = 7910;  % primary sludge pumping
eqn_sc_olc = 63572;  % secondary clarifier
eqn_stbnr_olc = 0;  % 5-stage Bardenpho, new reactors
```

```
eqn_stber_olc = 0;  % 5-stage Bardenpho, existing reactors
eqn_stbcr_olc = ((242.4*((6*(eqn_stbnr_hp_anam) + 6*(eqn_stbnr_hp_anx1m) + 12*
(eqn_stber_hp_anx2m))^0.3731)))*unit_operator;  % 5-stage Bardenpho, combined (new + existing)
reactors
eqn_stbras_olc = (7360)*(qconras_operation_mgd^0.3350);  % 5-stage Bardenpho, RAS pumping
eqn_stbir_olc = (480)*q_internal_operation_mgd + 7448;  % 5-stage Bardenpho, internal recycle
pumping
eqn_stbwas_olc = (11000)*(qconrctrwas_operation_mgd^0.1285);  % 5-stage Bardenpho, WAS pumping
eqn_blo_olc = ((26.56*(((qairstandlrctreff_delivered_mgd)*scfm_per_mgd)^0.5038)))*unit_operator;
% blowers
eqn_df1_olc = (4345)*(qsecforward_avg_mgd^0.3332)*unit_operator;  % denitrification filters -
configuration 1
eqn_cct_olc = 40877;  % chlorine contact tank
eqn_isbpfr_olc = 21958;  % incinerator scrubber blowdown TS plug flow reactor
eqn_isbras_olc = (11000)*(qconisbras_operation_mgd^0.1285);  % incinerator scrubber blowdown TS
RAS pumping
eqn_isbsc_olc = 11288;  % incinerator scrubber blowdown TS secondary clarification
eqn_isbwas_olc = (11000)*(qconisbwas_operation_mgd^0.1285);  % incinerator scrubber blowdown TS
WAS pumping
eqn_gt_olc = 14400;  % gravity thickners for primary solids
eqn_gbt_olc = (55600)*qconisbwas_operation_mgd;  % gravity belt thickeners for secondary solids
eqn_cent_olc = (1542204)*(qcentinf_avg_mgd^0.8273);  % centrifuges
eqn_poly_olc = (281.3)*(eqn_poly_py^0.5624);  % polymer feed system
eqn_inc_olc = 136438;  % incinerator
eqn_ah_olc = (1.437)*eqn_inc_ap;  % ash hauling

% Additional blower calculations
eqn_blo_olc_tunable = ((26.56*(((qair_tunableblowers_delivered_mgd)*scfm_per_mgd)^0.5038)))
*unit_operator;  % blowers
eqn_blo_olc_3fixed = ((26.56*(((qair_3fixedblowers_delivered_mgd)*scfm_per_mgd)^0.5038)))
*unit_operator;  % blowers
eqn_blo_olc_4fixed = ((26.56*(((qair_4fixedblowers_delivered_mgd)*scfm_per_mgd)^0.5038)))
*unit_operator;  % blowers
eqn_blo_olc_3_1_fixed = ((26.56*(((qair_3_1_fixedblowers_delivered_mgd)*scfm_per_mgd)^0.5038)))
*unit_operator;  % blowers

% SECTION 3.3.3
% ------- MAINTENANCE LABOR COST (MLC), ALL IN UNITS OF "$/YR"
eqn_pc_mlc = 16400;  % primary clarifier
eqn_psp_mlc = 4360;  % primary sludge pumping
eqn_sc_mlc = 29191;  % secondary clarifier
eqn_stbnr_mlc = 0;  % 5-stage Bardenpho, new reactors
eqn_stber_mlc = 0;  % 5-stage Bardenpho, existing reactors
eqn_stbcr_mlc = ((42.6*((6*(eqn_stbnr_hp_anam) + 6*(eqn_stbnr_hp_anx1m) + 12*
(eqn_stber_hp_anx2m))^0.5956)))*unit_operator;  % 5-stage Bardenpho, combined (new + existing)
reactors
eqn_stbras_mlc = (4475)*(qconras_operation_mgd^0.3360);  % 5-stage Bardenpho, RAS pumping
eqn_stbir_mlc = (319)*q_internal_operation_mgd + 7563;  % 5-stage Bardenpho, internal recycle
pumping
eqn_stbwas_mlc = (7411)*(qconrctrwas_operation_mgd^0.1482);  % 5-stage Bardenpho, WAS pumping
eqn_blo_mlc = (6.05*(((qairstandlrctreff_delivered_mgd)*scfm_per_mgd)^0.6037))*unit_operator;  %
blowers
eqn_df1_mlc = (675)*(qsecforward_avg_mgd^0.727)*unit_operator;  % denitrification filters -
configuration 1
eqn_cct_mlc = 7413;  % chlorine contact tank
eqn_isbpfr_mlc = 11118;  % incinerator scrubber blowdown TS plug flow reactor
```

```
eqn_isbras_mlc = (6400)*(qconisbras_operation_mgd^0.1520);  % incinerator scrubber blowdown TS RAS pumping
eqn_isbsc_mlc = 6549;  % incinerator scrubber blowdown TS secondary clarification
eqn_isbwas_mlc = (7411)*(qconisbwas_operation_mgd^0.1482);  % incinerator scrubber blowdown TS WAS pumping
eqn_gt_mlc = 7550;  % gravity thickners for primary solids
eqn_gbt_mlc = (9229)*(qconisbwas_operation_mgd^1.084);  % gravity belt thickeners for secondary solids
eqn_cent_mlc = (216232)*(qcentinf_avg_mgd^0.8914);  % centrifuges
eqn_poly_mlc = 0;  % polymer feed system
eqn_inc_mlc = 47134;  % incinerator
eqn_ah_mlc = 0;  % ash hauling

% Additional blower calculations
eqn_blo_mlc_tunable = (6.05*(((qair_tunableblowers_delivered_mgd)*scfm_per_mgd)^0.6037))*unit_operator;
eqn_blo_mlc_3fixed = (6.05*(((qair_3fixedblowers_delivered_mgd)*scfm_per_mgd)^0.6037))*unit_operator;
eqn_blo_mlc_4fixed = (6.05*(((qair_4fixedblowers_delivered_mgd)*scfm_per_mgd)^0.6037))*unit_operator;
eqn_blo_mlc_3_1_fixed = (6.05*(((qair_3_1_fixedblowers_delivered_mgd)*scfm_per_mgd)^0.6037))*unit_operator;

% SECTION 3.3.4
% ------- MATERIAL & SUPPLY COST (MSC), ALL IN UNITS OF "$/YR"
eqn_pc_msc = 11200;  % primary clarifier
eqn_psp_msc = 265;  % primary sludge pumping
eqn_sc_msc = 24396;  % secondary clarifier
eqn_stbnr_msc = 0;  % 5-stage Bardenpho, new reactors
eqn_stber_msc = 0;  % 5-stage Bardenpho, existing reactors
eqn_stbcr_msc = eqn_stbcr_cec*((3.57*(26.6^(-0.2602)))/100);  % 5-stage Bardenpho, combined (new + existing) reactors
eqn_stbras_msc = (85.6)*(qconras_operation_mgd^1.067);  % 5-stage Bardenpho, RAS pumping
eqn_stbir_msc = (825)*(q_internal_operation_mgd^0.9277);  % 5-stage Bardenpho, internal recycle pumping
eqn_stbwas_msc = (483)*(qconrctrwas_operation_mgd^0.2385);  % 5-stage Bardenpho, WAS pumping
eqn_blo_msc = eqn_blo_cec*((3.57*(26.6^(-0.2602)))/100);  % blowers
eqn_df1_msc = 0.005*eqn_df1_cec;  % denitrification filters - configuration 1
eqn_cct_msc = 9990;  % chlorine contact tank
eqn_isbpfr_msc = 11908;  % incinerator scrubber blowdown TS plug flow reactor
eqn_isbras_msc = (657)*(qconisbras_operation_mgd^0.3345);  % incinerator scrubber blowdown TS RAS pumping
eqn_isbsc_msc = 4048;  % incinerator scrubber blowdown TS secondary clarification
eqn_isbwas_msc = (483)*(qconisbwas_operation_mgd^0.2385);  % incinerator scrubber blowdown TS WAS pumping
eqn_gt_msc = 2890;  % gravity thickners for primary solids
eqn_gbt_msc = 0;  % gravity belt thickeners for secondary solids
eqn_cent_msc = (373450)*(qcentinf_avg_mgd^0.9701);  % centrifuges
eqn_poly_msc = (0.151)*(eqn_poly_py^0.8563);  % polymer feed system
eqn_inc_msc = 158910;  % incinerator
eqn_ah_msc = (198.7)*(eqn_inc_ap^0.9229);  % ash hauling

% Additional blower calculations
eqn_blo_msc_tunable = eqn_blo_cec_tunable*((3.57*(26.6^(-0.2602)))/100);
eqn_blo_msc_3fixed = eqn_blo_cec_3fixed*((3.57*(26.6^(-0.2602)))/100);
eqn_blo_msc_4fixed = eqn_blo_cec_4fixed*((3.57*(26.6^(-0.2602)))/100);
```

```
eqn_blo_msc_3_1_fixed = eqn_blo_cec_3_1_fixed*((3.57*(26.6^(-0.2602)))/100);

% SECTION 3.3.5
% ------- CHEMICAL COST (CC), ALL IN UNITS OF "$/YR"
eqn_pc_cc = 0;  % primary clarifier
eqn_psp_cc = 0;  % primary sludge pumping
eqn_sc_cc = 0;  % secondary clarifier
eqn_stbnr_cc = 0;  % 5-stage Bardenpho, new reactors
eqn_stber_cc = 0;  % 5-stage Bardenpho, existing reactors
eqn_stbcr_cc = eqn_stbcr_hac*unit_hac + eqn_df_fecl3*unit_fecl3;  % 5-stage Bardenpho, combined
(new + existing) reactors
eqn_stbras_cc = 0;  % 5-stage Bardenpho, RAS pumping
eqn_stbir_cc = 0;  % 5-stage Bardenpho, internal recycle pumping
eqn_stbwas_cc = 0;  % 5-stage Bardenpho, WAS pumping
eqn_blo_cc = 0;  % blowers
eqn_df1_cc = eqn_df1_hac*unit_hac;  % denitrification filters - configuration 1
eqn_cct_cc = eqn_cct_cl*unit_hypo;  % chlorine contact tank
eqn_isbpfr_cc = 0;  % incinerator scrubber blowdown TS plug flow reactor
eqn_isbras_cc = 0;  % incinerator scrubber blowdown TS RAS pumping
eqn_isbsc_cc = 0;  % incinerator scrubber blowdown TS secondary clarification
eqn_isbwas_cc = 0;  % incinerator scrubber blowdown TS WAS pumping
eqn_gt_cc = 0;  % gravity thickners for primary solids
eqn_gbt_cc = eqn_gbt_py*unit_poly;  % gravity belt thickeners for secondary solids
eqn_cent_cc = 0;  % centrifuges
eqn_poly_cc = eqn_poly_py*unit_poly;  % polymer feed system
eqn_inc_cc = 0;  % incinerator
eqn_ah_cc = 0;  % ash hauling


% SECTION 3.3.6
% ------- ENERGY COST (EC), ALL IN UNITS OF "$/YR"
eqn_pc_ec = eqn_pc_ee*unit_elec;  % primary clarifier
eqn_psp_ec = eqn_psp_ee*unit_elec;  % primary sludge pumping
eqn_sc_ec = eqn_sc_ee*unit_elec;  % secondary clarifier
eqn_stbnr_ec = eqn_stbnr_ee*unit_elec;  % 5-stage Bardenpho, new reactors
eqn_stber_ec = eqn_stber_ee*unit_elec;  % 5-stage Bardenpho, existing reactors
eqn_stbcr_ec = eqn_stbcr_ee*unit_elec;  % 5-stage Bardenpho, combined (new + existing) reactors
eqn_stbras_ec = eqn_stbras_ee*unit_elec;  % 5-stage Bardenpho, RAS pumping
eqn_stbir_ec = eqn_stbir_ee*unit_elec;  % 5-stage Bardenpho, internal recycle pumping
eqn_stbwas_ec = eqn_stbwas_ee*unit_elec;  % 5-stage Bardenpho, WAS pumping
eqn_blo_ec = eqn_blo_ee*unit_elec;  % blowers
eqn_df1_ec = eqn_df1_ee*unit_elec;  % denitrification filters - configuration 1
eqn_cct_ec = eqn_cct_ee*unit_elec;  % chlorine contact tank
eqn_isbpfr_ec = eqn_isbpfr_ee*unit_elec;  % incinerator scrubber blowdown TS plug flow reactor
eqn_isbras_ec = eqn_isbras_ee*unit_elec;  % incinerator scrubber blowdown TS RAS pumping
eqn_isbsc_ec = eqn_isbsc_ee*unit_elec;  % incinerator scrubber blowdown TS secondary
clarification
eqn_isbwas_ec = eqn_isbwas_ee*unit_elec;  % incinerator scrubber blowdown TS WAS pumping
eqn_gt_ec = eqn_gt_ee*unit_elec;  % gravity thickners for primary solids
eqn_gbt_ec = eqn_gbt_ee*unit_elec;  % gravity belt thickeners for secondary solids
eqn_cent_ec = eqn_cent_ee*unit_elec;  % centrifuges
eqn_poly_ec = eqn_poly_ee*unit_elec;  % polymer feed system
eqn_inc_ec = eqn_inc_ee*unit_elec + eqn_inc_fo*unit_oil + eqn_inc_ng*unit_gas;  % incinerator
eqn_ah_ec = eqn_ah_ee*unit_elec;  % ash hauling

% Additional blower calculations
```

```
eqn_blo_ec_tunable = eqn_blo_ee_tunable*unit_elec;
eqn_blo_ec_3fixed = eqn_blo_ee_3fixed*unit_elec;
eqn_blo_ec_4fixed = eqn_blo_ee_4fixed*unit_elec;
eqn_blo_ec_3_1_fixed = eqn_blo_ee_3_1_fixed*unit_elec;

% SECTION 3.3.7
% ------- AMORTIZATION COST (AC), ALL IN UNITS OF "$/YR"
% Note:  Amortization costs are the annual cost associated with a loan at
% a fixed interest rate for specific capital and equipment costs.
% Amortization costs OR capital and equipment costs should be included in
% final calculations, but not both.  The present worth of the amortization
% costs is equivalent to the present worth of their associated capital and
% equipment costs.
eqn_pc_ac = eqn_pc_cec*((interest/(((1 + interest)^40) - 1)) + interest);  % primary clarifier
eqn_psp_ac = eqn_psp_cec*((interest/(((1 + interest)^40) - 1)) + interest);  % primary sludge↙
pumping
eqn_sc_ac = eqn_sc_cec*((interest/(((1 + interest)^40) - 1)) + interest);  % secondary clarifier
eqn_stbnr_ac = eqn_stbnr_cec*((interest/(((1 + interest)^40) - 1)) + interest);  % 5-stage↙
Bardenpho, new reactors
eqn_stber_ac = eqn_stber_cec*((interest/(((1 + interest)^40) - 1)) + interest);  % 5-stage↙
Bardenpho, existing reactors
eqn_stbcr_ac = eqn_stbcr_cec*((interest/(((1 + interest)^40) - 1)) + interest);  % 5-stage↙
Bardenpho, combined (new + existing) reactors
eqn_stbras_ac = eqn_stbras_cec*((interest/(((1 + interest)^40) - 1)) + interest);  % 5-stage↙
Bardenpho, RAS pumping
eqn_stbir_ac = eqn_stbir_cec*((interest/(((1 + interest)^40) - 1)) + interest);  % 5-stage↙
Bardenpho, internal recycle pumping
eqn_stbwas_ac = eqn_stbwas_cec*((interest/(((1 + interest)^40) - 1)) + interest);  % 5-stage↙
Bardenpho, WAS pumping
eqn_blo_ac = eqn_blo_cec*((interest/(((1 + interest)^40) - 1)) + interest); % blowers
eqn_df1_ac = eqn_df1_cec*((interest/(((1 + interest)^40) - 1)) + interest);  % denitrification↙
filters - configuration 1
eqn_cct_ac = eqn_cct_cec*((interest/(((1 + interest)^40) - 1)) + interest);  % chlorine contact↙
tank
eqn_isbpfr_ac = eqn_isbpfr_cec*((interest/(((1 + interest)^40) - 1)) + interest);  % incinerator↙
scrubber blowdown TS plug flow reactor
eqn_isbras_ac = eqn_isbras_cec*((interest/(((1 + interest)^40) - 1)) + interest);  % incinerator↙
scrubber blowdown TS RAS pumping
eqn_isbsc_ac = eqn_isbsc_cec*((interest/(((1 + interest)^40) - 1)) + interest);  % incinerator↙
scrubber blowdown TS secondary clarification
eqn_isbwas_ac = eqn_isbwas_cec*((interest/(((1 + interest)^40) - 1)) + interest);  % incinerator↙
scrubber blowdown TS WAS pumping
eqn_gt_ac = eqn_gt_cec*((interest/(((1 + interest)^40) - 1)) + interest);  % gravity thickners↙
for primary solids
eqn_gbt_ac = eqn_gbt_cec*((interest/(((1 + interest)^40) - 1)) + interest); % two 1m GBTs,↙
gravity belt thickeners for secondary solids
eqn_cent_ac = eqn_cent_cec*((interest/(((1 + interest)^40) - 1)) + interest);  % centrifuges
eqn_poly_ac = eqn_poly_cec*((interest/(((1 + interest)^40) - 1)) + interest);  % polymer feed↙
system
eqn_inc_ac = eqn_inc_cec*((interest/(((1 + interest)^40) - 1)) + interest);  % incinerator
eqn_ah_ac = eqn_ah_cec*((interest/(((1 + interest)^40) - 1)) + interest);  % ash hauling

% Additional blower calculations
eqn_blo_ac_tunable = eqn_blo_cec_tunable*((interest/(((1 + interest)^40) - 1)) + interest);
eqn_blo_ac_3fixed = eqn_blo_cec_3fixed*((interest/(((1 + interest)^40) - 1)) + interest);
eqn_blo_ac_4fixed = eqn_blo_cec_4fixed*((interest/(((1 + interest)^40) - 1)) + interest);
```

```
eqn_blo_ac_3_1_fixed = eqn_blo_cec_3_1_fixed*((interest/(((1 + interest)^40) - 1)) + interest);


% SECTION 3.4
% ------------------ TOTALS FOR SOURCES OF ENVI IMPACTS ------------------
eqn_total_ve = eqn_pc_ve + eqn_psp_ve + eqn_sc_ve + eqn_stbnr_ve + eqn_stber_ve ...
    + eqn_stbcr_ve + eqn_stbras_ve + eqn_stbir_ve + eqn_stbwas_ve + eqn_blo_ve ...
    + eqn_df1_ve + eqn_cct_ve + eqn_isbpfr_ve + eqn_isbras_ve + eqn_isbsc_ve ...
    + eqn_isbwas_ve + eqn_gt_ve + eqn_gbt_ve + eqn_cent_ve + eqn_poly_ve ...
    + eqn_inc_ve + eqn_ah_ve;
eqn_total_vsc = eqn_pc_vsc + eqn_psp_vsc + eqn_sc_vsc + eqn_stbnr_vsc + eqn_stber_vsc ...
    + eqn_stbcr_vsc + eqn_stbras_vsc + eqn_stbir_vsc + eqn_stbwas_vsc + eqn_blo_vsc ...
    + eqn_df1_vsc + eqn_cct_vsc + eqn_isbpfr_vsc + eqn_isbras_vsc + eqn_isbsc_vsc ...
    + eqn_isbwas_vsc + eqn_gt_vsc + eqn_gbt_vsc + eqn_cent_vsc + eqn_poly_vsc ...
    + eqn_inc_vsc + eqn_ah_vsc;
eqn_total_vwc = eqn_pc_vwc + eqn_psp_vwc + eqn_sc_vwc + eqn_stbnr_vwc + eqn_stber_vwc ...
    + eqn_stbcr_vwc + eqn_stbras_vwc + eqn_stbir_vwc + eqn_stbwas_vwc + eqn_blo_vwc ...
    + eqn_df1_vwc + eqn_cct_vwc + eqn_isbpfr_vwc + eqn_isbras_vwc + eqn_isbsc_vwc ...
    + eqn_isbwas_vwc + eqn_gt_vwc + eqn_gbt_vwc + eqn_cent_vwc + eqn_poly_vwc ...
    + eqn_inc_vwc + eqn_ah_vwc;
eqn_total_ba = eqn_pc_ba + eqn_psp_ba + eqn_sc_ba + eqn_stbnr_ba + eqn_stber_ba ...
    + eqn_stbcr_ba + eqn_stbras_ba + eqn_stbir_ba + eqn_stbwas_ba + eqn_blo_ba ...
    + eqn_df1_ba + eqn_cct_ba + eqn_isbpfr_ba + eqn_isbras_ba + eqn_isbsc_ba ...
    + eqn_isbwas_ba + eqn_gt_ba + eqn_gbt_ba + eqn_cent_ba + eqn_poly_ba ...
    + eqn_inc_ba + eqn_ah_ba;
eqn_total_ee = eqn_pc_ee + eqn_psp_ee + eqn_sc_ee + eqn_stbnr_ee + eqn_stber_ee ...
    + eqn_stbcr_ee + eqn_stbras_ee + eqn_stbir_ee + eqn_stbwas_ee + eqn_blo_ee ...
    + eqn_df1_ee + eqn_cct_ee + eqn_isbpfr_ee + eqn_isbras_ee + eqn_isbsc_ee ...
    + eqn_isbwas_ee + eqn_gt_ee + eqn_gbt_ee + eqn_cent_ee + eqn_poly_ee ...
    + eqn_inc_ee + eqn_ah_ee;
eqn_total_cl = eqn_pc_cl + eqn_psp_cl + eqn_sc_cl + eqn_stbnr_cl + eqn_stber_cl ...
    + eqn_stbcr_cl + eqn_stbras_cl + eqn_stbir_cl + eqn_stbwas_cl + eqn_blo_cl ...
    + eqn_df1_cl + eqn_cct_cl + eqn_isbpfr_cl + eqn_isbras_cl + eqn_isbsc_cl ...
    + eqn_isbwas_cl + eqn_gt_cl + eqn_gbt_cl + eqn_cent_cl + eqn_poly_cl ...
    + eqn_inc_cl + eqn_ah_cl;
eqn_total_py = eqn_pc_py + eqn_psp_py + eqn_sc_py + eqn_stbnr_py + eqn_stber_py ...
    + eqn_stbcr_py + eqn_stbras_py + eqn_stbir_py + eqn_stbwas_py + eqn_blo_py ...
    + eqn_df1_py + eqn_cct_py + eqn_isbpfr_py + eqn_isbras_py + eqn_isbsc_py ...
    + eqn_isbwas_py + eqn_gt_py + eqn_gbt_py + eqn_cent_py + eqn_poly_py ...
    + eqn_inc_py + eqn_ah_py;
eqn_total_sd = eqn_pc_sd + eqn_psp_sd + eqn_sc_sd + eqn_stbnr_sd + eqn_stber_sd ...
    + eqn_stbcr_sd + eqn_stbras_sd + eqn_stbir_sd + eqn_stbwas_sd + eqn_blo_sd ...
    + eqn_df1_sd + eqn_cct_sd + eqn_isbpfr_sd + eqn_isbras_sd + eqn_isbsc_sd ...
    + eqn_isbwas_sd + eqn_gt_sd + eqn_gbt_sd + eqn_cent_sd + eqn_poly_sd ...
    + eqn_inc_sd + eqn_ah_sd;
eqn_total_hac = eqn_pc_hac + eqn_psp_hac + eqn_sc_hac + eqn_stbnr_hac + eqn_stber_hac ...
    + eqn_stbcr_hac + eqn_stbras_hac + eqn_stbir_hac + eqn_stbwas_hac + eqn_blo_hac ...
    + eqn_df1_hac + eqn_cct_hac + eqn_isbpfr_hac + eqn_isbras_hac + eqn_isbsc_hac ...
    + eqn_isbwas_hac + eqn_gt_hac + eqn_gbt_hac + eqn_cent_hac + eqn_poly_hac ...
    + eqn_inc_hac + eqn_ah_hac;
eqn_total_fo = eqn_pc_fo + eqn_psp_fo + eqn_sc_fo + eqn_stbnr_fo + eqn_stber_fo ...
    + eqn_stbcr_fo + eqn_stbras_fo + eqn_stbir_fo + eqn_stbwas_fo + eqn_blo_fo ...
    + eqn_df1_fo + eqn_cct_fo + eqn_isbpfr_fo + eqn_isbras_fo + eqn_isbsc_fo ...
    + eqn_isbwas_fo + eqn_gt_fo + eqn_gbt_fo + eqn_cent_fo + eqn_poly_fo ...
    + eqn_inc_fo + eqn_ah_fo;
eqn_total_ng = eqn_pc_ng + eqn_psp_ng + eqn_sc_ng + eqn_stbnr_ng + eqn_stber_ng ...
```

```
    + eqn_stbcr_ng + eqn_stbras_ng + eqn_stbir_ng + eqn_stbwas_ng + eqn_blo_ng ...
    + eqn_df1_ng + eqn_cct_ng + eqn_isbpfr_ng + eqn_isbras_ng + eqn_isbsc_ng ...
    + eqn_isbwas_ng + eqn_gt_ng + eqn_gbt_ng + eqn_cent_ng + eqn_poly_ng ...
    + eqn_inc_ng + eqn_ah_ng;
eqn_total_ap = eqn_pc_ap + eqn_psp_ap + eqn_sc_ap + eqn_stbnr_ap + eqn_stber_ap ...
    + eqn_stbcr_ap + eqn_stbras_ap + eqn_stbir_ap + eqn_stbwas_ap + eqn_blo_ap ...
    + eqn_df1_ap + eqn_cct_ap + eqn_isbpfr_ap + eqn_isbras_ap + eqn_isbsc_ap ...
    + eqn_isbwas_ap + eqn_gt_ap + eqn_gbt_ap + eqn_cent_ap + eqn_poly_ap ...
    + eqn_inc_ap + eqn_ah_ap;

% SECTION 3.5
% ------------------ TOTALS FOR SOURCES OF COSTS ------------------
eqn_total_cec = eqn_pc_cec + eqn_psp_cec + eqn_sc_cec + eqn_stbnr_cec + eqn_stber_cec ...
    + eqn_stbcr_cec + eqn_stbras_cec + eqn_stbir_cec + eqn_stbwas_cec + eqn_blo_cec ...
    + eqn_df1_cec + eqn_cct_cec + eqn_isbpfr_cec + eqn_isbras_cec + eqn_isbsc_cec ...
    + eqn_isbwas_cec + eqn_gt_cec + eqn_gbt_cec + eqn_cent_cec + eqn_poly_cec ...
    + eqn_inc_cec + eqn_ah_cec;
eqn_total_olc = eqn_pc_olc + eqn_psp_olc + eqn_sc_olc + eqn_stbnr_olc + eqn_stber_olc ...
    + eqn_stbcr_olc + eqn_stbras_olc + eqn_stbir_olc + eqn_stbwas_olc + eqn_blo_olc ...
    + eqn_df1_olc + eqn_cct_olc + eqn_isbpfr_olc + eqn_isbras_olc + eqn_isbsc_olc ...
    + eqn_isbwas_olc + eqn_gt_olc + eqn_gbt_olc + eqn_cent_olc + eqn_poly_olc ...
    + eqn_inc_olc + eqn_ah_olc;
eqn_total_mlc = eqn_pc_mlc + eqn_psp_mlc + eqn_sc_mlc + eqn_stbnr_mlc + eqn_stber_mlc ...
    + eqn_stbcr_mlc + eqn_stbras_mlc + eqn_stbir_mlc + eqn_stbwas_mlc + eqn_blo_mlc ...
    + eqn_df1_mlc + eqn_cct_mlc + eqn_isbpfr_mlc + eqn_isbras_mlc + eqn_isbsc_mlc ...
    + eqn_isbwas_mlc + eqn_gt_mlc + eqn_gbt_mlc + eqn_cent_mlc + eqn_poly_mlc ...
    + eqn_inc_mlc + eqn_ah_mlc;
eqn_total_msc = eqn_pc_msc + eqn_psp_msc + eqn_sc_msc + eqn_stbnr_msc + eqn_stber_msc ...
    + eqn_stbcr_msc + eqn_stbras_msc + eqn_stbir_msc + eqn_stbwas_msc + eqn_blo_msc ...
    + eqn_df1_msc + eqn_cct_msc + eqn_isbpfr_msc + eqn_isbras_msc + eqn_isbsc_msc ...
    + eqn_isbwas_msc + eqn_gt_msc + eqn_gbt_msc + eqn_cent_msc + eqn_poly_msc ...
    + eqn_inc_msc + eqn_ah_msc;
eqn_total_cc = eqn_pc_cc + eqn_psp_cc + eqn_sc_cc + eqn_stbnr_cc + eqn_stber_cc ...
    + eqn_stbcr_cc + eqn_stbras_cc + eqn_stbir_cc + eqn_stbwas_cc + eqn_blo_cc ...
    + eqn_df1_cc + eqn_cct_cc + eqn_isbpfr_cc + eqn_isbras_cc + eqn_isbsc_cc ...
    + eqn_isbwas_cc + eqn_gt_cc + eqn_gbt_cc + eqn_cent_cc + eqn_poly_cc ...
    + eqn_inc_cc + eqn_ah_cc;
eqn_total_ec = eqn_pc_ec + eqn_psp_ec + eqn_sc_ec + eqn_stbnr_ec + eqn_stber_ec ...
    + eqn_stbcr_ec + eqn_stbras_ec + eqn_stbir_ec + eqn_stbwas_ec + eqn_blo_ec ...
    + eqn_df1_ec + eqn_cct_ec + eqn_isbpfr_ec + eqn_isbras_ec + eqn_isbsc_ec ...
    + eqn_isbwas_ec + eqn_gt_ec + eqn_gbt_ec + eqn_cent_ec + eqn_poly_ec ...
    + eqn_inc_ec + eqn_ah_ec;
eqn_total_ac = eqn_pc_ac + eqn_psp_ac + eqn_sc_ac + eqn_stbnr_ac + eqn_stber_ac ...
    + eqn_stbcr_ac + eqn_stbras_ac + eqn_stbir_ac + eqn_stbwas_ac + eqn_blo_ac ...
    + eqn_df1_ac + eqn_cct_ac + eqn_isbpfr_ac + eqn_isbras_ac + eqn_isbsc_ac ...
    + eqn_isbwas_ac + eqn_gt_ac + eqn_gbt_ac + eqn_cent_ac + eqn_poly_ac ...
    + eqn_inc_ac + eqn_ah_ac;



% SECTION 3.6.1
% ------------------ SUMMARY CALCULATIONS FOR COSTS -----------------------

direct_costs_and_construction = eqn_total_cec*(1 + dc_profit);
indirect_costs = direct_costs_and_construction*ic_ratio;
interest_during_construction = (((direct_costs_and_construction/(1 + dc_profit)) + indirect_costs↙
```

```
...
    + land_costs)*construction_period*interest)/2;
o_and_m_costs = eqn_total_olc + eqn_total_mlc + eqn_total_msc + eqn_total_cc + eqn_total_ec;
land_present_worth = land_costs*(1-((1.03^plant_lifetime)*((1/(1 + interest))^plant_lifetime)));

present_worth = present_worth_factor*(o_and_m_costs) + direct_costs_and_construction ...
    + indirect_costs + land_present_worth + interest_during_construction; % note AC not included.
AC or CEC should be included depending on payment schedule.
present_worth_construction = direct_costs_and_construction + indirect_costs + land_present_worth
+ interest_during_construction;
present_worth_operation = present_worth_factor*(o_and_m_costs);

% SECTION 3.7
% BLOWER CALCULATIONS
cec_without_blower = eqn_total_cec - eqn_blo_cec;
olc_without_blower = eqn_total_olc - eqn_blo_olc;
mlc_without_blower = eqn_total_mlc - eqn_blo_mlc;
msc_without_blower = eqn_total_msc - eqn_blo_msc;
cc_without_blower = eqn_total_cc - eqn_blo_cc;
ec_without_blower = eqn_total_ec - eqn_blo_ec;
ac_without_blower = eqn_total_ac - eqn_blo_ac;

% Simulated Blower Calcs
direct_costs_and_construction_blo = eqn_blo_cec*(1 + dc_profit);
indirect_costs_blo = direct_costs_and_construction_blo*ic_ratio;
o_and_m_costs_blo = eqn_blo_olc + eqn_blo_mlc + eqn_blo_msc + eqn_blo_ec;
present_worth_blo = present_worth_factor*(o_and_m_costs_blo) + direct_costs_and_construction_blo
...
    + indirect_costs_blo; % note AC not included.  AC or CEC should be included depending on
payment schedule.
present_worth_construction_blo = direct_costs_and_construction_blo + indirect_costs_blo;
present_worth_operation_blo = present_worth_factor*(o_and_m_costs_blo);


% Tunable Blower Calcs
direct_costs_and_construction_tunable = eqn_blo_cec_tunable*(1 + dc_profit);
indirect_costs_tunable = direct_costs_and_construction_tunable*ic_ratio;
o_and_m_costs_tunable = eqn_blo_olc_tunable + eqn_blo_mlc_tunable + eqn_blo_msc_tunable +
eqn_blo_ec_tunable;
present_worth_tunable = present_worth_factor*(o_and_m_costs_tunable) +
direct_costs_and_construction_tunable ...
    + indirect_costs_tunable; % note AC not included.  AC or CEC should be included depending on
payment schedule.
present_worth_construction_tunable = direct_costs_and_construction_tunable +
indirect_costs_tunable;
present_worth_operation_tunable = present_worth_factor*(o_and_m_costs_tunable);

% 3 Fixed Blower Calcs
direct_costs_and_construction_3fixed = eqn_blo_cec_3fixed*(1 + dc_profit);
indirect_costs_3fixed = direct_costs_and_construction_3fixed*ic_ratio;
o_and_m_costs_3fixed = eqn_blo_olc_3fixed + eqn_blo_mlc_3fixed + eqn_blo_msc_3fixed +
eqn_blo_ec_3fixed;
present_worth_3fixed = present_worth_factor*(o_and_m_costs_3fixed) +
direct_costs_and_construction_3fixed ...
    + indirect_costs_3fixed; % note AC not included.  AC or CEC should be included depending on
payment schedule.
```

```
present_worth_construction_3fixed = direct_costs_and_construction_3fixed + indirect_costs_3fixed;
present_worth_operation_3fixed = present_worth_factor*(o_and_m_costs_3fixed);

% 4 Fixed Blower Calcs
direct_costs_and_construction_4fixed = eqn_blo_cec_4fixed*(1 + dc_profit);
indirect_costs_4fixed = direct_costs_and_construction_4fixed*ic_ratio;
o_and_m_costs_4fixed = eqn_blo_olc_4fixed + eqn_blo_mlc_4fixed + eqn_blo_msc_4fixed +↙
eqn_blo_ec_4fixed;
present_worth_4fixed = present_worth_factor*(o_and_m_costs_4fixed) +↙
direct_costs_and_construction_4fixed ...
    + indirect_costs_4fixed; % note AC not included.  AC or CEC should be included depending on↙
payment schedule.
present_worth_construction_4fixed = direct_costs_and_construction_4fixed + indirect_costs_4fixed;
present_worth_operation_4fixed = present_worth_factor*(o_and_m_costs_4fixed);

% 3-1 Fixed Blower Calcs
direct_costs_and_construction_3_1_fixed = eqn_blo_cec_3_1_fixed*(1 + dc_profit);
indirect_costs_3_1_fixed = direct_costs_and_construction_3_1_fixed*ic_ratio;
o_and_m_costs_3_1_fixed = eqn_blo_olc_3_1_fixed + eqn_blo_mlc_3_1_fixed + eqn_blo_msc_3_1_fixed +↙
eqn_blo_ec_3_1_fixed;
present_worth_3_1_fixed = present_worth_factor*(o_and_m_costs_3_1_fixed) +↙
direct_costs_and_construction_3_1_fixed ...
    + indirect_costs_3_1_fixed; % note AC not included.  AC or CEC should be included depending↙
on payment schedule.
present_worth_construction_3_1_fixed = direct_costs_and_construction_3_1_fixed +↙
indirect_costs_3_1_fixed;
present_worth_operation_3_1_fixed = present_worth_factor*(o_and_m_costs_3_1_fixed);

% SECTION 3.8
% ------------------ SUMMARY CALCULATIONS FOR ENVIRONMENTAL IMPACTS -------

total_earthwork_m3 = eqn_total_ve*m3_per_cuft;
total_concrete_m3 = (eqn_total_vsc + eqn_total_vwc)*m3_per_cuft;
total_electricity_kWh = eqn_total_ee*plant_lifetime;
total_chlorine_kg = eqn_total_cl*plant_lifetime*kg_per_lb;
total_polymer_kg = eqn_total_py*plant_lifetime*kg_per_lb;
total_sand_kg = eqn_total_sd*kg_per_lb;
total_acetate_kg = eqn_total_hac*plant_lifetime*kg_per_lb; % XXX NEED TO CHANGE TO ACETATE (price↙
too)
total_fuel_oil_kg = eqn_total_fo*plant_lifetime*kg_per_gal_fo;
total_nat_gas_mj = eqn_total_ng*plant_lifetime*mj_per_1000cuft_ng;
total_ash_prod_cuyd = eqn_total_ap*plant_lifetime;
total_biomass_to_incin_kg = qcentcake_avg_mgd*xcentcake_conc_avg*lbs_mg_per_mg_L*365.↙
25*plant_lifetime*kg_per_lb;

total_scod_kg = (scodsecforward_conc_avg/1000)*(qfiltereff_avg - qconisb)*365.25*plant_lifetime;
total_nh3_kg = (snhlrctrceff2_conc_avg/1000)*(qfiltereff_avg - qconisb)*365.25*plant_lifetime;
total_no3_kg = (snoafiltereff_conc_avg/1000)*(qfiltereff_avg - qconisb)*365.25*plant_lifetime;
total_tp_kg = (stpfiltereff_conc_avg/1000)*(qfiltereff_avg - qconisb)*365.25*plant_lifetime;
total_orgn_kg = (sndfiltereff_conc_avg/1000)*(qfiltereff_avg - qconisb)*365.25*plant_lifetime;
total_effluent_n_kg = (tneff_conc_avg/1000)...
    *(qfiltereff_avg - qconisb)*365.25*plant_lifetime;
total_n_denit_kg = ((tn_rctr_loading_avg/1000) - (tnrctrwas_mass_removal_avg/1000)...
     - (tneff_conc_avg*qfiltereff_avg/1000))*365.25*plant_lifetime;
total_nit_emissions_kg_n_chandran = n2o_emissions_aer_avg_chandran*365.25*plant_lifetime/1000;
total_n2o_kg_n_chandran = (ef_n2o_effluent*total_effluent_n_kg) + (ef_n2o_wwt*total_n_denit_kg) +↙
```

```
(total_nit_emissions_kg_n_chandran);
total_n2o_kg_chandran = total_n2o_kg_n_chandran*(44/14);

total_n2o_kg_n = (ef_n2o_effluent*total_effluent_n_kg) + (ef_n2o_wwt*total_n_denit_kg);
total_n2o_kg = total_n2o_kg_n*(44/14);

total_fecl3_kg = eqn_df_fecl3*kg_per_lb*plant_lifetime;

% Ecoinvent TRACI impact factors for various energy sources AT POWERPLANT
traci_elec_from_coal_per_kwh_at_plant = [1.187591419; 0.390177177; 0.002221807; 9.822427629;...
0.002131507; 0.004741905; 5.40587E-09; 3.773857916; 0.002557531];
traci_elec_from_oil_per_kwh_at_plant = [1.150243117; 0.753081951; 0.001933608; 7.648202809;...
0.003352631; 0.000979762; 1.38795E-07; 0.31776372; 0.004053251];
traci_elec_from_nat_gas_per_kwh_at_plant = [0.677834003; 0.309540447; 0.000785553; 4.419290895;...
0.00142717; 9.2562E-05; 4.0827E-10; 0.086550208; 0.000434769];
traci_elec_from_nuclear_per_kwh_at_plant = [0.012779618; 0.004720564; 0.002307635; 27.71013109;...
7.7249E-05; 4.98271E-05; 6.83933E-08; 0.644061466; 4.42082E-05];
traci_elec_from_hydro_per_kwh_at_plant = [0.003718048; 0.00083282; 1.39893E-05; 0.065704639;...
2.39448E-05; 8.88328E-06; 2.33928E-10; 0.00620693; 1.38148E-05];
traci_elec_other_renew_per_kwh_at_plant = [0.011273546; 0.002695647; 0.000213662; 1.021464849;...
2.64942E-05; 5.90386E-05; 6.82229E-10; 0.05754407; 2.53817E-05];

% 2009 Percentages for Virginia (from EIA dataset)
% percent_coal = 0.3703;
% percent_oil = 0.0122;
% percent_nat_gas = 0.1213;
% percent_nuclear = 0.4659;
% percent_hydro = 0.0231;
% percent_other_renew = 1 - percent_coal - percent_oil - percent_nat_gas - percent_nuclear -...
percent_hydro;

% 2010 Percentages for Virginia (from EIA dataset)
percent_coal = 0.3419;
percent_oil = 0.0174;
percent_nat_gas = 0.2283;
percent_nuclear = 0.3569;
percent_hydro = 0.0201;
percent_other_renew = 1 - percent_coal - percent_oil - percent_nat_gas - percent_nuclear -...
percent_hydro;

traci_elec_impact_factor_set = percent_coal*traci_elec_from_coal_per_kwh_at_plant +...
percent_oil*traci_elec_from_oil_per_kwh_at_plant ...
    + percent_nat_gas*traci_elec_from_nat_gas_per_kwh_at_plant +...
percent_nuclear*traci_elec_from_nuclear_per_kwh_at_plant ...
    + percent_hydro*traci_elec_from_hydro_per_kwh_at_plant +...
percent_other_renew*traci_elec_other_renew_per_kwh_at_plant;

traci_elec_acid_per_kwh_VA_at_grid = (traci_elec_impact_factor_set(2,1))/(1-elec_grid_loss);
traci_elec_carc_per_kwh_VA_at_grid = (traci_elec_impact_factor_set(3,1))/(1-elec_grid_loss);
traci_elec_eco_per_kwh_VA_at_grid = (traci_elec_impact_factor_set(8,1))/(1-elec_grid_loss);
traci_elec_eut_per_kwh_VA_at_grid = (traci_elec_impact_factor_set(6,1))/(1-elec_grid_loss);
traci_elec_ghg_per_kwh_VA_at_grid = (traci_elec_impact_factor_set(1,1))/(1-elec_grid_loss);
traci_elec_noncarc_per_kwh_VA_at_grid = (traci_elec_impact_factor_set(4,1))/(1-elec_grid_loss);
traci_elec_ozone_per_kwh_VA_at_grid = (traci_elec_impact_factor_set(7,1))/(1-elec_grid_loss);
traci_elec_resp_per_kwh_VA_at_grid = (traci_elec_impact_factor_set(5,1))/(1-elec_grid_loss);
traci_elec_smog_per_kwh_VA_at_grid = (traci_elec_impact_factor_set(9,1))/(1-elec_grid_loss);
```

```
% US low voltage AT GRID average according to ecoinvent Ecoinvent - NOT
% USED IN THIS ANALYSIS, SWITCHED TO VIRGINIA AVERAGES
traci_elec_acid_per_kwh_US_at_grid = 0.298336873681986;
traci_elec_carc_per_kwh_US_at_grid = 0.00329265180842366;
traci_elec_eco_per_kwh_US_at_grid = 2.66596686387885;
traci_elec_eut_per_kwh_US_at_grid = 0.00341655833809891;
traci_elec_ghg_per_kwh_US_at_grid = 0.834482665126872;
traci_elec_noncarc_per_kwh_US_at_grid = 19.5781473622734;
traci_elec_ozone_per_kwh_US_at_grid = 2.21524561647287E-08;
traci_elec_resp_per_kwh_US_at_grid = 0.00158835031178773;
traci_elec_smog_per_kwh_US_at_grid = 0.0016118747430855;


% SECTION 3.9
% BLOWER CALCULATIONS
total_electricity_kWh_without_blo = total_electricity_kWh - eqn_blo_ee*plant_lifetime;
total_electricity_kWh_blo = eqn_blo_ee*plant_lifetime;
total_electricity_kWh_tunable = eqn_blo_ee_tunable*plant_lifetime;
total_electricity_kWh_3fixed = eqn_blo_ee_3fixed*plant_lifetime;
total_electricity_kWh_4fixed = eqn_blo_ee_4fixed*plant_lifetime;
total_electricity_kWh_3_1_fixed = eqn_blo_ee_3_1_fixed*plant_lifetime;

% ------------------ Acidification, H+ moles eq -------------------------
traci_earthwork_acid_per_m3 = 0.284014683919029;
traci_construct_acid_per_m3conc = 93.4514506644663;
traci_sand_acid_per_kg = 0.00100301546821799;
traci_elec_acid_per_kwh = traci_elec_acid_per_kwh_VA_at_grid;
traci_cl_acid_per_kg = 1.41188067615791;
traci_poly_acid_per_kg = 1.69596973104071;
traci_meoh_acid_per_kg = 0.0692074161874319;
traci_hac_acid_per_kg = 0.31835109;
traci_ng_acid_per_MJ = 0.0283772611354627;
traci_fo_acid_per_kg = 0.260350210010743;
traci_incin_acid_per_kg = 0.00640083809185792;
traci_scod_acid_per_kg = 0;
traci_nh3_acid_per_kg = 0;
traci_snd_acid_per_kg = 0;
traci_sno_acid_per_kg = 0;
traci_tp_acid_per_kg = 0;
traci_n2o_acid_per_kg = 0;
traci_fecl3_acid_per_kg = 0.21154228;

total_acidification = traci_earthwork_acid_per_m3*total_earthwork_m3 +↙
traci_construct_acid_per_m3conc*total_concrete_m3 ...
    + traci_sand_acid_per_kg*total_sand_kg + traci_elec_acid_per_kwh*total_electricity_kWh ...
    + traci_cl_acid_per_kg*total_chlorine_kg + traci_poly_acid_per_kg*total_polymer_kg ...
     + traci_ng_acid_per_MJ*total_nat_gas_mj ...
    + traci_fo_acid_per_kg*total_fuel_oil_kg + traci_incin_acid_per_kg*total_biomass_to_incin_kg↙
...
    + traci_scod_acid_per_kg*total_scod_kg + traci_nh3_acid_per_kg*total_nh3_kg ...
    + traci_snd_acid_per_kg*total_orgn_kg + traci_sno_acid_per_kg*total_no3_kg ...
    + traci_tp_acid_per_kg*total_tp_kg + traci_n2o_acid_per_kg*total_n2o_kg +↙
traci_hac_acid_per_kg*total_acetate_kg + traci_fecl3_acid_per_kg*total_fecl3_kg;

construction_acidification = traci_earthwork_acid_per_m3*total_earthwork_m3 +↙
```

```
traci_construct_acid_per_m3conc*total_concrete_m3 ...
    + traci_sand_acid_per_kg*total_sand_kg;
operation_acidification = total_acidification - construction_acidification;

total_acidification_without_blo = total_acidification -
traci_elec_acid_per_kwh*total_electricity_kWh_without_blo;
total_acidification_blo = traci_elec_acid_per_kwh*total_electricity_kWh_blo;
total_acidification_tunable = traci_elec_acid_per_kwh*total_electricity_kWh_tunable;
total_acidification_3fixed = traci_elec_acid_per_kwh*total_electricity_kWh_3fixed;
total_acidification_4fixed = traci_elec_acid_per_kwh*total_electricity_kWh_4fixed;
total_acidification_3_1_fixed = traci_elec_acid_per_kwh*total_electricity_kWh_3_1_fixed;

% ------------------ Carcinogenics, kg benzen eq -------------------------
traci_earthwork_carc_per_m3 = 0.000296881763576155;
traci_construct_carc_per_m3conc = 4.46180126989716;
traci_sand_carc_per_kg = 1.12117585777685E-05;
traci_elec_carc_per_kwh = traci_elec_carc_per_kwh_VA_at_grid;
traci_cl_carc_per_kg = 0.0367616664603576;
traci_poly_carc_per_kg = 0.00239591438733397;
traci_meoh_carc_per_kg = 0.000585068348098974;
traci_hac_carc_per_kg = 0.0055544045;
traci_ng_carc_per_MJ = 7.29371481156214E-05;
traci_fo_carc_per_kg = 0.000752825301253302;
traci_incin_carc_per_kg = 0.000653800214096913;
traci_scod_carc_per_kg = 0;
traci_nh3_carc_per_kg = 0;
traci_snd_carc_per_kg = 0;
traci_sno_carc_per_kg = 0;
traci_tp_carc_per_kg = 0;
traci_n2o_carc_per_kg = 0;
traci_fecl3_carc_per_kg = 0.0085691286;

total_carcinogenics = traci_earthwork_carc_per_m3*total_earthwork_m3 +
traci_construct_carc_per_m3conc*total_concrete_m3 ...
    + traci_sand_carc_per_kg*total_sand_kg + traci_elec_carc_per_kwh*total_electricity_kWh ...
    + traci_cl_carc_per_kg*total_chlorine_kg + traci_poly_carc_per_kg*total_polymer_kg ...
    + traci_ng_carc_per_MJ*total_nat_gas_mj ...
    + traci_fo_carc_per_kg*total_fuel_oil_kg + traci_incin_carc_per_kg*total_biomass_to_incin_kg
...
    + traci_scod_carc_per_kg*total_scod_kg + traci_nh3_carc_per_kg*total_nh3_kg ...
    + traci_snd_carc_per_kg*total_orgn_kg + traci_sno_carc_per_kg*total_no3_kg ...
    + traci_tp_carc_per_kg*total_tp_kg + traci_n2o_carc_per_kg*total_n2o_kg +
traci_hac_carc_per_kg*total_acetate_kg + traci_fecl3_carc_per_kg*total_fecl3_kg;


construction_carcinogenics = traci_earthwork_carc_per_m3*total_earthwork_m3 +
traci_construct_carc_per_m3conc*total_concrete_m3 ...
    + traci_sand_carc_per_kg*total_sand_kg;
operation_carcinogenics = total_carcinogenics - construction_carcinogenics;

total_carcinogenics_without_blo = total_carcinogenics -
traci_elec_carc_per_kwh*total_electricity_kWh_without_blo;
total_carcinogenics_blo = traci_elec_carc_per_kwh*total_electricity_kWh_blo;
total_carcinogenics_tunable = traci_elec_carc_per_kwh*total_electricity_kWh_tunable;
total_carcinogenics_3fixed = traci_elec_carc_per_kwh*total_electricity_kWh_3fixed;
total_carcinogenics_4fixed = traci_elec_carc_per_kwh*total_electricity_kWh_4fixed;
```

```
total_carcinogenics_3_1_fixed = traci_elec_carc_per_kwh*total_electricity_kWh_3_1_fixed;

% ------------------ Ecotoxicity, kg 2,4-D eq -------------------------
traci_earthwork_eco_per_m3 = 0.193163211918173;
traci_construct_eco_per_m3conc = 2503.78889970454;
traci_sand_eco_per_kg = 0.0052591262298745;
traci_elec_eco_per_kwh = traci_elec_eco_per_kwh_VA_at_grid;
traci_cl_eco_per_kg = 23.4845016526237;
traci_poly_eco_per_kg = 2.073870790072;
traci_meoh_eco_per_kg = 0.398617410105989;
traci_hac_eco_per_kg = 3.7494548;
traci_ng_eco_per_MJ = 0.00797488475913521;
traci_fo_eco_per_kg = 0.487377856312679;
traci_incin_eco_per_kg = 1.7266907905355;
traci_scod_eco_per_kg = 0;
traci_nh3_eco_per_kg = 0;
traci_snd_eco_per_kg = 0;
traci_sno_eco_per_kg = 0;
traci_tp_eco_per_kg = 0;
traci_n2o_eco_per_kg = 0;
traci_fecl3_eco_per_kg = 4.3479181;

total_ecotoxicity = traci_earthwork_eco_per_m3*total_earthwork_m3 +↙
traci_construct_eco_per_m3conc*total_concrete_m3 ...
    + traci_sand_eco_per_kg*total_sand_kg + traci_elec_eco_per_kwh*total_electricity_kWh ...
    + traci_cl_eco_per_kg*total_chlorine_kg + traci_poly_eco_per_kg*total_polymer_kg ...
    + traci_ng_eco_per_MJ*total_nat_gas_mj ...
    + traci_fo_eco_per_kg*total_fuel_oil_kg + traci_incin_eco_per_kg*total_biomass_to_incin_kg↙
...
    + traci_scod_eco_per_kg*total_scod_kg + traci_nh3_eco_per_kg*total_nh3_kg ...
    + traci_snd_eco_per_kg*total_orgn_kg + traci_sno_eco_per_kg*total_no3_kg ...
    + traci_tp_eco_per_kg*total_tp_kg + traci_n2o_eco_per_kg*total_n2o_kg +↙
traci_hac_eco_per_kg*total_acetate_kg + traci_fecl3_eco_per_kg*total_fecl3_kg;

construction_ecotoxicity = traci_earthwork_eco_per_m3*total_earthwork_m3 +↙
traci_construct_eco_per_m3conc*total_concrete_m3 ...
    + traci_sand_eco_per_kg*total_sand_kg;
operation_ecotoxicity = total_ecotoxicity - construction_ecotoxicity;

total_ecotoxicity_without_blo = total_ecotoxicity -↙
traci_elec_eco_per_kwh*total_electricity_kWh_without_blo;
total_ecotoxicity_blo = traci_elec_eco_per_kwh*total_electricity_kWh_blo;
total_ecotoxicity_tunable = traci_elec_eco_per_kwh*total_electricity_kWh_tunable;
total_ecotoxicity_3fixed = traci_elec_eco_per_kwh*total_electricity_kWh_3fixed;
total_ecotoxicity_4fixed = traci_elec_eco_per_kwh*total_electricity_kWh_4fixed;
total_ecotoxicity_3_1_fixed = traci_elec_eco_per_kwh*total_electricity_kWh_3_1_fixed;

% ------------------ Eutrophication, kg N eq -------------------------
traci_earthwork_eut_per_m3 = 0.000751226339613574;
traci_construct_eut_per_m3conc = 2.70063425409446;
traci_sand_eut_per_kg = 6.47717581538685E-06;
traci_elec_eut_per_kwh = traci_elec_eut_per_kwh_VA_at_grid;
traci_cl_eut_per_kg = 0.0379904313969148;
traci_poly_eut_per_kg = 0.00548136412391987;
traci_meoh_eut_per_kg = 0.00073911332138954;
traci_hac_eut_per_kg = 0.0068118066;
```

```
traci_ng_eut_per_MJ = 7.38637169742344E-06;
traci_fo_eut_per_kg = 0.0021829408607144;
traci_incin_eut_per_kg = 0.00106785791093958;
traci_scod_eut_per_kg = 0.05;
traci_nh3_eut_per_kg = 0.7793;
traci_snd_eut_per_kg = 1;
traci_sno_eut_per_kg = 0.2367;
traci_tp_eut_per_kg = 2.38;
traci_n2o_eut_per_kg = 0;
traci_fecl3_eut_per_kg = 0.0064986913;

total_eutrophication = traci_earthwork_eut_per_m3*total_earthwork_m3 +...
traci_construct_eut_per_m3conc*total_concrete_m3 ...
    + traci_sand_eut_per_kg*total_sand_kg + traci_elec_eut_per_kwh*total_electricity_kWh ...
    + traci_cl_eut_per_kg*total_chlorine_kg + traci_poly_eut_per_kg*total_polymer_kg ...
    + traci_ng_eut_per_MJ*total_nat_gas_mj ...
    + traci_fo_eut_per_kg*total_fuel_oil_kg + traci_incin_eut_per_kg*total_biomass_to_incin_kg...
...
    + traci_scod_eut_per_kg*total_scod_kg + traci_nh3_eut_per_kg*total_nh3_kg ...
    + traci_snd_eut_per_kg*total_orgn_kg + traci_sno_eut_per_kg*total_no3_kg ...
    + traci_tp_eut_per_kg*total_tp_kg + traci_n2o_eut_per_kg*total_n2o_kg +...
traci_hac_eut_per_kg*total_acetate_kg + traci_fecl3_eut_per_kg*total_fecl3_kg;

construction_eutrophication = traci_earthwork_eut_per_m3*total_earthwork_m3 +...
traci_construct_eut_per_m3conc*total_concrete_m3 ...
    + traci_sand_eut_per_kg*total_sand_kg;
effluent_eutrophication = traci_scod_eut_per_kg*total_scod_kg + traci_nh3_eut_per_kg*total_nh3_kg...
...
    + traci_snd_eut_per_kg*total_orgn_kg + traci_sno_eut_per_kg*total_no3_kg ...
    + traci_tp_eut_per_kg*total_tp_kg + traci_n2o_eut_per_kg*total_n2o_kg;
ir_pumping_eutrophication = (eqn_stbir_ee*plant_lifetime)*traci_elec_eut_per_kwh;
aeration_eutrophication = ((eqn_stbcr_ee + eqn_isbpfr_ee)*plant_lifetime)*traci_elec_eut_per_kwh;

percent_eut_from_eff = effluent_eutrophication/total_eutrophication;

operation_eutrophication = total_eutrophication - construction_eutrophication;

total_eutrophication_without_blo = total_eutrophication -...
traci_elec_eut_per_kwh*total_electricity_kWh_without_blo;
total_eutrophication_blo = traci_elec_eut_per_kwh*total_electricity_kWh_blo;
total_eutrophication_tunable = traci_elec_eut_per_kwh*total_electricity_kWh_tunable;
total_eutrophication_3fixed = traci_elec_eut_per_kwh*total_electricity_kWh_3fixed;
total_eutrophication_4fixed = traci_elec_eut_per_kwh*total_electricity_kWh_4fixed;
total_eutrophication_3_1_fixed = traci_elec_eut_per_kwh*total_electricity_kWh_3_1_fixed;

% ------------------ Global Warming, kg CO2 eq -------------------------
traci_earthwork_ghg_per_m3 = 0.533314207595925;
traci_construct_ghg_per_m3conc = 504.186356337375;
traci_sand_ghg_per_kg = 0.00240070717991179;
traci_elec_ghg_per_kwh = traci_elec_ghg_per_kwh_VA_at_grid;
traci_cl_ghg_per_kg = 5.89712621030092;
traci_poly_ghg_per_kg = 6.61330410703775;
traci_meoh_ghg_per_kg = 0.736311853776162;
traci_hac_ghg_per_kg = 1.5377906;
traci_ng_ghg_per_MJ = 0.0133469757888744;
traci_fo_ghg_per_kg = 0.424191009326254;
```

```
traci_incin_ghg_per_kg = 0.0123102737166984;
traci_scod_ghg_per_kg = 0;
traci_nh3_ghg_per_kg = 0;
traci_snd_ghg_per_kg = 0;
traci_sno_ghg_per_kg = 0;
traci_tp_ghg_per_kg = 0;
traci_n2o_ghg_per_kg = 300;
traci_fecl3_ghg_per_kg = 0.80021399;

total_global_warming = traci_earthwork_ghg_per_m3*total_earthwork_m3 +↙
traci_construct_ghg_per_m3conc*total_concrete_m3 ...
    + traci_sand_ghg_per_kg*total_sand_kg + traci_elec_ghg_per_kwh*total_electricity_kWh ...
    + traci_cl_ghg_per_kg*total_chlorine_kg + traci_poly_ghg_per_kg*total_polymer_kg ...
    + traci_ng_ghg_per_MJ*total_nat_gas_mj ...
    + traci_fo_ghg_per_kg*total_fuel_oil_kg + traci_incin_ghg_per_kg*total_biomass_to_incin_kg↙
...
    + traci_scod_ghg_per_kg*total_scod_kg + traci_nh3_ghg_per_kg*total_nh3_kg ...
    + traci_snd_ghg_per_kg*total_orgn_kg + traci_sno_ghg_per_kg*total_no3_kg ...
    + traci_tp_ghg_per_kg*total_tp_kg + traci_n2o_ghg_per_kg*total_n2o_kg +↙
traci_hac_ghg_per_kg*total_acetate_kg + traci_fecl3_ghg_per_kg*total_fecl3_kg;

construction_global_warming = traci_earthwork_ghg_per_m3*total_earthwork_m3 +↙
traci_construct_ghg_per_m3conc*total_concrete_m3 ...
    + traci_sand_ghg_per_kg*total_sand_kg;
operation_global_warming = total_global_warming - construction_global_warming;

blower_lifetime_ghg = eqn_blo_ee*traci_elec_ghg_per_kwh;

total_n2o_ghg_chandran = traci_n2o_ghg_per_kg*total_n2o_kg_chandran;
total_n2o_ghg_ef = total_n2o_kg*traci_n2o_ghg_per_kg;

total_global_warming_without_blo = total_global_warming -↙
traci_elec_ghg_per_kwh*total_electricity_kWh_without_blo;
total_global_warming_blo = traci_elec_ghg_per_kwh*total_electricity_kWh_blo;
total_global_warming_tunable = traci_elec_ghg_per_kwh*total_electricity_kWh_tunable;
total_global_warming_3fixed = traci_elec_ghg_per_kwh*total_electricity_kWh_3fixed;
total_global_warming_4fixed = traci_elec_ghg_per_kwh*total_electricity_kWh_4fixed;
total_global_warming_3_1_fixed = traci_elec_ghg_per_kwh*total_electricity_kWh_3_1_fixed;


% ------------------ Non carcinogenics, kg toluen eq ---------------------
traci_earthwork_noncarc_per_m3 = 2.37128725478146;
traci_construct_noncarc_per_m3conc = 47257.5722247246;
traci_sand_noncarc_per_kg = 0.101238214485853;
traci_elec_noncarc_per_kwh = traci_elec_noncarc_per_kwh_VA_at_grid;
traci_cl_noncarc_per_kg = 249.190733825231;
traci_poly_noncarc_per_kg = 66.9879851412649;
traci_meoh_noncarc_per_kg = 4.59667071637409;
traci_hac_noncarc_per_kg = 39.045569;
traci_ng_noncarc_per_MJ = 0.414926026335273;
traci_fo_noncarc_per_kg = 8.29523994186839;
traci_incin_noncarc_per_kg = 5.69171842267862;
traci_scod_noncarc_per_kg = 0;
traci_nh3_noncarc_per_kg = 0;
traci_snd_noncarc_per_kg = 0;
traci_sno_noncarc_per_kg = 0;
```

```
traci_tp_noncarc_per_kg = 0;
traci_n2o_noncarc_per_kg = 0;
traci_fecl3_noncarc_per_kg = 54.048977;

total_noncarcinogenics = traci_earthwork_noncarc_per_m3*total_earthwork_m3 +...
traci_construct_noncarc_per_m3conc*total_concrete_m3 ...
    + traci_sand_noncarc_per_kg*total_sand_kg + traci_elec_noncarc_per_kwh*total_electricity_kWh...
...
    + traci_cl_noncarc_per_kg*total_chlorine_kg + traci_poly_noncarc_per_kg*total_polymer_kg ...
    + traci_ng_noncarc_per_MJ*total_nat_gas_mj ...
    + traci_fo_noncarc_per_kg*total_fuel_oil_kg +...
traci_incin_noncarc_per_kg*total_biomass_to_incin_kg ...
    + traci_scod_noncarc_per_kg*total_scod_kg + traci_nh3_noncarc_per_kg*total_nh3_kg ...
    + traci_snd_noncarc_per_kg*total_orgn_kg + traci_sno_noncarc_per_kg*total_no3_kg ...
    + traci_tp_noncarc_per_kg*total_tp_kg + traci_n2o_noncarc_per_kg*total_n2o_kg +...
traci_hac_noncarc_per_kg*total_acetate_kg + traci_fecl3_noncarc_per_kg*total_fecl3_kg;

construction_noncarcinogenics = traci_earthwork_noncarc_per_m3*total_earthwork_m3 +...
traci_construct_noncarc_per_m3conc*total_concrete_m3 ...
    + traci_sand_noncarc_per_kg*total_sand_kg;
operation_noncarcinogenics = total_noncarcinogenics - construction_noncarcinogenics;

total_noncarcinogenics_without_blo = total_noncarcinogenics -...
traci_elec_noncarc_per_kwh*total_electricity_kWh_without_blo;
total_noncarcinogenics_blo = traci_elec_noncarc_per_kwh*total_electricity_kWh_blo;
total_noncarcinogenics_tunable = traci_elec_noncarc_per_kwh*total_electricity_kWh_tunable;
total_noncarcinogenics_3fixed = traci_elec_noncarc_per_kwh*total_electricity_kWh_3fixed;
total_noncarcinogenics_4fixed = traci_elec_noncarc_per_kwh*total_electricity_kWh_4fixed;
total_noncarcinogenics_3_1_fixed = traci_elec_noncarc_per_kwh*total_electricity_kWh_3_1_fixed;

% ------------------ Ozone depletion, kg CFC-11 eq ---------------------
traci_earthwork_ozone_per_m3 = 6.50524354362008E-08;
traci_construct_ozone_per_m3conc = 2.09770112944236E-05;
traci_sand_ozone_per_kg = 2.82421775895205E-10;
traci_elec_ozone_per_kwh = traci_elec_ozone_per_kwh_VA_at_grid;
traci_cl_ozone_per_kg = 4.30654967386225E-07;
traci_poly_ozone_per_kg = 2.02799374082863E-09;
traci_meoh_ozone_per_kg = 1.63544351939341E-07;
traci_hac_ozone_per_kg = 0.0000002806394;
traci_ng_ozone_per_MJ = 3.63535773696086E-11;
traci_fo_ozone_per_kg = 4.50197908465043E-07;
traci_incin_ozone_per_kg = 2.33571129134719E-09;
traci_scod_ozone_per_kg = 0;
traci_nh3_ozone_per_kg = 0;
traci_snd_ozone_per_kg = 0;
traci_sno_ozone_per_kg = 0;
traci_tp_ozone_per_kg = 0;
traci_n2o_ozone_per_kg = 0;
traci_fecl3_ozone_per_kg = 0.000001051082;

total_ozone_depletion = traci_earthwork_ozone_per_m3*total_earthwork_m3 +...
traci_construct_ozone_per_m3conc*total_concrete_m3 ...
    + traci_sand_ozone_per_kg*total_sand_kg + traci_elec_ozone_per_kwh*total_electricity_kWh ...
    + traci_cl_ozone_per_kg*total_chlorine_kg + traci_poly_ozone_per_kg*total_polymer_kg ...
    + traci_ng_ozone_per_MJ*total_nat_gas_mj ...
    + traci_fo_ozone_per_kg*total_fuel_oil_kg +...
```

```
traci_incin_ozone_per_kg*total_biomass_to_incin_kg ...
    + traci_scod_ozone_per_kg*total_scod_kg + traci_nh3_ozone_per_kg*total_nh3_kg ...
    + traci_snd_ozone_per_kg*total_orgn_kg + traci_sno_ozone_per_kg*total_no3_kg ...
    + traci_tp_ozone_per_kg*total_tp_kg + traci_n2o_ozone_per_kg*total_n2o_kg +...
traci_hac_ozone_per_kg*total_acetate_kg + traci_fecl3_ozone_per_kg*total_fecl3_kg;

construction_ozone_depletion = traci_earthwork_ozone_per_m3*total_earthwork_m3 +...
traci_construct_ozone_per_m3conc*total_concrete_m3 ...
    + traci_sand_ozone_per_kg*total_sand_kg;
operation_ozone_depletion = total_ozone_depletion - construction_ozone_depletion;


total_ozone_depletion_without_blo = total_ozone_depletion -...
traci_elec_ozone_per_kwh*total_electricity_kWh_without_blo;
total_ozone_blo = traci_elec_ozone_per_kwh*total_electricity_kWh_blo;
total_ozone_depletion_tunable = traci_elec_ozone_per_kwh*total_electricity_kWh_tunable;
total_ozone_depletion_3fixed = traci_elec_ozone_per_kwh*total_electricity_kWh_3fixed;
total_ozone_depletion_4fixed = traci_elec_ozone_per_kwh*total_electricity_kWh_4fixed;
total_ozone_depletion_3_1_fixed = traci_elec_ozone_per_kwh*total_electricity_kWh_3_1_fixed;

% ------------------ Respiratory effects, kg PM2.5 eq ----------------------
traci_earthwork_resp_per_m3 = 0.00108549309226895;
traci_construct_resp_per_m3conc = 0.742926615735013;
traci_sand_resp_per_kg = 4.46906282528081E-06;
traci_elec_resp_per_kwh = traci_elec_resp_per_kwh_VA_at_grid;
traci_cl_resp_per_kg = 0.00834552570864515;
traci_poly_resp_per_kg = 0.00694554288783989;
traci_meoh_resp_per_kg = 0.00026500222017138;
traci_hac_resp_per_kg = 0.0017466346;
traci_ng_resp_per_MJ = 0.000134088619757101;
traci_fo_resp_per_kg = 0.00122232705009103;
traci_incin_resp_per_kg = 1.57023213588824E-05;
traci_scod_resp_per_kg = 0;
traci_nh3_resp_per_kg = 0;
traci_snd_resp_per_kg = 0;
traci_sno_resp_per_kg = 0;
traci_tp_resp_per_kg = 0;
traci_n2o_resp_per_kg = 0;
traci_fecl3_resp_per_kg = 0.0013226108;

total_respiratory = traci_earthwork_resp_per_m3*total_earthwork_m3 +...
traci_construct_resp_per_m3conc*total_concrete_m3 ...
    + traci_sand_resp_per_kg*total_sand_kg + traci_elec_resp_per_kwh*total_electricity_kWh ...
    + traci_cl_resp_per_kg*total_chlorine_kg + traci_poly_resp_per_kg*total_polymer_kg ...
    + traci_ng_resp_per_MJ*total_nat_gas_mj ...
    + traci_fo_resp_per_kg*total_fuel_oil_kg + traci_incin_resp_per_kg*total_biomass_to_incin_kg...
...
    + traci_scod_resp_per_kg*total_scod_kg + traci_nh3_resp_per_kg*total_nh3_kg ...
    + traci_snd_resp_per_kg*total_orgn_kg + traci_sno_resp_per_kg*total_no3_kg ...
    + traci_tp_resp_per_kg*total_tp_kg + traci_n2o_resp_per_kg*total_n2o_kg +...
traci_hac_resp_per_kg*total_acetate_kg + traci_fecl3_resp_per_kg*total_fecl3_kg;

construction_respiratory = traci_earthwork_resp_per_m3*total_earthwork_m3 +...
traci_construct_resp_per_m3conc*total_concrete_m3 ...
    + traci_sand_resp_per_kg*total_sand_kg;
operation_respiratory = total_respiratory - construction_respiratory;
```

```
total_respiratory_without_blo = total_respiratory -↙
traci_elec_resp_per_kwh*total_electricity_kWh_without_blo;
total_respiratory_blo = traci_elec_resp_per_kwh*total_electricity_kWh_blo;
total_respiratory_tunable = traci_elec_resp_per_kwh*total_electricity_kWh_tunable;
total_respiratory_3fixed = traci_elec_resp_per_kwh*total_electricity_kWh_3fixed;
total_respiratory_4fixed = traci_elec_resp_per_kwh*total_electricity_kWh_4fixed;
total_respiratory_3_1_fixed = traci_elec_resp_per_kwh*total_electricity_kWh_3_1_fixed;

% ------------------ Smog, g NOx eq ---------------------
traci_earthwork_smog_per_m3 = 0.00611150732100021;
traci_construct_smog_per_m3conc = 1.1250050351559;
traci_sand_smog_per_kg = 1.82458779395028E-05;
traci_elec_smog_per_kwh = traci_elec_smog_per_kwh_VA_at_grid;
traci_cl_smog_per_kg = 0.0124886906893279;
traci_poly_smog_per_kg = 0.0125775810663426;
traci_meoh_smog_per_kg = 0.0010637836217357;
traci_hac_smog_per_kg = 0.0039354782;
traci_ng_smog_per_MJ = 1.31979590947921E-05;
traci_fo_smog_per_kg = 0.00166580679526272;
traci_incin_smog_per_kg = 0.000127500318238714;
traci_scod_smog_per_kg = 0;
traci_nh3_smog_per_kg = 0;
traci_snd_smog_per_kg = 0;
traci_sno_smog_per_kg = 0;
traci_tp_smog_per_kg = 0;
traci_n2o_smog_per_kg = 0;
traci_fecl3_smog_per_kg = 0.0016565214;

total_smog = traci_earthwork_smog_per_m3*total_earthwork_m3 +↙
traci_construct_smog_per_m3conc*total_concrete_m3 ...
    + traci_sand_smog_per_kg*total_sand_kg + traci_elec_smog_per_kwh*total_electricity_kWh ...
    + traci_cl_smog_per_kg*total_chlorine_kg + traci_poly_smog_per_kg*total_polymer_kg ...
    + traci_ng_smog_per_MJ*total_nat_gas_mj ...
    + traci_fo_smog_per_kg*total_fuel_oil_kg + traci_incin_smog_per_kg*total_biomass_to_incin_kg↙
...
    + traci_scod_smog_per_kg*total_scod_kg + traci_nh3_smog_per_kg*total_nh3_kg ...
    + traci_snd_smog_per_kg*total_orgn_kg + traci_sno_smog_per_kg*total_no3_kg ...
    + traci_tp_smog_per_kg*total_tp_kg + traci_n2o_smog_per_kg*total_n2o_kg +↙
traci_hac_smog_per_kg*total_acetate_kg + traci_fecl3_smog_per_kg*total_fecl3_kg;

construction_smog = traci_earthwork_smog_per_m3*total_earthwork_m3 +↙
traci_construct_smog_per_m3conc*total_concrete_m3 ...
    + traci_sand_smog_per_kg*total_sand_kg;
operation_smog = total_smog - construction_smog;

total_smog_without_blo = total_smog - traci_elec_smog_per_kwh*total_electricity_kWh_without_blo;
total_smog_blo = traci_elec_smog_per_kwh*total_electricity_kWh_blo;
total_smog_tunable = traci_elec_smog_per_kwh*total_electricity_kWh_tunable;
total_smog_3fixed = traci_elec_smog_per_kwh*total_electricity_kWh_3fixed;
total_smog_4fixed = traci_elec_smog_per_kwh*total_electricity_kWh_4fixed;
total_smog_3_1_fixed = traci_elec_smog_per_kwh*total_electricity_kWh_3_1_fixed;

% ------------------ REPORTING ---------------------
```

```
additional_pw_tunable = present_worth_tunable - present_worth_blo;
additional_pw_3fixed = present_worth_3fixed - present_worth_blo;
additional_pw_4fixed = present_worth_4fixed - present_worth_blo;
additional_pw_3_1_fixed = present_worth_3_1_fixed - present_worth_blo;

additional_ghg_tunable = total_global_warming_tunable - total_global_warming_blo;
additional_ghg_3fixed = total_global_warming_3fixed - total_global_warming_blo;
additional_ghg_4fixed = total_global_warming_4fixed - total_global_warming_blo;
additional_ghg_3_1_fixed = total_global_warming_3_1_fixed - total_global_warming_blo;


output_101 = lhs_set;
output_102 = config;
output_103 = season;
output_104 = actual_srt_d;
output_105 = present_worth;
output_106 = present_worth_construction;
output_107 = present_worth_operation;
output_108 = present_worth_construction_blo;
output_109 = present_worth_operation_blo;
output_110 = construction_acidification;
output_111 = construction_carcinogenics;
output_112 = construction_ecotoxicity;
output_113 = construction_eutrophication;
output_114 = construction_global_warming;
output_115 = construction_noncarcinogenics;
output_116 = construction_ozone_depletion;
output_117 = construction_respiratory;
output_118 = construction_smog;
output_119 = operation_acidification;
output_120 = operation_carcinogenics;
output_121 = operation_ecotoxicity;
output_122 = operation_eutrophication;
output_123 = operation_global_warming;
output_124 = operation_noncarcinogenics;
output_125 = operation_ozone_depletion;
output_126 = operation_respiratory;
output_127 = operation_smog;
output_128 = tneff_conc_avg;
output_129 = ir_ratio;
output_130 = additional_pw_tunable;
output_131 = additional_pw_3fixed;
output_132 = additional_pw_4fixed;
output_133 = additional_pw_3_1_fixed;
output_134 = additional_ghg_tunable;
output_135 = additional_ghg_3fixed;
output_136 = additional_ghg_4fixed;
output_137 = additional_ghg_3_1_fixed;

output_138 = total_electricity_kWh;
output_139 = total_effluent_n_kg;
output_140 = total_n_denit_kg;
output_141 = total_concrete_m3;
output_142 = eqn_stbir_cec;
output_143 = total_acetate_kg;
output_144 = qairstandlrctreff_avg;
```

```
% output_145 =
% output_146 =
% output_147 =
% output_148 =
% output_149 =
% output_150 =
% output_151 =
% output_152 =

                    % APPEND DATA TO FILE
                    line62 = sprintf('%d \t %d \t %d \t %d \t %d \t %d \t %d \t %d \t %d \t %d \t↙
%d \t %d \t %d \t %d \t %d \t %d \t %d \t %d \t %d \t %d \t %d \t %d \t %d \t %d \t %d \t %d↙
\t %d \t %d \t %d \t %d \t %d \t %d \t %d \t %d \t %d \t %d \t %d \t %d \t %d \t %d \t %d↙
\t %d', ...
                                output_101, output_102, output_103, output_104, output_105,↙
output_106, ...
        output_107, output_108, output_109, output_110, output_111, output_112, ...
        output_113, output_114, output_115, output_116, output_117, output_118, ...
        output_119, output_120, output_121, output_122, output_123, output_124, ...
        output_125, output_126, output_127, output_128, output_129, output_130, ...
        output_131, output_132, output_133, output_134, output_135, output_136, ...
        output_137, output_138, output_139, output_140, output_141, output_142, output_143,↙
output_144);

                    fid=fopen(processeddatafilename,'a');
                    fprintf(fid, '%s \r\n', line62);
                    fclose('all'); %this used to be fclose(fid), but then I got the error
                    % "??? Error using ==> fprintf Invalid file identifier.  Use fopen to↙
generate a valid file identifier. Error in ==> full_space_run_draft_03 at 416
                    % a little more digging revealed that too many files
                    % were open (511), and this program had run 511
                    % times.  Now use fclose('all').

lhs_set_output_set(k,config) = lhs_set;
config_output_set(k,config) = config;
season_output_set(k,config) = season;
actual_srt_d_output_set(k,config) = actual_srt_d;
present_worth_output_set(k,config) = present_worth;
present_worth_construction_output_set(k,config) = present_worth_construction;
present_worth_operation_output_set(k,config) = present_worth_operation;
present_worth_blower_construction_output_set(k,config) = present_worth_construction_blo;
present_worth_blower_operation_output_set(k,config) = present_worth_operation_blo;
construction_acidification_output_set(k,config) = construction_acidification;
construction_carcinogenics_output_set(k,config) = construction_carcinogenics;
construction_ecotoxicity_output_set(k,config) = construction_ecotoxicity;
construction_eutrophication_output_set(k,config) = construction_eutrophication;
construction_global_warming_output_set(k,config) = construction_global_warming;
construction_noncarcinogenics_output_set(k,config) = construction_noncarcinogenics;
construction_ozone_depletion_output_set(k,config) = construction_ozone_depletion;
construction_respiratory_output_set(k,config) = construction_respiratory;
construction_smog_output_set(k,config) = construction_smog;
operation_acidification_output_set(k,config) = operation_acidification;
operation_carcinogenics_output_set(k,config) = operation_carcinogenics;
operation_ecotoxicity_output_set(k,config) = operation_ecotoxicity;
operation_eutrophication_output_set(k,config) = operation_eutrophication;
operation_global_warming_output_set(k,config) = operation_global_warming;
```

```
operation_noncarcinogenics_output_set(k,config) = operation_noncarcinogenics;
operation_ozone_depletion_output_set(k,config) = operation_ozone_depletion;
operation_respiratory_output_set(k,config) = operation_respiratory;
operation_smog_output_set(k,config) = operation_smog;
tneff_conc_avg_output_set(k,config) = tneff_conc_avg;
ir_ratio_output_set(k,config) = ir_ratio;

additional_pw_tunable_output_set(k,config) = additional_pw_tunable;
additional_pw_3fixed_output_set(k,config) = additional_pw_3fixed;
additional_pw_4fixed_output_set(k,config) = additional_pw_4fixed;
additional_pw_3_1_fixed_output_set(k,config) = additional_pw_3_1_fixed;
additional_ghg_tunable_output_set(k,config) = additional_ghg_tunable;
additional_ghg_3fixed_output_set(k,config) = additional_ghg_3fixed;
additional_ghg_4fixed_output_set(k,config) = additional_ghg_4fixed;
additional_ghg_3_1_fixed_output_set(k,config) = additional_ghg_3_1_fixed;


end

summer_simulations = 0;
winter_simulations = 0;

for j = 1:number_of_simulations
    if (season_output_set(j,1) == 12)
       winter_simulations = winter_simulations + 1;
    elseif (season_output_set(j,1) == 28)
        summer_simulations = summer_simulations + 1;
    end
end

% config_1_summer_tn_set = zeros(summer_simulations,1);
% config_1_winter_tn_set = zeros(winter_simulations,1);
% config_2_summer_tn_set = zeros(summer_simulations,1);
% config_2_winter_tn_set = zeros(winter_simulations,1);

winter_sims = winter_simulations
summer_sims = summer_simulations

% config_1_tn_set = zeros(number_of_simulations/2,1);
% config_2_tn_set = zeros(number_of_simulations/2,1);



%INSERT ADDITIONAL SUMMARY CALCULATIONS USING "_output_set" data.

toc
end
```

Appendix I
Photobioreactor Experimental Setup

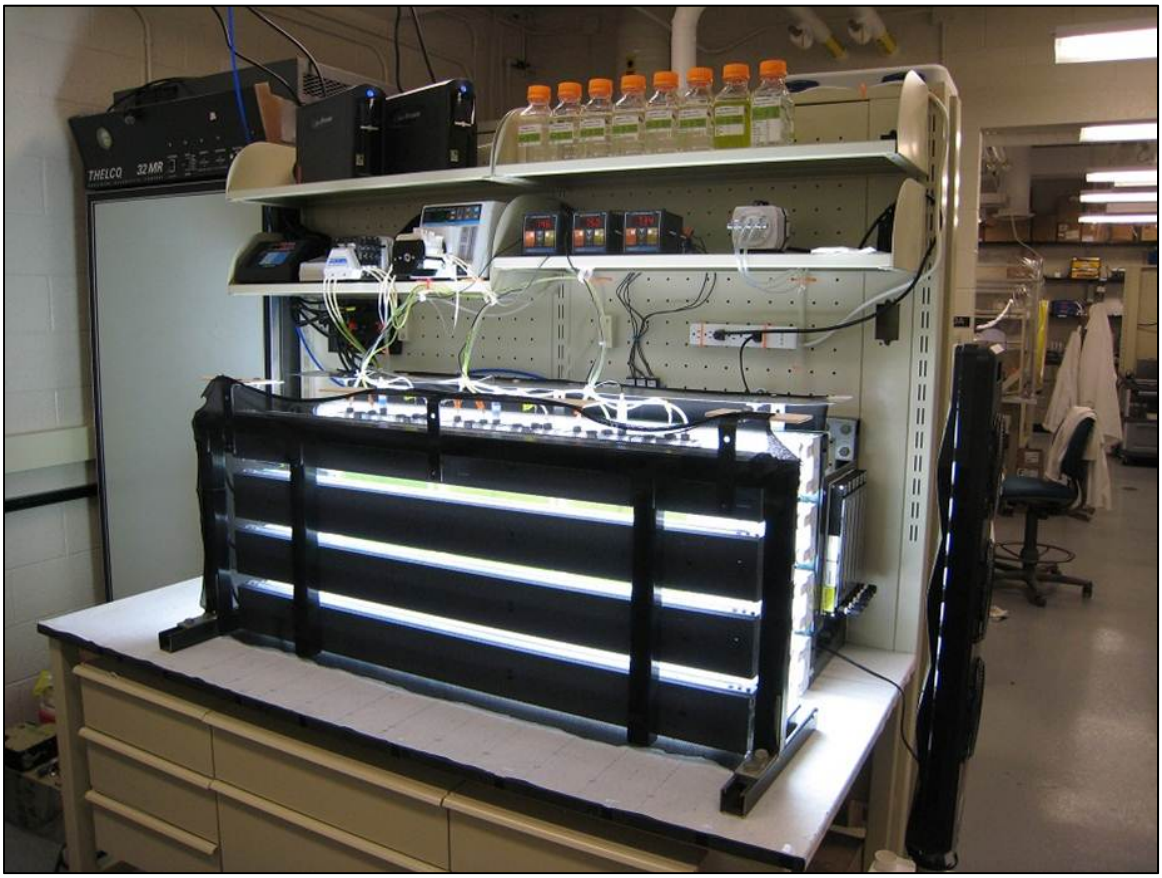

Figure I.1. Picture of full photobioreactor setup.

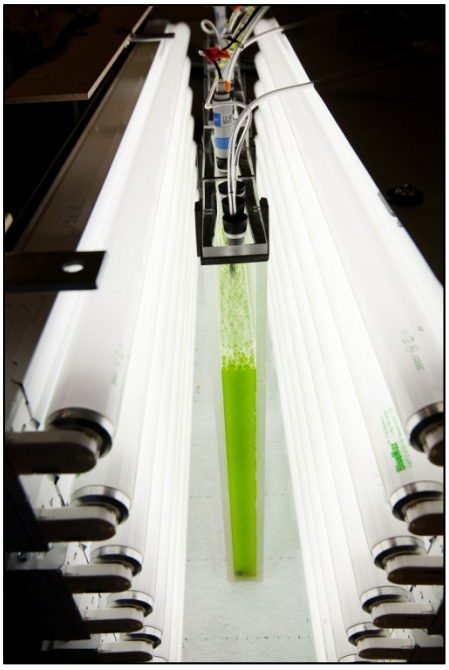

Figure I.2. Picture of photobioreactors and lighting.

Appendix J

Microscope Images from Photobioreactor Experimentation

All microscope images were taken using 40x and 100x objectives on a Zeiss Axio Observer epi-fluorescence microscope with an inverted stage (Carl Zeiss MicroImaging, Inc.). Images were taken either with transmitted light, phase contrast, or fluorescence with one of the following Zeiss filter sets: set 49, DAPI, W/424920 (**DAPI**); set 38, HE EGFP, W/424920 (**GFP**); set 20, CY3, W/424931 (**Rhodamine**); FL filter set 14, Ex BP510-560, shift free (**Alexa 546**). All fluorescence in images is the result of auto-fluorescence. No dyes were added.

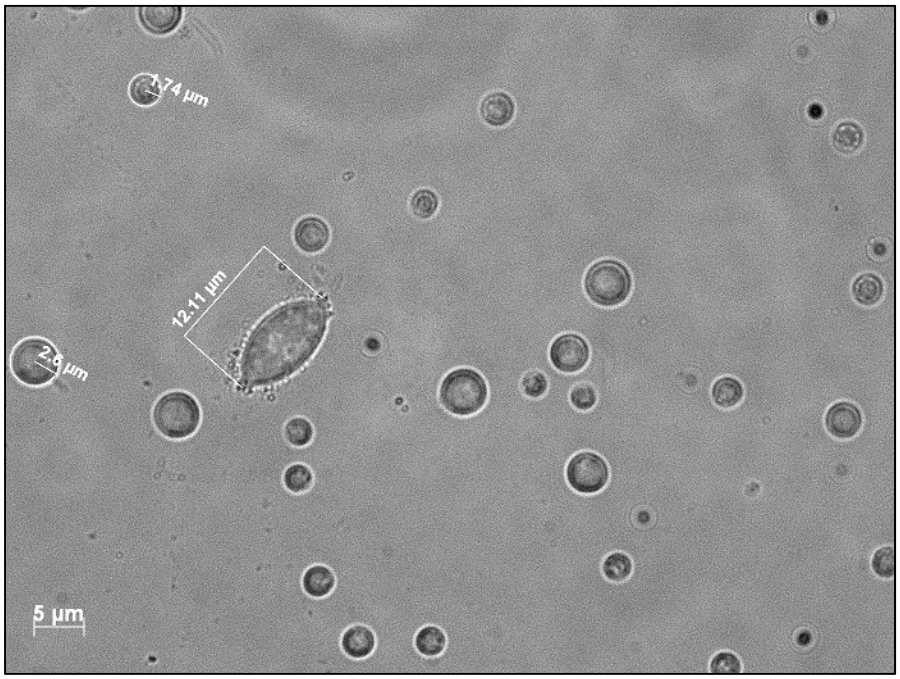

Figure J.1. Example of a transmitted light image of biomass in Photobioreactor 1. This image was taken after 4 days of batch operation under lit, nitrogen-deplete conditions.

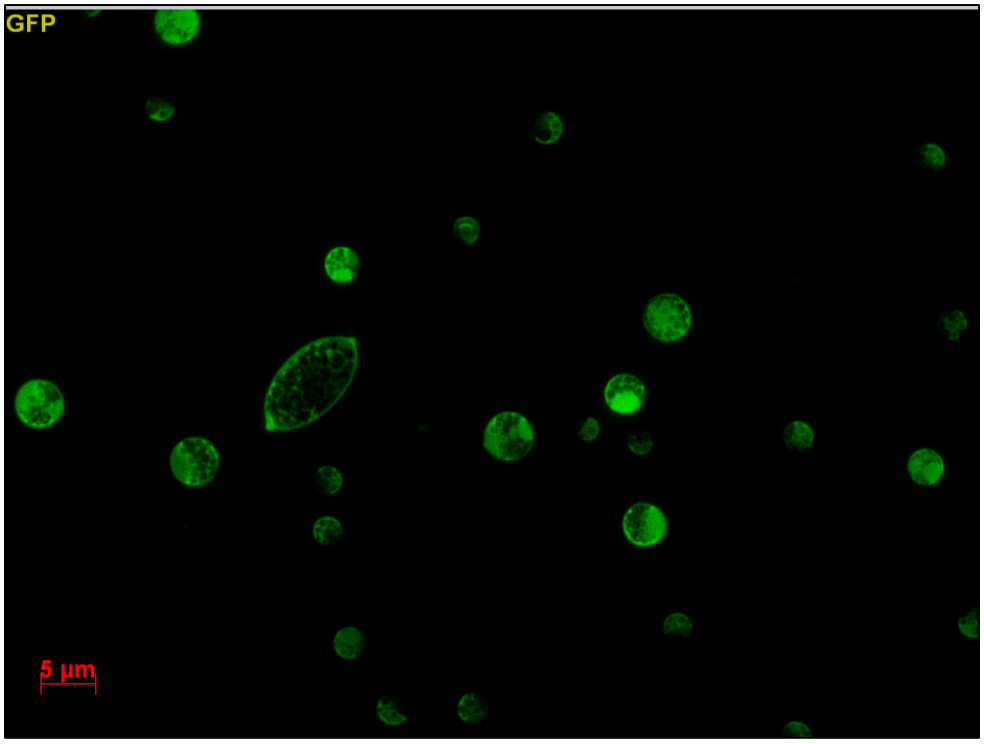

Figure J.2. Example of epifluorescence image of biomass from Photobioreactor 1. This image was taken after 4 days of batch operation under lit, nitrogen-deplete conditions.

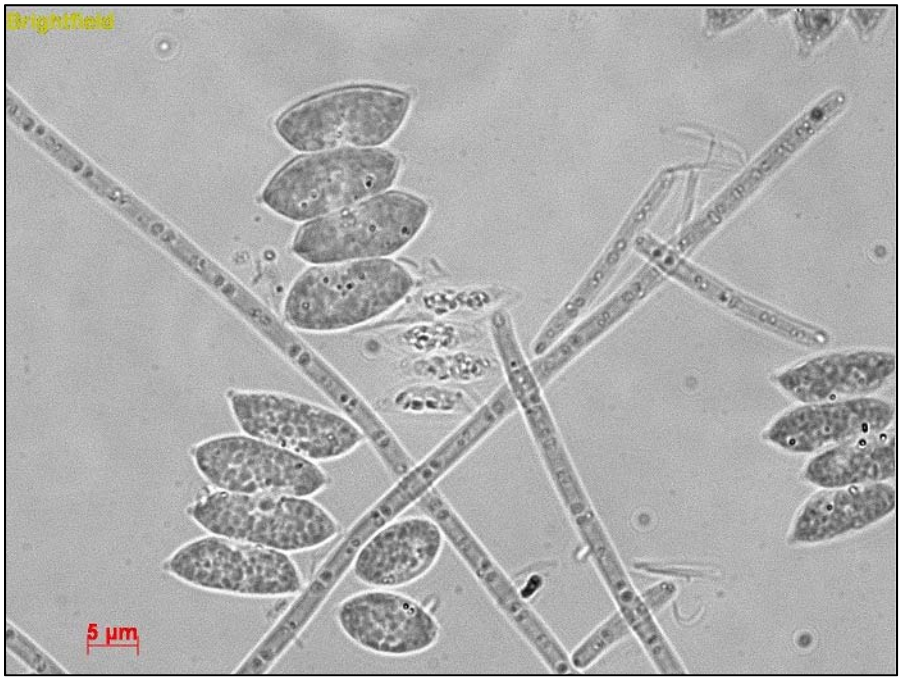

Figure J.3. Example of a transmitted light image of biomass in Photobioreactor 2. This image was taken after 4 days of batch operation under lit, phosphorus-deplete conditions.

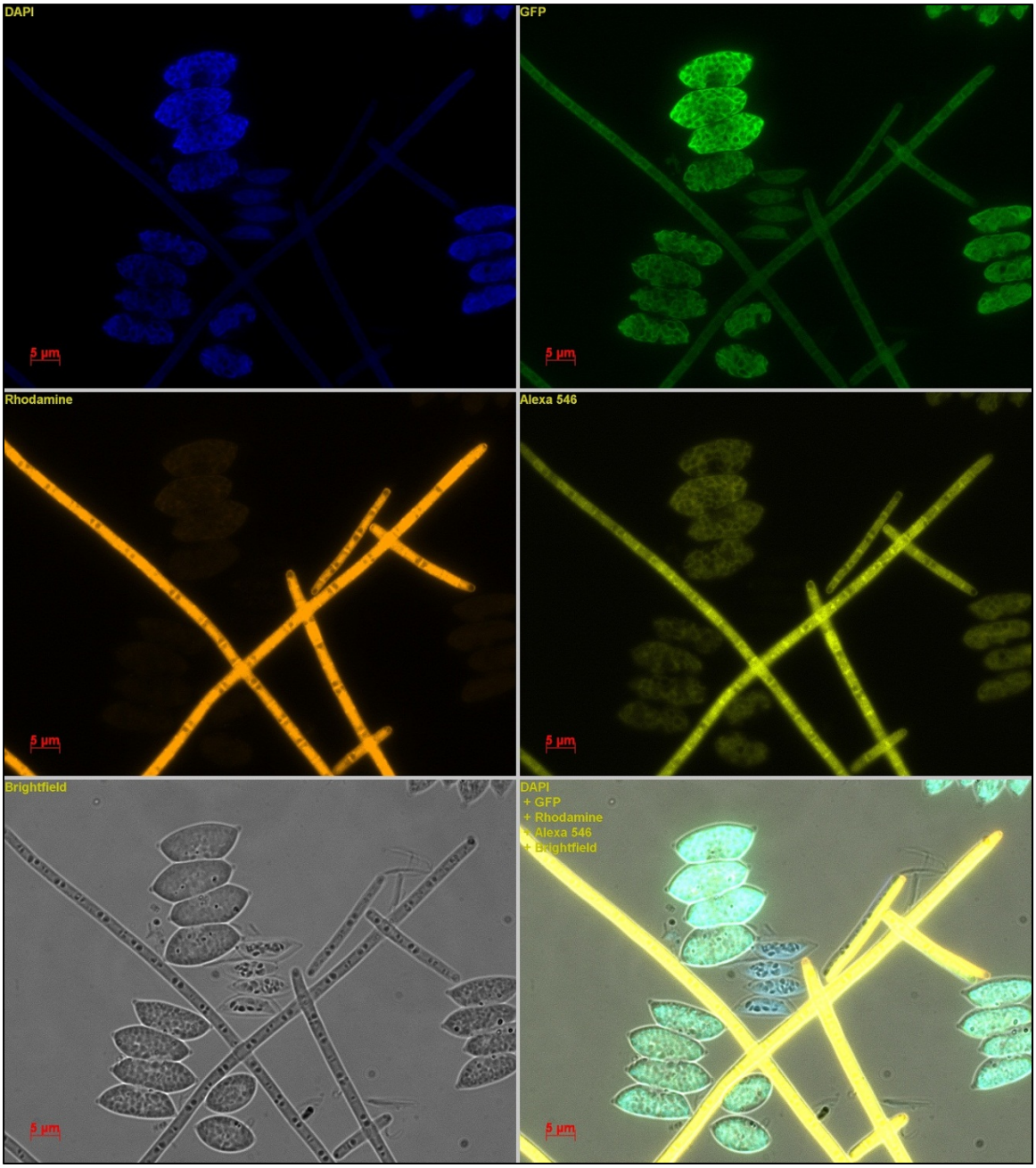

Figure J.4. Example of epifluorescence image of biomass from Photobioreactor 2. This image was taken after 4 days of batch operation under lit, phosphorus-deplete conditions.

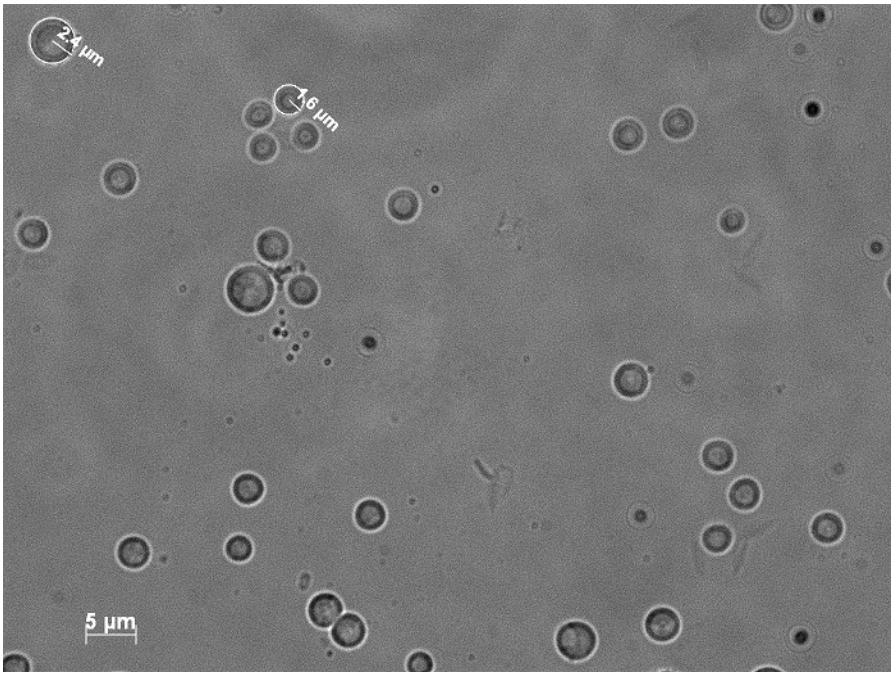

Figure J.5. Example of a transmitted light image of biomass in Photobioreactor 3. This image was taken after 4 days of batch operation under lit, nitrogen-deplete conditions.

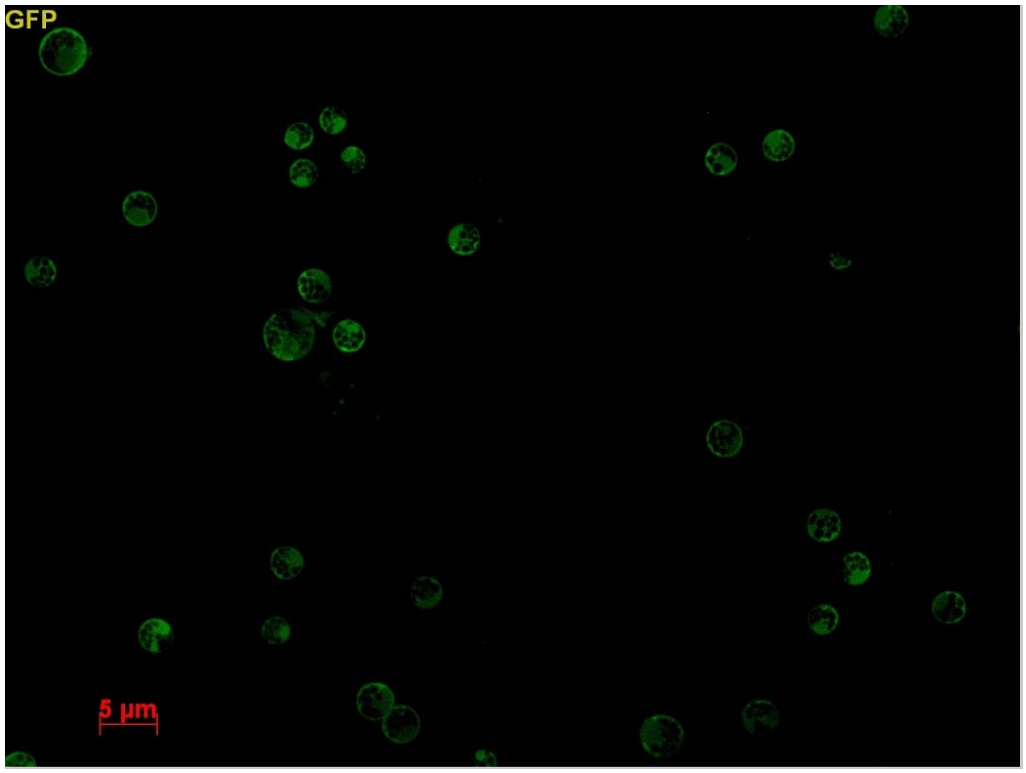

Figure J.6. Example of epifluorescence image of biomass from Photobioreactor 3. This image was taken after 4 days of batch operation under lit, nitrogen-deplete conditions.

Appendix K

Linear Equations for Phototrophic Process Model

Table K.1. Compiled linear equations for all reactions.

#	Equation	Units
1[a]	$r_{NADH2} = 0 = {}^{2}/_{3}\, r_2 + (2\delta_X - 0.1)\, r_3 + {}^{11}/_{6}\, r_5 - r_6 - {}^{45}/_{51}\, r_9 + {}^{38}/_{51}\, r_{10}$	moles $NADH_2$·hour^{-1}
2	$r_{ATP} = 0 = {}^{2}/_{3}\, r_2 - (\alpha_m - \tfrac{1}{2}\,\delta_N)\, r_3 - \left(\alpha_X + \frac{m_{ATP}}{\mu}\right) r_4 + {}^{1}/_{2}\, r_5 + \delta_{PO}\, r_6 - {}^{1}/_{6}\, r_7 - {}^{1}/_{6}\, r_8 - {}^{23}/_{51}\, r_9 - {}^{2}/_{51}\, r_{10}$	moles ATP·hour^{-1}
3	$r_{precursors} = 0 = r_3 - r_4$	C-moles precursors·hour^{-1}
4	$r_{acetyl\text{-}CoA} = 0 = {}^{2}/_{3}\, r_2 - (1 + \delta_x + \delta_N)\, r_3 - r_5 - {}^{50}/_{51}\, r_9 + {}^{50}/_{51}\, r_{10}$	C-moles acetyl-CoA·hour^{-1}
5	$r_{g3p} = 0 = r_1 - r_2 - r_7 + r_8$	C-moles G3P·hour^{-1}
6	$r_{biomass} = r_4$	C-moles biomass·hour^{-1}
7	$r_{PG} = r_7 - r_8$	C-moles PG·hour^{-1}
8	$r_{TAG} = r_9 - r_{10}$	C-moles TAG·hour^{-1}
9	$r_{O2} = r_1 - {}^{1}/_{2}\, r_6$	moles O_2·hour^{-1}
10	$r_{CO2} = -r_1 + {}^{1}/_{3}\, r_2 + (\delta_x + \delta_N)\, r_3 + r_5 - {}^{1}/_{51}\, r_9 + {}^{1}/_{51}\, r_{10}$	C-moles CO_2·hour^{-1}
11[b]	$4\, r_1 + 4\, (-{}^{1}/_{2}\, r_6) = {}^{290}/_{51}\, r_{TAG} + 4\, r_{PG} + 5.8\, r_{biomass}$	-

[a] Assumes $FADH_2 = {}^{2}/_{3}\, NADH_2$.

[b] Degree of reduction balance, based on [293], assuming a TAG elemental composition of $C_{51}H_{98}O_6$. Also, carbon in biomass is reduced 21/5 and nitrogen 8/5 (total of 29/5).

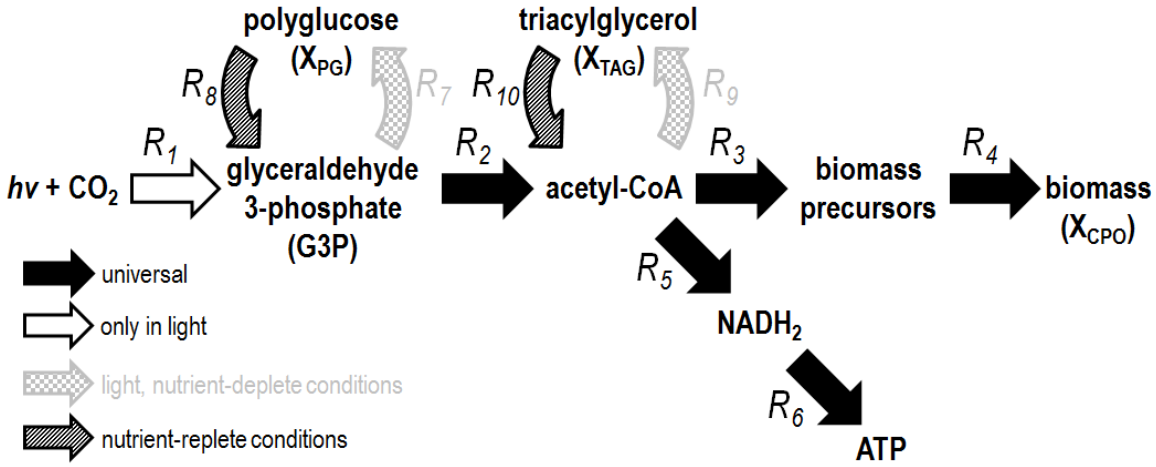

Figure K.1. Schematic representation of the lumped sum metabolic model under <u>nutrient-replete</u> conditions (i.e., sufficient nutrients for growth).

Table K.2. Linear equations for <u>nutrient-replete</u> metabolism of X_{CPO}.

#	Equation	Units
1[a]	$r_{NADH2} = 0 = {}^{2}/_{3}\, r_2 + (2\delta_X - 0.1)\, r_3 + {}^{11}/_{6}\, r_5 - r_6 + {}^{38}/_{51}\, r_{10}$	moles $NADH_2$·hour^{-1}
2	$r_{ATP} = 0 = {}^{2}/_{3}\, r_2 - (\alpha_m - \tfrac{1}{2}\,\delta_N)\, r_3 - \left(\alpha_X + \frac{m_{ATP}}{\mu}\right) r_4 + {}^{1}/_{2}\, r_5 + \delta_{PO}\, r_6 - {}^{1}/_{6}\, r_8 - {}^{2}/_{51}\, r_{10}$	moles ATP·hour^{-1}
3	$r_{precursors} = 0 = r_3 - r_4$	C-moles precursors·hour^{-1}
4	$r_{acetyl\text{-}CoA} = 0 = {}^{2}/_{3}\, r_2 - (1 + \delta_x + \delta_N)\, r_3 - r_5 + {}^{50}/_{51}\, r_{10}$	C-moles acetyl-CoA·hour^{-1}
5	$r_{g3p} = 0 = r_1 - r_2 + r_8$	C-moles G3P·hour^{-1}
6	$r_{biomass} = r_4$	C-moles biomass·hour^{-1}
7	$r_{PG} = - r_8$	C-moles PG·hour^{-1}
8	$r_{TAG} = - r_{10}$	C-moles TAG·hour^{-1}
9	$r_{O2} = r_1 - {}^{1}/_{2}\, r_6$	moles O_2·hour^{-1}
10	$r_{CO2} = - r_1 + {}^{1}/_{3}\, r_2 + (\delta_x + \delta_N)\, r_3 + r_5 + {}^{1}/_{51}\, r_{10}$	C-moles CO_2·hour^{-1}
11[b]	$4\, r_1 + 4\, (- {}^{1}/_{2}\, r_6) = {}^{290}/_{51}\, r_{TAG} + 4\, r_{PG} + 5.8\, r_{biomass}$	-

[a] Assumes $FADH_2 = {}^{2}/_{3}\, NADH_2$.
[b] Degree of reduction balance, based on [293], assuming a TAG elemental composition of $C_{51}H_{98}O_6$. Also, carbon in biomass is reduced 21/5 and nitrogen 8/5 (total of 29/5).

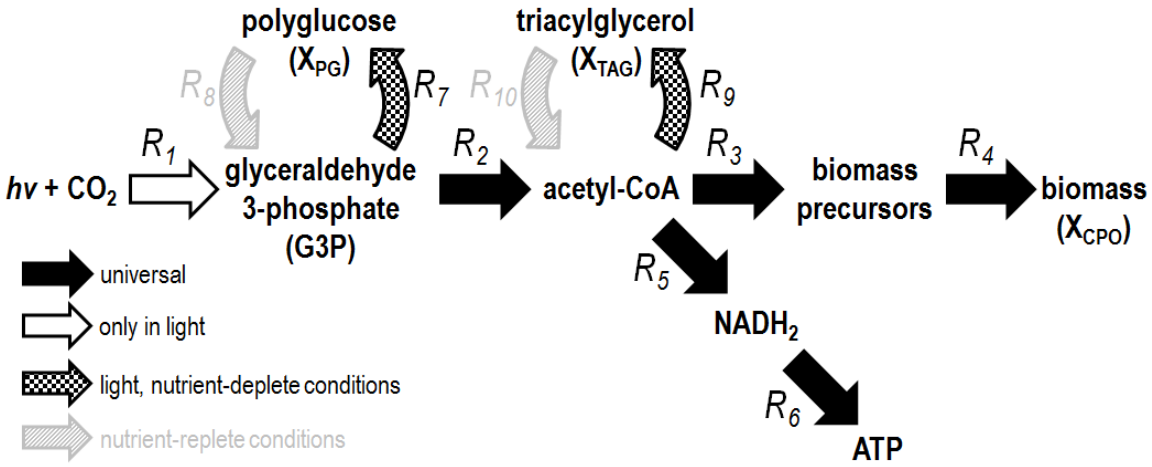

Figure K.2. Schematic representation of the lumped sum metabolic model under <u>nutrient-deplete</u> conditions.

Table K.3. Linear equations for <u>nutrient-deplete</u> metabolism of X_{CPO}.

#	Equation	Units
1[a]	$r_{NADH2} = 0 = {}^{2}/_{3}\, r_2 + (2\delta_X - 0.1)\, r_3 + {}^{11}/_{6}\, r_5 - r_6 - {}^{45}/_{51}\, r_9$	moles $NADH_2$·hour^{-1}
2	$r_{ATP} = 0 = {}^{2}/_{3}\, r_2 - (\alpha_m - \frac{1}{2}\,\delta_N)\, r_3 - \left(\alpha_X + \frac{m_{ATP}}{\mu}\right) r_4 + {}^{1}/_{2}\, r_5 + \delta_{PO}\, r_6 - {}^{1}/_{6}\, r_7 - {}^{23}/_{51}\, r_9$	moles ATP·hour^{-1}
3	$r_{precursors} = 0 = r_3 - r_4$	C-moles precursors·hour^{-1}
4	$r_{acetyl\text{-}CoA} = 0 = {}^{2}/_{3}\, r_2 - (1 + \delta_x + \delta_N)\, r_3 - r_5 - {}^{50}/_{51}\, r_9$	C-moles acetyl-CoA·hour^{-1}
5	$r_{g3p} = 0 = r_1 - r_2 - r_7$	C-moles G3P·hour^{-1}
6	$r_{biomass} = r_4$	C-moles biomass·hour^{-1}
7	$r_{PG} = r_7$	C-moles PG·hour^{-1}
8	$r_{TAG} = r_9$	C-moles TAG·hour^{-1}
9	$r_{O2} = r_1 - {}^{1}/_{2}\, r_6$	moles O_2·hour^{-1}
10	$r_{CO2} = -r_1 + {}^{1}/_{3}\, r_2 + (\delta_x + \delta_N)\, r_3 + r_5 - {}^{1}/_{51}\, r_9$	C-moles CO_2·hour^{-1}
11[b]	$4\, r_1 + 4\,(-{}^{1}/_{2}\, r_6) = {}^{290}/_{51}\, r_{TAG} + 4\, r_{PG} + 5.8\, r_{biomass}$	-

[a] Assumes $FADH_2 = {}^{2}/_{3}\, NADH_2$.

[b] Degree of reduction balance, based on [293], assuming a TAG elemental composition of $C_{51}H_{98}O_6$.

Appendix L
Mathematica Linear Equation Solutions for Phototrophic Process Model

Notes:

1. Headers on the top right of files are unique to a given linear solution.
2. There are 3 solutions for nutrient-replete conditions:
    a. q_{phot}
    b. q_{CO2}
    c. q_{O2}
3. There are 3 solutions for nutrient-deplete conditions:
    a. q_{phot}
    b. q_{CO2}
    c. q_{O2}
4. Rates (r) have been converted to specific rates (q) by applying the following substitutions:
    a. $r_{biomass} = \mu \cdot X_{CPO}$
    b. $r_1 = q_{phot} \cdot X_{CPO}$
    c. $r_{PG} = q_{PG} \cdot X_{CPO}$
    d. $r_{TAG} = q_{TAG} \cdot X_{CPO}$
5. Note that $r_{biomass}$, r_{PG}, and r_{TAG} are the rates of X_{CPO}, X_{PG}, and X_{TAG} formation, respectively.

In[1]:=
```
Clear["Global`*"]
```

In[2]:=
```
Solve[{(2/3)*r2 + (2+δx - (1/10))*r3 + (11/6)*r5 - r6 + (38/51)*r10 == 0,
  (2/3)*r2 - (αm - ((1/2)*δN))*r3 - (αx + (matp/μ))*r4 + (1/2)*r5 + δPO*r6 - (1/6)*r8 - (2/51)*r10 == 0,
  r3 - r4 == 0, (2/3)*r2 - (1 + δx + δN)*r3 - r5 + (50/51)*r10 == 0, r1 - r2 + r8 == 0,
  r4biomass - r4 == 0, r8pg + r8 == 0, r10tag + r10 == 0}, r1, {r2, r3, r4, r5, r6, r8, r10}]
```

Out[2]=
$$\left\{\left\{r1 \to -\frac{1}{170\,(9+17\,\delta PO)\,\mu}\right.\right.$$
$$(-1530\,matp\,r4biomass - 690\,r10tag\,\mu - 765\,r4biomass\,\mu - 1275\,r8pg\,\mu - 1530\,r4biomass\,\alpha m\,\mu -$$
$$1530\,r4biomass\,\alpha x\,\mu - 3890\,r10tag\,\delta PO\,\mu - 2958\,r4biomass\,\delta PO\,\mu - 2890\,r8pg\,\delta PO\,\mu -$$
$$\left.\left.2805\,r4biomass\,\delta N\,\delta PO\,\mu - 765\,r4biomass\,\delta x\,\mu + 255\,r4biomass\,\delta PO\,\delta x\,\mu)\right\}\right\}$$

In[3]:=
```
{-1/(170 (9 + 17 δPO) μ)
  (-1530 matp r4biomass - 690 r10tag μ - 765 r4biomass μ - 1275 r8pg μ - 1530 r4biomass αm μ -
    1530 r4biomass αx μ - 3890 r10tag δPO μ - 2958 r4biomass δPO μ - 2890 r8pg δPO μ -
    2805 r4biomass δN δPO μ - 765 r4biomass δx μ + 255 r4biomass δPO δx μ)} /. r10tag → qtag
```

Out[3]=
$$\left\{-\frac{1}{170\,(9+17\,\delta PO)\,\mu}\right.$$
$$(-1530\,matp\,r4biomass - 690\,qtag\,\mu - 765\,r4biomass\,\mu - 1275\,r8pg\,\mu - 1530\,r4biomass\,\alpha m\,\mu -$$
$$1530\,r4biomass\,\alpha x\,\mu - 3890\,qtag\,\delta PO\,\mu - 2958\,r4biomass\,\delta PO\,\mu - 2890\,r8pg\,\delta PO\,\mu -$$
$$\left.2805\,r4biomass\,\delta N\,\delta PO\,\mu - 765\,r4biomass\,\delta x\,\mu + 255\,r4biomass\,\delta PO\,\delta x\,\mu)\right\}$$

In[4]:=
```
{-1/(170 (9 + 17 δPO) μ)
  (-1530 matp r4biomass - 690 qtag μ - 765 r4biomass μ - 1275 r8pg μ - 1530 r4biomass αm μ -
    1530 r4biomass αx μ - 3890 qtag δPO μ - 2958 r4biomass δPO μ - 2890 r8pg δPO μ -
    2805 r4biomass δN δPO μ - 765 r4biomass δx μ + 255 r4biomass δPO δx μ)} /. r4biomass → μ
```

Out[4]=
$$\left\{-\frac{1}{170\,(9+17\,\delta PO)\,\mu}(-1530\,matp\,\mu - 690\,qtag\,\mu - 1275\,r8pg\,\mu - 3890\,qtag\,\delta PO\,\mu - 2890\,r8pg\,\delta PO\,\mu -\right.$$
$$\left.765\,\mu^2 - 1530\,\alpha m\,\mu^2 - 1530\,\alpha x\,\mu^2 - 2958\,\delta PO\,\mu^2 - 2805\,\delta N\,\delta PO\,\mu^2 - 765\,\delta x\,\mu^2 + 255\,\delta PO\,\delta x\,\mu^2)\right\}$$

In[5]:=
```
{-1/(170 (9 + 17 δPO) μ)
  (-1530 matp μ - 690 qtag μ - 1275 r8pg μ - 3890 qtag δPO μ - 2890 r8pg δPO μ - 765 μ^2 - 1530 αm μ^2 -
    1530 αx μ^2 - 2958 δPO μ^2 - 2805 δN δPO μ^2 - 765 δx μ^2 + 255 δPO δx μ^2)} /. r8pg → qpg
```

Out[5]=
$$\left\{-\frac{1}{170\,(9+17\,\delta PO)\,\mu}(-1530\,matp\,\mu - 1275\,qpg\,\mu - 690\,qtag\,\mu - 2890\,qpg\,\delta PO\,\mu - 3890\,qtag\,\delta PO\,\mu - 765\,\mu^2 -\right.$$
$$\left.1530\,\alpha m\,\mu^2 - 1530\,\alpha x\,\mu^2 - 2958\,\delta PO\,\mu^2 - 2805\,\delta N\,\delta PO\,\mu^2 - 765\,\delta x\,\mu^2 + 255\,\delta PO\,\delta x\,\mu^2)\right\}$$

In[6]:=
$$\text{Collect}\left[\frac{1}{170\,(9+17\,\delta\text{PO})\,\mu}\right.$$
$$\left(-1530\,\text{matp}\,\mu-1275\,\text{qpg}\,\mu-690\,\text{qtag}\,\mu-2890\,\text{qpg}\,\delta\text{PO}\,\mu-3890\,\text{qtag}\,\delta\text{PO}\,\mu-765\,\mu^2-1530\,\alpha\text{m}\,\mu^2-\right.$$
$$\left.\left.1530\,\alpha\text{x}\,\mu^2-2958\,\delta\text{PO}\,\mu^2-2805\,\delta\text{N}\,\delta\text{PO}\,\mu^2-765\,\delta\text{x}\,\mu^2+255\,\delta\text{PO}\,\delta\text{x}\,\mu^2\right),\{\mu,\text{qtag},\text{matp},\text{qpg}\},\text{Simplify}\right]$$

Out[6]=
$$\frac{9\,\text{matp}}{9+17\,\delta\text{PO}}+\frac{\text{qpg}\,(15+34\,\delta\text{PO})}{18+34\,\delta\text{PO}}+\frac{\text{qtag}\,(69+389\,\delta\text{PO})}{153+289\,\delta\text{PO}}+$$
$$\frac{3\,(15+30\,\alpha\text{m}+30\,\alpha\text{x}+58\,\delta\text{PO}+55\,\delta\text{N}\,\delta\text{PO}+15\,\delta\text{x}-5\,\delta\text{PO}\,\delta\text{x})\,\mu}{90+170\,\delta\text{PO}}$$

In[7]:=
$$\text{qphot}=\frac{9\,\text{matp}}{9+17\,\delta\text{PO}}+\frac{\text{qpg}\,(15+34\,\delta\text{PO})}{18+34\,\delta\text{PO}}+\frac{\text{qtag}\,(69+389\,\delta\text{PO})}{153+289\,\delta\text{PO}}+$$
$$\frac{3\,(15+30\,\alpha\text{m}+30\,\alpha\text{x}+58\,\delta\text{PO}+55\,\delta\text{N}\,\delta\text{PO}+15\,\delta\text{x}-5\,\delta\text{PO}\,\delta\text{x})\,\mu}{90+170\,\delta\text{PO}}$$

Out[7]=
$$\frac{9\,\text{matp}}{9+17\,\delta\text{PO}}+\frac{\text{qpg}\,(15+34\,\delta\text{PO})}{18+34\,\delta\text{PO}}+\frac{\text{qtag}\,(69+389\,\delta\text{PO})}{153+289\,\delta\text{PO}}+$$
$$\frac{3\,(15+30\,\alpha\text{m}+30\,\alpha\text{x}+58\,\delta\text{PO}+55\,\delta\text{N}\,\delta\text{PO}+15\,\delta\text{x}-5\,\delta\text{PO}\,\delta\text{x})\,\mu}{90+170\,\delta\text{PO}}$$

In[8]:=
```
Clear["Global`*"]
```

In[9]:=
```
Solve[{r3 - r4 == 0, (2/3)*r2 - (1 + δx + δN)*r3 - r5 + (50/51)*r10 == 0,
    r1 - r2 + r8 == 0, r4biomass - r4 == 0, r8pg + r8 == 0, r10tag + r10 == 0,
    rco2 + r1 - (1/3)*r2 - (δx + δN)*r3 - r5 - (1/51)*r10 == 0}, rco2, {r2, r3, r4, r5, r6, r8, r10}]
```

Out[9]=
$$\{\{rco2 \to -r10tag - r4biomass - r8pg\}\}$$

In[10]:=
```
{-r10tag - r4biomass - r8pg} /. r8pg → qpg
```

Out[10]=
$$\{-qpg - r10tag - r4biomass\}$$

In[11]:=
```
{-qpg - r10tag - r4biomass} /. r10tag → qtag
```

Out[11]=
$$\{-qpg - qtag - r4biomass\}$$

In[12]:=
```
{-qpg - qtag - r4biomass} /. r4biomass → μ
```

Out[12]=
$$\{-qpg - qtag - \mu\}$$

In[13]:=
```
qco2 = -qpg - qtag - μ
```

Out[13]=
$$-qpg - qtag - \mu$$

In[14]:=
```
Clear["Global`*"]
```

In[15]:=
```
Solve[{(2/3)*r2 + (2*δx - (1/10))*r3 + (11/6)*r5 - r6 + (38/51)*r10 == 0, r3 - r4 == 0,
  (2/3)*r2 - (αm - ((1/2)*δN))*r3 - (αx + (matp/μ))*r4 + (1/2)*r5 + δPO*r6 - (1/6)*r8 - (2/51)*r10 == 0,
  r4biomass - r4 == 0, r8pg + r8 == 0, r10tag + r10 == 0,
  4*r1 - 4*(1/2)*r6 - (290/51)*r10tag - 4*r8pg - (29/5)*r4biomass == 0,
  ro2 - r1 + (1/2)*r6 == 0}, ro2, {r2, r3, r4, r5, r6, r8, r10}]
```

Out[15]=
$$\left\{\left\{ro2 \to \frac{1450\,r10tag + 1479\,r4biomass + 1020\,r8pg}{1020}\right\}\right\}$$

In[16]:=
```
{ro2 -> 1/1020 (1450 r10tag + 1479 r4biomass + 1020 r8pg)} /. r8pg -> qpg
```

Out[16]=
$$\left\{ro2 \to \frac{1020\,qpg + 1450\,r10tag + 1479\,r4biomass}{1020}\right\}$$

In[17]:=
```
{(1020 qpg + 1450 r10tag + 1479 r4biomass)/1020} /. r10tag -> qtag
```

Out[17]=
$$\left\{\frac{1020\,qpg + 1450\,qtag + 1479\,r4biomass}{1020}\right\}$$

In[18]:=
```
{(1020 qpg + 1450 qtag + 1479 r4biomass)/1020} /. r4biomass -> μ
```

Out[18]=
$$\left\{\frac{1020\,qpg + 1450\,qtag + 1479\,\mu}{1020}\right\}$$

In[19]:=
```
{(1020 qpg + 1450 qtag + 1479 μ)/1020} /. r1 -> q1
```

Out[19]=
$$\left\{\frac{1020\,qpg + 1450\,qtag + 1479\,\mu}{1020}\right\}$$

In[20]:=
```
qo2 = (1020 qpg + 1450 qtag + 1479 μ)/1020
```

Out[20]=
$$\frac{1020\,qpg + 1450\,qtag + 1479\,\mu}{1020}$$

In[21]:=
```
Clear["Global`*"]
```

In[22]:=
```
Solve[{(2/3)*r2 + (2*δx - (1/10))*r3 + (11/6)*r5 - r6 - (45/51)*r9 == 0,
  (2/3)*r2 - (αm - ((1/2)*δN))*r3 - (αx + (matp/μ))*r4 + (1/2)*r5 + δPO*r6 - (1/6)*r7 - (23/51)*r9 == 0,
  r3 - r4 == 0, (2/3)*r2 - (1 + δx + δN)*r3 - r5 - (50/51)*r9 == 0, r1 - r2 - r7 == 0,
  r4biomass - r4 == 0, r8pg - r7 == 0, r10tag - r9 == 0}, r1, {r2, r3, r4, r5, r6, r7, r9}]
```

Out[22]=
$$\{\{r1 \to -(-1530\,matp\,r4biomass - 1440\,r10tag\,\mu - 765\,r4biomass\,\mu - 1785\,r8pg\,\mu - 1530\,r4biomass\,\alpha m\,\mu - 1530\,r4biomass\,\alpha x\,\mu - 4100\,r10tag\,\delta PO\,\mu - 2958\,r4biomass\,\delta PO\,\mu - 2890\,r8pg\,\delta PO\,\mu - 2805\,r4biomass\,\delta N\,\delta PO\,\mu - 765\,r4biomass\,\delta x\,\mu + 255\,r4biomass\,\delta PO\,\delta x\,\mu)/(170\,(9 + 17\,\delta PO)\,\mu)\}\}$$

In[23]:=
```
{-(-1530 matp r4biomass - 1440 r10tag μ - 765 r4biomass μ -
    1785 r8pg μ - 1530 r4biomass αm μ - 1530 r4biomass αx μ - 4100 r10tag δPO μ -
    2958 r4biomass δPO μ - 2890 r8pg δPO μ - 2805 r4biomass δN δPO μ -
    765 r4biomass δx μ + 255 r4biomass δPO δx μ)/(170 (9 + 17 δPO) μ)} /. r10tag → qtag
```

Out[23]=
$$\{(1530\,matp\,r4biomass + 1440\,qtag\,\mu + 765\,r4biomass\,\mu + 1785\,r8pg\,\mu + 1530\,r4biomass\,\alpha m\,\mu + 1530\,r4biomass\,\alpha x\,\mu + 4100\,qtag\,\delta PO\,\mu + 2958\,r4biomass\,\delta PO\,\mu + 2890\,r8pg\,\delta PO\,\mu + 2805\,r4biomass\,\delta N\,\delta PO\,\mu + 765\,r4biomass\,\delta x\,\mu - 255\,r4biomass\,\delta PO\,\delta x\,\mu)/(170\,(9 + 17\,\delta PO)\,\mu)\}$$

In[24]:=
```
{(1530 matp r4biomass + 1440 qtag μ + 765 r4biomass μ +
    1785 r8pg μ + 1530 r4biomass αm μ + 1530 r4biomass αx μ + 4100 qtag δPO μ +
    2958 r4biomass δPO μ + 2890 r8pg δPO μ + 2805 r4biomass δN δPO μ +
    765 r4biomass δx μ - 255 r4biomass δPO δx μ)/(170 (9 + 17 δPO) μ)} /. r8pg → qpg
```

Out[24]=
$$\{(1530\,matp\,r4biomass + 1785\,qpg\,\mu + 1440\,qtag\,\mu + 765\,r4biomass\,\mu + 1530\,r4biomass\,\alpha m\,\mu + 1530\,r4biomass\,\alpha x\,\mu + 2890\,qpg\,\delta PO\,\mu + 4100\,qtag\,\delta PO\,\mu + 2958\,r4biomass\,\delta PO\,\mu + 2805\,r4biomass\,\delta N\,\delta PO\,\mu + 765\,r4biomass\,\delta x\,\mu - 255\,r4biomass\,\delta PO\,\delta x\,\mu)/(170\,(9 + 17\,\delta PO)\,\mu)\}$$

In[25]:=
```
{(1530 matp r4biomass + 1785 qpg μ + 1440 qtag μ +
    765 r4biomass μ + 1530 r4biomass αm μ + 1530 r4biomass αx μ + 2890 qpg δPO μ +
    4100 qtag δPO μ + 2958 r4biomass δPO μ + 2805 r4biomass δN δPO μ +
    765 r4biomass δx μ - 255 r4biomass δPO δx μ)/(170 (9 + 17 δPO) μ)} /. r4biomass → μ
```

Out[25]=
$$\{(1530\,matp\,\mu + 1785\,qpg\,\mu + 1440\,qtag\,\mu + 2890\,qpg\,\delta PO\,\mu + 4100\,qtag\,\delta PO\,\mu + 765\,\mu^2 + 1530\,\alpha m\,\mu^2 + 1530\,\alpha x\,\mu^2 + 2958\,\delta PO\,\mu^2 + 2805\,\delta N\,\delta PO\,\mu^2 + 765\,\delta x\,\mu^2 - 255\,\delta PO\,\delta x\,\mu^2)/(170\,(9 + 17\,\delta PO)\,\mu)\}$$

In[26]:=
```
Collect[{(1530 matp μ + 1785 qpg μ + 1440 qtag μ + 2890 qpg δPO μ + 4100 qtag δPO μ + 765 μ^2 +
    1530 αm μ^2 + 1530 αx μ^2 + 2958 δPO μ^2 + 2805 δN δPO μ^2 + 765 δx μ^2 - 255 δPO δx μ^2)/
  (170 (9 + 17 δPO) μ), {μ, qtag, matp, qpg}, Simplify]
```

Out[26]=
$$\frac{9\,matp}{9 + 17\,\delta PO} + \frac{qpg\,(21 + 34\,\delta PO)}{18 + 34\,\delta PO} + \frac{qtag\,(144 + 410\,\delta PO)}{153 + 289\,\delta PO} + \frac{3\,(15 + 30\,\alpha m + 30\,\alpha x + 58\,\delta PO + 55\,\delta N\,\delta PO + 15\,\delta x - 5\,\delta PO\,\delta x)\,\mu}{90 + 170\,\delta PO}$$

In[27]:=
```
qphot = 9 matp/(9 + 17 δPO) + qpg (21 + 34 δPO)/(18 + 34 δPO) + qtag (144 + 410 δPO)/(153 + 289 δPO) +
  3 (15 + 30 αm + 30 αx + 58 δPO + 55 δN δPO + 15 δx - 5 δPO δx) μ/(90 + 170 δPO)
```

Out[27]=
$$\frac{9\,matp}{9 + 17\,\delta PO} + \frac{qpg\,(21 + 34\,\delta PO)}{18 + 34\,\delta PO} + \frac{qtag\,(144 + 410\,\delta PO)}{153 + 289\,\delta PO} + \frac{3\,(15 + 30\,\alpha m + 30\,\alpha x + 58\,\delta PO + 55\,\delta N\,\delta PO + 15\,\delta x - 5\,\delta PO\,\delta x)\,\mu}{90 + 170\,\delta PO}$$

In[28]:=
```
Clear["Global`*"]
```

In[29]:=
```
Solve[{r3 - r4 == 0, (2/3)*r2 - (1 + δx + δN)*r3 - r5 - (50/51)*r9 == 0,
    r1 - r2 - r7 == 0, r4biomass - r4 == 0, r8pg - r7 == 0, r10tag - r9 == 0,
    rco2 + r1 - (1/3)*r2 - (δx + δN)*r3 - r5 + (1/51)*r9 == 0}, rco2, {r2, r3, r4, r5, r7, r9}]
```

Out[29]=
$$\{\{rco2 \to -r10tag - r4biomass - r8pg\}\}$$

In[30]:=
```
{-r10tag - r4biomass - r8pg} /. r8pg → qpg
```

Out[30]=
$$\{-qpg - r10tag - r4biomass\}$$

In[31]:=
```
{-qpg - r10tag - r4biomass} /. r10tag → qtag
```

Out[31]=
$$\{-qpg - qtag - r4biomass\}$$

In[32]:=
```
{-qpg - qtag - r4biomass} /. r4biomass → μ
```

Out[32]=
$$\{-qpg - qtag - \mu\}$$

In[33]:=
```
qco2 = -qpg - qtag - μ
```

Out[33]=
$$-qpg - qtag - \mu$$

In[34]:=
```
Clear["Global`*"]
```

In[35]:=
```
Solve[{(2/3)*r2 + (2*δx - (1/10))*r3 + (11/6)*r5 - r6 - (45/51)*r9 == 0,
  (2/3)*r2 - (αm - ((1/2)*δN))*r3 - (αx + (matp/μ))*r4 + (1/2)*r5 + δPO*r6 - (1/6)*r7 - (23/51)*r9 == 0,
  r3 - r4 == 0, r4biomass - r4 == 0, r8pg - r7 == 0, r10tag - r9 == 0,
  4*r1 - 4*(1/2)*r6 - (290/51)*r10tag - 4*r8pg - (29/5)*r4biomass == 0,
  ro2 - r1 + (1/2)*r6 == 0}, ro2, {r2, r3, r4, r5, r6, r7, r9}]
```

Out[35]=
$$\left\{\left\{ro2 \to \frac{1450\,r10tag + 1479\,r4biomass + 1020\,r8pg}{1020}\right\}\right\}$$

In[36]:=
```
{(1450 r10tag + 1479 r4biomass + 1020 r8pg)/1020} /. r8pg → qpg
```

Out[36]=
$$\left\{\frac{1020\,qpg + 1450\,r10tag + 1479\,r4biomass}{1020}\right\}$$

In[37]:=
```
{(1020 qpg + 1450 r10tag + 1479 r4biomass)/1020} /. r10tag → qtag
```

Out[37]=
$$\left\{\frac{1020\,qpg + 1450\,qtag + 1479\,r4biomass}{1020}\right\}$$

In[38]:=
```
{(1020 qpg + 1450 qtag + 1479 r4biomass)/1020} /. r4biomass → μ
```

Out[38]=
$$\left\{\frac{1020\,qpg + 1450\,qtag + 1479\,\mu}{1020}\right\}$$

In[39]:=
```
qo2 = (1020 qpg + 1450 qtag + 1479 μ)/1020
```

Out[39]=
$$\frac{1020\,qpg + 1450\,qtag + 1479\,\mu}{1020}$$

References

1. World Health Organization; United Nations Children's Fund Joint Monitoring Program for Water Supply and Sanitation *Progress on Drinking Water and Sanitation: Special Focus on Sanitation*; UNICEF, New York and WHO, Geneva: 2008.
2. Rockström, J.; Steffen, W.; Noone, K.; Persson, A.; Chapin, F. S.; Lambin, E. F.; Lenton, T. M.; Scheffer, M.; Folke, C.; Schellnhuber, H. J.; Nykvist, B.; de Wit, C. A.; Hughes, T.; van der Leeuw, S.; Rodhe, H.; Sörlin, S.; Snyder, P. K.; Costanza, R.; Svedin, U.; Falkenmark, M.; Karlberg, L.; Corell, R. W.; Fabry, V. J.; Hansen, J.; Walker, B.; Liverman, D.; Richardson, K.; Crutzen, P.; Foley, J. A., A safe operating space for humanity. *Nature* **2009,** *461*, (7263), 472-475.
3. Unknown, Water-analysis for sanitary purposes. *The British Medical Journal* **1869,** *2*, (445), 32-33.
4. Unknown, The disposal of sewage. *The British Medical Journal* **1872,** *2*, (606), 168-169.
5. Ardern, E.; Lockett, W. T., Experiments on the oxidation of sewage without the aid of filters. *J. Society of Chemical Industry* **1914,** *33*, (10), 523-539.
6. Grady Jr., C. P. L.; Daigger, G. T.; Love, N. G.; Filipe, C. D. M., *Biological Wastewater Treatment*. Third Edition ed.; CRC Press: Boca Raton, FL, 2011; p 1022.
7. Metcalf & Eddy, I.; Tchobanoglous, G.; Burton, F. L.; Stensel, H. D., *Wastewater Engineering: Treatment and Reuse*. 4th ed.; McGraw-Hill: New York, 2003; p 1819.
8. Barnard, J. L., Biological nutrient removal without the addition of chemicals. *Water Res.* **1975,** *9*, 485-490.
9. Lettinga, G.; Roersma, R.; Grin, P., Anaerobic treatment of raw domestic sewage at ambient temperatures using a granular bed UASB reactor. *Biotechnol. Bioeng.* **1983,** *25*, (7), 1701-1724.
10. Jetten, M. S. M.; Strous, M.; van de Pas-Schoonen, K. T.; Schalk, J.; van Dongen, U.; van de Graaf, A. A.; Logemann, S.; Muyzer, G.; van Loosdrecht, M. C. M.; Kuenen, J. G., The anaerobic oxidation of ammonium. *Fems Microbiology Reviews* **1998,** *22*, (5), 421-437.
11. Daigger, G. T., Evolving urban water and residuals management paradigms: water reclamation and reuse, decentralization, and resource recovery. *Water Environ. Res.* **2009,** *81*, (8), 809-823.
12. Larsen, T. A.; Gujer, W., Separate management of anthropogenic nutrient solutions (human urine). *Water Science and Technology* **1996,** *34*, (3-4), 87-94.
13. Mihelcic, J. R.; Crittenden, J. C.; Small, M. J.; Shonnard, D. R.; Hokanson, D. R.; Zhang, Q.; Chen, H.; Sorby, S. A.; James, V. U.; Sutherland, J. W.; Schnoor, J. L., Sustainability science and engineering: the emergence of a new metadiscipline. *Environmental Science & Technology* **2003,** *37*, (23), 5314-5324.
14. Clark, W. C.; Dickson, N. M., Sustainability science: the emerging research program. *Proceedings of the National Academy of Sciences - U.S.A.* **2003,** *100*, (14), 8059-8061.

15. Holling, C. S., Understanding the complexity of economic, ecological, and social systems. *Ecosystems* **2001,** *4*, 390-405.
16. Gunderson, L. H.; Holling, C. S., *Panarchy: Understanding Transformations in Human and Natural Systems*. Island Press: Washington, DC, 2002.
17. Ostrom, E., A diagnostic approach for going beyond panaceas. *Proceedings of the National Academy of Sciences - U.S.A.* **2008,** *104*, (39), 15181-15187.
18. Clark, W. C., Sustainability science: a room of its own. *Proceedings of the National Academy of Sciences - U.S.A.* **2007,** *104*, (6), 1737-1738.
19. American Society of Civil Engineers *Report Card for American Infrastructure*; 2009.
20. Zimmerman, J. B.; Mihelcic, J. R.; Smith, J., Global stressors on water quality and quantity. *Environ. Sci. Technol.* **2008,** *42*, (12), 4247-4254.
21. U.S. Environmental Protection Agency *Despite Progress, EPA Needs to Improve Oversight of Wastewater Upgrades in the Chesapeake Bay Watershed*; Washington, D.C., January 8, 2008.
22. Gleick, P. H., Water in crisis: paths to sustainable water use. *Ecol. Applications* **1998,** *8*, (3), 571-579.
23. Matos, R.; Cardoso, A.; Ashley, R.; Duarte, P.; Molinari, A.; Schulz, A., *Performance Indicators for Wastewater Services*. IWA Publishing: London, 2003.
24. Guest, J. S.; Skerlos, S. J.; Barnard, J. L.; Beck, M. B.; Daigger, G. T.; Hilger, H.; Jackson, S. J.; Karvazy, K.; Kelly, L.; Macpherson, L.; Mihelcic, J. R.; Pramanik, A.; Raskin, L.; van Loosdrecht, M. C. M.; Yeh, D.; Love, N. G., A new planning and design paradigm to achieve sustainable resource recovery from wastewater. *Environ. Sci. Technol.* **2009,** *43*, (16), 6126-6130.
25. Allen, D. T.; Shonnard, D. R., Environmentally conscious design of chemical processes and products: a collaborative internet-based modeling approach. *AICHE Journal* **2001,** *47*, (9), 1906-1910.
26. Anastas, P. T.; Kirchhoff, M. M., Origins, current status, and future challenges of green chemistry. *Accounts of Chemical Research* **2002,** *35*, (9), 686-694.
27. Ullman, D. G., *The Mechanical Design Process, Second Edition*. McGraw-Hill: New York, 1997; p 340.
28. Ramani, K.; Ramanujan, D.; Bernstein, W. Z.; Zhao, F.; Sutherland, J.; Handwerker, C.; Choi, J. K.; Kim, H.; Thurston, D., Integrated sustainable life cycle design: a review. *Journal of mechanical design* **2010,** *132*, (9), 091004-1 - 091004-15.
29. Grimm, N. B.; Faeth, S. H.; Golubiewski, N. E.; Redman, C. L.; Wu, J.; Bai, X.; Briggs, J. M., Global change and the ecology of cities. *Science* **2008,** *319*, 756-760.
30. Beck, M. B. *Cities as Forces of Good in the Environment: Sustainability in the Water Sector*; Warnell School of Forestry and Natural Resources, University of Georgia: Athens, Georgia (ISBN: 978-1-61584-248-4), 2011.
31. Boyle, C.; Mudd, G.; Mihelcic, J. R.; Anastas, P.; Collins, T.; Culligan, P.; Edwards, M.; Gabe, J.; Gallagher, P.; Handy, S.; Kao, J. J.; Krumdieck, S.; Lyles, L. D.; Mason, I.; McDowall, R.; Pearce, A.; Riedy, C.; Russell, J.; Schnoor, J. L.; Trotz, M.; Venables, R.; Zimmerman, J. B.; Fuchs, V.; Miller, S.; Page, S.; Reeder-Emery, K., Delivering sustainable infrastructure that supports the urban built environment. *Environ. Sci. Technol.* **2010,** *44*, (13), 4836-4840.
32. Dietz, M. E., Low impact development practices: A review of current research and recommendations for future directions. *Water Air and Soil Pollution* **2007,** *186*, (1-4), 351-363.
33. Sartori, I.; Hestnes, A. G., Energy use in the life cycle of conventional and low-energy buildings: A review article. *Energy and Buildings* **2007,** *39*, (3), 249-257.
34. Mora, E. P., Life cycle, sustainability and the transcendent quality of building materials. *Building and Environment* **2007,** *42*, (3), 1329-1334.

35. Verstraete, W.; de Caveye, P. V.; Diamantis, V., Maximum use of resources present in domestic "used water". *Bioresource Technology* **2009,** *100*, (23), 5537-5545.
36. Lazzarin, R. M.; Gasparella, A., Technical and economical analysis of heat recovery in building ventilation systems. *Applied Thermal Engineering* **1998,** *18*, (1-2), 47-67.
37. Larsen, T. A.; Alder, A. C.; Eggen, R. I. L.; Maurer, M.; Lienert, J., Source separation: will we see a paradigm shift in wastewater handling? *Environ. Sci. Technol.* **2009,** *43*, (16), 6121-6125.
38. Corominas, L.; Foley, J.; Guest, J. S.; Hospido, A.; Larsen, H. F.; Shaw, A., Towards a standard method for life cycle assessments (LCA) of wastewater treatment. In *Watermatex - 8th IWA Symposium on System Analysis and Integrated Assessment*, IWA: San Sebastian, Spain, 2011.
39. Peters, G. M.; Rowley, H. V., Environmental comparison of biosolids management systems using life cycle assessment. *Environmental Science & Technology* **2009,** *43*, (8), 2674-2679.
40. Marks, J.; Martin, B.; Zadoroznyj, M., How Australians order acceptance of recycled water: national baseline data. *J. Sociology* **2008,** *44*, (1), 83-99.
41. Lundin, M.; Bengtsson, M.; Molander, S., Life cycle assessment of wastewater systems: influence of system boundaries and scale on calculated environmental loads. *Environ. Sci. Technol.* **2000,** *34*, (1), 180-186.
42. Lienert, J.; Larsen, T. A., High acceptance of urine source separation in seven European countries - a review. *Environ. Sci. Technol.* **accepted**.
43. Montgomery, M. A.; Elimelech, M., Water and sanitation in developing countries: including health in the equation. *Environ. Sci. Technol.* **2007,** *41*, (1), 17-24.
44. Fry, L. M.; Mihelcic, J. R.; Watkins, D. W., Water and nonwater-related challenges of achieving global sanitation coverage. *Environ. Sci. Technol.* **2008,** *42*, (12), 4298-4304.
45. Mihelcic, J. R.; Fry, L. M.; Myre, E. A.; Philips, L. D.; Barkdoll, B. D., *Field Guide to Environmental Engineering for Development Workers: Water, Sanitation, and Indoor Air*. American Society of Civil Engineers (ASCE) Press: Reston, VA, 2009; p 550.
46. McConville, J. R.; Mihelcic, J. R., Adapting life-cycle thinking tools to evaluate project sustainability in international water and sanitation development work. *Environ. Eng. Sci.* **2007,** *24*, (7), 937-948.
47. Phillips, H. M.; Sahlstedt, K. E.; Frank, K.; Bratby, J.; Brennan, W.; Rogowski, S.; Pier, D.; Anderson, W.; Mulas, M.; Copp, J. B.; Shirodkar, N., Wastewater treatment modelling in practice: a collaborative discussion of the state of the art. *Water Sci. Technol.* **2009,** *59*, (4), 695-704.
48. Belia, E.; Amerlinck, Y.; Benedetti, L.; Johnson, B.; Sin, G.; Vanrolleghem, P. A.; Gernaey, K. V.; Gillot, S.; Neumann, M. B.; Rieger, L.; Shaw, A.; Villez, K., Wastewater treatment modelling: dealing with uncertainties. *Water Sci. Technol.* **2009,** *60*, (8), 1929-1941.
49. Rebitzer, G.; Hunkeler, D.; Jolliet, O., LCC - the economic pillar of sustainability: methodology and application to wastewater treatment. *Environmental Progress* **2003,** *22*, (4), 241-249.
50. ISO *14040:1997 - Environmental management - Life cycle assessment - Principles and framework*; Switzerland, 1997.
51. ISO *14044:2006 - Environmental management - Life cycle assessment - Requirements and guidelines*; Switzerland, 2006.
52. Ashley, R.; Blackwood, D.; Butler, D.; Jowitt, P.; Davies, J.; Smith, H.; Gilmour, D.; Oltean-Dumbrava, C., Making asset investment decisions for wastewater systems that include sustainability. *J. Environ. Engineering - ASCE* **2008,** *134*, (3), 200-209.

53. van Hise, C. R., Preservation of the phosphates and the conservation of the soil. *Annals of the American Academy of Political and Social Science* **1909**, 215-226.
54. Tchobanoglous, G.; Burton, F. L.; Stensel, H. D., *Wastewater Engineering: Treatment and Reuse*. 4th ed.; McGraw-Hill: New York, 2003; p 1819.
55. Lettinga, G.; Hulshoff Pol, L. W., UASB-process design for various types of wastewaters. *Water Sci. Technol* **1991,** *24*, (8), 87-107.
56. Logan, B. E.; Hamelers, B.; Rozendal, R. A.; Schrorder, U.; Keller, J.; Freguia, S.; Aelterman, P.; Verstraete, W.; Rabaey, K., Microbial fuel cells: methodology and technology. *Environmental Science & Technology* **2006,** *40*, (17), 5181-5192.
57. Le Corre, K. S.; Valsami-Jones, E.; Hobbs, P.; Parsons, S. A., Phosphorus recovery from wastewater by struvite crystallization: a review. *Critical Reviews in Environmental Science and Technology* **2009,** *39*, (6), 433-477.
58. Chisti, Y., Biodiesel from microalgae. *Biotechnology Advances* **2007,** *25*, (3), 294-306.
59. Rich, L. G., *Unit Processes of Sanitary Engineering*. John Wiley & Sons, Inc.: United States, 1963.
60. Mara, D. D., *Domestic Wastewater Treatment in Developing Countries*. 1 ed.; Earthscan Publications: London, 2004.
61. Lardon, L.; Helias, A.; Sialve, B.; Steyer, J. P.; Bernard, O., Life-cycle assessment of biodiesel production from microalgae. *Environ. Sci. Technol.* **2009,** *43*, (17), 6475-6481.
62. Mata, T. M.; Martins, A. A.; Caetano, N. S., Microalgae for biodiesel production and other applications: a review. *Renewable & Sustainable Energy Reviews* **2010,** *14*, (1), 217-232.
63. Bradley, B. R.; Daigger, G. T. In *A sustainable development approach to wastewater infrastructure*, Water Environment Federation Technical Exhibition and Conference, 2000; 2000.
64. Palme, U.; Lundin, M.; Tillman, A. M.; Molander, S., Sustainable development indicators for wastewater systems - researchers and indicator users in a co-operative case study. *Resources Conservation and Recycling* **2005,** *43*, (3), 293-311.
65. World Commission on Environment and Development (WCED) *Our Common Future*; United Nations: 1987.
66. Kates, R. W.; Clark, W. C.; Corell, R.; Hall, J. M.; Jaeger, C. C.; Lowe, I.; McCarthy, J. J.; Schellnhuber, H. J.; Bolin, B.; Dickson, N. M.; Faucheux, S.; Gallopin, G. C.; Grubler, A.; Huntley, B.; Jager, J.; Jodha, N. S.; Kasperson, R. E.; Mabogunje, A.; Matson, P.; Mooney, H.; Moore, B.; O'Riordan, T.; Svedin, U., Sustainability science. *Science* **2001,** *292*, (5517), 641-642.
67. Reiss, R., Sustainability from the CEO Perspective. *Forbes* September 13, 2011.
68. Wikipedia Sustainability. http://en.wikipedia.org/wiki/Sustainability
69. Jerneck, A.; Olsson, L.; Ness, B.; Anderberg, S.; Baier, M.; Clark, E.; Hickler, T.; Hornborg, A.; Kronsell, A.; Lovbrand, E.; Persson, J., Structuring sustainability science. *Sustainability Science* **2011,** *6*, (1), 69-82.
70. Kajikawa, Y., Research core and framework of sustainability science. *Sustain. Sci.* **2008,** *3*, (2), 215-239.
71. Schoolman, E. D.; Guest, J. S.; Bush, K. F.; Bell, A. R., How interdisciplinary is sustainability research? Analyzing the structure of an emerging scientific field. *Sustain. Sci.* **in press**.
72. Benedetti, L.; Dirckx, G.; Bixio, D.; Thoeye, C.; Vanrolleghem, P. A., Environmental and economic performance assessment of the integrated urban wastewater system. *J. Environ. Management* **2008,** *88*, (4), 1262-1272.

73. Lundie, S.; Peters, G. M.; Beavis, P. C., Life cycle assessment for sustainable metropolitan water systems planning. *Environ. Sci. Technol.* **2004,** *38*, (13), 3465-3473.
74. Pasqualino, J. C.; Meneses, M.; Abella, M.; Castells, F., LCA as a decision support tool for the environmental improvement of the operation of a municipal wastewater treatment plant. *Environ. Sci. Technol.* **2009,** *43*, (9), 3300-3307.
75. Mihelcic, J. R.; Myre, E. A.; Fry, L. M.; Philips, L. D.; Barkdoll, B. D., *Field Guide in Environmental Engineering for Development Workers: Water, Sanitation, Indoor Air*. American Society of Civil Engineers (ASCE) Press: Reston, VA, 2009.
76. Lin, C., Identifying lowest-emission choices and environmental Pareto frontiers for wastewater treatment. *J. Industrial Ecology* **2011,** *15*, (3), 367-380.
77. Lim, S. R.; Park, J. M., Environmental impact minimization of a total wastewater treatment network system from a life cycle perspective. *J. Environ. Management* **2009,** *90*, 1454-1462.
78. Biswas, P.; Bose, P.; Tare, V., Optimal choice of wastewater treatment train by multi-objective optimization. *Engineering Optimization* **2007,** *39*, (2), 125-145.
79. International Council for Science *ICSU Series on Science for Sustainable Development. No. 9: Science and Technology for Sustainable Development*; 2002; p 30.
80. Beck, M. B.; Jiang, F.; Shi, F.; Villarroel Walker, R., Technology, Sustainability, and Business: Cities as Forces for Good in the Environment. In *Integrated Urban Water Management in Temperate Climates*, Maksimovic, C., Ed. UNESCO/Taylor & Francis: London, in press.
81. Li, F. Y.; Wichmann, K.; Otterpohl, R., Review of the technological approaches for grey water treatment and reuses. *Science of the Total Environment* **2009,** *407*, (11), 3439-3449.
82. Funamizu, N.; Iida, M.; Sakakura, Y.; Takakuwa, T., Reuse of heat energy in wastewater: implementation examples in Japan. *Water Sci. Technol.* **2001,** *43*, (10), 277-285.
83. Driver, J.; Lijmbach, D.; Steen, I., Why recover phosphorus for recycling, and how? *Environmen. Technol.* **1999,** *20*, 651-662.
84. Kleerebezem, R.; van Loosdrecht, M. C. M., Mixed culture biotechnology for bioenergy production. *Curr. Opin. Biotechnol.* **2007,** *18*, (3), 207-212.
85. Rozendal, R. A.; Leone, E.; Keller, J.; Rabaey, K., Efficient hydrogen peroxide generation from organic matter in a bioelectrochemical system. *Electrochemistry Communications* **2009,** *11*, (9), 1752-1755.
86. Public Utilities Board of Singapore NEWater. Accessed December 12, 2011, Internet: http://www.pub.gov.sg/water/Pages/NEWater.aspx.
87. Schroedel, R. B., Jr.; Cavagnaro, P. V.; Mukira, D. In *Digester gas powers energy conservation at Baltimore's Back River WWTP*, WEF Sustainability, National Harbor, United States, 2008; National Harbor, United States, 2008.
88. Clarens, A. F.; Resurreccion, E. P.; White, M. A.; Colosi, L. M., Environmental life cycle comparison of algae to other bioenergy feedstocks. *Environ. Sci. Technol.* **2010,** *44*, 1813-1819.
89. Water Environment Federation *Renewable Energy Generation from Wastewater - Water Environment Federation Position Statement*; Alexandria, Virginia, 2011.
90. Henze, M.; Grady, C. P. L.; Gujer, W.; Marais, G. V. R.; Matsuo, T., A general-model for single-sludge waste-water treatment systems. *Water Res.* **1987,** *21*, (5), 505-515.

91. Gujer, W.; Henze, M.; Mino, T.; Matsuo, T.; Wentzel, M. C.; Marais, G. v. R., The activated sludge model no. 2: biological phosphorus removal. *Water Sci. Technol.* **1995,** *31*, (2), 1-11.
92. Henze, M.; Gujer, W.; Mino, T.; Matsuo, T.; Wentzel, M. C.; Marais, G. v. R.; van Loosdrecht, M. C. M., Activated sludge model No. 2d, ASM2D. *Water Sci. Technol.* **1999,** *39*, (1), 165-182.
93. Gujer, W.; Henze, M.; Mino, T.; van Loosdrecht, M., Activated Sludge Model No. 3. *Water Sci. Technol.* **1999,** *39*, (1), 183-193.
94. Batstone, D. J.; Keller, J.; Angelidaki, I.; Kalyuzhnyi, S. V.; Pavlostathis, S. G.; Rozzi, A.; Sanders, W. T. M.; Siegrist, H.; Vavilin, V. A., The IWA Anaerobic Digestion Model No 1 (ADM1). *Water Sci. Technol.* **2001,** *45*, (10), 65-73.
95. Batstone, D. J.; Keller, J.; Angelidaki, I.; Kalyuzhnyi, S. V.; Pavlostathis, S. G.; Rozzi, A.; Sanders, W. T. M.; Siegrist, H.; Vavilin, V. A. *Anaerobic Digestion Model No. 1 (ADM1)*; International Water Association: London, 2002; p 77.
96. Nopens, I.; Batstone, D. J.; Copp, J. B.; Jeppsson, U.; Volcke, E.; Alex, J.; Vanrolleghem, P. A., An ASM/ADM model interface for dynamic plant-wide simulation. *Water Res.* **2009,** *43*, (7), 1913-1923.
97. Volcke, E. I. P.; van Loosdrecht, M. C. M.; Vanrolleghem, P. A., Continuity-based model interfacing for plant-wide simulation: A general approach. *Water Res.* **2006,** *40*, (15), 2817-2828.
98. Zaher, U.; Grau, P.; Benedetti, L.; Ayesa, E.; Vanrolleghem, P. A., Transformers for interfacing anaerobic digestion models to pre- and post-treatment processes in a plant-wide modelling context. *Environmental Modelling & Software* **2007,** *22*, (1), 40-58.
99. Vanrolleghem, P. A.; Rosen, C.; Zaher, U.; Copp, J.; Benedetti, L.; Ayesa, E.; Jeppsson, U., Continuity-based interfacing of models for wastewater systems described by Petersen matrices. *Water Sci. Technol.* **2005,** *52*, (1-2), 493-500.
100. Seco, A.; Ribes, J.; Serralta, J.; Ferrer, J., Biological nutrient removal model No. 1 (BNRM1). *Water Sci. Technol.* **2004,** *50*, (6), 69-78.
101. Jones, R. M.; Dold, P. L.; Takacs, I.; Chapman, K.; Wett, B.; Murthy, S.; O'Shaughnessy, M. In *Simulation for operation and control of reject water treatment processes*, Proceedings of the Water Environment Federation 80th Annual Technical Exhibition and Conference (WEFTEC), San Diego, CA, 2007; San Diego, CA, 2007.
102. Grau, P.; de Gracia, M.; Vanrolleghem, P. A.; Ayesa, E., A new plant-wide modelling methodology for WWTPs. *Water Res.* **2007,** *41*, (19), 4357-4372.
103. Grau, P.; Copp, J.; Vanrolleghem, P. A.; Takacs, I.; Ayesa, E., A comparative analysis of different approaches for integrated WWTP modelling. *Water Sci. Technol.* **2009,** *59*, (1), 141-147.
104. Daigger, G. T., A practitioners perspective on the uses and future developments for wastewater treatment modelling. *Water Science and Technology* **2011,** *63*, (3), 516-526.
105. Roels, J. A., *Energetics and Kinetics in Biotechnology*. Elsevier Biomedical Press BV: Amsterdam, The Netherlands, 1983; p 330.
106. Filipe, C. D. M.; Daigger, G. T.; Grady, C. P. L., Stoichiometry and kinetics of acetate uptake under anaerobic conditions by an enriched culture of phosphorus-accumulating organisms at different pHs. *Biotechnology and Bioengineering* **2001,** *76*, (1), 32-43.
107. Smolders, G. J. F.; Vandermeij, J.; Van Loosdrecht, M. C. M.; Heijnen, J. J., A structured metabolic model for anaerobic and aerobic stoichiometry and kinetics of

the biological phosphorus removal process. *Biotechnology and Bioengineering* **1995,** *47*, (3), 277-287.
108. Smolders, G. J. F.; Vandermeij, J.; Van Loosdrecht, M. C. M.; Heijnen, J. J., Stoichiometric model of the aerobic metabolism of the biological phosphorus removal process. *Biotechnology and Bioengineering* **1994,** *44*, (7), 837-848.
109. Smolders, G. J. F.; Vandermeij, J.; Van Loosdrecht, M. C. M.; Heijnen, J. J., Model of the anaerobic metabolism of the biological phosphorus removal process - stoichiometry and pH influence. *Biotechnology and Bioengineering* **1994,** *43*, (6), 461-470.
110. Filipe, C. D. M.; Daigger, G. T.; Grady Jr., C. P. L., A metabolic model for acetate uptake under anaerobic conditions by glycogen accumulating organisms: stoichiometry, kinetics, and the effects of pH. *Biotechnology and Bioengineering* **2001,** *76*, (1), 17-31.
111. Zeng, R.; Yuan, Z.; van Loosdrecht, M. C. M.; Keller, J., Proposed modifications to metabolic model for glycogen-accumulating organisms under anaerobic conditions. *Biotechnol. Bioeng.* **2001,** *80*, (3), 277-279.
112. van Aalst-van Leeuwen, M. A.; Pot, M. A.; van Loosdrecht, M. C. M.; Heijnen, J. J., Kinetic modeling of poly(beta-hydroxybutyrate) production and consumption by *Paracoccus pantotrophus* under dynamic substrate supply. *Biotechnology and Bioengineering* **1997,** *55*, (5), 773-782.
113. van Loosdrecht, M. C. M.; Pot, M. A.; Heijnen, J. J., Importance of bacterial storage polymers in bioprocesses. *Water Sci. Technol.* **1997,** *35*, (1), 41-47.
114. Boyle, N. R.; Morgan, J. A., Flux balance analysis of primary metabolism in *Chlamydomonas reinhardtii*. *BMC Systems Biology* **2009,** *3*.
115. Manichaikul, A.; Ghamsari, L.; Hom, E. F. Y.; Lin, C. W.; Murray, R. R.; Chang, R. L.; Balaji, S.; Hao, T.; Shen, Y.; Chavali, A. K.; Thiele, I.; Yang, X. P.; Fan, C. Y.; Mello, E.; Hill, D. E.; Vidal, M.; Salehi-Ashtiani, K.; Papin, J. A., Metabolic network analysis integrated with transcript verification for sequenced genomes. *Nature Methods* **2009,** *6*, (8), 589-592.
116. Walker, W. E.; Harremoes, P.; Rotmans, J.; van der Sluijs, J. P.; van Asselt, M. B. A.; Janssen, P.; Krayer von Krauss, M. P., Defining uncertainty: a conceptual basis for uncertainty management in model-based decision support. *Integrated Assessment* **2003,** *4*, (1), 5-17.
117. Flores-Alsina, X.; Rodriguez-Roda, I.; Sin, G.; Gernaey, K. V., Uncertainty and sensitivity analysis of control strategies using benchmark simulation model No1 (BSM1). *Water Sci. Technol.* **2009,** *59*, (3), 491-499.
118. Grady, C. P. L.; Smets, B. F.; Barbeau, D. S., Variability in kinetic parameter estimates: a review of possible causes and a proposed terminoloty. *Water Res.* **1996,** *30*, (3), 742-748.
119. Cox, C. D., Statistical distributions of uncertainty and variability in activated sludge model parameters. *Water Environ. Res.* **2004,** *76*, 2672-2685.
120. Ekama, G. A., Using bioprocess stoichiometry to build a plant-wide mass balance based steady-state WWTP model. *Water Res.* **2009,** *43*, (8), 2101-2120.
121. Sin, G.; Van Hulle, S. W. H.; De Pauw, D. J. W.; van Griensven, A.; Vanrolleghem, P. A., A critical comparison of systematic calibration protocols for activated sludge models: A SWOT analysis. *Water Res.* **2005,** *39*, (12), 2459-2474.
122. Roels, J. A., Application of macroscopic principles to microbial metabolism. *Biotechnology & Bioengineering* **1980,** *22*, (12), 2457-2514.
123. Bixio, D.; Parmentier, G.; Rousseau, D.; Verdonck, F.; Meirlaen, J.; Vanrolleghem, P. A.; Thoeye, C., A quantitative risk analysis tool for design/simulation of wastewater treatment plants. *Water Sci. Technol.* **2002,** *46*, (4-5), 301-307.

124. Sin, G.; Gernaey, K. V.; Neumann, M. B.; van Loosdrecht, M. C. M.; Gujer, W., Uncertainty analysis in WWTP model applications: A critical discussion using an example from design. *Water Res.* **2009,** *43*, (11), 2894-2906.
125. Benedetti, L.; Bixio, D.; Claeys, F.; Vanrolleghem, P. A., Tools to support a model-based methodology for emission/immission and benefit/cost/risk analysis of wastewater systems that considers uncertainty. *Environmental Modelling & Software* **2008,** *23*, (8), 1082-1091.
126. Sin, G.; Gernaey, K. V.; Neumann, M. B.; van Loosdrecht, M. C. M.; Gujer, W., Global sensitivity analysis in wastewater treatment model applications: prioritizing sources of uncertainty. *Wat. Res.* **2011,** *45*, (2), 639-651.
127. Benedetti, L.; Bixio, D.; Vanrolleghem, P. A., Assessment of WWTP design and upgrade options: balancing costs and risks of standards' exceeance. *Water Sci. Technol.* **2006,** *54*, (6-7), 371-378.
128. Hospido, A.; Moreira, M. T.; Feijoo, G., A comparison of municipal wastewater treatment plants for big centres of population in Galicia (Spain). *International Journal of Life Cycle Assessment* **2008,** *13*, (1), 57-64.
129. Benetto, E.; Nguyen, D.; Lohmann, T.; Schmitt, B.; Schosseler, P., Life cycle assessment of ecological sanitation system for small-scale wastewater treatment. *Science of the Total Environment* **2009,** *407*, (5), 1506-1516.
130. Foley, J.; de Haas, D.; Hartley, K.; Lant, P., Comprehensive life cycle inventories of alternative wastewater treatment systems. *Water Research* **2010,** *44*, (5), 1654-1666.
131. Golueke, C. G.; Oswald, W. J.; Gotaas, H. B., Anaerobic digestion of algae. *Applied Microbiol.* **1957,** *5*, (1), 47-55.
132. Golueke, C. G.; Oswald, W. J., Power from solar energy: via algae-produced methane. *Solar Energy* **1963,** *7*, (3), 86-92.
133. Golueke, C. G.; Oswald, W. J., Biological conversion of light energy to the chemical energy of methane. *Applied Microbiol.* **1959,** *7*, (4), 219-227.
134. Goldman, J. C., Outdoor algal mass cultures - I. Applications. *Water Res.* **1979,** *13*, (1), 1-19.
135. Benemann, J. R.; Weissman, J. C.; Koopman, B. L.; Oswald, W. J., Energy production by microbial photosynthesis. *Nature* **1977,** *268*, (5615), 19-23.
136. Sialve, B.; Bernet, N.; Bernard, O., Anaerobic digestion of microalgae as a necessary step to make microalgal biodiesel sustainable. *Biotechnol. Advances* **2009,** *27*, 409-416.
137. Samson, R.; LeDuy, A., Detailed study of anaerobic digestion of *Spirulina maxima* algal biomass. *Biotechnology & Bioengineering* **1986,** *28*, (7), 1014-1023.
138. Samson, R.; LeDuy, A., Biogas production from anaerobic digestion of *Spriulina maxima* algal biomass. *Biotechnology and Bioengineering* **1982,** *24*, (8), 1919-1924.
139. Samson, R.; LeDuy, A., Improved performance of anaerobic digestion of *Spirulina maxima* algal biomass by addition of carbon-rich wastes. *Biotechnology Letters* **1983,** *5*, (10), 677-682.
140. Samson, R.; LeDuy, A., Influence of mechanical and thermochemical pretreatments on anaerobic digestion of *Spirulina maxima* algal biomass. *Biotechnology Letters* **1983,** *5*, (10), 671-676.
141. Velasquez-Orta, S. B.; Curtis, T. P.; Logan, B. E., Energy from algae using microbial fuel cells. *Biotechnology & Bioengineering* **2009,** *103*, (6), 1068-1076.
142. He, Z.; Kan, J.; Mansfeld, F.; Angenent, L. T.; Nealson, K. H., Self-sustained phototrophic microbial fuel cells based on the synergistic cooperation between photosynthetic microorganisms and heterotrophic bacteria. *Environ. Sci. Technol.* **2009,** *43*, (5), 1648-1654.

143. Strik, D. P. B. T. B.; Hamelers, H. V. M.; Buisman, C. J. N., Solar energy powered microbial fuel cell with reversible bioelectrode. *Environ. Sci. Technol.* **in press**.
144. De Schamphelaire, L.; Verstraete, W., Revival of the biological sunlight-to-biogas energy conversion system. *Biotechnology & Bioengineering* **2009,** *103*, (2), 296-304.
145. Converti, A.; Casazza, A. A.; Ortiz, E. Y.; Perego, P.; Del Borghi, M., Effect of temperature and nitrogen concentration on the growth and lipid content of *Nannochloropsis oculata* and *Chlorella vulgaris* for biodiesel production. *Chemical Engineering and Processing* **2009,** *48*, 1146-1151.
146. Guschina, I. A.; Harwood, J. L., Lipids and lipid metabolism in eukaryotic algae. *Progress in Lipid Research* **2006,** *45*, 160-186.
147. Harwood, J. L.; Guschina, I. A., The versatility of algae and their lipid metabolism. *Biochimie* **2009,** *91*, 679-684.
148. Chiu, S. Y.; Kao, C. Y.; Tsai, M. T.; Ong, S. C.; Chen, C. H.; Lin, C. S., Lipid accumulation and CO2 utilization of *Nannochloropsis oculata* in response to CO2 aeration. *Bioresource Technology* **2009,** *100*, 833-838.
149. Vardon, D. R.; Sharma, B. K.; Scott, J.; Yu, G.; Wang, Z. C.; Schideman, L.; Zhang, Y. H.; Strathmann, T. J., Chemical properties of biocrude oil from the hydrothermal liquefaction of *Spirulina* algae, swine manure, and digested anaerobic sludge. *Bioresource Technology* **2011,** *102*, (17), 8295-8303.
150. Chisti, Y., Biodiesel from microalgae beats bioethanol. *Trends in Biotechnology* **2008,** *26*, (3), 126-131.
151. Wijffels, R. H.; Barbosa, M. J., An outlook on microalgal biofuels. *Science* **2010,** *329*, (5993), 796-799.
152. Whyte, J. N. C., Biochemical composition and energy content of six species of phytoplankton used in mariculture of bivalves. *Aquaculture* **1987,** *60*, (3-4), 231-241.
153. Chu, F. L. E.; Dupuy, J. L.; Webb, K. L., Polysaccharide composition of five algal species used as food larvae of the American oyster, *Crassostrea virginica*. *Aquaculture* **1982,** *29*, (3-4), 241-252.
154. Hu, Q.; Sommerfeld, M.; Jarvis, E.; Ghirardi, M.; Posewitz, M.; Seibert, M.; Darzins, A., Microalgal triacylglycerols as feedstocks for biofuel production: perspectives and advances. *The Plant Journal* **2008,** *54*, 621-639.
155. Courchesne, N. M. D.; Parisien, A.; Wang, B.; Lan, C. Q., Enhancement of lipid production using biochemical, genetic and transcription factor engineering approaches. *J. Biotechnology* **2009,** *141*, 31-41.
156. Rodolfi, L.; Zittelli, G. C.; Bassi, N.; Padovani, G.; Biondi, N.; Bonini, G.; Tredici, M. R., Microalgae for oil: strain selection, induction of lipid synthesis and outdoor mass cultivation in a low-cost photobioreactor. *Biotechnology & Bioengineering* **2009,** *102*, (1), 100-112.
157. Mansour, M. P.; Frampton, D. M. F.; Nichols, P. D.; Volkman, J. K.; Blackburn, S. I., Lipid and fatty acid yield of nine stationary-phase microalgae: applications and unusual C24-C28 polyunsaturated fatty acids. *J. Appl. Phycol.* **2005,** *17*, 287-300.
158. Christenson, L.; Sims, R., Production and harvesting of microalgae for wastewater treatment, biofuels, and bioproducts. *Biotechnol. Advances* **2011,** *29*, (6), 686-702.
159. Wang, B.; Lan, C. Q., Biomass production and nitrogen and phosphorus removal by the green alga *Neochloris oleoabundans* in simulated wastewater and secondary municipal wastewater effluent. *Bioresource Technology* **2011,** *102*, (10), 5639-5644.
160. Su, Y. Y.; Mennerich, A.; Urban, B., Municipal wastewater treatment and biomass accumulation with a wastewater-born and settleable algal-bacterial culture. *Water Research* **2011,** *45*, (11), 3351-3358.

161. Cho, S.; Luong, T. T.; Lee, D.; Oh, Y. K.; Lee, T., Reuse of effluent water from a municipal wastewater treatment plant in microalgae cultivation for biofuel production. *Bioresource Technology* **2011,** *102*, (18), 8639-8645.
162. Sturm, B. S. M.; Lamer, S. L., An energy evaluation of coupling nutrient removal from wastewater with algal biomass production. *Applied Energy* **2011,** *88*, (10), 3499-3506.
163. Sydney, E. B.; da Silva, T. E.; Tokarski, A.; Novak, A. C.; de Carvalho, J. C.; Woiciecohwski, A. L.; Larroche, C.; Soccol, C. R., Screening of microalgae with potential for biodiesel production and nutrient removal from treated domestic sewage. *Applied Energy* **2011,** *88*, (10), 3291-3294.
164. Zhou, W. G.; Li, Y. C.; Min, M.; Hu, B.; Chen, P.; Ruan, R., Local bioprospecting for high-lipid producing microalgal strains to be grown on concentrated municipal wastewater for biofuel production. *Bioresource Technology* **2011,** *102*, (13), 6909-6919.
165. Brown, M. R.; Jeffrey, S. W.; Volkman, J. K.; Dunstan, G. A., Nutritional properties of microalgae for mariculture. *Aquaculture* **1997,** *151*, 315-331.
166. Cornet, J. F.; Dussap, C. G.; Gros, J. B., Kinetics and Energetics of Photosynthetic Micro-Organisms in Photobioreactors: Application to *Spirulina* Growth. In *Bioprocess and Algae Reactor Technology, Apoptosis*, Scheper, T., Ed. Springer / Heidelberg: Berlin, 1998; Vol. 59.
167. Hu, Q., Environmental Effects on Cell Composition. In *Handbook of Microalgal Culture: Biotechnology and Applied Phycology*, Richmond, A., Ed. Blackwell Science Ltd.: Oxford, UK, 2004; p 566.
168. Cuhel, R. L.; Ortner, P. B.; Lean, D. R. S., Night synthesis of protein by algae. *Limnology and Oceanography* **1984,** *29*, (4), 731-744.
169. Dismukes, G. C.; Carrieri, D.; Bennette, N.; Ananyev, G. M.; Posewitz, M. C., Aquatic phototrophs: efficient alternatives to land-based crops for biofuels. *Curr. Opin. Biotechnol.* **2008,** *19*, 235-240.
170. Varzakas, T. H.; Arvanitoyannis, I. S.; Baltas, H., The politics and science behind GMO acceptance. *Critical Reviews in Food Science and Nutrition* **2007,** *47*, 335-361.
171. Briones, A.; Raskin, L., Diversity and dynamics of microbial communities in engineered environments and their implications for process stability. *Curr. Opin. Biotechnol.* **2003,** *14*, 270-276.
172. Griffiths, M. J.; Harrison, S. T. L., Lipid productivity as a key characteristic for choosing algal species for biodiesel production. *J. Applied Phycol.* **2009,** *21*, 493-507.
173. Unknown, A new parasitic green alga. *Nature* **1877,** *15*, (384), 416.
174. Unknown, Algae in water supplies. *Science* **1904,** *19*, (495), 963.
175. Franks, P. J. S., Models of harmful algal blooms. *Limnology and Oceanography* **1997,** *42*, (5), 1273-1282.
176. Scavia, D.; Liu, Y., Exploring estuarine nutrient susceptibility. *Environ. Sci. Technol.* **2009,** *43*, (10), 3474-3479.
177. Maynard, H. E.; Ouki, S. K.; Williams, S. C., Tertiary lagoons: a review of removal mechanisms and performance. *Water Res.* **1999,** *33*, (1), 1-13.
178. Hoffmann, J. P., Wastewater treatment with suspended and nonsuspended algae. *J. Phycol.* **1998,** *34*, 757-763.
179. Hashimoto, S.; Furukawa, K., Nutrient removal from secondary effluent by filamentous algae. *J. Fermentation Bioengineering* **1989,** *67*, (1), 62-69.
180. Roeselers, G.; van Loosdrecht, M. C. M.; Muyzer, G., Phototrophic biofilms and their potential applications. *J. Applied Phycol.* **2008,** *20*, 227-235.

181. Jupsin, H.; Praet, E.; Vasel, J. L., Dynamic mathematical model of high rate algal ponds (HRAP). *Water Sci. Technol.* **2003,** *48*, (2), 197-204.
182. Bordel, S.; Guieysse, B.; Munoz, R., Mechanistic model for the reclamation of industrial wastewaters using algal-bacterial photobioreactors. *Environ. Sci. Technol.* **2009,** *43*, (9), 3200-3207.
183. Wolf, G.; Picioreanu, C.; van Loosdrecht, M. C. M., Kinetic modeling of phototrophic biofilms: the PHOBIA model. *Biotechnology & Bioengineering* **2007,** *97*, (5), 1064-1079.
184. Staal, M.; Thar, R.; Kuhl, M.; van Loosdrecht, M. C. M.; Wolf, G.; De Brouwer, J. F. C.; Rijstenbil, J. W., Carbon isotope fractionation in developing natural phototrophic biofilms. *Biogeosciences Discussions* **2007,** *4*, (1), 69-98.
185. Neu, T. R.; Lawrence, J. R., Development and structure of microbial biofilms in river water studied by confocal laser scanning microscopy. *FEMS Microbiology Ecology* **1997,** *24*, 11-25.
186. Horn, H.; Neu, T. R.; Wulkow, M., Modelling the structure and function of extracellular polymeric substances in biofilms with new numerical techniques. *Water Sci. Technol.* **2001,** *43*, (6), 121-127.
187. Merrick, J. M., Metabolism of reserve materials. In *The Photosynthetic Bacteria*, Clayton, R. K.; Sistrom, W. R., Eds. Plenum Press: New York, 1978.
188. Dircks, K.; Henze, M.; van Loosdrecht, M. C. M.; Mosbaek, H.; Aspegren, H., Storage and degradation of poly-beta-hydroxybutyrate in activated sludge under aerobic conditions. *Water Res.* **2001,** *35*, (9), 2277-2285.
189. Oki, T.; Kanae, S., Global hydrological cycles and world water resources. *Science* **2006,** *313*, (5790), 1068-1072.
190. Conley, D. J.; Paerl, H. W.; Howarth, R. W.; Boesch, D. F.; Seitzinger, S. P.; Havens, K. E.; Lancelot, C.; Likens, G. E., Controlling eutrophication: nitrogen and phosphorus. *Science* **2009,** *323*, (5917), 1014-1015.
191. Kolpin, D. W.; Furlong, E. T.; Meyer, M. T.; Thurman, E. M.; Zaugg, S. D.; Barber, L. B.; Buxton, H. T., Pharmaceuticals, hormones, and other organic wastewater contaminants in US streams, 1999-2000: A national reconnaissance. *Environmental Science & Technology* **2002,** *36*, (6), 1202-1211.
192. Beck, M. B.; Jiang, F.; Shi, F.; Villarroel Walker, R., Technology, Sustainability, and Business: Cities as Forces of Good in the Environment. In *Integrated Urban Water Management in Temperate Climates*, Maksimovic, C., Ed. UNESCO and Taylor & Francis: London, in press.
193. Daigger, G. T., New approaches and technologies for wastewater management. *Bridge* **2008,** *38*, (3), 38-45.
194. Public Utilities Board of Singapore *Press Release: Sembcorp NEWater to start building Changi NEWater Plant in April*; February 28, 2008.
195. Lahnsteiner, J.; Lempert, G., Water management in Windhoek, Namibia. *Water science and technology* **2007,** *55*, (1-2), 441-448.
196. Logan, B. E.; Hamelers, B.; Rozendal, R.; Schroder, U.; Keller, J.; Freguia, S.; Aelterman, P.; Verstraete, W.; Rabaey, K., Microbial fuel cells: methodology and technology. *Environmental science & technology* **2006,** *40*, (17), 5181-5192.
197. National Biosolids Partnership *2006-2007 Annual Report - Environmental Stewardship: a decade of progress in implementing a national model EMS program for the water quality profession*; Alexandria, United States, 2007.
198. Water UK *Recycling of Biosolids to Land*; London, England, 2006.
199. de-Bashan, L. E.; Bashan, Y., Recent advances in removing phosphorus from wastewater and its future use as a fertilizer (1997-2003). *Water research* **2004,** *38*, 4222-4246.

200. Kvarnstrom, E.; Emilsson, K.; Stintzing, A. R.; Johansson, M.; Jonsson, H.; Petersens, E. a.; Schonning, C.; Christensen, J.; Hellstrom, D.; Qvarnstrom, L.; Ridderstolpe, P.; Drangert, J.-O. *Urine Diversion: One Step Towards Sustainable Sanitation*; Stockholm Environment Institute: Stockholm, Sweden, 2006.
201. Parris, T. M.; Kates, R. W., Characterizing a sustainability transition: goals, targets, trends, and driving forces. *Proceedings of the National Academy of Sciences* **2003,** *100*, (14), 8068-8073.
202. City of San Diego *The 2005 Urban Water Management Plan*; San Diego, United States, 2005.
203. Hartley, T. W., Public perception and participation in water reuse. *Desalination* **2006,** *187*, 115-126.
204. Po, M.; Kaercher, J. D.; Nancarrow, B. E. *Literature Review of Factors Influencing Public Perceptions of Water Reuse*; CSIRO Land and Water: December 2003.
205. Lupton, D., *Risk*. Routledge: London, 1999.
206. Saravanan, V. S.; McDonald, G. T.; Mollinga, P. P., Critical review of integrated water resources management: moving beyond polarised discourse. *Natural Resources Forum* **2009,** *33*, 76-86.
207. Jasanoff, S., *Designs on Nature: Science and Democracy in Europe and the United States*. Princeton University Press: Princeton, New Jersey, 2005; p 380.
208. World Water Assessment Programme *The United Nations World Water Development Report 3: Water in a Changing World*; Paris: UNESCO, and London: Earthscan, 2009.
209. Starkl, M.; Brunner, N.; Flogl, W.; Wimmer, J., Design of an institutional decision-making process: The case of urban water management. *Journal of Environmental Management* **2009,** *90*, (2), 1030-1042.
210. Cheng, H.; Hu, Y.; Zhao, J., Meeting China's water shortage crisis: current practices and challenges. *Environ. Sci. Technol.* **2009,** *43*, (2), 240-244.
211. Haffejee, M.; Brent, A. C., Evaluation of an integrated asset life-cycle management (ALCM) model and assessment of practices in the water utility sector. *Water SA* **2008,** *34*, (2), 285-290.
212. Hokanson, D. R.; Zhang, Q.; Cowden, J. R.; Troschinetz, A. M.; Mihelcic, J. R.; Johnson, D. M., "Challenges to implementing drinking water technologies in developing world countries," Environmental Engineer: Applied Research and Practice, Vol. I, Winter, 2007. *Environmental Engineer, the Magazine of the American Academy of Environmental Engineers* **2007,** *43*, (1), 31-38.
213. Atkinson, G.; Mourato, S., Environmental cost-benefit analysis. *Annu. Rev. Environ. Resour.* **2008,** *33*, 317-344.
214. Hunkeler, D.; Rebitzer, G. G., The future of life cycle assessment. *International Journal of Life Cycle Assessment* **2005,** *10*, (5), 305-308.
215. Rebitzer, G. G.; Hunkeler, D., Life cycle costing in LCM: ambitions, opportunities, and limitations. *International Journal of Life Cycle Assessment* **2003,** *8*, (5), 253-256.
216. Hunkeler, D., Societal LCA methodology and case study. *Int. J. Life Cycle Assess.* **2006,** *11*, (6), 371-382.
217. Mendoza, G. A.; Martins, H., Multi-criteria decision analysis in natural resource management: a critical review of methods and new modelling paradigms. *Forest Ecology and Management* **2006,** *230*, 1-22.
218. Giupponi, C.; Jakeman, A. J.; Karssenberg, D.; Hare, M. P., *Sustainable Management of Water Resources: an Integrated Approach*. Edward Elgar Publishing: Northampton, MA, 2006.

219. Mihelcic, J. R.; Myre, E. A.; Fry, L. M.; Phillips, L. D.; Barkdoll, B. D., *Field Guide in Environmental Engineering for Development Workers: Water, Sanitation, Indoor Air*. American Society of Civil Engineers (ASCE) Press: Reston, VA, 2009.
220. Presidential/Congressional Commission on Risk Assessment and Risk Management, Framework for Environmental Health and Risk Management. In Washington, DC, 1997; Vol. 1.
221. U.S. EPA *Response to Congress on use of decentralized wastewater treatment systems*; EPA 832-R-97-001b; Washington, D.C., 1997.
222. Etnier, C., Research needs for decentralized wastewater treatment in an energy-constrained future. *Water Environment Research* **2007,** *79*, (2), 123-124.
223. Brown, R. R., Social and Institutional Considerations. In *Data Requirements for Integrated Urban Water Management*, Fletcher, T. D.; Deletic, A., Eds. UNESCO Publishing, Taylor & Francis: Paris, France, 2008; p 337.
224. Carson, R. T., Contingent valuation: a user's guide. *Environmental science & technology* **2000,** *34*, (8), 1413-1418.
225. Gasparatos, A.; El-Haram, M.; Horner, M., The argument against a reductionist approach for measuring sustainable development performance and the need for methodological pluralism. *Accounting Forum* **2009,** *33*, (3), 245-256.
226. Pahl-Wostl, C., Towards sustainability in the water sector - the importance of human actors and processes of social learning. *Aquat. Sci.* **2002,** *64*, 394-411.
227. Daigger, G. T.; Crawford, G. V., Enhancing water system security and sustainability by incorporating centralized and decentralized water reclamation and reuse into urban water management systems. *Journal of Environmental Engineering Management* **2007,** *17*, (1), 1-10.
228. Ostrom, E., A general framework for analyzing sustainability of social-ecological systems. *Science* **2009,** *325*, (5939), 419-422.
229. CRD Wastewater Treatment Made Clear. http://www.wastewatermadeclear.ca/ (March 9, 2009),
230. Wolstenholme, E. F., Qualitative vs quantitative modelling: the evolving balance. *Journal of the Operational Research Society* **1999,** *50*, (4), 422-428.
231. Sterman, J., *Business Dynamics: Systems Thinking and Modeling for a Complex World*. McGraw Hill: Columbus, Ohio, 2000.
232. Tippett, J., The value of combining a systems view of sustainability with a participatory protocol for ecologically informed design in river basins. *Environ. Modelling & Software* **2005,** *20*, 119-139.
233. Shafir, E.; Simonson, I.; Tversky, A., Reason-based choice. *Cognition* **1993,** *49*, 11-36.
234. Slovic, P.; Finucane, M. L.; Peters, E.; MacGregor, D. G., The affect heuristic. *European J. Operational Research* **2007,** *177*, 1333-1352.
235. Stave, K. A., A system dynamics model to facilitate public understanding of water management options in Las Vegas, Nevada. *Journal of Environmental Management* **2003,** *67*, (4), 303-313.
236. Conklin, J. E., *Dialogue Mapping: Building Shared Understanding of Wicked Problems*. John Wiley & Sons Ltd: West Sussex, England, 2006; p 242.
237. Stepp, M. D.; Winebrake, J. J.; Hawker, J. S.; Skerlos, S. J., Greenhouse gas mitigation policies and the transportation sector: The role of feedback effects on policy effectiveness. *Energy Policy* **2009,** *37*, (7), 2774-2787.
238. Belton, V.; Stewart, T. J., *Multiple Criteria Decision Analysis: An Integrated Approach*. Kluwer Academic Publisher: Boston, MA, 2002.

239. Wang, J. J.; Jing, Y. Y.; Zhang, C. F.; Zhao, J. H., Review on multi-criteria decision analysis aid in sustainable energy decision-making. *Renewable and Sustainable Energy Reviews* **2009,** *13*, 2263-2278.
240. Hajkowicz, S.; Collins, K., A review of multiple criteria analysis for water resource planning and management. *Water Resources Management* **2007,** *21*, (9), 1553-1566.
241. Borsuk, M. E.; Maurer, M.; Lienert, J.; Larsen, T. A., Charting a path for innovative toilet technology using multicriteria decision analysis. *Environmental Science & Technology* **2008,** *42*, (6), 1855-1862.
242. Hyde, K. M.; Maier, H. R.; Colby, C. B., Reliability-based approach to multicriteria decision analysis for water resources. *J. Water Resources Planning and Management - ASCE* **2004,** *130*, (6), 429-438.
243. Slovic, P., The construction of preference. *American Psychologist* **1995,** *50*, (5), 364-371.
244. Refsgaard, J. C.; van der Sluijs, J. P.; Højberg, A. L.; Vanrolleghem, P. A., Uncertainty in the environmental modelling process - A framework and guidance. *Environmental Modelling & Software* **2007,** *22*, 1543-1556.
245. Hämäläinen, R. P.; Alaja, S., The threat of weighting biases in environmental decision analysis. *Ecological Economics* **2008,** *68*, 556-569.
246. Ascough, J. C.; Maier, H. R.; Ravalico, J. K.; Strudley, M. W., Future research challenges for incorporation of uncertainty in environmental and ecological decision-making. *Ecological Modelling* **2008,** *219*, (3-4), 383-399.
247. Zendehdel, K.; Rademaker, M.; De Baets, B.; Van Huylenbroeck, G., Qualitative valuation of environmental criteria through a group consensus based on stochastic dominance. *Ecological Economics* **2008,** *67*, 253-264.
248. Rodriguez-Garcia, G.; Molinos-Senante, M.; Hospido, A.; Hernandez-Sancho, F.; Moreira, M. T.; Feijoo, G., Environmental and economic profile of six typologies of wastewater treatment plants. *Water Res.* **2011,** *45*, (18), 5997-6010.
249. Printemps, C.; Baudin, A.; Dormoy, T.; Zug, M.; Vanrolleghem, P. A., Optimisation of a large WWTP thanks to mathematical modelling. *Water Sci. Technol.* **2004,** *50*, (7), 113-122.
250. Rivas, A.; Irizar, I.; Ayesa, E., Model-based optimisation of wastewater treatment plants design. *Environ. Modelling & Software* **2008,** *23*, 435-450.
251. Marshall, J. D.; Toffel, M. W., Framing the elusive concept of sustainability: a sustainability hierarchy. *Environ. Sci. Technol.* **2005,** *39*, (3), 673-682.
252. Guest, J. S.; Skerlos, S. J.; Daigger, G. T.; Corbett, J. R. E.; Love, N. G., The use of qualitative system dynamics to identify sustainability characteristics of decentralized wastewater management alternatives. *Water Sci. Technol.* **2010,** *61*, (6), 1637-1644.
253. Gallego, A.; Hospido, A.; Moreira, M. T.; Feijoo, G., Environmental performance of wastewater treatment plants for small populations. *Resources Conservation and Recycling* **2008,** *52*, (6), 931-940.
254. Gaterell, M. R.; Griffin, P.; Lester, J. N., Evaluation of environmental burdens associated with sewage treatment processes using life cycle assessment techniques. *Environmental Technology* **2005,** *26*, (3), 231-249.
255. Lundin, M.; Olofsson, M.; Pettersson, G. J.; Zetterlund, H., Environmental and economic assessment of sewage sludge handling options. *Resources Conservation and Recycling* **2004,** *41*, (4), 255-278.
256. Wang, J. S.; Hamburg, S. P.; Pryor, D. E.; Chandran, K.; Daigger, G. T., Emissions credits: opportunity to promote integrated nitrogen management in the wastewater sector. *Environ. Sci. Technol.* **2011,** *45*, (15), 6239–6246.

257. Gori, R.; Jiang, L. M.; Sobhani, R.; Rosso, D., Effects of soluble and particulate substrate on the carbon and energy footprint of wastewater treatment processes. *Water Res.* **2011,** *45*, (18), 5858-5872.
258. U.S. Environmental Protection Agency *Process Design and Cost Estimating Algorithms for the Computer Assisted Procedure for Design and Evaluation of Wastewater Treatment Systems (CAPDET)*; Office of Water Program Operations: Washington, D.C., 1982; p 1700.
259. Foley, J. M.; Rozendal, R. A.; Hertle, C. K.; Lant, P. A.; Rabaey, K., Life cycle assessment of high-rate anaerobic treatment, microbial fuel cells, and microbial electrolysis cells. *Environmental Science & Technology* **2010,** *44*, (9), 3629-3637.
260. Doka, G., Life Cycle Inventories of Waste Treatment Services. ecoinvent report No. 13. Swiss Centre for Life Cycle Inventories, Dübendorf. **2009**.
261. Zimmermann, P.; Doka, G.; Huber, F.; Labhardt, A.; Menard, M., *Ökoinventare von Entsorgungsprozessen: Grundlagen zur Integration der Entsorgung in Ökobilanzen*. ESU-Reihe, 1/96, Gruppe Energie-Stoffe-Umwelt ESU, Laboratorium für Energiesysteme, Institut für Energietechnik, ETH Zürich, Switzerland, 1996.
262. Grabski, C.; Fahner, S.; Bührer, H.; Leuenberger, H., Ökobilanz einer kläranlage (life cycle assessment of a sewage treatment plant). *Korrespondenz Abwasser* **1996,** *43*, (6), 1053-1056.
263. Fahner, S.; Bührer, H.; Grabski, C. Ökobilanz einer kommunalen ARA: am Beispiel der ARA “Ergolz I” in Sissach, BL (in Swiss German). IBB Ingenieurschule beider Basel, 1995.
264. IPCC *2006 IPCC Guidelines for National Greenhouse Gas Inventories*; Hayama, Kanagawa, Japan, 2006.
265. Bare, J., TRACI 2.0: the tool for the reduction and assessment of chemical and other environmental impacts 2.0. *Clean Techn Environ Policy* **in press**.
266. McKay, M. D.; Beckman, R. J.; Conover, W. J., A comparison of three methods for selecting values of input variables in the analysis of output from a computer code. *Technometrics* **1979,** *21*, (2), 239-245.
267. U.S. Energy Information Administration *1990-2010 Net Generation by State by Type of Producer by Energy Source (EIA-906, EIA-920, and EIA-923)*; Washington, D.C., 2011.
268. Ahn, J. H.; Kim, S.; Park, H.; Rahm, B.; Pagilla, K.; Chandran, K., N_2O emissions from activated sludge processes, 2008-2009: results of a national monitoring survey in the United States. *Environmental Science & Technology* **2010,** *44*, (12), 4505-4511.
269. Seitzinger, S. P.; Kroeze, C., Global distribution of nitrous oxide production and N inputs in freshwater and coastal marine ecosystems. *Global Biogeochemical Cycles* **1998,** *12*, (1), 93-113.
270. ICIS, Chemical Pricing Database. In 2011.
271. Ruhl, H. A.; Rybicki, N. B., Long-term reductions in anthropogenic nutrients link to improvements in Chesapeake Bay habitat. *Proceedings of the National Academy of Sciences* **2010,** *107*, (38), 16566-16570.
272. Birch, M. B. L.; Gramig, B. M.; Moomaw, W. R.; Doering, O. C.; Reeling, C. J., Why Metrics Matter: Evaluating Policy Choices for Reactive Nitrogen in the Chesapeake Bay Watershed. *Environmental Science & Technology* **2011,** *45*, (1), 168-174.
273. John, R. P.; Anisha, G. S.; Nampoothiri, K. M.; Pandey, A., Micro and macroalgal biomass: a renewable source for bioethanol. *Bioresource Technol.* **2011,** *102*, (1), 186-193.

274. Yang, Z.; Guo, R.; Xu, X.; Fan, X.; Luo, S., Hydrogen and methane production from lipid-extracted microalgal biomass residues. *Int. J. Hydrogen Energy* **2011,** *36*, (5), 3465-3470.
275. Furusato, E.; Asaeda, T., A dynamic model of darkness tolerance for phytoplankton: model description. *Hydrobiologia* **2009,** *619*, 67-88.
276. Harris, E. H.; Stern, D.; Witman, G., *The Chlamydomonas Sourcebook. Second Edition*. Academic Press: New York, 2009; Vol. 1-3.
277. Siaut, M.; Cuine, S.; Cagnon, C.; Fessler, B.; Nguyen, M.; Carrier, P.; Beyly, A.; Beisson, F.; Triantaphylides, C.; Li-Beisson, Y. H.; Peltier, G., Oil accumulation in the model green alga *Chlamydomonas reinhardtii*: characterization, variability between common laboratory strains and relationship with starch reserves. *BMC Biotechnology* **2011,** *11*, (7).
278. Allen, M. M.; Stanier, R. Y., Growth and division of some unicellular blue-green algae. *Journal of General Microbiology* **1968,** *51*, 199-&.
279. Allen, M. M., Simple conditions for growth of unicellular blue-green algae on plates. *Journal of Phycology* **1968,** *4*, (1), 1-&.
280. MacIntyre, H. L.; Cullen, J. J., Using Cultures to Investigate the Physiological Ecology of Microalgae. In *Algal Culturing Techniques*, Hendersen, R. A., Ed. Elsevier Academic Press: London, 2005.
281. Barbosa, M. J.; Zijffers, J. W.; Nisworo, A.; Vaes, W.; van Schoonhoven, J.; Wijffels, R. H., Optimization of biomass, vitamins, and carotenoid yield on light energy in a flat-panel reactor using the A-stat technique. *Biotechnology and Bioengineering* **2005,** *89*, (2), 233-242.
282. Pruvost, J.; Van Vooren, G.; Cogne, G.; Legrand, J., Investigation of biomass and lipids production with Neochloris oleoabundans in photobioreactor. *Bioresource Technology* **2009,** *100*, (23), 5988-5995.
283. Lowry, O. H.; Rosebrough, N. J.; Farr, A. L.; Randall, R. J., Protein measurement with the folin phenol reagent. *Journal of Biological Chemistry* **1951,** *193*, (1), 265-275.
284. Khunjar, W. O.; Love, N. G., Sorption of carbamazepine, 17 alpha-ethinylestradiol, iopromide and trimethoprim to biomass involves interactions with exocellular polymeric substances. *Chemosphere* **2011,** *82*, (6), 917-922.
285. Levine, R. B.; Pinnarat, T.; Savage, P. E., Biodiesel production from wet algal biomass through in situ lipid hydrolysis and supercritical transesterification. *Energy & Fuels* **2010,** *24*, 5235-5243.
286. European Committee for Standardization *Standard EN14103: Determination of Ester and Linolenic Acid Methyl Ester Content*; Brussels, Belgium, 2003.
287. Dubois, M.; Gilles, K. A.; Hamilton, J. K.; Rebers, P. A.; Smith, F., Colorimetric method for determination of sugars and related substances. *Analytical Chemistry* **1956,** *28*, (3), 350-356.
288. Granum, E.; Myklestad, S. M., A simple combined method for determination of beta-1,3-glucan and cell wall polysaccharides in diatoms. *Hydrobiologia* **2002,** *477*, (1-3), 155-161.
289. APHA; AWWA; WEF, *Standard Methods for the Examination of Water and Wastewater. 21st Edition*. Washington, D.C., 2006.
290. Richmond, A., *Handbook of Microalgal Culture: Biotechnology and Applied Phycology*. Blackwell Science Ltd.: Ames, Iowa, 2004; p 566.
291. Alric, J., Cyclic electron flow around photosystem I in unicellular green algae. *Photosynthesis Research* **2010,** *106*, (1-2), 47-56.
292. Peltier, G.; Tolleter, D.; Billon, E.; Cournac, L., Auxiliary electron transport pathways in chloroplasts of microalgae. *Photosynthesis Research* **2010,** *106*, (1-2), 19-31.

293. Roels, J. A., Application of macroscopic principles to microbial metabolism. *Biotechnology and Bioengineering* **1980,** *22*, (12), 2457-2514.
294. Verduyn, C.; Stouthamer, A. H.; Scheffers, W. A.; Vandijken, J. P., A theoretical evaluation of growth yields of yeasts. *Antonie Van Leeuwenhoek International Journal of General and Molecular Microbiology* **1991,** *59*, (1), 49-63.
295. Stouthamer, A. H., A theoretical study on the amount of ATP required for synthesis of microbial cell material. *Antonie Van Leeuwenhoek* **1973,** *39*, (3), 545-565.
296. Williams, P. J. L.; Laurens, L. M. L., Microalgae as biodiesel & biomass feedstocks: Review & analysis of the biochemistry, energetics & economics. *Energy & Environmental Science* **2010,** *3*, (5), 554-590.
297. Work, V. H.; Radakovits, R.; Jinkerson, R. E.; Meuser, J. E.; Elliott, L. G.; Vinyard, D. J.; Laurens, L. M. L.; Dismukes, G. C.; Posewitz, M. C., Increased lipid accumulation in the *Chlamydomonas reinhardtii* sta7-10 starchless isoamylase mutant and increased carbohydrate synthesis in complemented strains. *Eukaryotic Cell* **2010,** *9*, (8), 1251-1261.
298. Nelson, D. L.; Cox, M. M., *Lehninger Principles of Biochemistry, Fourth Edition*. W.H. Freeman: 2004; p 1,100.
299. Pirt, S. J., Tansley Review No. 4 - The thermodynamic efficiency (quantum demand) and dynamics of photosynthetic growth. *New Phytologist* **1986,** *102*, (1), 3-37.
300. Gommers, P. J. F.; Vanschie, B. J.; Vandijken, J. P.; Kuenen, J. G., Biochemical limits to microbial growth yields: an analysis of mixed substrate utilization. *Biotechnology and Bioengineering* **1988,** *32*, (1), 86-94.
301. Beeftink, H. H.; Vanderheijden, R. T. J. M.; Heijnen, J. J., Maintenance requirements: energy supply from simultaneous endogenouos respiration and substrate consumption. *FEMS Microbiology Ecology* **1990,** *73*, (3), 203-209.
302. Jiang, Y.; Hebly, M.; Kleerebezem, R.; Muyzer, G.; van Loosdrecht, M. C. M., Metabolic modeling of mixed substrate uptake for polyhydroxyalkanoate (PHA) production. *Water Research* **2011,** *45*, (3), 1309-1321.
303. Beun, J. J.; Verhoef, E. V.; Van Loosdrecht, M. C. M.; Heijnen, J. J., Stoichiometry and kinetics of poly-beta-hydroxybutyrate metabolism under denitrifying conditions in activated sludge cultures. *Biotechnology and Bioengineering* **2000,** *68*, (5), 496-507.
304. Johnson, K.; Kleerebezem, R.; van Loosdrecht, M. C. M., Model-Based Data Evaluation of Polyhydroxybutyrate Producing Mixed Microbial Cultures in Aerobic Sequencing Batch and Fed-Batch Reactors. *Biotechnology and Bioengineering* **2009,** *104*, (1), 50-67.
305. Roessler, P. G., UDPglucose pyrophosphorylase activity in the diatom *Cyclotella cryptica* - pathway of chrysolaminarin biosynthesis. *Journal of Phycology* **1987,** *23*, (3), 494-498.
306. National Renewable Energy Laboratory *A Look Back at the U.S. Department of Energy's Aquatic Species Program: Biodiesel from Algae*; Golden, Colorado, 1998; p 328.
307. Noctor, G.; Foyer, C. H., Homeostasis of adenylate status during photosynthesis in a fluctuating environment. *Journal of Experimental Botany* **2000,** *51*, 347-356.
308. Klausmeier, C. A.; Litchman, E.; Levin, S. A., Phytoplankton growth and stoichiometry under multiple nutrient limitation. *Limnology and Oceanography* **2004,** *49*, (4), 1463-1470.
309. Droop, M. R., VITAMIN B12 AND MARINE ECOLOGY .4. KINETICS OF UPTAKE GROWTH AND INHIBITION IN MONOCHRYSIS LUTHERI. *Journal of the Marine Biological Association of the United Kingdom* **1968,** *48*, (3), 689-&.

310. Flynn, K. J.; Fasham, M. J. R.; Hipkin, C. R., Modelling the interactions between ammonium and nitrate uptake in marine phytoplankton. *Phil. Trans. R. Soc. Lond. B* **1997,** *352*, (1361), 1625-1645.
311. Droop, M. R., Nutrient status of algal cells in continuous culture. *Journal of the Marine Biological Association of the United Kingdom* **1974,** *54*, (4), 825-855.
312. Droop, M. R., NUTRIENT STATUS OF ALGAL CELLS IN BATCH CULTURE. *Journal of the Marine Biological Association of the United Kingdom* **1975,** *55*, (3), 541-555.
313. Ross, O. N.; Geider, R. J., New cell-based model of photosynthesis and photo-acclimation: accumulation and mobilisation of energy reserves in phytoplankton. *Marine Ecology Progress Series* **2009,** *383*, 53-71.
314. Eilers, P. H. C.; Peeters, J. C. H., A model for the relationship between light intensity and the rate of photosynthesis in phytoplankton. *Ecological Modelling* **1988,** *42*, (3-4), 199-215.
315. Duarte, P.; Ferreira, J. G., Dynamic modelling of photosynthesis in marine and estuarine ecosystems. *Environmental Modeling and Assessment* **1997,** *2*, (1-2), 83-93.
316. Falkowski, P. G.; Wirick, C. D., A simulation model of the effects of vertical mixing on primary productivity. *Marine Biology* **1981,** *65*, (1), 69-75.
317. Dias, J. M. L.; Serafim, L. S.; Lemos, P. C.; Reis, M. A. M.; Oliveira, R., Mathematical modelling of a mixed culture cultivation process for the production of polyhydroxybutyrate. *Biotechnology and Bioengineering* **2005,** *92*, (2), 209-222.
318. Herbert, D., Some principles on continuous culture. In *Recent Progress in Microbiology*, Tunevall, G., Ed. Almqvist & Wiksell: Stockholm, 1958; pp 381-396.
319. Pirt, S. J., Maintenance energy of bacteria in growing cultures. *Proceedings of the Royal Society of London Series B-Biological Sciences* **1965,** *163*, (991), 224-231.
320. Henze, M.; Gujer, W.; Mino, T.; van Loosdrecht, M. *Actived Sludge Models ASM1, ASM2, ASM2d and ASM3*; International Water Association: London, 2000.
321. Petersen, E. E., *Chemical Reaction Analysis*. Prentice-Hall: Englewood Cliffs, NJ, 1965; p 276.
322. Falkowski, P. G.; Laroche, J., ACCLIMATION TO SPECTRAL IRRADIANCE IN ALGAE. *Journal of Phycology* **1991,** *27*, (1), 8-14.
323. Favier-Teodorescu, L.; Cornet, J. F.; Dussap, C. G., Modelling continuous culture of Rhodospirillum rubrum in photobioreactor under light limited conditions. *Biotechnology Letters* **2003,** *25*, (4), 359-364.
324. Klausmeier, C. A.; Litchman, E.; Daufresne, T.; Levin, S. A., Optimal nitrogen-to-phosphorus stoichiometry of phytoplankton. *Nature* **2004,** *429*, (6988), 171-174.
325. Zhao, J. Y.; Ramin, M.; Cheng, V.; Arhonditsis, G. B., Competition patterns among phytoplankton functional groups: How useful are the complex mathematical models? *Acta Oecologica-International Journal of Ecology* **2008,** *33*, (3), 324-344.
326. Steele, J. H., Environmental control of photosynthesis in the sea. *Limnology and Oceanography* **1962,** *7*, (2), 137-150.
327. Flynn, K. J.; Hipkin, C. R., Interactions between iron, light, ammonium, and nitrate: Insights from the construction of a dynamic model of algal physiology. *Journal of Phycology* **1999,** *35*, (6), 1171-1190.
328. Helmes, R.; Huijbregts, M. A. J.; Henderson, A. D.; Jolliet, O., Spatially explicit fate factors of freshwater phosphorous emissions at the global scale. *Int. J. Life Cycle Assess.* **in revision**.
329. Mutel, C. L.; Hellweg, S., Regionalized life cycle assessment: computational methodology and application to inventory databases. *Environmental Science & Technology* **2009,** *43*, (15), 5797-5803.

330. Reap, J.; Roman, F.; Duncan, S.; Bras, B., A survey of unresolved problems in life cycle assessment - Part 2: impact assessment and interpretation. *Int. J. Life Cycle Assess.* **2008,** *13*, 374-388.
331. Daigger, G. T., Tools for future success: emerging trends that are changing the nature of water quality management. *Water Environment & Technology* **2003,** *15*, (12), 38-45.
332. Drechsel, P.; Kunze, D., *Waste Composting for Urban and Peri-urban Agriculture: Closing the Rural-Urban Nutrient Cycle in Sub-Saharan Africa*. CABI Publishing: New York, 2001.
333. Orecchini, F., A "measurable" definition of sustainable development based on closed cycles of resources and its application to energy systems. *Sustain. Sci.* **2007,** *2*, 245-252.
334. Stenstrom, M. K.; Rosso, D., Energy conservation and recovery: two requirements for sustainable wastewater treatment. *Water Environment Research* **2007,** *79*, (8), 819-820.
335. King, C. W.; Holman, A. S.; Webber, M. E., Thirst for energy. *Nature Geoscience* **2008,** *1*, 283-286.
336. Beck, M. M. B., Vulnerability of water quality in intensively developing urban watersheds. *Environmental Modelling and Software* **2005,** *20*, (4), 381-400.
337. Baron, J. S.; Poff, N. L.; Angermeier, P. L.; Dahm, C. N.; Gleick, P. H.; Hairston Jr., N. G.; Jackson, R. B.; Johnston, C. A.; Richter, B. D.; Steinman, A. D., Meeting ecological and societal needs for freshwater. *Ecological Applications* **2002,** *12*, (5), 1247-1260.
338. Magid, J.; Eilersen, A. M.; Wrisberg, S.; Henze, M., Possibilities and barriers for recirculation of nutrients and organic matter from urban to rural areas: a technical theoretical framework applied to the medium-sized town Hillerod, Denmark. *Ecological engineering* **2006,** *28*, 44-54.
339. Berndtsson, J. C., Experiences from the implementation of a urine separation system: goals, planning, reality. *Building Environ.* **2006,** *41*, 427-437.
340. Rosso, D.; Stenstrom, M. K., The carbon-sequestration potential of municipal wastewater treatment. *Chemosphere* **2008,** *70*, (8), 1468-1475.
341. Bogner, J.; Pipatti, R.; Hashimoto, S.; Diaz, C.; Mareckova, K.; Diaz, L.; Kjeldsen, P.; Monni, S.; Faaij, A.; Gao, Q.; Zhang, T.; Ahmed, M. A.; Sutamihardja, R. T. M.; Gregory, R., Mitigation of global greenhouse gas emissions from waste: conclusions and strategies from the Intergovernmental Panel on Climate Change (IPCC) Fourth Assessment Report - Working Group III (Mitigation). *Waste management & research* **2008,** *26*, 11-32.
342. Bunn, S. E.; Arthington, A. H., Basic principles and ecological consequences of altered flow regimes for aquatic biodiversity. *Environmental Management* **2002,** *30*, (4), 492-507.
343. Gatzweiler, F. W., Organizing a public ecosystem service economy for sustaining biodiversity. *Ecol. Economics* **2006,** *59*, 296-304.
344. International Water Association *Sanitation 21: simple approaches to complex sanitation*; 2006.
345. Montgomery, M. A.; Bartram, J.; Elimelech, M., Increasing functional sustainability of water and sanitation supplies in rural sub-Saharan Africa. *Environmental engineering science* **2009,** *26*, (5), 1017-1023.
346. Bithas, K., The sustainable residential water use: sustainability, efficiency and social equity. The European experience. *Ecological Economics* **2008,** *68*, (1-2), 221-229.

347. Lienert, J.; Larsen, T. A., Considering user attitude in early development of environmentally friendly technology: a case study of NoMix toilets. *Environmental Science & Technology* **2006,** *40*, (16), 4838-4844.
348. Ozerol, G.; Newig, J., Evaluating the success of public participation in water resources management: five key constituents. *Water Policy* **2008,** *10*, 639-655.
349. Beck, M. B. *Grand challenges of the future for environmental modeling*; NSF: Washington, DC, 2008.
350. Maurer, M.; Pronk, W.; Larsen, T. A., Treatment processes for source-separated urine. *Water research* **2006,** *40*, 3151-3166.
351. Wilsenach, J. A.; van Loosdrecht, M. C. M., Effects of separate urine collection on advanced nutrient removal processes. *Environmental science & technology* **2004,** *38*, (4), 1208-1215.
352. Clauwaert, P.; Aelterman, P.; Pham, T. H.; De Schamphelaire, L.; Carballa, M.; Rabaey, K.; Verstraete, W., Minimizing losses in bio-electrochemical systems: the road to applications. *Appl. Microbiol. Biotechnol.* **2008,** *79*, (6), 901-913.
353. Czepiel, P.; Crill, P.; Harriss, R., Nitrous oxide emissions from municipal wastewater treatment. *Environ. Sci. Technol.* **1995,** *29*, (9), 2352-2356.
354. Institute, E. P. R. *Water & Sustainability (Volume 4): U.S. Electricity Consumption for Water Supply & Treatment - The Next Half Century*; Palo Alto, 2002.
355. California Energy Commission *2005 Integrated Energy Policy Report*; CEC-100-2005-007-CTD, September 2005.
356. Tsagarakis, K. P.; Mara, D. D.; Angelakis, A. N., Application of cost criteria for selection of municipal wastewater treatment systems. *Water, air, and soil pollution* **2003,** *142*, (1), 187-210.
357. United States Environmental Protection Agency, Inventory of U.S. Greenhouse Gas Emissions and Sinks: 1990-2007. In Washington, DC, EPA 430-R-09-004, 2009.
358. Angelakis, A. N.; Durham, B., Water recycling and reuse in EUREAU countries: trends and challenges. *Desalination* **2008,** *218*, 3-12.
359. Miller, G. W., Integrated concepts in water reuse: managing global water needs. *Desalination* **2006,** *187*, 65-75.